HUMAN HEPATIC NATURAL KILLER CELLS IN HEALTH AND MALIGNANCY

This thesis is submitted to the University of Dublin for the degree of

Doctor of Philosophy (Ph.D)

By
Cathal Harmon
B.Sc (Hons)

School of Biochemistry and Immunology
Trinity College Dublin
Supervisor: Prof. Cliona O'Farrelly

Declaration

I declare that this thesis has not been submitted as an exercise for a degree at this or any other university and it is entirely my own work. I agree to deposit this thesis in the University's open access institutional repository or allow the Library to do so on my behalf, subject to Irish Copyright Legislation and Trinity College Library conditions of use and acknowledgement.

_____

Cathal Harmon

2018

General abstract

The adult human liver is described as an immunologically tolerogenic organ, maintaining a homeostatic environment while bombarded by dietary antigens, microbial products and metabolic by-products. The liver is also a site of immunosurveillance, scouring the portal vein and liver parenchyma for viral infection, malignant cells and toxic products. This balance is achieved through the unique immune repertoire of the liver. A predominance of immunoregulatory myeloid cells and cytotoxic innate lymphocytes, especially natural killer (NK) cells, creates a microenvironment skewed toward tolerance but primed to respond to pathogenic threats. We hypothesise that liver resident NK cells have adapted to this microenvironment, altering their phenotype and function in order to maintain an immunologically competent but naturally tolerogenic immune repertoire. We further hypothesised that tumour induced changes to the microenvironment compromise liver resident NK cell tumour immunity. In this project, we aimed to characterise NK cell subpopulations in healthy donor liver and metastatic liver tumours, focusing on the effect of the hepatic microenvironment on the differentiation and function of these populations.

NK cells account for nearly 50% of hepatic lymphocytes, making it the most NK cell populated organ in the body. Unlike their peripheral blood counterparts, hepatic NK cells express an activated phenotype and display increased cytotoxicity toward tumour cells *in vitro.* However, this increased cytotoxic function is not accompanied by the usual production of classic pro-inflammatory cytokines, like IFN-γ. In this study, we have identified a population of tissue resident NK cells characterised by a unique transcription factor profile, $Eomes^{hi}$ $Tbet^{lo}$, and expression of the tissue homing receptor CXCR6 whose ligand (CXCL16) is constitutively expressed by liver sinusoidal endothelial cells.

When placed in culture, these cells revert to a more conventional phenotype but maintain CXCR6 expression. When this system is supplemented with conditioned medium from

healthy liver tissue, hepatic NK cells maintain their Eomes^{hi} Tbet^{lo} phenotype, indicating that the liver microenvironment plays an important role in defining their phenotype. We have identified TGF-β as the factor responsible for maintaining this phenotype and suppressing pro-inflammatory cytokine production.

Hepatic NK cells appear ideally suited for tumour surveillance. The tumour microenvironment is classically considered an anti-inflammatory environment; however tumour growth, angiogenesis and eventual metastasis requires an inflammatory environment, often provided by the immune cells trying to prevent the spread of cancer. Eomes^{hi} Tbet^{lo} hepatic NK cells have the potential to target tumour cells without contributing to the inflammatory environment which causes significant tissue damage and promotes tumour progression. In our cohort of colorectal liver metastasis (CRLM), NK cells are significantly depleted from these tumours, specifically the liver resident CD56^{bright} NK cells. Culture with conditioned media from tumours selectively induces apoptosis of liver resident NK cells *in vitro*. Accumulation of lactate in the tissue microenvironment causes a decrease in intracellular pH, increased mitochondrial stress and production of ROS which induces apoptosis. This process can be abrogated by treatment with a mitochondrial ROS scavenger.

We have identified a unique population of tissue resident anti-tumour NK cells in human liver. This population is compromised in CRLM through changes in the metabolic microenvironment. We propose that patients will benefit from metabolic targeted therapies which would restrict tumour growth, reduce lactate production and restore liver resident NK cell immunity. This is the first time tumour metabolism has been identified as a key immune evasion technique in CRLM and provides a novel avenue for therapeutic approaches.

Table of contents

Acknowledgements

After four years in Trinity, I have many happy memories to look back on. The relationships and bonds that I have forged here will last a life time (if they can still stand me when I move on). As I reflect on my time here, I realise how much I've changed and my world has changed. A PhD is a difficult thing, something I underestimated from the start. After many a long night, early morning and failed experiment I feel like I've truly given my blood, sweat and tears to this project (not literally blood because that would be unethical). I couldn't have made it this far without the love and support of my family and friends.

To my parents Sheila and Jimmy, you've given everything to your family and supported me without question (despite worrying I'd never buy a house). You've put up with me living at when I should be long gone. I want to thank you for everything you've done for me, listening to me whine and complain, picking me up late at night in the rain, always being there when I needed reassuring word. To my brothers and sisters, thank you for always being there to support me. You've all inspired me over the years to become the best I can be.

For the last 4 years I've had second family in the comparative immunology lab. I've probably spent more time with this family than my real family. Cliona O'Farrelly, my supervisor, has brought together an incredible group of people. Cliona was the mentor every young researcher needs; supportive, dedicated, enthusiastic and willing to give her students the freedom they need to develop as an independent thinker. I owe you more than I can ever repay. It is clear you care deeply for all of your students and I don't think we show our appreciation for that nearly enough. Over the years the lab has changed quite a bit and now at the end I feel like last of one era of the lab moving on.

Team Liver

Without Ronan Fahey this project would not have been possible. Ronan spent four years building the scientific and collaborative basis for this research. He helped me a lot in those early days, spending several late nights with me processing livers when he could have been in Kennedys with everyone else. Ronan I am eternally grateful to you for making life so easy for me. The staff in the pathology never got over the retirement of "hot liver guy" and I could never replace you in their eyes. I tried my best to fill your shoes.

Sarah Whelan……that is all.

Haha I kid. After a cool start, Sarah and I became like family, forming one third of the toblerone trio. It's amazing the bond you develop over a hundred mouse livers at ten o'clock at night. Always there with a suggestion or reassurance, I've missed our science chats so much. You were also instrumental in developing my love life, thanks for the recommendation.

Ann Byrne we didn't get enough time together but I'm glad you're happy down under. I miss the trips to the bank (even though I wasn't invited most of the time). You could always make me laugh, except when you were rocking a bun and then I stayed well away for fear of getting a death stare. Good luck with your PhD, you'll do fantastic.

Dalal, after Ronan and Sarah left, I was a very lonely on team liver. You've been a huge help over the last couple of years. It's been a privilege to watch you develop into an outstanding researcher. And thank you for the introduction to Kuwaiti tea and cookies. You are the undisputed champion of lab baking too.

Kim is the latest addition to team liver and the last student I supervised (although I think you did more supervision than me). You've given me a whole new perspective on science and how to approach problems. I have no doubt you'll do great things in the lab and beyond. Never stop telling people about what you do.

Team HCV

Auntie Mags and I started at the same time in the lab but she became irreplaceable overnight. On top of managing a lab, doing lab work and generally getting whatever needed to be done, done, Mag has had to listen to every one of us complain and vent. And like Peig Sayers born again she always had some sage advice or pearl of wisdom. There is no way to thank you for all the time you've given me. I'm sure you would have rather been listening to Pat Kenny than my problems. I'm sorry for the pencil shavings on your keyboard.

Mark "Sharkey" Robinson is a post-doc I hope to emulate. He's been a huge help in developing this project. He's thought me a lot about writing and helped make me a better communicator. I'll always cherish the times we went for drinks and talked science. All I ask is that you let Tom play for Ireland.

Lena my neighbour on the other side of Das Border. Thank you for sharing German Wednesdays with us. Das Strauss Uberwicht will live on with me forever.

Gerard Roche the funniest man to ever inhabit this lab. I hope you still dream. Stay away from those bears in the mountains.

Jaime has only been in the lab short time but I really enjoyed having him in the lab. A social media mogul in the making, I think you'll achieve a lot in the coming years. AS someone at the end take my advice, there will be a time when you don't think it's worth it but trust me it is.

Team NK

Uma Turkleton, the second member of the toblerone. When you left the lab it was like a light went out. It has never been the same. You were my mentor in everything NK cell related and so much more. Even after you'd left you were always there with advice or to ask how my wee lass was. You've been an inspiration to me in work and in life. I have to confess it was me that used up all of your antibody and left the empty tube in your box. You were too scary to admit it to you.

The NK cells are in safe hands with Louise Glover. You couldn't ask for a safer pair of hands. You are the first non-NK cell person that's ever been interested in learning about NK cells I've met.

Team Bovine

Fernando and Anne were the bovine tag team when I started in the lab. I learned a lot from them over the years. Fernando was the most popular man in TBSI because he could solve everyone's protein problems. The lab has been a lot quieter since you left. Anne my next door neighbour, I'm sorry I left my music playing all night while you were trying to write.

Amy thanks for all the photos of cervical mucus while I had my morning coffee. I always looked forward to seeing your data because your intro grossed me out.

drum roll Now for the main event. PAUL. KELLY. The man. The cow whisperer. I could write pages and pages about Paul but I've promised him I won't embarrass him in a published format. Don't worry Appendix II The Paul Kelly Chronicles is available on demand. Paul it's been an absolute pleasure spending the last few years working together. You never fail to make me laugh. Despite offering me pizza in return for a mental breakdown, every day you made life a little bit easier for me. I've no doubt you'll have this cow lark sorted out soon.

Sarah Swoboda. We haven't had much time to get to know each other but I'm confident the bovine projects are in good hands with you. Best of luck in the future.

Outside the lab there are still so many people to thank. For the last year we've been sharing the lab with the real slim Sheady et al. Thanks for the advice Fred and sitting through so many talks about flipping NK cells, are they even real? To Sarah Case and Emer Hackett, you guys came in like a wrecking ball (see I know pop music). The lab has gotten a new lease of life since you guys joined. I've learnt so much about bags of quilts from Emer. Little Sarah you have to take care of Paul now, don't let him put his t shirt on upside down (haha Pual thought he was safe).

To the Bowie lab, who I've had the pleasure of sharing a reading room with for four years. Thanks for the memories, I'm sorry Uma and Fiona were so loud.

Thanks to Lydia Lynch and her lab for all her help and advice over the years. Your time has been invaluable to helping me progress to this point. I hope we can work together again in the future.

To the staff of St. Vincent's University Hospital, none of this would have been possible without your work. To the nurses, the transplant co-ordinators, pathologists, and surgeons' thank you, you do truly inspiring work. This project couldn't compare to the help you give in one day to these patients. I would especially like to thank Diarmaid Houlihan, Justin Geoghegan, Emir Hoti, Keno Mentor and Fiona Hand for contributing directly to the development of this project. You're help has been invaluable over the years. I only hope that this work will help your patients one day.

Last but by no means least, thank you Claire. You've made the last couple of years the best of my life. I know it's been difficult sometimes and you have the patience of a saint. You've always been there for me when I needed it, always brightening my day. I hope I can repay that debt with the love and affection you showed me during my most difficult times.

There are so many other friends I can't mention here. I could fill another thesis with the names of people who've supported me through the last four years. Know that I appreciate what you've done for me and that I'll try to pay you back one day. Thank you all. This work is for you.

Ethics Statement

This study was approved by the Research Ethics Committee of St. Vincent's University Hospital and Trinity College Dublin. Informed written consent was obtained from all study participants except when anonymised buffy coat packs (obtained from the Irish Blood Transfusion Service) were used.

Associated Publications

Harmon, C., Robinson, M.W., Fahey, R., Whelan, S., Houlihan, D.D., Geoghegan, J., and C. O'Farrelly (2016). Tissue-resident Eomes^{hi} T-bet^{lo} CD56^{bright} NK cells with reduced proinflammatory potential are enriched in the adult human liver. *European Journal of Immunology*, 46(9). https://doi.org/10.1002/eji.201646559

Harmon, C., Sanchez-Fueyo, A., O'Farrelly, C., and D.D. Houlihan (2016). Natural Killer Cells and Liver Transplantation: Orchestrators of Rejection or Tolerance? *American Journal of Transplantation* 16(3), 751–7. https://doi.org/10.1111/ajt.13565

Robinson, M.W., **Harmon, C.,** and O'Farrelly, C., (2016). Liver immunology and its role in inflammation and homeostasis. *Cellular and Molecular Immunology,* 13(3). https://doi.org/10.1038/cmi.2016.3

Further Publications

Coughlan, A.M., **Harmon, C.,** Whelan, S., O'Brien, E.C., O'Reilly, V.P., Crotty, P., Kelly, P., Ryan, M., Hickey, F.B., O'Farrelly, C., and Little, M.A. (2016). Myeloid engraftment in humanized mice: Impact of granulocyte-colony stimulating factor treatment and transgenic mouse strain. *Stem Cells and Development*, 25(7). https://doi.org/10.1089/scd.2015.0289

Glover, L.E., Crosby, D., Thiruchelvam, U., **Harmon, C.,** Chorcora, C.N., Wingfield, M.B., and O'Farrelly, C., (2018). Uterine natural killer cell progenitor populations predict successful implantation in women with endometriosis-associated infertility. *American Journal of Reproductive Immunology*, e12817. https://doi.org/10.1111/aji.12817

Hand, F., **Harmon, C.,** Elliott, L.A., Caiazza, F., Lavelle, A., Maguire, D., Hoti, E., Nolan, N., Geoghegan, J.G., Ryan, E.J., and O'Farrelly, C., (2018) Depleted polymorphonuclear leukocytes in human metastatic liver reflect an altered immune microenvironment associated with recurrent metastasis. *Cancer Immunology, Immunotherapy,* Accepted Manuscript.

List of figures

List of Tables

Abbreviations

αCHC	Alpha- cyano-4-hydroxycinnamate
AIH	Autoimmune hepatitis
AHR	Aryl hydrocarbon receptor
ALD	Alcoholic liver disease

ASCT2	Alanine, serine, cysteine-preferring transporter 2
ATM	Ataxia-telangiectasia mutated
ATP	Adenosine Triphosphate
ATR	ATM and RAD3-related
BAD	BCL2 associated agonist of cell death
BAX	BCL2 associated X, apoptosis regulator,
BAT-3	HLA-B associated transcript 3
BID	BH3 interacting domain death agonist
BSA	Bovine serum albumin
B_2M	Beta-2 microglobulin
CD	Cluster of differentiation
CCL	Chemokine (c-c motif) ligand
CCR	Chemokine (c-c motif) receptor
CILCP	Common innate lymphoid cell precursor
CMV	Cytomegalovirus
CRC	Colorectal cancer
CRLM	Colorectal liver metastasis
CTLA-4	Cytotoxic T-lymphocyte associated protein 4
CTV	Cell trace violet
CXCL	Chemokine (C-X-C motif) ligand
DAA	Direct acting anti-viral
DAMP	Danger associated molecular pattern
DC	Dendritic cell
DFFAB	DNA fragmentation factor A/B
DMSO	Dimethyl sulfoxide
DNAM1	DNAX accessory molecule-1
dNTP	Dinucleotide triphosphate
DTT	Dithiothreitol
EDTA	Ethylenediaminetetraacetic acid
EMT	Epithelial-mesenchymal transition
Eomes	Eomesodermin
ER	Endoplasmic reticulum
FADD	FAS-associated death domain

FASL	FAS ligand
FBS	Fetal bovine serum
FMO	Fluorescence minus one
FVS	Fixable viability stain
GATA3	GATA Binding Protein 3
GI	Gastrointestinal
GF	Growth factor
GM-CSF	Granulocyte-monocyte colony stimulating factor
GLUT1	Glucose transporter 1
HBV	Hepatitis B virus
HBSS	Hank's buffered salt solution
HCC	Hepatocellular carcinoma
HCV	Hepatitis C virus
HIV	Human immunodeficiency virus
HLA	Human leukocyte antigen
HMNC	Hepatic mononuclear cell
hnRNP-K	Heterogeneous nuclear ribonucleoprotein K
HPSC	Hematopoietic stem cell
HSC	Hepatic stellate cell
IDO	Indolemine-2,3-oxygenase
ID2	Inhibitor Of DNA Binding 2
IFN-γ	Interferon gamma
iNKT	Invariant natural killer T cell
IL-	Interleukin
ILC	Innate lymphoid cell
KC	Kupffer cell
KIR	Killer cell immunoglobulin-like receptor
KLRG1	Killer-cell lectin like receptor G1
LAK	Lymphokine-activated killer cell
LAMP-1	Lysosomal-associated membrane protein 1
LCIS	Live cell imaging solution
LCM	Liver conditioned media
LCMV	Lymphocytic Choriomeningitis Virus
LDH	Lactate dehydrogenase

LIR	Leukocyte immunoglobulin like receptor
LB	Liver biopsy
LP	Liver perfusate
LSEC	Liver sinusoidal endothelial cell
LTi	Lymphoid tissue-inducer
mAb	Monoclonal antibody
MAIT	Mucosal associated invariant T cell
MAMP	Microbial associated molecular pattern
MCT	Monocarboxylate transporter
MMP	Matrix metalloproteinase
MDSC	Myeloid derived suppressor cell
MFI	Mean fluorescence intensity
MHC	Major histocompatibility complex
MIC-A/B	MHC class I polypeptide-related sequence A/B
NAD	Nicotinamide adenine dinucleotide
NAFLD	Non-alcoholic fatty liver disease
NASH	Non-alcoholic steatohepatitis
NCR	Natural cytotoxicity receptor
NFIL3	Nuclear Factor, Interleukin 3 Regulated
NK	Natural killer cell
NKp	Natural killer cell progenitor
NKT	Natural killer T cell
NSG	Nod-SCID-gamma receptor
OD	Optical density
PB	Peripheral blood
PBC	Primary biliary cirrhosis
PBMC	Peripheral blood mononuclear cell
PBS	Phosphate buffered saline
PDGF	Platelet-derived growth factor
PD-L1	Programmed death-ligand 1
PI	Propidium Iodide
PLZF	Promyelocytic leukaemia zinc finger
PMA	Phorbol 12-myristate 13-acetate
PRR	Pattern recognition receptor

PSC	Primary Sclerosing cholangitis
qPCR	Quantitative polymerase chain reaction
RANTES	Regulated on activation, normal T cell expressed and secreted
RAS	Rat sarcoma
RLU	Relative luminescence units
RORα	RAR-related orphan receptor alpha
RORγt	RAR-related orphan receptor gamma
RPMI	Roswell Park Memorial Institute
ROS	Reactive oxygen species
RTM	Resting transport media
SLT	Secondary lymphoid tissue
TCA	Tricarboxylic acid cycle
TGF-β	Transforming growth factor beta
TIGIT	T-cell immunoreceptor with Ig and ITIM domains
TLR	Toll-like receptor
TNF-α	Tumour necrosis factor alpha
TNFR	TNF-α receptor
TRAIL	Tumour necrosis factor (TNF)-related apoptosis inducing ligand
TRAIL-R	Tumour necrosis factor (TNF)-related apoptosis inducing ligand receptor
ULBP	UL-16 binding protein
UW	University of Wisconsin
VEGF	Vascular endothelial growth factor

CHAPTER 1: General Introduction

1.1 The liver as an immunological organ

The liver is the central metabolic organ of the human body, essential for the processing, transport and storage of carbohydrates, lipids, proteins and nutrients. In recent times the plethora of immunological functions the liver also performs has become apparent. The liver is essential to the systemic immune system, producing acute phase proteins, complement, clotting factors and various cytokines and chemokines (Crispe, 2009; O'Farrelly et al., 2005; Robinson et al., 2016). The liver is highly vascularised, but unusually receives 80% of its blood supply from the venous system, via the portal vein. This blood supply drains the gastrointestinal tract, so is enriched in: nutrients, dietary antigens, as well as bacterial components and toxins from the gut microflora. The liver must tolerate this immunogenic load while still providing immunosurveillance for hepatotrophic and systemic infections, as well as malignant cells. Upon entering the liver, venous blood from the gut mixes with oxygen rich blood from the hepatic artery and drains through the hepatic sinusoids to the central veins through plates of hepatocytes. The sinusoids are lined by specialised liver sinusoidal endothelial cells (LSECs) that contain numerous fenestrations, allowing blood to pass through the LSEC layer to the underlying hepatocytes (Knolle and Wohlleber, 2016).

This organization allows for rapid exchange of molecules from the blood into hepatocytes and vice versa. This allows the metabolism of nutrients by hepatocytes and facilitates the removal and degradation of immunogenic molecules (e.g. bacterial endotoxin) in the liver. Pattern recognition receptors (PRRs) expressed by hepatocytes and liver-resident macrophages (known as Kupffer cells (KC)), bind to microbial associated molecular patterns (MAMPs) (Janeway, 1992; Takeuchi and Akira, 2010) and damage associated molecular patterns (DAMPs), which are present in high quantities in the blood arriving from the portal vein. Upon binding, these MAMPs and DAMPs are phagocytosed and subsequently degraded by hepatocytes and KCs, without the production of inflammatory mediators that usually accompany PRR signaling. This detoxification of blood from the gut protects the rest of the

body from excessive immune activation and influences the unique immunological environment within the liver.

1.1.1 Hepatic tolerance

The concept that the liver is an immunologically tolerant organ arose in the transplantation field when it was first observed in pigs that allogeneic liver transplantation was significantly better tolerated than other allogeneic organ transplants which induced rapid rejection (Calne et al., 1969). Moreover, organs (e.g. skin graft) transplanted from the same donor after liver transplantation are better tolerated than grafts from a third party. In humans, liver transplantation does not require HLA matching, in contrast to other solid organs which require close matching. This concept of tolerance is further supported by the low levels of immunosuppression generally required by liver transplant recipients (Geissler and Schlitt, 2009). Indeed, in some individuals, immunosuppression can be completely stopped following liver transplantation without subsequent graft rejection (Benitez et al., 2013; Garza et al., 2013; Li et al., 2004; Martinez-llordella et al., 2006, 2007, 2008). Furthermore, the ability of hepatic tolerance to induce systemic tolerance to co-transplanted organs highlights the powerful tolerogenic properties of the liver (Simpson et al., 2006).

The liver is often described as an immunologically tolerant organ (Calne et al., 1969; O'Farrelly and Crispe, 2002). This early description was based on several observations of the ability of the liver to clear pathogenic stimuli without inducing a systemic immune response. Animal models have demonstrated that antigens absorbed through the portal tract fail to induce an antibody response or immunological memory (Cantor and Dumont, 1967). Endotoxin, or lipopolysaccharide (LPS), tolerance is a unique feature of the hepatic immune system. The hepatic blood supply contains low levels of endotoxin, up to 1ng/ml of lipopolysaccharide LPS is detectable in the portal vein, which is removed from the circulation by the liver without further immune activation. In fact, Kupffer cells treated with LPS

produce IL-10 and prostaglandins, potent immunosuppressive cytokines which inhibit T cell activity (Callery et al., 1991; Groux et al., 1996; Knolle et al., 1995). The liver therefore acts as an antigenic barrier, capable of clearing threats but without eliciting a systemic response. This unique immunological balance is achieved through the specialised immune repertoire of the liver.

1.1.2 Immunological landscape of the liver

The liver acts as an important barrier between the gut and the systemic circulation. Not surprisingly the liver has developed several layers of regulation in order to minimize immune activation in response to harmless dietary and commensal antigens. Parenchymal cells, such as hepatocytes and cholangiocytes, as well as non-parenchymal LSECs and stellate cells act as primary antigen sensing cells. These cells express a range of PRRs (Jenne and Kubes, 2013; Seki and Brenner, 2008; Wu et al., 2010) and variable levels of MHC molecules which are capable of antigen presentation to naïve T cells (Crispe, 2009; Thomson and Knolle, 2010). Under homeostatic conditions this process induces T cell anergy and clonal deletion due to the absence of co-stimulatory molecules and expression of PD-L1 molecules (Bowen et al., 2004; Wuensch et al., 2010). While the liver naturally tends towards tolerance and the prevention of inflammation, it is also poised to respond rapidly to hepatotrophic and systemic pathogens through a variety of innate and adaptive immune cells (**Figure 1-1**).

1.1.3 Hepatic immune repertoire

The tolerogenic environment of the liver is often attributed to the unique repertoire of hepatic leukocytes. The liver is home to several populations of immunoregulatory cells, arrays of cytotoxic innate lymphocytes, as well as conventional T cells and antigen presenting cells. Kupffer cells account for up to 80% of human macrophages; however they are derived from an independent self-renewing pool of liver resident cells, rather than classical myelomonocytic bone marrow derived populations (Gomez Perdiguero et al., 2014; Tacke

and Zimmermann, 2014). These cells constitutively secrete IL-10 in response to LPS, express T cell inhibitory receptors, such as PD-L1, and can induce Treg cell differentiation *in vivo* (Heymann et al., 2015). Similarly, hepatic myeloid dendritic cells (DC) are less potent activators of T cells and produce significantly more IL-10 compared to spleen derived myeloid DCs (Bamboat et al., 2009; De Creus et al., 2005; Goddard et al., 2004). Hepatic plasmacytoid DCs also appear phenotypically immature and indeed are not effective T cell activators *ex vivo,* however, activation via growth factors or Toll-like receptor (TLR) agonists induces maturation and effective antigen presentation (Kingham et al., 2007). Hepatic plasmacytoid DCs have also been shown to be capable of IL-10 production and activation of Treg cells (Tokita et al., 2008). The presentation of antigens in the liver biases T cells towards tolerance due to a lack of co-stimulatory molecules and $CD4^+$ T cell help required for efficient T cell differentiation (Bowen et al., 2004; Wuensch et al., 2010). The liver also maintains mechanisms by which it can respond to hepatotrophic infections with an adaptive immune response, demonstrated by the presence of a small but distinct population of pro-inflammatory $CD141^+$ DCs (Kelly et al., 2014).

In addition to populations of antigen presenting cells, components of the adaptive immune system are also present in healthy liver. The liver is particularly enriched in cytotoxic $CD8^+$ T cells, activated T cells, and memory T cells (Norris et al., 1998; Pruvot et al., 1995). Activation of T cells in the liver can result in anergy and deletion, leading to the liver having been described as a 'graveyard' for T cells (Huang et al., 1994; Mehal et al., 1999). However this theory has been reconsidered in recent years, tissue-resident T cells (Trm) have been identified in human liver from virally infected patients and those who have previously cleared viral infection and provide a rapid first line defense against hepatotrophic viruses (Lugli et al., 2016; Pallett et al., 2017; Schenkel and Masopust, 2014).

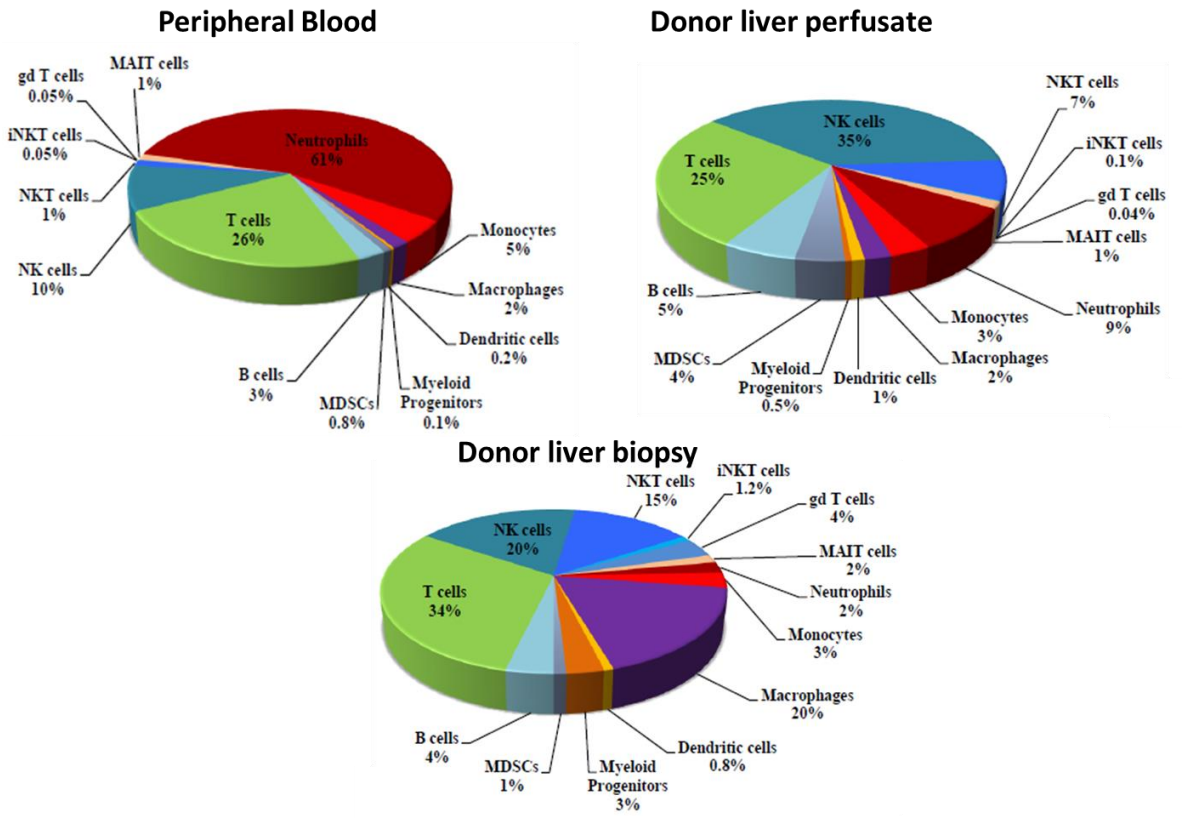

Figure 1- 1 The liver is an organ of predominately innate immunity

The adult human liver is enriched with innate immune cells, including tissue resident macrophages (Kupffer cells), γδ T cells, iNKT cells, and NK cells. Some populations appear resistant to perfusion, as smaller populations of Kupffer cells, γδ T cells and iNKT cells are present in perfusion fluid. NK cells are highly enriched in this perfusion fluid. (Adapted from Fahey et al. unpublished). (NK cell- natural killer cell, NKT cell- natural killer T cell, MAIT cell- mucosal associated invariant T cell, iNKT cell- invariant natural killer T cell, MDSC- myeloid derived suppressor cell).

Moreover, T cells are present in many liver pathologies, where they overcome local tolerance and chronic inflammation occurs. Populations of B cells are also present in the human liver, where they account for up to 8% of the total lymphocyte population (Norris et al., 1998). Specific hepatic B cell subpopulations, such as the innate-like $CD5^+$ B cell population, are further expanded in the liver during hepatotrophic viral infection (Curry et al., 2003; Racanelli et al., 2001).

This tolerogenic environment of healthy liver which is not conducive to T cell mediated immunity is compensated for by a varied repertoire of innate lymphoid cells with potent cytotoxic and trans-activatory abilities. The diverse range of innate lymphocytes in the adult liver includes natural killer (NK) cells, natural killer T (NKT) cells (including populations of CD1d-restricted invariant NKT cells), mucosal-associated invariant T (MAIT) cells, γδ T cells and innate lymphoid cell (ILC) group 1-3 family members (Doherty et al., 1999; Dusseaux et al., 2011; Forkel et al., 2017; Kenna et al., 2004, 2003). Hepatic innate lymphocyte populations are potent cytokine producers and influence both innate and adaptive immune responses in the liver. The repertoire of liver innate lymphocytes is strikingly different between mice and humans. In mice, NKT cells and NK cells make up to 40% and 10% of total liver lymphocytes respectively, while in humans, these percentages are reversed, with NK cells predominating (Gao et al., 2008). iNKT cells are essential in the switch from inflammation to resolution in liver inflammation (Liew et al., 2017; Park et al., 2009). γδ T cells have diverse functions in hepatic inflammation and malignancy, capable of inducing hepatocyte and tumour apoptosis but also limiting inflammation (Hammerich and Tacke, 2014). These functions appear to depend on the predominant class of γδ T cell present (Vδ1-Vδ3). MAIT cells account for a sizable proportion of hepatic T cells (20-50%) (Jo et al., 2014), and though their role in liver immunity is only beginning to become evident, there is increasing evidence that they are an important population in bacterial and viral infection (Kurioka et al., 2016). ILC family members have only recently been described in human liver

with a predominance of ILC2, which produce pro-fibrotic IL-13 in response to liver produced IL-33 and TSLP (Forkel et al., 2017)

1.2 Natural killer (NK) cells

1.2.1 Innate lymphoid cell family

The ILC family is made up of a collection of lymphoid cells lacking antigen specific receptors which derive from a common innate lymphoid cell precursor (CILCP) (Constantinides et al., 2014; Zook and Kee, 2016).The family is divided into three groups based on function and phenotype, closely matching T cell subsets (Tc, T_{h1}, T_{h2}, $T_{h17/22}$) (**Figure 1-2**). Group 1 ILC family members produce T_{h1} type cytokines such as IFN-γ and TNF-α (Zhang et al., 2018). NK cells are group 1 innate lymphoid cells (ILC), important in anti-viral and tumour immunity (Spits and Di Santo, 2011). ILC1 cells are dependent on the transcription factor Tbet for their differentiation. NK cells are differentiated from other ILC1 member by their cytotoxic function and requirement for Eomes and IL-15 (Serafini et al., 2015). ILC2 cells produce a range of T_{h2} like cytokines including IL-4, IL-13 and IL-5. These cells are dependent on the transcription factors GATA3 and RORα, as well as IL-7 for their differentiation (Serafini et al., 2015; Walker and McKenzie, 2013).

Group 3 ILCs are made up of a number of cell types including natural cytotoxicity receptor positive and negative (NCR^+/NCR^-) ILC3 cells and lymphoid tissue inducer cells. These cells rely on the transcription factor RORγt and IL-7 for their differentiation. They are characterised by IL-17 and IL-22 production and are essential for lymphoid organ development and maintenance of intestinal barrier integrity (Montaldo et al., 2015).

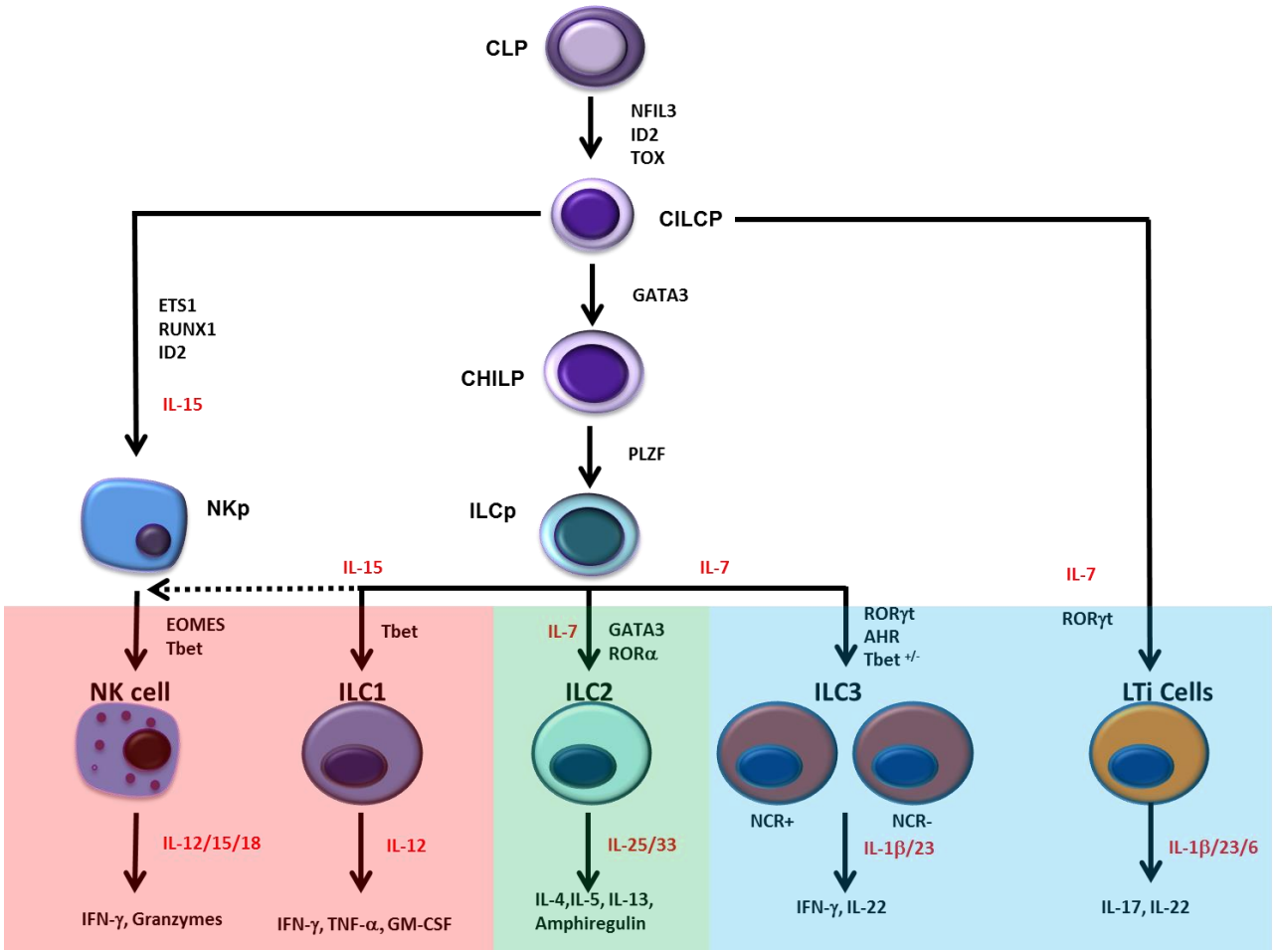

Figure 1- 2 Differentiation of Innate lymphoid cell family

Innate lymphoid family and their progenitors. ILC family members are differentiated by their use of transcription factors (black), essential cytokines (red) and their functions. ILC1 family (red box) is made up of NK cells and non-cytotoxic ILC1 cells. ILC2 (green box) are functionally similar to Th2 cells. ILC3 (blue box) contains three family member NCR^{+} ILC3, NCR^{-} ILC3 and lymphoid tissue inducers (LTi).CLP-common lymphoid precursor, CILCP-common innate lymphoid cell precursor, CHILP-common helper innate lymphoid precursor, ILCp- innate lymphoid cell precursor, NKp- NK cell precursor, NK cell-natural killer cell, ILC-innate lymphoid cell, NCR-natural cytotoxicity receptor, GM-CSF- granulocyte, monocyte colony stimulating factor)

1.2.2 NK cell subsets and functions

NK cells represent 5-15% of peripheral blood lymphocytes (Cooper et al., 2001a) and are found in large numbers in healthy gut, liver, uterus and bone marrow, where several heterogenous populations with diverse functions have been identified (Freud et al., 2017; Lysakova-Devine and O'Farrelly, 2014). Human NK cells are defined phenotypically by the expression of the adhesion molecule CD56 and the absence of CD3. Density of CD56 and CD16 expression defines two distinct sub-populations, $CD56^{bright}$ $CD16^{+/-}$ and $CD56^{dim}$ $CD16^{+}$ NK cells (Cooper et al., 2001a; Farag and Caligiuri, 2006; Lanier et al., 1986). In the blood, $CD56^{dim}$ account for 90% of NK cells, with 10% $CD56^{bright}$. Classically these subsets have been considered functionally distinct, with $CD56^{bright}$ NK cells the primary producers of inflammatory and regulatory cytokines, while $CD56^{dim}$ NK cells produce less cytokine but have greater cytotoxic activity (Cooper et al., 2001a; Maria et al., 2011; Poli et al., 2009). However, it is becoming increasingly clear that the diversity of NK cells is much greater than previously appreciated. Furthermore, the context in which NK cells become activated and the mechanism by which they are activated can lead to drastically different effector functions in both $CD56^{bright}$ and $CD56^{dim}$ NK cells, blurring this functional distinction(De Maria et al., 2011; Eisenhardt et al., 2012; Freud et al., 2017; Jiang et al., 2011; Juelke et al., 2010; Nielsen et al., 2012; Wagner et al., 2017). Following activation, NK cells provide a functional bridge between the innate and adaptive arms of the immune systems by augmenting early adaptive immune responses through the production of IFN-γ and TNF-α. IFN-γ acts as a co-stimulatory signal to antigen specific T cells, enhancing antigen specific proliferation and further IFN-γ production (Cooper et al., 2001a; Poli et al., 2009). However, initial descriptions of NK cells and their functions did not capture the true heterogeneity of NK cell subsets and the variety of tissue specific functions they carry out, which are now being identified (Freud et al., 2017; Horowitz et al., 2013; Lysakova-Devine and O'Farrelly, 2014).

1.2.3 NK cell activation

Unlike T cells, NK cells are capable of target recognition and lysis without prior antigen priming (Caligiuri, 2008; Cooper et al., 2001a; Vivier et al., 2008). NK cells recognize target cells through a complex mechanism of balancing activatory and inhibitory receptors. In health, NK cells are constantly interacting with MHC and MHC-like molecules expressed by all cells via a range of surface receptors. This usually results in an inhibitory signal being sent to the NK cell which prevents activation (**Figure 1-3A**). Activation can occur through the absence of MHC binding to inhibitory receptors (missing self, **Figure 1-3B**) or through the binding of activatory receptors to stress induced molecules (induced self, **Figure 1-3C**), such as MIC-A, MIC-B or ULBP family proteins (Colucci et al., 2002; Kruse et al., 2014). Recognition of missing or altered self is carried out by a range of cytotoxicity receptors, which can transmit inhibitory or activatory signals, including killer cell immunoglobulin-like receptors (KIR), C-type lection like NKG2 receptors, natural cytotoxicity receptors (NCR) and the signalling lymphocytic activation molecule (SLAM) families. Additionally, other receptor families can also regulate NK cell activation including leukocyte immunoglobulin-like receptor (LIR/ILT), killer cell lectin-like receptor G1 (KLRG1) and DNAM-1 (Bottino et al., 2003; Ito et al., 2006; Martinet et al., 2015; Shiroishi et al., 2006). The KIR and NKG2 families regulate NK cell cytolysis through the recognition of MHC class I and MHC class I-like molecules (Borrego et al., 2006; Cooper et al., 2001a; Parham, 2005). NCR ligands have been less well characterised by comparison and appear to recognise a number of pathogen associated molecules (hemagglutinin, mycolic acids and Duffy binding-like-1α peptides) as well as cellular targets such as heparin sulphates, BAT-3 and B7-H6 (Kruse et al., 2014). In addition NCRs can recognise growth factors in the tumour microenvironment and glycoproteins such a complement factor P (Barrow et al., 2017; Narni-Mancinelli et al., 2017). Unlike other NK cell receptors the SLAM receptors work through homotypic recognition, with the exception of 2B4 which recognises CD48 (Brown et al., 1998; Veillette,

2006). The SLAM receptors contribute to the "missing self" immunosurveillance mechanism and appear to be important in NK cell education (Chen et al., 2016; Dong et al., 2009).

Upon activation NK cells degranulate resulting in the release of lysosome contents, including perforin and granzymes. Perforin oligomerization forms a pore-like structure which inserts into the cell membrane through two membrane-penetrating regions (TMH1/2) (Law et al., 2010; Voskoboinik et al., 2015). These molecules are rapidly endocytosed, forming giant endosomes containing perforin and granzymes (Keefe et al., 2005). It is thought that pores form in the endosomes allowing granzymes to pass into the cytosol of target cells and induce apoptosis through a series of mechanisms. Granzyme B has been the most widely studied of these, which cleaves pro-caspases 3/7, BID and translocates to the nucleus to activate DNA fragmentation factor A/B (DFFAB) (Rousalova and Krepela, 2010; Voskoboinik, Whisstock and Trapani, 2015).

Granzyme A mediates apoptosis-like cell death via a different pathway involving disruption of chromatin structural proteins, preventing DNA repair, replication and transcription (SET complex) (Fan et al., 2002; Pinkoski and Green, 2003). Granzyme K has been less well described but induces a caspase-independent apoptosis characterised by mitochondrial dysfunction (MacDonald et al., 1999). It causes caspase-independent nuclear fragmentation and nuclear condensation and single-stranded DNA breaks by targeting the SET complex (T Zhao et al., 2007). Similar to granzyme B, granzyme K can target BID for cleavage and activate mitochondrial mediated cytochrome C release (Tongbiao Zhao et al., 2007). Additionally, all human granzymes cleave DNA/RNA-binding protein heterogeneous nuclear ribonucleoprotein K (hnRNP-K), which regulates pre-mRNA processing (van Domselaar et al., 2012).

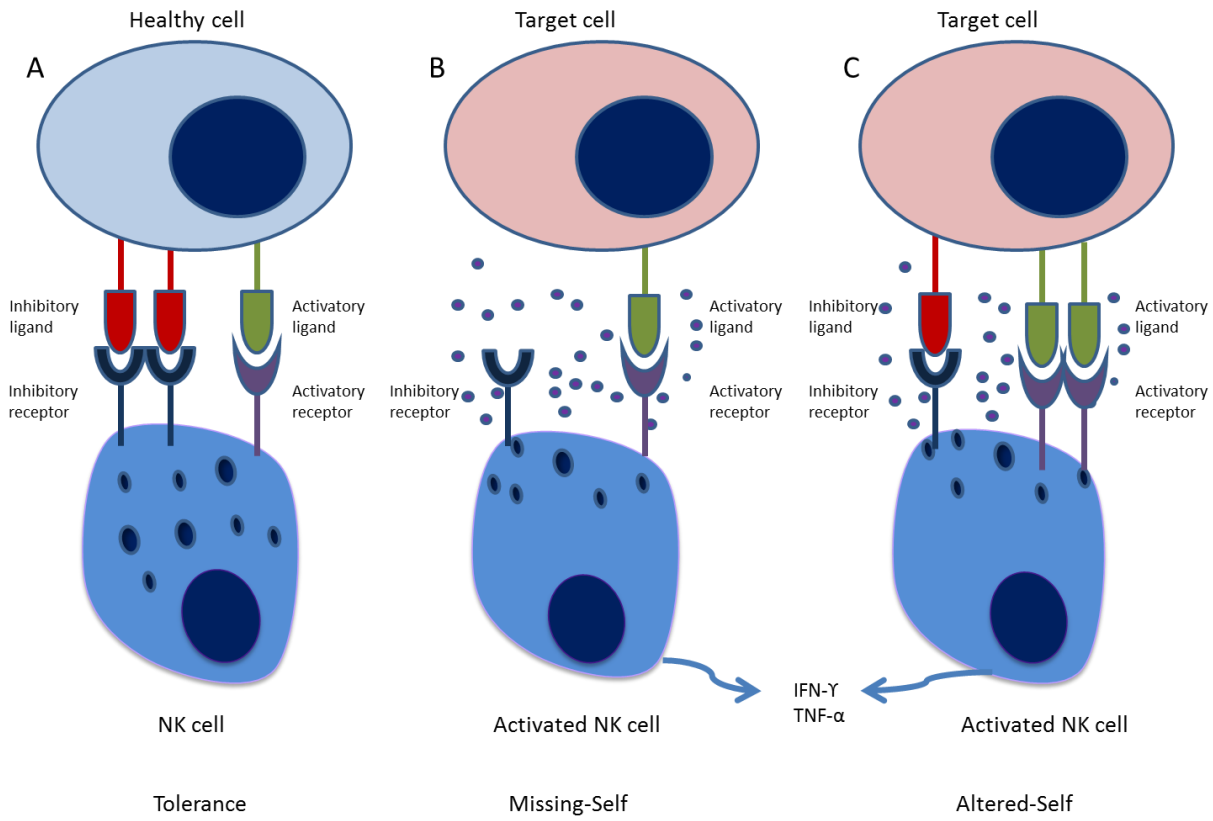

Figure 1- 3 Mechanisms of natural killer cell activation

(A) Tolerance. NK cells are tolerant of healthy cells; the engagement of their inhibitory receptor dampens the signal received from their activatory receptor. **(B) Missing Self**. Virally infected or tumour cells may lose MHC Class I expression. This results in the loss of an inhibitory signal and activation of the NK cell, which releases cytotoxic granules and pro-inflammatory cytokines. **(C) Altered Self.** NK cells may also be activated by "stressed" cells. These cells up regulate activatory ligands, overcoming the inhibitory signal. (Adapted from Harmon et al. 2016 *Am J Transplant*).

Alternatively, NK cells can activate caspase mediated death pathways through binding of TRAIL or FAS to their respective ligands (Elmore, 2007; Smyth et al., 2005). This process leads to recruitment of the FADD complex and cleavage of pro-caspase 8/10. Caspase-8 can then activate intrinsic apoptosis pathway through BID cleavage or extrinsic cell death pathway via activation of caspase 3 and initiation of apoptosis (de Miguel et al., 2016).

At the same time, pro-inflammatory cytokines are produced, such as IFN-γ and TNF-α, which have anti-viral, immune activating functions and can induce apoptosis in tumour cells (Arase et al., 1996; Cooper et al., 2001b; Vivier et al., 2008). Cytokine production is dependent on a metabolic switch, shifting the cell toward a more glycolytic phenotype (Keating et al., 2016).

1.2.4 NK cell cytotoxicity receptors

NK cells activation is regulated through a variety of receptors which can transmit inhibitory and activatory signals. Loss of inhibitory signalling can result in activation through "missing self". Alternatively, increased activatory signalling can overcome inhibitory signal and allow the recognition of "altered self". Structurally, NK cell receptors can be broadly be divided into c-type lectin like receptors and immunoglobulin-like receptors. The C-type lectin-like NKG2 receptors form heterodimers with CD94 which recognize the non-classical MHC molecule, HLA-E (Pegram et al., 2011). Depending on the NKG2 molecule paired to CD94, an activatory or inhibitory receptor will be formed. The inhibitory signal produced by NKG2A binding overrides activatory NKG2C signalling (Beziat et al., 2011).

NKG2D is an activatory receptor which recognizes stress induced ligands, such as MIC-A, and –B, and ULBP family members (induced self) (Bauer et al., 1999; Pegram et al., 2011). Expression of these stress molecules occurs during viral infection and malignancy (Lanier, 2015). While it is included in the natural-killer group 2 receptor family, it is biologically quite distinct from NKG2A/C. NKG2D forms a heterodimer and lacks an intracellular signalling

motif, instead associating with DAP10 for signal transduction (Nausch and Cerwenka, 2008; Raulet, 2003)

The immunoglobulin-like families include KIRs, NCRs, and SLAM receptors. The killer cell KIR family is made up of inhibitory and activating receptors that recognize HLA-A, -B and –C and share highly homologous extracellular domains but differ in their cytoplasmic signalling motifs (Vilches and Parham, 2002). In humans, KIRs are coded for by 14 highly polymorphic genes, which segregate independently of HLA but are not necessarily found in every individual (Middleton and Gonzelez, 2010). As a result, there is variation in the number and type of KIR genes inherited. KIRs are distributed clonally among NK cells, resulting in highly heterogeneous populations. Normally, NK cell cytolysis is suppressed by the binding of inhibitory KIRs to self HLA. In virally infected and tumour cells, HLA expression is down regulated and the inhibitory signal to NK cells is lost, resulting in NK cell cytolysis (missing self). The mechanism of activating KIRs is poorly understood; they appear highly homologous to inhibitory KIRs but show lower ligand avidity (Vilches and Parham, 2002). Hepatic NK cells have lower levels of KIR expression, which are further decreased in hepatic malignancy (Burt et al., 2009; Hydes et al., 2018, 2015; Norris et al., 2003).

The natural cytotoxicity receptor (NCR) family is made up of three receptors containing immunoglobulin-like domains; NKp30, NKp44 and NKp46. Activation of NK cells through NCRs have been associated with tumour cells, and viral and bacterial infection (Esin et al., 2013; Mandelboim et al., 2001; Mavoungou et al., 2007). NK cells have significant interactions with other immune cells, such as DCs (Cooper et al., 2004; Simhadri et al., 2008). Immature DCs express the NKp30 ligand BAT-3, which induces DC cell death upon engagement with NKp30 (Simhadri et al., 2008). Platelet-derived growth factor-DD (PDGF-DD) has recently been described as a ligand for NKp44 and is essential for control of tumour spread in a B16 melanoma model (Barrow et al., 2017). PDGF has been implicated in the

progression of several human gastrointestinal cancers and contributes to epithelial-mesenchymal transition (EMT) (Heldin, 2013). Furthermore, activation of NK cells through NKp46 has been shown to be essential for maintaining tissue structure in the setting of malignancy. Loss of NKp46 or IFN-γ has been shown to correlate with extracellular matrix remodelling, aggressive tumour growth and metastases (Glasner et al., 2018). Furthermore NKp46 has been shown to interact with glycoproteins such as complement factor P (Narni-Mancinelli et al., 2017).

The SLAM receptor family is made up of nine members, all of which are members of the CD2 superfamily (Dragovich and Mor, 2018). NK cells express three member sof the SLAM family; 2B4, NK-, T- and B-cell antigen (NTB) and CD2-like receptor activating cytotoxic cells (CRACC) (Cannons et al., 2011). 2B4 has been shown to act primarily as a co-receptor on human NK cells and it's activatory effects require ligation of another cytoxicity receptor (Bryceson et al., 2006; Sivori et al., 2000). Similarly, NTB and CRACC appear to work in synergy with activation of other receptors such as NKG2D and NKp46 (Bottino et al., 2001; Cruz-Munoz et al., 2009). The majority of SLAM receptors interact with self-ligands in homotypic interaction, with the notable exception of 2B4 which recognises CD48 (Brown et al., 1998; Dong et al., 2009). SLAM receptors associate with SH-2 domain of SAP adaptor molecules to enable signal transduction (Sayos et al., 1998). SLAM receptors and SAP signalling are essential for the control of EBV, as demonstrated by uncontrolled viral infection of patients with X-linked lymphoproliferative disease, which is characterised by inadequate cytotoxicity in T and NK cells (Latour and Veillette, 2003; Sayos et al., 1998; Veillette, 2006). Furthermore, SLAM receptor interactions play an important role in NK cell education, critical for the acquisition of cytotoxic effector function (Chen et al., 2016; He and Tian, 2017).

1.2.5 NK cell mediated immunity

NK cells were originally identified in mice and characterised by their ability to spontaneously lyse tumour cells (Herberman et al., 1975a, 1975b, Kiessling et al., 1975a, 1975b). Nearly a decade later, the underlying mechanisms by which NK cells recognise their targets was discovered (Kärre et al., 1985; Ljunggren and Kärre, 1990). The "missing self" mechanism was proposed, whereby NK cells recognise malignant or virally infected cells due to the loss of MHC Class I molecules (**Figure 1-2B**). However, the "missing-self" pathway did not explain why some MHC-sufficient tumour cells were also targeted for lysis. The discovery of "stress induced" molecules which acted as ligands for NKG2D, such as MIC-A and ULBPs, led to the characterisation of the altered-self pathway of NK cell recognition (Bauer et al., 1999; Diefenbach et al., 2000). Since the original characterisation of NK cells as anti-tumour lymphocytes, they have been implicated in protection against several malignancies in both human and mouse (Stojanovic and Cerwenka, 2011; Zamai et al., 2007).

In addition to their anti-tumour roles, NK cells are essential for the control of viral infection. While congenital deficiencies of NK cells in humans are rare (and life limiting), mice lacking NK cells have demonstrated significant pathology and viral persistence (Bancroft et al., 1981; Biron et al., 1989; Bukowski et al., 1983; Orange, 2002; Shellam et al., 1981). Much of the early work on the protective role of NK cells in viral infection focused on human and murine CMV and herpes viruses (Arase et al., 2002; Cosman et al., 2001; Uhrberg et al., 1997), over the years, NK cells have been characterised in a plethora of viral infections, such as HIV, HCV and HBV (Björkström et al., 2010; Funke et al., 2011; Golden-Mason et al., 2008; Protzer et al., 2012). NK cells are rapidly activated by virally infected cells and act as an early source of IFN-γ which then drives an antigen specific T cell response and in some cases viral clearance (Pollmann, Rölle & Hofmann, 2017).

1.2.6 Immune regulation

In recent years, NK cells have been highlighted as potent immunoregulatory cells, involved in limiting inflammation. Several studies demonstrate that NK cells can regulate T-cell responses under various conditions (Cerboni et al., 2007; Peppa et al., 2013; Su et al., 2001; Waggoner et al., 2012). For example, alloantigen activated T cells express stress induced NKG2D ligands MIC-A and ULBP proteins via an ATM/ATR-dependent mechanism and become susceptible to autologous NK cell lysis *in vitro* (Cerboni et al., 2007). A significant body of work has emerged demonstrating that NK cells play an important role in regulating virus specific T cells. In chronic HBV infection, antiviral T cell responses are profoundly diminished. NK cells contribute to this in a contact dependent fashion inducing caspase-8-mediated apoptosis of TRAIL-R2 expressing T cells (Peppa et al., 2013). The immunoregulatory effects of NK cells are not limited to T cells however; additional studies demonstrate that antigen-presenting cells are vulnerable to deletion by activated NK cells consequently diminishing virus-specific $CD4^+$ and $CD8^+$ T cell responses. NK cells have been shown to lyse immature dendritic cells at sites of inflammation (Cooper et al., 2004). During murine lymphocytic choriomeningitis virus (LCMV) infection (a model resembling chronic HCV infection), NK cells were essential for controlling T cell mediated pathology, targeting $CD4^+$ T cells for cytolysis, thus indirectly inhibiting $CD8^+$ T cell activity (Waggoner et al., 2012).

These data have led some to hypothesise that NK cells could play an essential role in solid organ transplantation, especially liver transplantation (Adenugba, 2017; Harmon et al., 2016; Villard, 2011). Based on these data and other studies of viral infection, one might assume that following liver transplantation, both donor and recipient NK cells may target graft specific recipient T cells and promote a tolerogenic environment for the new liver. Due to the inherent limitations of liver biopsies, studies of intrahepatic NK cells in this setting have been limited. Interestingly, in non-HCV infected liver transplant recipients who go on to develop

immunosuppression-free tolerance, NK cell numbers in the peripheral blood and NK related gene transcripts were predictive of positive outcome (Benitez et al., 2013; García de la Garza et al., 2015; Martinez-llordella et al., 2007). While not conclusive these data provide tantalising evidence of an important role for liver NK cells in mediating tolerance following liver transplantation. Direct manipulation of the graft to prime donor liver NK cells (Reddy et al., 2008) or using viral vaccines to prime recipient T cells (for donor NK lysis) prior to implantation may provide novel mechanisms to promote operational tolerance. However, identifying the particular subset of NK cell involved in this protection will be essential to the efficacy of any future treatments.

1.3 Diversity of natural killer cells

Classically NK cells have been defined as a non-T, non-B cell lymphocyte that demonstrates rapid production of IFN-γ following stimulation and mediate cellular cytotoxicity (Freud et al., 2017; Vivier et al., 2008). However, it has become increasingly evident that the NK cell lineage is remarkably diverse in terms of developmental, phenotypic, and functional profiles. Even in peripheral blood, mass cytometry and genetic studies have revealed a previously unappreciated heterogeneity in NK cell phenotype (Horowitz et al., 2013). The recognition of tissue resident and memory NK cells has challenged many assumptions about how and where NK cells develop and function. In recent years, tissue resident NK cells have been identified in organs such as, liver (Aw Yeang et al., 2017a; Cuff et al., 2016; Harmon et al., 2016; Hudspeth et al., 2015; Hydes et al., 2017; Marquardt et al., 2015; Stegmann et al., 2016), gut (Takayama et al., 2010) lungs (Marquardt et al., 2017; Robinson et al., 1984), uterus (Koopman et al., 2003; Manaster et al., 2008; Moffett-King, 2002) as well as lymphoid organs such as lymph nodes (Fehniger et al., 2003; Lugthart et al., 2016), tonsils (Ferlazzo et al., 2004) and the thymus (Vosshenrich et al., 2006) (**Figure 1-4**). Many of these tissue resident populations have tissue specific functions and features. Uterine NK cells have been the most completely characterised because of their involvement in embryo implantation and

pregnancy. Uterine NK cells are essential for spiral artery formation and provide a source of growth factors during implantation (Fu et al., 2017; Manaster et al., 2008; Robson et al., 2012).The origin of these tissue resident populations remains contentious. Whether tissue resident NK cells develop through classical bone marrow differentiation or mature locally from tissue progenitors remains unclear. Haematopoietic progenitors have been identified in a number of organs including; lymph nodes, gut, liver, and uterus (Chiossone et al., 2014; Crosbie et al., 1999; Freud et al., 2005; Glover et al., 2018; Lynch et al., 2006; Moroso et al., 2011).

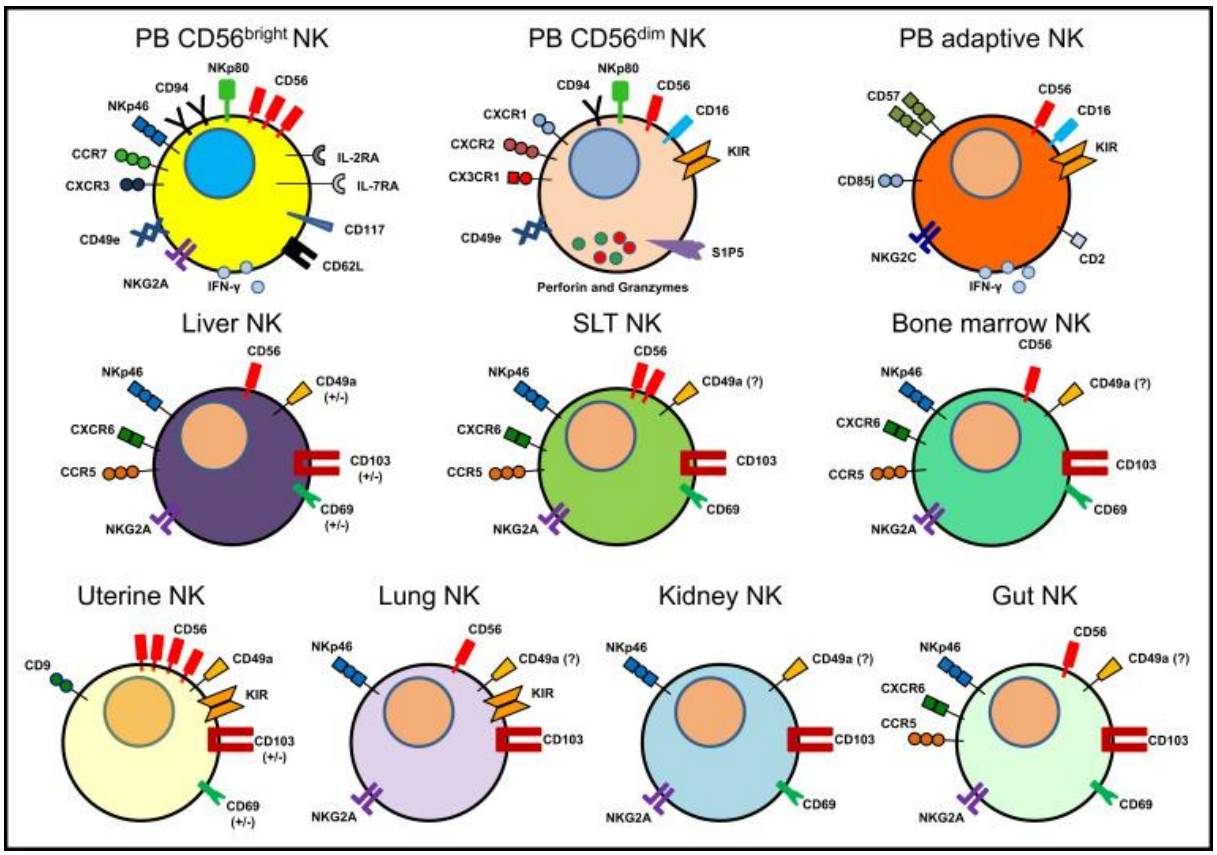

Figure 1- 4 Diversity of human natural killer cells

NK cells reside in a number of tissues, as well as the peripheral blood (PB). The phenotype of NK cells from PB, liver, secondary lymphoid tissue (SLT), bone marrow, uterus, lung, kidney and gut are shown above. (From Freud et al. (2017) Immunity, 47 (5), pp. 820-833.)

1.4 Hepatic NK cells

1.4.1 Immunophenotype

Just a year after the identification of NK cells as a bona fide immune cell lineage, Wisse and colleagues identified "Pit" cells in rat liver sinusoids, so called because of their characteristic small dense granules which resemble fruit pips or pits (Bouwens and Wisse, 1992; Wisse et al., 1976). Initially thought to play a role in endocrine production (their granules resemble endocrine granules), they were later described as large granular lymphocytes with cytotoxicity equivalent to lymphokine-activated killer cells (LAK) (Peng et al., 2016; Wisse et al., 1997). These NK cells constitute the largest proportion of lymphoid cells in the human liver, comprising 30-50% of hepatic lymphocytes (Hata et al., 1990; Moroso et al., 2010; Norris et al., 1998). Over 45% of the hepatic NK cells are $CD56^{bright}$ however the ratio of $CD56^{bright}$:$CD56^{dim}$ is highly variable between individuals (Harmon et al., 2016; Hudspeth et al., 2015; Moroso et al., 2010; Stegmann et al., 2016). Phenotypically, hepatic NK cells have an activated phenotype with increased expression of CD69, a marker of tissue residency (Mackay et al., 2015; Moroso et al., 2010; Shiow et al., 2006), and the natural cytotoxicity receptor NKp44. However, a higher proportion of hepatic NK cells express the inhibitory receptor $NKG2A^{+}$ (**Figure 1-5**), suggesting a tension between activation and tolerance of HLA expressing cells. They are functionally distinct from their peripheral blood counterparts, as they contain significantly more preformed granzymes and perforins and are capable of twice the level of cytotoxicity (Moroso et al., 2010).

There is accumulating evidence that the adult liver supports lymphopoeisis, and at least a proportion of hepatic NK cells may differentiate *in situ* from haematopoietic progenitors in the liver (Crosbie et al., 1999; Moroso et al., 2011; Shi et al., 2013; Wang et al., 2012). NK cell precursors, isolated from adult liver, have been differentiated into functionally mature $CD56^{bright}$ and $CD56^{dim}$ NK cells, *in vitro* (Moroso et al., 2011). In addition, donor NK cells have been identified within liver grafts up to two years after transplant (Cuff et al., 2016; Shi

et al., 2013). Whether these cells are evidence of long lived "memory-like" NK cells or locally differentiated remains unclear. More recently, a significant population of $CD49a^+$ $Eomes^-$ NK cells has been identified in the adult human liver (Marquardt et al., 2015; Martrus et al., 2017). Due to the low prevalence of these cells in human liver, it has led us and others to hypothesise that other populations of tissue-resident NK cells reside in the liver.

1.4.2 Liver resident natural killer cells

Recent murine studies have characterised a repertoire of hepatic innate lymphoid cells. While murine studies remain somewhat unclear about the presence of bona fide liver resident NK cells there is evidence of liver resident ILC populations. Parabiosis experiments identified a population of NK cells which do not recirculate and remain resident within the liver. These NK cells have an unconventional phenotype, lacking the essential NK cell transcription factor Eomes and possessing an immature $TRAIL^+$ $DX5^-$ phenotype (Daussy et al., 2014; Gordon et al., 2012). These cells are liver resident, express the chemokine receptor CXCR6, appear to have undergone clonal expansion and show memory-like enhanced function when challenged with viral or allergen stimuli (Daussy et al., 2014; Gordon et al., 2012; Paust et al., 2011). These cells rely on T-bet expression and deletion of this gene leads to a profound loss of liver resident NK cells (Cuff and Male, 2017; Daussy et al., 2014). It was proposed that these represented an immature progenitor which could differentiate into $TRAIL^-$ $DX5^+$ mature NK cells. However, the bone marrow contains only low levels of these cells and they do not differentiate further after adoptive transfer (Peng et al., 2013).

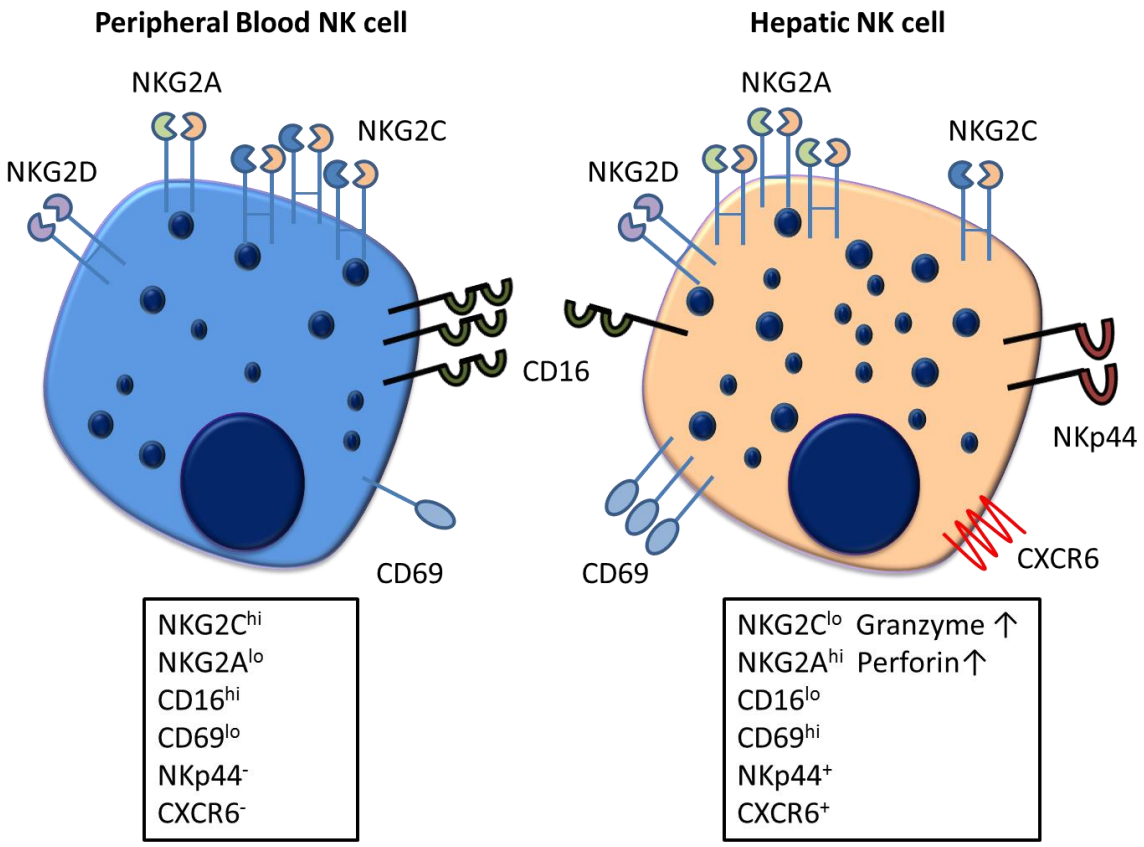

Figure 1- 5 Phenotypic differences between hepatic and peripheral blood natural killer cells

Hepatic NK cells show significant phenotypical differences compared to peripheral blood NK cells. The liver is enriched with $CD56^{bright}$ $CD16^{-}$ NK cells. These cells appear immature with higher expression of the inhibitory receptor NKG2A. However they have an activated phenotype, expressing higher levels of CD69 and NKp44. Hepatic NK cells produce significantly more granzymes and perforins, which correlate with their increased cytotoxicity. Sub-populations of hepatic NK cells express CXCR6 and TRAIL. This is thought to mark a liver resident population which does not recirculate. (Adapted from Harmon et al. 2016 *Am J Transplant*)

While these cells were initially thought to represent a specialised subset of NK cells, more recent studies have highlighted some key differences between liver resident "NK" cells and conventional NK cells. Despite expressing NCRs and requiring IL-15 for survival and differentiation, these liver resident NK cells appear to originate from a distinct $PLZF^+$ innate lymphoid precursor. Fate mapping of the progeny of these cells excluded conventional NK cells but included substantial numbers of liver resident NK-like cells (Constantinides et al., 2014). Additionally, liver resident "NK" cells express high levels of CD49a, CXCR6 and CD69, markers not normally seen on NK cells in the peripheral blood (Paust et al., 2011; Peng et al., 2013). It is now thought that these cells are more likely to be an ILC1 cell which closely resembles an NK cell (Marotel et al., 2016).

Functionally, these ILC1 cells produce significant amounts of IFN-γ and TNF-α, but also GM-CSF (Daussy et al., 2014; Sojka et al., 2014a). They degranulate less efficiently than conventional NK cells but express higher levels of TRAIL which can induce caspase mediated cell death (Takeda et al., 2005). A human counterpart to these cells has recently been identified and at the time was considered a NK cell subset. This $Eomes^-$ $CD49a^+$ subset represented a small proportion of liver NK cells (0.1-12%). Similar to murine liver resident ILC1 cells, these human cells degranulate poorly and produce significantly more cytokines, such as IFN-γ, TNF-α and GM-CSF (Marquardt et al., 2015; Martrus et al., 2017). It has been theorised that the hepatic microenvironment represses the expression of Eomes, in contrast to the bone marrow where T-bet is repressed and conventional NK cells are produced. While this theory is gaining acceptance in the murine setting, the challenge of replicating the hepatic environment and studying its effect on both conventional NK cells and liver resident NK cells has not been satisfactorily addressed. We propose to approach this question using liver conditioned media, a rich source of tissue derived cytokines and growth factors, which mimics the natural liver microenvironment.

More recently, a series of human studies have identified a bona fide NK cell subset which appears to reside within in the liver sinusoid and does not re-enter circulation (Aw Yeang et al., 2017; Cuff et al., 2016; Harmon et al., 2016; Hudspeth et al., 2015; Hydes et al., 2018; Stegmann et al., 2016). This population will be discussed in detail in the following chapters.

1.4.3 Functions of hepatic NK cells

Classically, the function of NK cells was to protect against viral infection and malignancy, linking the innate and adaptive immune systems. This is certainly true of hepatic NK cells as well. The liver acts as a filter through which the draining blood supply of the gut passes. Due to the tolerogenic nature of the liver, pathogens may escape detection or fail to illicit an appropriate response through the phagocytosis-antigen presentation pathway (Robinson, Harmon and O'Farrelly, 2016). Therefore it is not surprising that the liver is populated by large populations of cytotoxic innate lymphocytes, such as NK cells. Without the need for antigen priming, NK cells can quickly and efficiently eliminate virally infected or tumour cells passing through the liver (Smyth et al., 2005). In addition, the liver is also subjected to constant exposure to toxins and toxic by-products of metabolism.

It is surprising then that the incidence of *de novo* hepatic malignancy, in the absence of chronic disease, is remarkably rare. While this process has never been characterised, and may be uncharacterisable, we hypothesise that the innate immune cells of the liver remove dysplastic cells before they advance to the malignant stage.

In recent times, the diversity of NK cell functions has been expanded. We now know that NK cells residing in different tissues are phenotypically and functionally distinct (Björkström et al., 2016; Freud et al., 2017; Lysakova-Devine and O'Farrelly, 2014). These functions go beyond the role of protection against pathogens and range from vascular tissue remodelling (Robson et al., 2012), metabolic regulation (Lynch et al., 2009) and immunoregulation (Peppa et al., 2013). In the liver, NK cells play a pivotal role in the regulation of fibrosis and

maintenance of tissue homeostasis. During acute liver injury hepatic stellate cells (HSCs) become activated by cytokines, such as TNF-α, IL-6, platelet-derived growth factor (PDGF), and TGF-β (Senoo, 2004). This leads to activation and proliferation of HSCs and their differentiation into myofibroblasts, which are potent producers of extra-cellular matrix components, including α-smooth muscle actin and type I collagen (Hellerbrand et al., 1999). This trans-differentiation leads to an alteration in the expression of activating and inhibitory receptor ligands, such that they become targets for deletion by NK cells via TRAIL-, FasL-, and NKG2D-dependent mechanisms (Gao, 2010; Gao and Radaeva, 2013; Glässner et al., 2012; Radaeva et al., 2006; Tosello-Trampont et al., 2017, 2016). This function has been attributed to a population of $CXCR3^{+}$ $CD56^{bright}$ NK cells which become dysfunctional in chronic inflammatory conditions such as HCV (Eisenhardt et al., 2012). This process can become dysregulated and NK cells can contribute to the development of liver pathology.

1.4.4 NK cells in liver disease

Classically the main causes of liver disease have been viral infection, autoimmunity and malignancy. Between 1993-2003, these diseases accounted for 90% of liver transplantations in Ireland. However, in recent years there has been a surge in life-style associated diseases such as alcoholic liver disease (ALD), and obesity related non-alcoholic fatty liver disease (NAFLD) and non-alcoholic steatohepatitis (NASH). These are progressive diseases which often advance to cirrhosis and malignancy.

With the advent of direct acting anti-viral drugs (DAAs) for the treatment of HCV and vaccination against HBV, the burden of diseases caused by infection look set to drop in coming years. While significant research has been carried out into the role of NK cells in these diseases, in an era where disease eradication is possible in up to 95% of patients, a significant shift in research focus will be required in coming years. Harnessing innate resistance to produce novel vaccines is of particular interest (Pashine et al., 2005).

Hepatic autoimmune disease encompasses three major disorders (with additional overlapping syndromes); autoimmune hepatitis (AIH), primary sclerosing cholangitis (PSC) and primary biliary cirrhosis (PBC). While these disorders are predominantly mediated by autoreactive T cells, NK cells contribute to cellular damage, exacerbating tissue disruption and inflammation (Karlsen et al., 2007; Takeda et al., 2008; Wiencke, 2001). However, it is unclear whether this damage is caused by liver resident or NK cells recruited to the site of inflammation from the periphery.

Fatty liver disease now effects up to 30% of the world's population and is climbing rapidly (Lazo et al., 2013; Younossi et al., 2017, 2016). The pathogenesis of this condition is relatively unclear. It has become clear that high fat diets have profound effects, not only on metabolic activities, but also the immune system as well. Mice placed on high fat diets have significantly reduced NK cell cytotoxicity and in humans NK cells are depleted from the peripheral blood of obese patients and overweight children (Lamas, Martínez, & Marti, 2004; O'Shea et al., 2010; Tobin et al., 2017). NK cells have been linked to inflammation in adipose tissue and some of the metabolic changes associated with obesity (Theurich et al., 2017; Wensveen et al., 2015). While NK cells appear to contribute to the pro-inflammatory environment of the obese liver, targeting hepatocytes and cholangiocytes for cell death (Feldstein et al., 2003), this is balanced by the anti-fibrotic effects of hepatic NK cells (Radaeva et al., 2006; Tosello-Trampont et al., 2017, 2016). These conflicting roles are seen in many liver diseases and may represent the functional diversity of NK cells which has not yet been fully elucidated.

All of these conditions, if left untreated, advance to cirrhosis and eventually malignancy. This process appears to have a profound effect on hepatic immunity and results in a breakdown of tumour surveillance.

1.5 Hepatic malignancy

Primary cancer of the liver can be divided into two categories, malignancy of the hepatocyte (hepatocellular carcinoma (HCC)) and malignancy of the biliary system (cholangiocarcinoma). HCC is the fifth most common cancer worldwide, with the majority of cases (85%) reported in developing countries (Ferlay et al., 2015; McGlynn et al., 2015). HCC is most common in HBV endemic countries in Asia, such as China and Mongolia. HCC generally occurs after decades of chronic hepatic inflammation, progressing from fibrosis to cirrhosis and eventually tumour development. Despite the livers constant exposure to harmful toxins, dietary and gut antigens, HCC in the absence of a chronic inflammatory disease is rare. HCC most commonly develops on a background of chronic viral infection, such as HCV and HBV (El-Serag, 2012; Waller et al., 2015). In western countries, HCC is associated with HCV, chronic alcohol consumption and autoimmunity (McGlynn et al., 2015). While the development of direct acting antiviral (DAAs) will reduce the number of patients progressing to HCC, this reduction is in stark contrast to the increase in the number of patients with non-viral inflammatory diseases progressing to HCC in the developed world. These include autoimmune diseases (AIH, PSC and PBC), obesity related hepatic disease (NASH, NAFLD) and alcohol related cirrhosis (ALD). Interestingly, in all of these conditions tumours only develop after years of tissue damage and it appears hepatic immunity is maintained during the progression to advanced liver disease.

The role of natural killer cells in HCC is complicated by the variability in the underlying disease and its effect on NK cells functions. In HCV, chronic activation and inflammation leads to NK cell dysfunction and loss of immunosurveillance (Golden-Mason and Rosen, 2013; Kawarabayashi, 2000; Lunemann et al., 2014). NK cells have both anti-viral functions in HBV but also contribute to tissue damage and chronic inflammation (Maini and Peppa, 2013). Chronic alcohol consumption can impair NK cell cytotoxicity through suppression of TRAIL and NKG2D expression while also inhibiting IFN-γ production (Il-Jeong et al., 2008).

The use of liver NK cells as an immunotherapy in HCC has been trialled in several studies with some success. Donor liver NK cells are isolated at the time of transplantation and infused to patients who suffer a relapse of HCC after transplant (Bahjat et al., 2007; Nishida et al., 2013; Ohira et al., 2012)

1.5.1 Liver metastasis

Considering the extensive repertoire of anti-tumour cells in the liver and the significant pathology required for the development of HCC, it is surprising that the liver is a common site of tumour metastasis, second only to lymph nodes (Disibio and French, 2008). Metastatic tumours arise in a distant site of the body, evade local immune surveillance, and extravasate into the peripheral blood or lymph system. These cells are then deposited in capillary beds where their movement is arrested due the small size and low blood pressure of these blood vessels. Here, the tumour cells extravasate into the surrounding tissue, proliferate and form new blood vessels through angiogenesis (Chambers et al., 2002). The anatomy of the liver makes it an ideal site for this process to occur. The network of narrow liver sinusoids and low blood pressure from the portal vein blood supply provide ample opportunity for tumours cells to enter the liver parenchyma.

Colorectal cancer (CRC) is the third most common cancer worldwide, with approximately 1.3 million new cases per year (Ferlay et al., 2015). In Ireland, the rate of CRC has changed little in the last 20 years (**Figure 1-6A**). Up to 50% of CRC patients will go on to develop a metastatic tumour in the liver (Hugen et al., 2014). Up to 20% of patients will present with a stage IV metastatic tumour at diagnosis (**Figure 1-6B**). If left untreated, the average survival is between 5-20 months (Arnaud et al., 1984; Simmonds, 2000). The only curative treatment is surgical removal of the tumour, usually in combination with chemotherapy or monoclonal antibody therapy (anti-VEGF) (Misiakos, 2011). Unfortunately, only 20-25% of patients with liver metastases are eligible for surgical resection. Of these, 60-70% will develop a recurrent liver tumour or metastasis of another organ (Tomlinson et al., 2007). 5 year survival in stage

IV patients is 13.4% in Ireland (**Figure 1-6C**) which is in line with international standards (Nathan et al., 2010). The overall mortality of CRC is decreasing (**Figure 1-6D**); in part due to screening programmes and the development of new therapies. Immunotherapies have reshaped the cancer landscape, revolutionising the treatment of malignancy (Pardoll, 2012; Sagiv-Barfi et al., 2018). Checkpoint inhibitor therapies have recently been rolled out in CRC trials; while many patients benefit from these therapies (especially microsatellite unstable tumours) the prognosis for advanced metastatic tumours remains poor (Becht et al., 2016; Jacobs et al., 2015; Markman and Shiao, 2015). How these tumours evade the hepatic immune repertoire, dominated by NK cells, remain unclear and may represent a novel treatment target.

1.5.2 NK cells and tumour immunity

Originally characterised by their ability to spontaneously lyse tumour cells, NK cells have been implicated in the response to a range of tumour cells in both humans and mice (Gorelik and Herberman, 1986; Kiessling et al., 1975b; Riccardi et al., 1980). These studies showed that depletion of NK cells led to enhanced tumour growth, widespread metastases and adoptive transfer of NK cells restored resistance to tumour dissemination. This data was supported by observations in patients with metastatic disease, who had functional abnormalities in their peripheral blood NK cells, as well as liver NK cells (Hata et al., 1991; Krasnova et al., 2015; López-Soto et al., 2017; Whiteside and Herberman, 1994). In addition, longitudinal studies have correlated low peripheral blood NK cell cytotoxicity with an increased risk of cancer development (Imai et al., 2000; Jobin et al., 2017). NK cells have been shown to be particularly adept at preventing tumour metastases (Brodbeck et al., 2014; López-Soto et al., 2017).

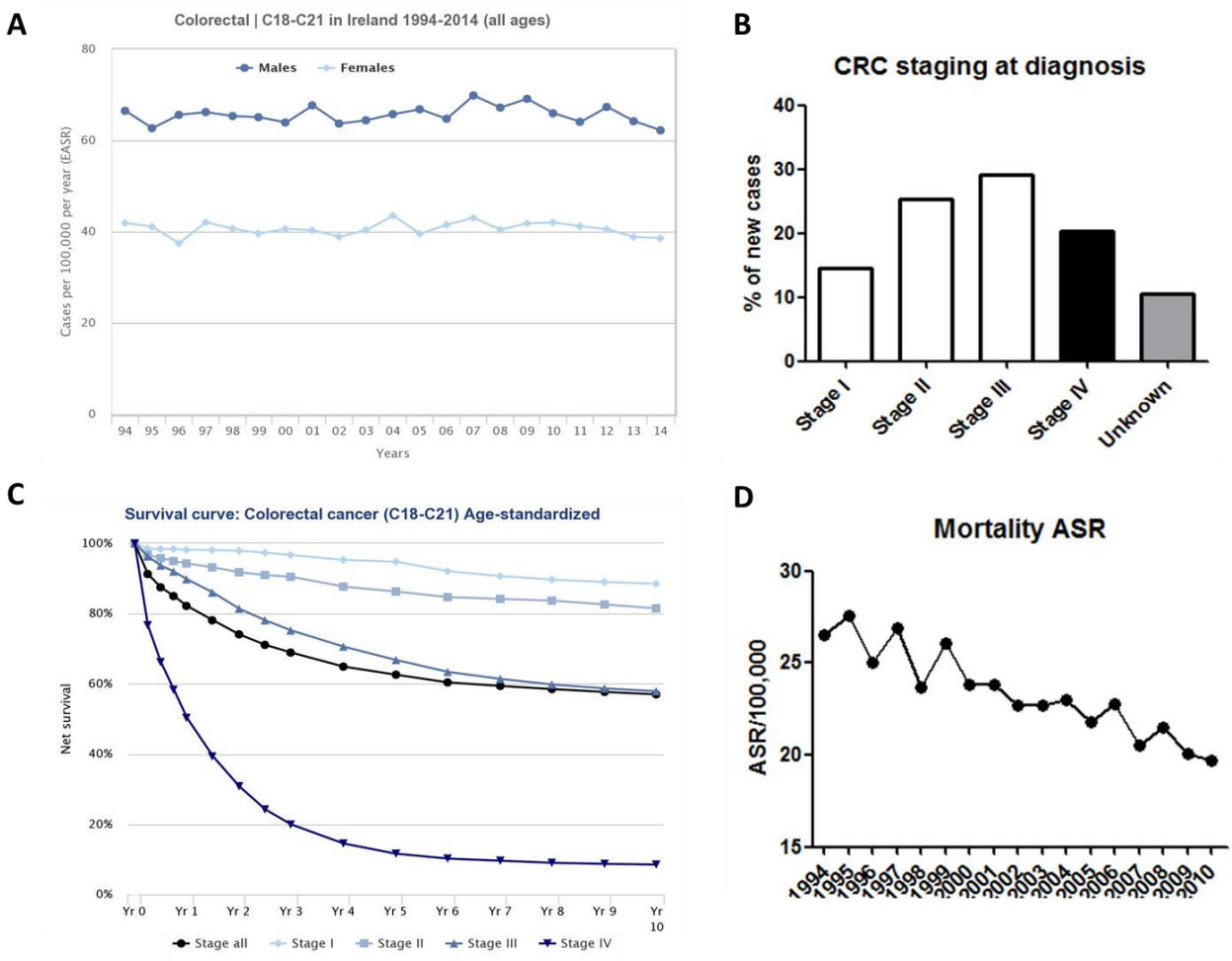

Figure 1- 6 Colorectal cancer incidence and mortality statistics

(A) Age standardised incidence of colorectal cancer in males (dark blue) and females (light blue). **(B)** Percentage of new colorectal cancer diagnoses in Stages I-IV. **(C)** 10-year survival curve for patients with colorectal cancer based on stage of disease (I-IV). **(D)** Age standardised mortality rate for colorectal cancer (1994-2010). Source: National Cancer Registry Ireland.

These studies suggested that NK cell based therapies might be an attractive proposition and many clinical trials were carried out during the 1980s and 1990s, using IL-2 treatment to boost NK cell activity or *ex vivo* IL-2 treated autologous NK cells as immunotherapies for renal cell carcinoma and metastatic melanoma (Atkins et al., 1999; Grimm et al., 1982). The efficacy of NK cell based therapies to already established metastases proved disappointing (Barlozzari et al., 1983; Introna and Mantovani, 1983; Stojanovic and Cerwenka, 2011). In addition, long term administration of IL-2 produced significant side effects, such as capillary leak syndrome, hypotension and atrial fibrillation. With the development of checkpoint inhibitors and tumour specific T cell therapies (CAR-T cells), NK cell based therapies have fallen out of favour. It is important to note however that many modern checkpoint inhibitors also enhance NK cell function, as T and NK cells share inhibitory ligands, and clinical studies to date have failed to assess the impact of checkpoint inhibitors on NK cell function (Childs and Carlsten, 2015; Chiossone and Vivier, 2017). In addition, NK cell based cellular therapies have shown promise when used in combination with in situ delivery systems, for examples in the case of primary and metastatic liver tumours (Adotevi et al., 2018; Nishida et al., 2013). Furthermore, CAR-NK cells are an area of increasing interest. Due to their more limited life span (removing the requirement for suicide gene incorporation), failure to illicit cytokine storm side effects and, do not cause graft versus host disease and are characterised by their serial killing nature, providing a more robust anti-tumour response with fewer side effects (Glienke et al., 2015; Klingemann, 2014). However, some obstacles still reaming in the mass production of NK cells due to the requirement for feeder cells for expansion (often malignant cell lines), sufficient T cell depletion, and pre-enrichment during isolation. Selection of specific NK cell subsets also complicated the development of CAR-NK therapies, since some subsets (adaptive NK cells) display superior anti-tumour activity (Oei et al., 2018).

1.5.3 Evasion of hepatic anti-tumour immunity

While many therapies have focused on enhancing the systemic response to tumour cells, targeting the mechanisms by which tumour cells evade immunosurveillance may prove a more fruitful pursuit. Infiltration of tumours by NK cells has been shown to be a positive prognostic marker in several types of carcinoma, including gastrointestinal, lung, renal and liver cancers (Coca et al., 1997; Ishigami et al., 2000; Sznurkowski et al., 2014; Takanami et al., 2001; Villegas et al., 2002). However, in advanced primary tumours and metastatic tumours, the number of tumour infiltrating NK cells is often much lower than surrounding tissue, and in some cases they are functionally dysregulated (Carrega et al., 2008; Esendagli et al., 2008; Sceneay et al., 2012). It is unclear whether absence of NK cells is due to their inability to traffic to the tumour site or a depletion of NK cells at the site, via soluble factors or cell-cell interactions. Primary CRC tumours often have sparse NK cell infiltration (Halama et al., 2011) but peripheral blood NK cell levels and receptor expression are important predictors of disease-free survival after surgery (Rocca et al., 2016).

Tumour cells have developed several strategies to avoid detection by NK cells. Many tumour types upregulate MHC-class I and non-classical MHC molecule (such as HLA-G) expression, leading to increased inhibitory signalling and repressed NK cell activity (Pardoll, 2001; Rouas-Freiss et al., 2005a; Urosevic and Dummer, 2008). While this process would increase antigen presentation and potential recognition by T cells, in the absence of neoantigens (tumour specific antigens produced by genetic mutation) T cell immunity to tumours is limited (Le et al., 2017; Schumacher and Schreiber, 2015). In these settings, NK cells rely on the altered-self pathway to recognise tumour cells. Expression of NK activating ligands, such as MIC-A/B and NKp46 ligands, by tumour cells evolves as the tumour develops and can decline over time as clones expressing these ligands are killed by NK cells (Elboim et al., 2010; Guerra et al., 2008). This is similar to the process by which acquired resistance to checkpoint therapy occurs, as PD-L1 expressing clones die, negative clones are allowed to

expand and replace susceptible cells (Riaz et al., 2017; Sharma et al., 2017). Alternatively, tumour cells can shed ligands for NK cell receptors, blocking tumour cell recognition through those receptors. Soluble MIC and ULBP proteins have been detected in a number of malignancies including colon, liver and lung cancer (Doubrovina et al., 2003; Jinushi et al., 2005; Salih et al., 2006). Similarly, tumours shed soluble HLA-G which prevents NK cells activation through KIR2DL4 (Cabestre et al., 1999; Rouas-Freiss et al., 2005b; Urosevic and Dummer, 2008).

In addition, the soluble factors produced by tumours can alter the surrounding microenvironment and directly or indirectly affect NK cell function. A recently described pathway, mediated by TGF-β, leads to the conversion of NK cells to non-cytotoxic type 1 innate lymphoid cells (ILC1) (Cortez et al., 2017; Gao et al., 2017). TGF-β has been shown to suppress the cytotoxic activity and cytokine production of NK cells and T cells (Chen and Ten Dijke, 2016; Krneta et al., 2016; Laouar et al., 2005; Mamessier et al., 2011; Viel et al., 2016)

The importance of NK cells in liver neoplasms is less well characterised and varies depending on the source of tumour cells. Accumulation of NK cells has been linked with increased survival in HCC (Cai et al., 2008; Jinushi et al., 2005) and significantly worse survival rates in hepatic colorectal cancer metastasis (Pugh et al., 2014). However, it remains unclear as to which NK cell subset is of benefit in these tumours. Classically $CD56^{dim}$ NK cells have been regarded as the more potent cytotoxic cells (Cooper et al., 2001a). However, more recently it has been discovered that $CD56^{bright}$ NK cells display enhanced cytotoxicity after IL-15 activation and $CD56^{dim}$ NK cells can become potent cytokine producing cells (Maria et al., 2011; Wagner et al., 2017). This makes the liver repertoire of activated $CD56^{bright}$ NK cells a possible target for immune based therapies.

Previous work by our group has shown that NK cells are increased in tumour bearing liver from patients with CRC metastasis compared to donor liver; these NK cells had decreased

expression of inhibitory KIR receptors and CD94 and showed normal levels of cytotoxicity *ex vivo* (Norris et al., 2003). This led to the hypothesis that the factors present within the tumour microenvironment disrupt NK cell function.

1.5.4 Tumour microenvironment

Human tissues are a complex mixture of cells, stroma and soluble factors cooperating, as components of a healthy microenvironment, to perform the necessary functions of that specific tissue. Tumour cells derive from these healthy cells through accumulation of genetic and epigenetic alterations which lead to disruption of this finely tuned microenvironment. As a tumour develops it constantly interacts with the surrounding stromal cells, often altering their phenotype and function (Balkwill et al., 2012; Liotta and Kohn, 2001). The interaction between malignant and non-malignant cells creates a dysregulated microenvironment which promotes tumour growth through a variety of mechanisms. A complex and dynamic network of cytokines, growth factors, extra-cellular matrix degrading enzymes develop, while significant alterations in the tissue architecture takes place (Hanahan and Weinberg, 2011). Many similarities have been drawn been tumour progression and the natural wound healing process (Balkwill et al., 2012; Flier et al., 1986). However, while wound healing is a tightly regulated process, tumorigenesis involves the dysregulation of proliferation and differentiation (Hanahan and Weinberg, 2011; Velnar et al., 2009). While the innate immune system is well armed to recognise and remove dysplastic cells, tumour cells often hijack the immune system and promote a more tolerogenic environment. Tumour associated macrophages, myeloid derived suppressor cells, and tumour associated neutrophils have all been shown to actively repress the anti-tumour immune response through the production of anti-inflammatory cytokines (IL-10, TGF-β) (Fridlender et al., 2009; Qian and Pollard, 2010), degradation of essential amino acids through arginase and nitric oxide production (Bronte et al., 2003). These mechanisms limit NK cell activation and their ability to clear malignant cells (Allan et al., 2010; Cortez et al., 2017; Gao et al., 2017; Husain et al., 2013a).

Furthermore, TGF-β has been shown to polarise NK cells to a non-cytotoxic ILC1 type phenotype in tumour models (Cortez et al., 2017; Gao et al., 2017; Viel et al., 2016). In addition, these cells can also produce pro-tumorigenic growth factors such as VEGF (Drucker et al., 2005). Previous work by our group has highlighted several cytokines which are altered in CRC liver metastasis, including increased IL-10 and decreased IL-15 and TGF-β (Kelly et al., 2006, 2004).

Cell-cell interactions with cytotoxic lymphocytes also limit the ability of the immune system to clear tumour cells. Inhibitory signals such as PD-L1/2, CTLA-4 and TIGIT suppress activation of $CD8^+$ T cells and NK cells (Iwai et al., 2002; Krummel and Allison, 1995; Yu et al., 2009). Many of our current immunotherapies target these interactions, however, while limited initial success is observed, resistance to these immunotherapies rapidly emerges (Pardoll, 2012; Sharma et al., 2017). It is thought that many tumours may not have microenvironments conducive to a cytotoxic immune response and the tumour landscape must be altered before immune based therapies can be employed (Hanahan and Weinberg, 2011). We must therefore consider the indirect effects of tumour growth on immune and stromal cells as potential therapeutic targets.

1.6 Tumour metabolism

Throughout their life-span, human tissues require repair, proliferation and apoptosis to maintain normal functions. This is a tightly controlled process and in the absence of specific growth factors proliferation lags and cell death can occur (Mason and Rathmell, 2011). In contrast, tumour cells evade apoptosis, are self-sufficient in growth factor production and are insensitive to inhibition of proliferation resulting in limitless replicative potential (Hanahan and Weinberg, 2011). Proliferating cells require a constant supply of biomolecules in order to replicate cell structures and divide; these include cholesterol, fatty acids, nucleotides and non-essential amino acids (Vander Heiden et al., 2009). Tumours are comprised of rapidly

growing clones which must drastically alter their metabolism in order to meet the demands of relentless cell division. Biosynthesis requires a range of carbon intermediates which are provided primarily by the catabolism of glucose and glutamine. The first observation of altered metabolism in tumour cells was described ninety years ago by Otto Warburg (Warburg et al., 1927). This seminal work first described the phenomenon we now know as the Warburg effect. Tumour cells were shown to consume large amounts of glucose and produce lactic acid; we now know this process as glycolysis. In the intervening years several metabolic changes in tumour cells have been identified beyond their requirement for glucose. Hallmarks of cancer metabolism include dysregulated uptake of glucose and amino acids, use of opportunistic means of nutrient acquisition, increased use of biochemical intermediates for biosynthesis, increased demand for nitrogen, alteration in metabolite related gene expression and metabolic interactions with components of their microenvironment (Pavlova and Thompson, 2016). The requirement of glucose is well characterised and has even been used for diagnostic purposes utilising radiolabelled glucose to visualise tumours (DeBerardinis and Chandel, 2016; Som et al., 1980). Glutamine provides the building blocks of nitrogen based compounds such as nucleotides and non-essential amino acids (Altman et al., 2016). The requirement of glutamine for tumour cell survival was first described in cultured Hela cells (a tumour cell line immortalised from a cervical cancer), which require up to 100 fold higher concentrations of glutamine than healthy cells (Eagle, 1955). PI3K/Akt and RAS mutations have been shown to be the most common oncogenic mutations which drive dysregulated tumour metabolism (Barthel et al., 1999; Wieman et al., 2007; Ying et al., 2012).

Often tumour growth is restricted by blood supply, nutrient availability and hypoxia (Vaupel et al., 1989), therefore some have acquired mutations that allow them to continue proliferating in these hostile environments. RAS-mutant cells are capable of absorbing macromolecules through macropinocytosis and degrading them to base amino acids through lysosomal degradation (Commisso et al., 2013). In extreme cases, tumour cells have even been shown to

absorb live and apoptotic cells through entosis and phagocytosis respectively (Hamann et al., 2017; Krajcovic et al., 2013; Kroemer and Perfettini, 2014). During hypoxia, many oxygen dependent processes must be abandoned or supplemented by other pathways. For example, unsaturated fatty acids are in short supply due to loss of stearoyl-CoA desaturase activity. Therefore, the free fatty acid pool must be supplemented by harvesting free fatty acids from the environment (Kamphorst et al., 2013). In even more extreme cases of nutrient deprivation tumour cells can catabolize their own proteins and lipoproteins through autophagy to liberate amino acids and fatty acids (Boya et al., 2013).

The glycolysis pathway is the major source of these biochemical intermediates required for proliferation (**Figure 1-7**). Surprisingly, tumour cells only have a modest increase in ATP demand and therefore do not increase use of the TCA cycle under normoxic, glucose rich conditions (Lunt and Vander Heiden, 2011). It is now hypothesised that tumour cells uncouple glycolysis from oxidative phosphorylation in order to maintain biosynthesis. By converting excess pyruvate to lactate tumour cells can prevent negative feedback and consumption of NAD^+ during mitochondrial respiration and continue constant biosynthesis through glycolysis intermediates (Pavlova and Thompson, 2016).

Nitrogen supply is essential for the production of nucleotides in proliferating cells. This is mainly acquired through glutamine and thus is a major rate limiting step in tumour cell proliferation (Gaglio et al., 2009). C-MYC mutations have been shown to be important in regulating nucleotide production through glutamine uptake and metabolism (Hensley et al., 2013).

These alterations in tumour cell metabolism have far reaching consequences for neighbouring and distant cells. Tumour-associated fibroblasts, endothelial cells and innate and adaptive immune cells all undergo phenotypic and metabolic changes as a results of tumour growth (Hanahan and Coussens, 2012). Tumour metabolism restricts immune cell proliferation and

activation by limiting the available nutrients necessary for these activities. Cytotoxic T cells and NK cells require substantial metabolic reprogramming, requiring glucose and glutamine to drive a glycolytic shift in metabolism, in order to produce anti-tumour cytokines, such as IFN-γ and TNF-α, and cytotoxic functions (Assmann et al., 2017; Fox et al., 2005; Keating et al., 2016; Viel et al., 2016). In addition, tumour cells deplete the microenvironment of essential amino acids such as tryptophan required for proliferation of immune cells (Platten et al., 2012). Furthermore, tumour cells can convert tryptophan to kynurenine (via IDO production) which promotes T_{reg} cell differentiation and development of an immunosuppressive environment (Mezrich et al., 2010) (**Figure 1-8**).

1.6.1 Role of lactate in tumour progression

Accumulation of lactate in the tumour microenvironment affects a range of cell types and is an important mediator of tumour progression (**Figure 1-8**). In the case of nutrient deprivation, tumour cells can reabsorb lactate and convert it to glucose through the Cori cycle (Hu et al., 2017; Martínez-Reyes and Chandel, 2017). Lactate is secreted from tumour cells via a monocarboxylate transporter (MCT), which is coupled to the co-transport of hydrogen ions (H+). Lactate production and the expression of MCTs are prognostic of tumour progression and metastases (Brand et al., 2016; Carmona-Fontaine et al., 2017; Payen et al., 2017). Lactate secretion leads to the initiation of angiogenesis through the production of VEG-F from stromal cells (Sonveaux et al., 2012; Vegran et al., 2011). Lactic acid can also lead to the production of hyaluronic acid and matrix metalloproteinases (MMPs) by fibroblasts (Martínez-Zaguilán et al., 1996; Stern et al., 2002). This combination of effects promotes the migration and extravasation of tumour cells.

Lactate can also affect the phenotype and function of immune cells. Notably it can induce the differentiation of M2 macrophages and MDSC cells (Colegio et al., 2014; Husain et al., 2013a, 2013b), both of which suppress T cell and NK cell activity (Scott and Cleveland, 2016). Furthermore, lactate is capable of supressing DC antigen-presentation and T cell

activation, while also attenuating monocyte migration (Fischer et al., 2007; Goetze et al., 2011; Gottfried, 2006). Beyond simply suppressing the immune system, acidification of the tissue microenvironment can lead to the selective cell death of T cells and NK cells (Brand et al., 2016).

In addition, tumour cell subpopulations can utilize alternate lactate metabolism, even using it to fuel oxidative phosphorylation. In breast cancer, signals from tumour cells lead to increased lactate production by stromal cells (Whitaker-Menezes et al., 2011). This lactate is then taken up by tumour cells, converted to pyruvate and shuttled into the TCA cycle (Corbet and Feron, 2017; Hui et al., 2017; Martínez-Reyes and Chandel, 2017).

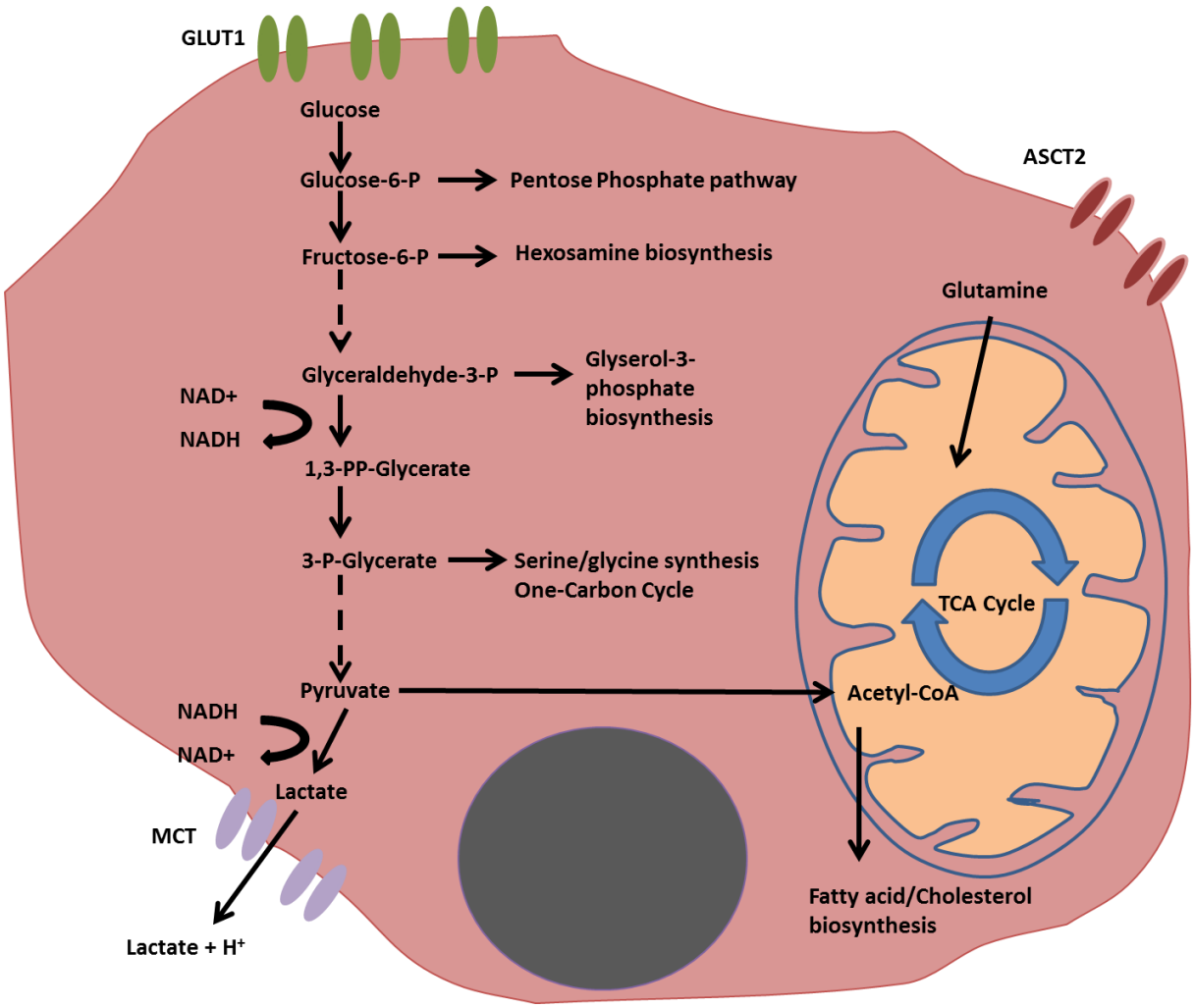

Figure 1- 7 Glycolytic intermediates fuel biosynthesis of essential molecules for proliferation

Diagram shows the biochemical intermediates produced by glycolysis which are used for biosynthesis of essential molecules for cell proliferation. Tumour cells favour glycolysis due to the range of intermediates produced and ability to produce the reducing molecule NAD+ by converting pyruvate to lactate. Dashed lines denote intermediates not shown as they have no biosynthetic function of interest. (NAD^+- nicotinamide adenine dinucleotide, NADH- NAD+ hydrogen, MCT- Monocarboxylate transporter, TCA- tricarboxylic acid cycle, ASCT2- Alanine, serine, cysteine-preferring transporter 2)

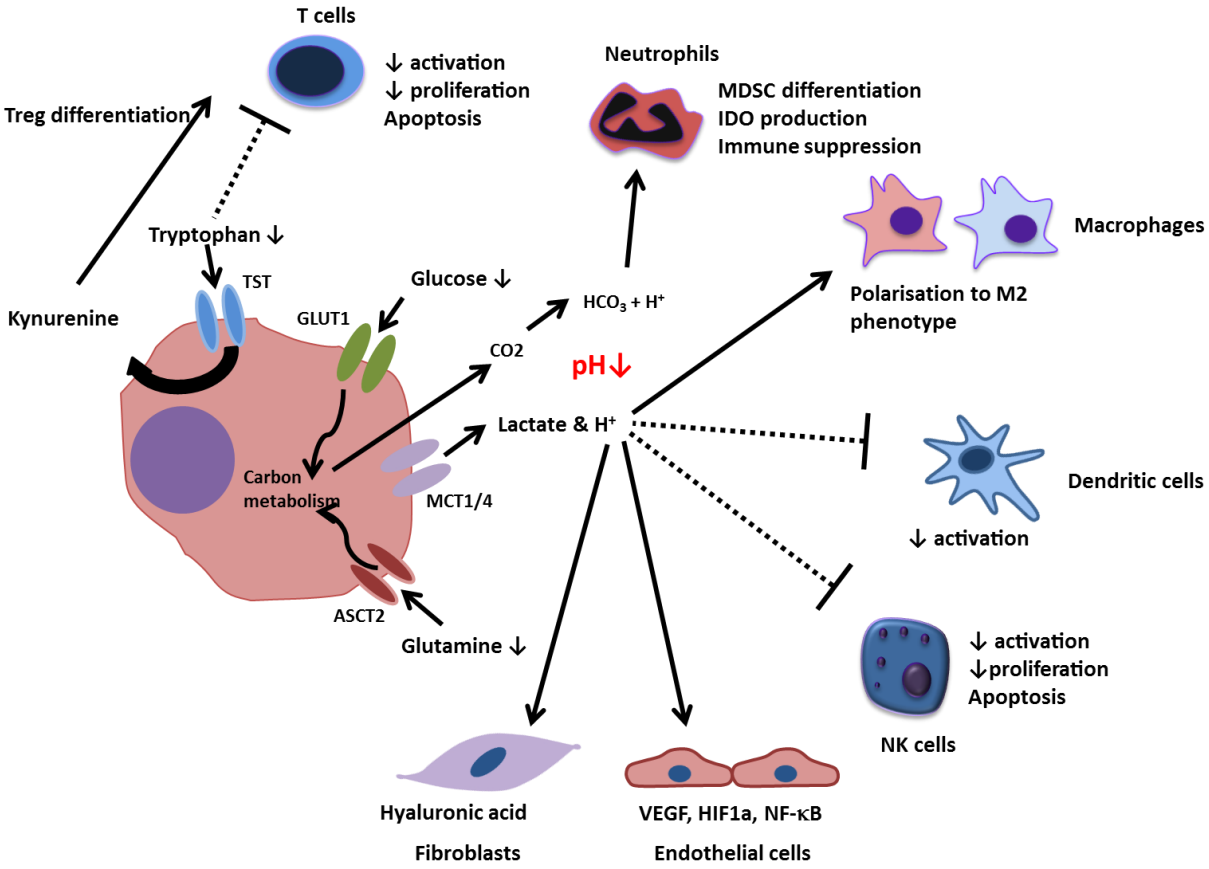

Figure 1- 8 Effect of tumour metabolism on the tumour microenvironment

Lactate is the main product of tumour glycolysis and is transported into the extracellular space by MCT1/4. In combination with CO_2, produced by the tumour, lactate decreases the pH of the microenvironment. Accumulation of lactate can lead to decreased activation of immune cells, including T-cells, NK cells and dendritic cells, can polarise macrophages to an M2 phenotype, lead to the differentiation of MDSC from myeloid cells. Lactate also induces angiogenesis and extracellular matrix remodelling through its effects on endothelial cells and fibroblasts. Additionally increased demand for glucose and glutamine by the tumour cell deprives neighbouring cells of necessary nutrients. The consumption of tryptophan and release of kynurenine by tumour cells leads to the differentiation of Treg cells. (IDO- Indolemine-2,3-dioxygenase, MDSC- Myeloid derived suppressor cell, VEGF- Vascular endothelial growth factor, HIF1a- Hypoxia inducible factor 1, ASCT2-Alanine, serine, cysteine-preferring transporter 2, MCT- Monocarboxylate transporter, TST-Tryptophan-selective transporter, GLUT1- Glucose transporter 1)

1.6.2 Therapeutic targeting of metabolic pathways

The treatment of cancer has long relied on targeting cell proliferation through the use of cytotoxic and DNA damaging chemotherapeutics (Cheung-Ong et al., 2013; Dasari and Tchounwou, 2014). However, these approaches have many off target side-effects including leukopenia, anaemia, nausea, hair loss, diarrhoea and emotional distress (Love et al., 1989). Despite the recognition of tumour metabolism as a defining feature of the disease by Warburg nearly 100 years ago, oncology has been slow to take advantage of this target. The first medical procedure utilizing this feature of cancer was the FDG-PET scan in the 1980's, which used radio labelled glucose to visualize tumours (Som et al., 1980). The broad spectrum of receptors, transporters, catalysing enzymes involved in tumour metabolism has led to the development of an array of metabolic therapies which are now beginning to enter the clinic, with varying degrees of success (Galluzzi et al., 2013; Tennant et al., 2010).

Anti-glycolytic drugs, such as metformin, were identified serendipitously to have a profound effect on cancer development. Diabetics treated with metformin have a significantly decreased rick of developing malignancy (Evans, 2005). While it has proven effective in a prophylactic setting, metformin is currently being trialled as an adjuvant treatment in breast cancer (NCT01101438) but remains to be shown to be effective in developed cancers. A range of other metabolic treatment approaches are currently under development and in clinical trials, these include those targeting glucose metabolism (Galluzzi et al., 2013; Tennant et al., 2010), glutamine metabolism (Altman et al., 2016), lactate transport (Noble et al., 2017; Polanski et al., 2014; Sonveaux et al., 2012, 2008), reversal of acidosis (Corbet and Feron, 2017; Pötzl et al., 2017), lipid metabolism and biosynthesis (Liu et al., 2017).

Targeting glycolysis, glutamine metabolism or lactate transport has multiple beneficial effects. By depriving tumour cells of essential nutrients it limits their biosynthetic and proliferative capacity, reducing tumour growth dramatically. Reducing glycolysis decreases the amount of lactate and protons produced by the cells, therefore increasing the pH of the

tumour microenvironment. This would create a more hospitable environment for the immune system to work within while also driving a stress response in tumour cells (Renner et al., 2017).

While an attractive target, metabolic therapies can also have their own side effects, specifically on the immune system. The realm of immunometabolism has become a topic of increasing interest. Metabolic changes underpin many of the immune functions we associate with tumour immunity (Mills et al., 2017; O'Neill et al., 2016). Glycolysis appears to be an essential pathway for T and NK cell activation (Buck et al., 2015; Keating et al., 2016; Viel et al., 2016). A fine tuning of the metabolic therapy approach is required to select pathways differentially used by tumour and non-tumour cells. Targeting lactate transport has proven effective in murine models and appears to have limited negative effects on T cells responses, possibly due to the preference of T cells to metabolise pyruvate through the TCA cycle (Gandhi et al., 2013; Husain et al., 2013a). Therefore, identifying tumours which would benefit from lactate targeted therapy may provide a novel therapeutic target in many cancers.

1.7 Hypothesis

We hypothesise that the adult human liver hosts a heterogeneous mix of tissue resident and transient populations of NK cells, and that the hepatic microenvironment is capable of altering the phenotype and function of subpopulations of these. In addition, we believe these potent anti-tumour cells are compromised in CRC liver metastasis, leading to tumour persistence and high rates of disease recurrence after surgical resection.

1.8 Aims

We will investigate the phenotype and function of hepatic NK cells in healthy donor liver and resected tumour bearing liver, focusing in particular on the following

- Composition of NK cell subpopulations in healthy human liver
- Expression of cytotoxicity receptors and cytotoxic molecules in NK cells from healthy and tumour bearing liver
- The cytotoxic function and cytokine production of hepatic NK cell subsets
- The expression of transcription factors governing NK cell differentiation and function
- The effect of liver microenvironment on the phenotype and function of NK cells
- Changes in the proportion and phenotype of NK cell subsets in tumour bearing liver
- The effect of tumour microenvironment on hepatic NK cells

CHAPTER 2: Materials and Methods

2.1 List of Reagents, materials and instruments used

Table 2-1: General reagents used

Reagent	Company	Location
Bovine serum albumin (BSA)	GE Healthcare	Buckinghamshire, UK
Collagenase IV	Sigma-Aldrich	Poole, UK
Dimethyl sulfoxide (DMSO)	Sigma-Aldrich	Poole, UK
Ethylenediaminetetracetic acid (EDTA)	Sigma-Aldrich	Poole, UK
Foetal bovine serum (FBS)	Gibco Invitrogen	Paisley, UK
Ficoll-Paque	GE Healthcare	Buckinghamshire, UK
Golgi-stop	BD Biosciences	Oxford, UK
Penicillin-streptomycin	Gibco Invitrogen	Paisley, UK
Sterile Phosphate buffered saline (PBS)	Gibco Invitrogen	Paisley, UK
rhIL-2	Peprotech	London, UK
rhIL-12	Peprotech	London, UK
rhIL-15	Peprotech	London, UK
RPMI 1640 + L-glutamine	Gibco Invitrogen	Paisley, UK
Sodium azide	Sigma-Aldrich	Poole, UK
Trypan blue	Sigma-Aldrich	Poole, UK
Trypsin 0.5% EDTA	Gibco	Paisley, UK
NK cell isolation kit	Miltenyi, Biotech	Bergisch-Gladbach, DE
Distilled, sterile, nuclease-free water	Gibco	Paisley, UK
Hank's balanced saline solution (HBSS)	Gibco	Paisley, UK
RNA Later	Ambion	Paisley, UK
Human AB serum	Gibco	Paisley, UK
Lactic Acid	Sigma-Aldrich	Poole, UK
Sodium Lactate	Sigma-Aldrich	Poole, UK
rhTGF-b	Peprotech	London, UK
rhIL-10	Peprotech	London, UK
HEPES	Sigma-Aldrich	Poole, UK

Reagent	Company	Location
PIPES	Sigma-Aldrich	Poole, UK
Hydrochloric Acid	Sigma-Aldrich	Poole, UK
Citric Acid	Sigma-Aldrich	Poole, UK
Phosphate Buffered Saline	Gibco	Paisley, UK
Sodium Chloride	Sigma-Aldrich	Poole, UK
Potassium Chloride	Sigma-Aldrich	Poole, UK
Magnesium Chloride	Sigma-Aldrich	Poole, UK
Calcium Chloride	Sigma-Aldrich	Poole, UK
Sodium Hydroxide	Sigma-Aldrich	Poole, UK
Lactate assay kit	Sigma-Aldrich	Poole, UK
Glucose detection kit	Abcam	Cambridge, UK
Intracellular ATP determination kit	Invitrogen	Paisley, UK
Intracellular pH detection kit	Invitrogen	Paisley, UK
Z-IETD-FMK	BD Biosciences	Oxford, UK

Table 2-2: Tissue culture materials

Material	Company	Location
6/12/24/96-well flat-bottom TC plates	Greiner Bio-One	Kremsmünster,Austria
96-well round-bottom TC plates	Corning Life Sciences	MA, USA
24 well transwell inserts 5.0um	Thermo Fisher Scientific	Paisley, UK
Cryovials	Thermo Scientific Nunc	Roskilde, DK
Polystyrene FACS tubes	BD Biosciences	Oxford, UK
LS separation columns	Miltenyi Biotech	Bergisch-Gladbach, Germany
0.2-μm mesh syringe filter	Sartorius	Göttingen, Germany
15/50mL centrifuge tubes	Greiner Bio-One	Kremsmünster,Austria
2mL cryovials	Thermo Fisher Scientific	Paisley, UK

Material	Company	Location
70-µm mesh cell strainer	Becton Dickinson	Flintshire, UK
3.5mL transfer pastettes	Sarstedt	Nümbrecht,Germany
40-µm mesh cell strainer	Becton Dickinson	Flintshire, UK
5/10/25mL serological pipettes	Greiner Bio-One	Kremsmünster,Austria
Falcon brand 50mL centrifuge tubes	Becton Dickinson	Flintshire, UK
Petri dishes	Greiner Bio-One	Kremsmünster,Austria
Scalpels	Swann Morton	Sheffield, UK
75/175cm^2 tissue culture flasks	Greiner Bio-One	Kremsmünster,Austria

Table 2-3: PCR materials

Material	Company	Location
100bp DNA Ladder	Invitrogen	Paisley, UK
GoTaq qPCR master mix	Promega	Madison, UK
HotStar Taq Plus DNA Polymerase	Qiagen	Crawley, UK
Oligo-dT Primers	Qiagen	Crawley, UK
Omniscript cDNA synthesis kit	Qiagen	Crawley, UK
PowerUp SYBR Green Master Mix	Applied Biosystems	Paisley, UK
SybrSafe DNA Gel Stain 10000X	Invitrogen	Paisley, UK
0.2mL nuclease-free microcentrifuge tubes	Sarstedt	Nümbrecht, DE
1.5/2.0mL sterile microcentrifuge tubes	Thermo Fisher Scientific	Paisley, UK
96-well plates	Thermo Fisher Scientific	Paisley, UK
Optical adhesive film	Applied Biosystems	Paisley, UK
P10/20/200/1000 sterile filtered pipette tips	Thermo Fisher Scientific	Paisley, UK
Stainless steel beads 3mm	Qiagen	Crawley, UK

Table 2-5: Primer used for qPCR

Gene	Forward Primer	Reverse Primer
HPRT	AGGCCATCACATTGTAGCCC	GTCCCCTGTTGACTGGTCATT
β_2M	GTGCTCGCGCTACTCTCTCTTT	GTCAACTTCAATGTCGGATGGA
GAPDH	CCACCCATGGCAAATTCC	CAGCATCGCCCCACTTG
RPS9	TGACCGGGTGGTTTGCTTA	ATACTCGCCGATCAGCTTCAG
SLC16A1	GGGTTATAAGGCAGCCTCGCT	TCCAACTGCTGGTGGCATTTT
SLC16A3	GAGTTTGGGATCGGCTACAG	CGGTTCACGCACACACTG
SLC2A1	CTGCTCATCAACCGCAAC	CTTCTTCTCCCGCATCATCT

Table 2-4: Equipment and software used

Equipment	Company
LSR Fortessa	BD Biosciences
FACS Canto	BD Biosciences
FlowJo v.7.6 software	Treestar Inc
Gel Logic 200 Imaging System	Kodak
NanoDrop Spectrophotometer	Thermo Fisher Scientific
StepOne Software v2.3	Applied Biosystems
StepOnePlus Real-Time PCR system	Applied Biosystems
Techne Prime Thermocycler	Bibby Scientific
Fluroskan Ascent FL	Labsystems

Table 2-5: Antibodies used for flow cytometric staining

Reagent	Conjugate	Catalogue Number	Company
CD3	Pacific blue	558117	BD Biosciences
CD3	PerCP-Cy5.5	560835	BD Biosciences
CD3	BV421	562426	BD Biosciences
CD16	Pe-Cy7	557744	BD Biosciences
CD16	BV605	563173	BD Biosciences
CD16	FITC	561308	BD Biosciences
CD45	BV510	563204	BD Biosciences
CD45	BV785	304048	Biolegend
CD49a	APC	328313	Biolegend
CD56	Alexa-Fluor 488	557699	BD Biosciences
CD56	V450	560360	BD Biosciences
CD56	BV650	564057	BD Biosciences
CD56	BV711	563169	BD Biosciences
CD71	PE-Vio770	130-115-073	Miltenyi
CD98	PE	130-105-708	Miltenyi
CD107a	APC-H7	561343	BD Biosciences
CD127	Alexa-Fluor 700	FAB306N	R&D
CXCR6	PE-CF594	356016	Biolegend
CCR5	AF700	359115	Biolegend
Eomes	FITC	11-4877-41	eBioscience
Granzyme B	Alexa-Fluor 700	561016	BD Biosciences
Granzyme A	Alexa-Fluor 488	507212	Biolegend
Granzyme K	Alexa-Fluor 647	370503	Biolegend
GLUT1	FITC	FAB1418F	R&D
Interferon-γ	Pe-Cy7	557643	BD Biosciences
NKG2A	APC	FAB1059A	R&D
NKG2C	Alexa-Fluor 488	FAB138G	R&D
NKG2D	PE	320805	Biolegend

Reagent	Conjugate	Catalogue Number	Company
NKp44	APC	325109	Biolegend
NKp46	Pe-cy7	562101	BD Biosciences
NKp46	BV785	563329	BD Biosciences
Perforin	PE-CF594	563763	BD Biosciences
Tbet	PE	12-5825-80	eBioscience
TRAIL	PE	550516	BD Biosciences
Mitotracker	Deep Red	8778S	Cell Signaling technologies
MitoSox	PE	M36008	Invitrogen
RORγτ	APC	17-6988-80	Biolegend
Tetramethylrhodamine (TMRM)	PE	T668	Invitrogen
FVS 780	NA	565388	BD Biosciences
Zombie Red	NA	423109	Biolegend
Zombie Yellow	NA	423103	Biolegend
Annexin V	FITC	640906	Biolegend
7-AAD Viability Dye	NA	00-6993-50	eBiosciences
pH Rodo Green	NA	P35373	Invitrogen
Cell Trace Violet (CTV)	NA	C34557	eBiosciences
123 Count Beads	NA	01-1234-42	eBiosciences
FOXP3 staining Buffer	NA	00-5523	eBiosciences
Red cell lysing buffer	NA	R7757	Sigma-Aldrich
Compensation Beads	NA	552843	BD Biosciences
Compensation beads (anti-REA)	NA	130-104-693	Miltenyi

2.2 Cell Culture

Cell culture and handling of blood samples was carried out according to strict standard operating procedures (SOPs) generated in the O'Farrelly lab based on best practice guidelines (Freshney, 2011). Cell culture was carried out in sterile conditions using laminar air flow hoods and sterile or autoclaved materials and reagents. Human blood and liver samples were treated as potentially infected and were processed and handled in accordance with relevant health and safety guidelines.

2.3 Liver perfusate collection

Healthy human liver samples were obtained from transplant donors **(Figure 2-1**). Healthy human livers were donated by brain-stem dead patients. Briefly, the donor liver organ is retrieved from the donor and is preserved in UW solution for transportation to the transplant theatre in St. Vincent's University hospital. The site of retrieval could be anywhere in Ireland, and collaboration with the United Kingdom (UK) means that some organs are sourced from the UK. All transplants are carried out within twelve hours of organ retrieval. The UW solution becomes enriched with cells during transport. This solution is known as resting transport medium (RTM) and it was collected in a one litre bottle for research. During liver transplantation, clamps are placed on inflow and outflow blood vessels of the recipient's liver. The explant diseased liver is removed, and the donor organ is grafted into the recipient. First, the recipient's hepatic vein is attached to the donor livers suprahepatic vena cava. The clamps remain in place on the recipient blood vessels to ensure that no recipient blood enters the donor liver and critically, that no UW solution enters the recipient. UW solution is high in potassium, which would cause cardiac arrest if allowed to circulate into the recipient. The liver is then perfused (under suction) with one litre of saline solution to remove the preservative (UW) solution from the organ. This liver flush solution enters the hepatic portal vein and is collected from the hepatic vena cava.

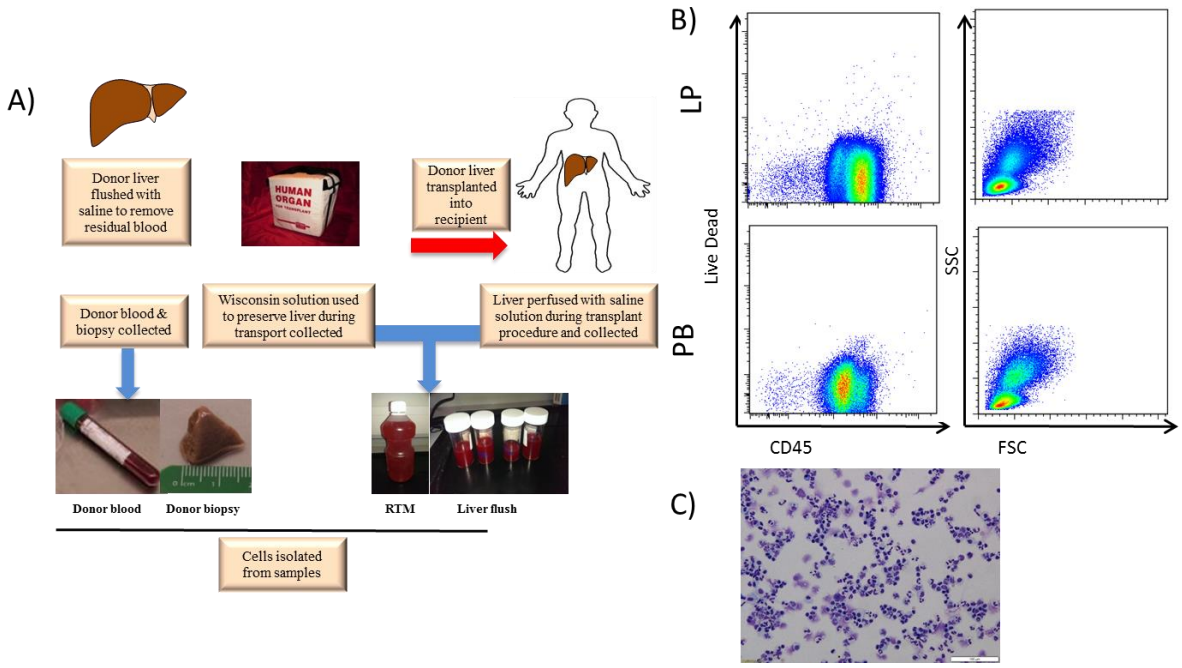

Figure 2- 1 Overview of sample acquisition from liver transplant

(A) During retrieval, the donor aorta and superior mesenteric vein are initially flushed with University of Wisconsin (UW) solution (ViaSpan, DuPont Pharmaceuticals Ltd., Herts, UK) at the time of exsanguination. Flushing of the liver with UW is continued after excision of the organ until the perfusate looks clear at which time the liver is packed in a bowl containing UW and stored on ice for transportation. During implantation, the liver is flushed with normal saline through the portal vein to wash out the UW before reperfusion. This liver perfusate is collected from the inferior vena cava for this study. Biopsies of donor liver tissue were collected at separate stages. Single cell suspensions were prepared as described in Chapter 2. **(B)** NK cells were identified from $CD45^{+}$ lymphocytes. Non-viable cells were excluded by FVS780 staining. **(C)** Cytospin of HMNCs showing heterogeneous populations of hepatic leukocytes.

2.4 Isolation of mononuclear cells from peripheral blood

Peripheral blood mononuclear cells (PBMCs) were isolated from heparin anticoagulated fresh blood sample tubes or buffy coat packs by Ficoll-Hypaque density gradient centrifugation using Ficoll-Paque™ PLUS (GE Healthcare). For buffy coats, blood was diluted by injecting 20ml of 1x sterile phosphate buffered saline (PBS) and mixing the buffy coat vigorously before blood was removed into a sterile container. Carefully, 35ml of blood was gradually layered onto 15ml of Ficoll in a 50ml falcon tube and centrifuged at 800 x g for 25 mins with brake set to 1. The buffy layer was then removed from each tube using a sterile Pasteur pipette and transferred into a fresh 50ml falcon. These PBMCs were washed twice by topping up the 50ml falcon with sterile 1x PBS and centrifuging at 300 x g for 5 mins, discarding the supernatant and resuspending the pelleted cells by vortexing each time. This cell pellet was again resuspended by vortexing and diluted in complete cell culture medium which consisted of a mixture of RPMI + L-glutamine, 10% v/v Foetal Calf Serum (FCS), 100U/ml penicillin and 100µg/ml streptomycin.

2.5 Isolation of hepatic mononuclear cells from liver perfusate

Hepatic mononuclear cells (HMNCs) were isolated by filtration of liver perfusate through 70µM filters (BD Biosciences) followed by centrifugation at 1500 rpm for 10 mins to remove debris. HMNCs were separated from the resulting solution by density gradient centrifugation using Ficoll-Paque™ PLUS (GE Healthcare) and any red blood cells present were removed by red cell lysis solution (Sigma). The resulting white blood cells were counted and viability calculated using trypan blue exclusion assay.

2.6 Isolation of hepatic mononuclear cells from liver tissue

Pieces of donor and explant liver biopsies were collected in RNA later, 10% formalin or frozen in liquid nitrogen for future studies when possible. The remainder of the biopsy was finely diced into <1mm pieces using scalpels and transferred to 50ml tubes containing

disruption enzyme mix solution (Collagenase type IV (0.05 %) (Sigma), DNAse I (10 mg/ml) (0.002 %) (Sigma), 2% FBS (Gibco) + 2% BSA (30% w/v) (GE Healthcare) diluted in hanks balanced salt solution (HBSS) (Gibco)). Samples were incubated at 37°C in a shaker rotating at 180rpm for 10-15 mins to digest the liver biopsy tissue. Debris was removed by filtration of the resulting mixture through 70µM filters (BD Biosciences) and collecting the filtrate in a 50ml falcon tube. Hepatocytes were removed by centrifugation at 30 x g for 3 mins at 4°C and collecting the supernatant. HMNCs were isolated by centrifugation at 300 x g for 10 mins at 4°C and collecting the pelleted cells. These cells were washed by resuspending the pellet in 20ml HBSS and centrifugation at 1500rpm for 5 mins. The supernatant was discarded and the remaining cell pellet was resuspended in RPMI. The resulting white blood cells were counted and viability calculated using trypan blue exclusion assay.

2.7 Cell viability and enumeration of cells

In order to count cells and assess cell viability, Trypan blue exclusion dye was used. Briefly, cells were diluted in Trypan blue at 1:20. Carefully, 10µl of the cell/Trypan blue solution was mounted to a Neubauer Haemocytometer and visualised using an inverted microscope. The numbers of cells in two or more grid sections were counted and an average for the number of cells in a 0.1mm x 1mm x 1mm section was calculated. Cells touching the top and right borders of each grid section were not counted to avoid counting the same cells twice. The average number of cells in one section is multiplied by 10^4 then by the dilution factor to give the number of cells per ml. Dead cells were unable to exclude the Trypan blue and therefore easily excluded in order to obtain a viable cell count.

2.8 Cryogenic storage and thawing out of cells

Cells were pelleted by centrifugation at 400 x g for 5 mins at 4°C, and the supernatant discarded. Freezing mixture containing 50% RMPI, 40% FCS and 10% DMSO (Gibco) was placed on ice for 5 mins. Cells were then mixed with freezing medium at a concentration of

10-25 x 10^6 cells per ml. Cells were immediately transferred to cryovials (Thermo Scientific) and placed in a cryo 1°C freezing container containing isopropanol and placed in a -80°C freezer overnight. Cells were transferred to long term storage in liquid nitrogen the next day. To reconstitute cells in medium and culture again, cryovials were thawed rapidly in a 37°C water bath and then transferred to a 15ml falcon tube containing pre-warmed complete medium. Cells were then pelleted by centrifugation at 400 x g for 5 mins, supernatant was discarded and cells were resuspended in appropriate complete medium. Cells were counted and cell viability assessed before being cultured at 37°C with 5% CO_2.

2.9 Magnetic bead enrichment of cells

NK cells were enriched using Miltenyi microbeads. Miltenyi microbeads are superparamagnetic particles with a diameter of 50nm conjugated to a mAb specific for the cell subset of interest. Negative selection was used to isolated NK cells. For negative selection cells were resuspended in 40µl/10^7 cells of MACS buffer (PBS with 0.5% bovine serum albumin (BSA) (GE Healthcare)). A biotin labelled antibody cocktail was added to the suspension and incubated for 5 mins at 4°C. Anti-biotin labelled magnetic beads were then added to the suspension and incubated for 10 mins at 4°C. The volume of the suspension was then adjusted to 500µl by addition of the required amount of cold MACS buffer. The suspension was then added to the pre-separation filter of the LS column inserted into the magnet apparatus. Unlabelled cells were eluted by washing the column with 3ml of cold MACS buffer. This filtered sample was then centrifuged at 300 x g for 10 mins and resuspended in RPMI. Cell yield was determined and cell viability and purity was assessed by flow cytometry.

2.10 Antibodies and flow cytometry

All of the antibodies used during the course of this work are listed in **Table 2.4**. Antibodies were titrated in order to determine the optimal concentration to use for staining. Fluorescence-minus-one (FMO) controls were used to set gates where necessary.

2.11 Principles of flow cytometry

Flow cytometry is a method by which multiple characteristics of single cells can be assessed rapidly. Cells in suspension are drawn into a single cell stream by surrounding isotonic sheath fluid and passed through an interrogation point. This point consists of a laser beam or beams which target the cells. Photodetectors in the flow cytometer can detect both transmitted and scattered light. Through the detection of visible light, cell subsets can be distinguished based on their physical characteristics. The size of the cell is measured by the forward scatter (FSC) of this visible light while the granularity of the cell is measured by the side scatter (SSC) of this light. In this way it is possible to distinguish between small non-granular cells (lymphocytes) and larger more granular cells (macrophages). As well as visible light, the photodetectors also detect fluorescent light that is emitted from fluorochromes which are conjugated to target cells after excitation by the laser beams. There is a wide range of fluorochromes and dyes that are excited at different wavelengths and therefore be detected by photodetectors of the flow cytometer. This is exploited in flow cytometry by conjugating these fluorochromes to mAbs specific to molecules of interest, allowing us to detect their presence or absence in different cell subsets. The fluorescence emitted by a fluorochrome conjugated to a mAb for a specific cell surface marker is interpreted by the flow cytometer software and given as mean fluorescence intensity (MFI), which correlates with the quantity of that specific marker on the cell surface.

2.12 Cell surface staining for flow cytometry

For flow cytometry analysis, $5 \times 10^5 – 1 \times 10^6$ cells were stained in polystyrene FACS tubes. Cells were washed with FACS buffer (PBS containing 1.5% v/v BSA and 0.2% sodium azide (NaN_3)) followed by centrifugation for 5 mins at 500 x g and carefully discarding the supernatant. Cells were then resuspended in 100µl of FACS buffer containing the required amounts of mAbs for surface markers being analysed. Cells were incubated for 30 mins at 4°C protected from light to allow binding of mAbs. Excess unbound antibodies were removed

by washing the cells twice with FACS buffer followed by centrifugation for 5 minutes at 500 x g and carefully discarding the supernatant. Essential controls were used for each flow cytometry experiment. Unstained cells were needed to adjust certain parameters on the flow cytometer, single stained controls (Compensation Beads stained with each individual fluorochrome being used) to carry out compensation and FMO controls (samples containing all but one of the fluorochrome labelled antibodies being used) to set the gating strategy where necessary.

2.13 Intracellular cytokine staining for flow cytometry

After cell surface staining, 100µl of fixation buffer (eBioscience) was added to each tube and incubated at room temperature for 20 mins. Permeabilisation buffer was prepared by diluting 1:10 Perm buffer in deionised water. 2ml of Perm buffer was added to each tube and centrifuged at 500 x g for 5 mins. Supernatant was decanted and intracellular antibodies added to each tube, incubated at room temperature for 30 mins. Cells were then washed with 2ml Permeabilisation buffer and centrifuged at 500 x g for 5 mins.

2.14 Intracellular transcription factor staining for flow cytometry

After cell surface staining 1ml of Perm/Fix buffer (eBiosciences) was added to each well and incubated at room temperature for 20 mins. This was prepared by diluting 1:4. Permeabilisation buffer was prepared by diluting 1:10 Perm buffer (eBiosciences) in deionised water. 2ml of Perm buffer was added to each tube and centrifuged at 500 x g for 5 mins. Supernatant was decanted and intracellular antibodies added to each tube, incubated at room temperature for 30 mins. Cells were then washed with 2ml Perm buffer and centrifuged at 500 x g for 5 mins.

2.15 Performing absolute cell counts by flow cytometry

In order to determine absolute cell counts from tissue samples, 123 Count eBeads (eBiosciences) were used in conjunction with flow cytometry. These are 7 µm microparticles

containing encapsulated dyes compatible with blue (488nm) and violet (405nm) excitation sources and emitting fluorescence between approximately 500nm and 750nm. They are supplied at a known concentration in 0.05% Tween-20 with 2mM sodium azide. Collecting carefully suspended and measured quantities of cell:bead mixtures on a flow cytometer makes the ratiometric enumeration of cells possible. After performing normal cell staining as described above samples were resuspended in 300µl FACS buffer. 123Count eBeads were vortexed for 15-30 seconds before use. 100µl of 123Count eBeads were added to each sample. Cell counts and bead counts were acquired on an LSR Fortessa. A minimum of 1 x 10^4 eBeads were acquired for each sample. The below equation was used to calculate the absolute count of cells in each tube.

$$Absolute\ count/ul = \frac{Cell\ count}{eBead\ Count} * eBead\ concentration$$

eBeads were provided at a concentration of 1.024 x 10^6/ml.

2.16 Fluorescence activated cell sorting (FACS)

Up to 4 x 10^7 cells were stained for cell sorting in a sterile polystyrene FACS tubes. Frozen liver perfusates were thawed and resuspended in Complete RPMI at a concentration of 3-4 x 10^6 cells/ml. Cells were then rested overnight at 37^{o}C in 12 well plates. Cells were washed by adding 2ml of sorting buffer (consisting of PBS supplemented with 2% v/v FCS) and resuspended in 100µl. The required amount of mAbs were added to the cell suspension and mixed well. Cells were incubated at 4°C for 1 hour to allow binding of the mAb with the cold temperature required to inhibit internalisation of the antibodies in the absence of sodium azide. Excess unbound antibodies were removed by washing with 2ml of sorting buffer followed by centrifugation at 500 x g for 5 minutes. Cells were resuspended in 200µl of sorting buffer for sorting on a BD Aria Fusion cell sorter. The sorted cells were centrifuged at 500 x g for 5 minutes, supernatant discarded and the cells resuspended in fresh complete RPMI. This was to wash out flow cytometer sheath fluid which contains growth inhibitors and would affect cell function.

2.17 Measuring NK cell degranulation and cytokine production

Degranulation of NK cells against target cells was measured using the CD107a externalisation assay. This method utilises the fact that the activation of NK cells leads to the degranulation of these cells at which point lysosomal associated membrane protein 1 (LAMP-1) or CD107a can be detected on the surface of the effector cells. The level of CD107a can be measured using flow cytometry and this has been shown to directly correlate with cell death.

Target cells were cultured in 96-well plates. The appropriate numbers of effector cells were then added at 5:1 effector: target (E:T) ratio along with mAb specific for CD107a. Following 60 minute incubation at 37°C, 50µM monensin (BD Biosciences) was added to the cells. The cells were cultured for a further 3 hours. Cells were then harvested and stained with

antibodies specific for: CD3, CD16, CD56, and IFN-γ. CD107a expression levels were determined by flow cytometric analysis.

2.18 Measuring direct cytotoxicity

Cell trace violet (CTV, eBiosciences) was reconstituted in 20µl DMSO to prepare a 5mM stock solution. This was further diluted in DMSO to 1mM working stock. Target cells for assay (K562 or SW620) were resuspended in 1ml warm PBS at a concentration of $1x10^6$/ml. 1µl of CTV working stock was added to 1ml cell suspension (1µM staining solution). Cells were incubated at 37^{o}C for 20 mins. 5ml of warm RPMI was added to quench staining. Cell suspension was centrifuged at 300 x g for 5 mins and resuspended in RPMI. Target cells were co-incubated with NK cells isolated from liver perfusate by FACS for 4 hours at 37^{o}C. Cell suspensions were stained with propidium iodide (PI) to assess cell death. Analysis was performed by gating on CTV^+ target cells and measuring PI positivity.

2.19 Measuring Mitochondrial Mass

Mitotracker Deep Red (Cell Signalling Technologies) was used to assess mitochondrial mass by FACS. This is a cell permeable probe containing a mildly thiol-reactive chloromethyl moiety. This dye passively diffuses across the plasma membrane and accumulates in the mitochondria. A 1 mM stock solution was prepared by reconstituting 50µg lyophilized dye with 91.98µl DMSO. A working concentration of 500nM was achieved by diluting stock directly in media. Samples were then incubated in dye media for 30 mins at 37^{o}C. Fluorescence was then measured on LSR Fortessa using an excitation of 633nm and emission detection at 670nm (FL3).

2.20 Measuring Mitochondrial Reactive Oxygen Species (ROS)

MitoSOX Red (Invitrogen) mitochondrial superoxide indicator is a novel fluorogenic dye for highly selective detection of superoxide in the mitochondria of live cells. MitoSOX Red

reagent is live-cell permeant and is rapidly and selectively targeted to the mitochondria. Once in the mitochondria, MitoSOX Red reagent is oxidized by superoxide and exhibits red fluorescence, oxidation of the probe is prevented by superoxide dismutase. A 5mM stock solution was prepared by reconstituting 50µg MitoSOX Red in 13µl DMSO. A working solution of 5µM was prepared by diluting the stock 1:1000 in HBSS. This staining solution was then applied to cells and incubated at 37^{o}C for 10 mins. Cells were washed in warm HBSS and run on a LSR Fortessa using excitation at 561nm and emission at 582nm (FL12).

2.21 Measuring Intracellular pH

pHrodo Green AM Intracellular pH Indicator (Invitrogen) is a novel fluorogenic probe used to measure intracellular pH in live cells. pHrodo Green is weakly fluorescent at neutral pH but increasingly fluorescent as the pH drops. This reagent can quantify cellular cytosolic pH in the range of 9-4 with a pKa of ~6.5. This pHrodo Green dye has been modified with AM ester groups, which results in an uncharged molecule that can permeate cell membranes. Once inside the cell, the lipophilic blocking groups are cleaved by nonspecific esterases, resulting in a compound that is retained within the intracellular space. pHrodo Green AM is supplied in a 1000x solution. Stock dye is diluted 1:10 in Powerload concentrate. This solution is further diluted 1:100 in Live Cell Imaging Solution (LCIS). LCIS is prepared by adding the following chemicals to PBS: 140mM NaCl, 2.5mM KCl, 1.8mM $CaCl_2$, 1mM $MgCl_2$, 20mM HEPES adjusted to pH 7.4. Remove media from cells and wash with LCIS. Replace LCIS with staining solution. Incubate at 37^{o}C for 30 mins. Fluorescence was read on LSR Fortessa at excitation 488nm and emission 530nm (FL1).

Intracellular pH calibration buffer kit was used to establish standard curves. Nigericin and Valinomycin were prepared in DMSO to a concentration of 20mM each. These were then combined in a 1:1 ratio and aliquoted. Calibration buffers were supplied at pH 5.5, 6.5 and 7.5. 10µl of Valinomycin/Nigericin was added to 10ml of desired calibration buffer. Fresh

cells were then incubated with respective calibration buffers for 5 mins at 37^{o}C. Valinomycin/Nigericin allows for permeabilisation of cells to protons. Fluorescence from these standards was then used to generate a standard curve and allowed the calculation of intracellular pH of samples.

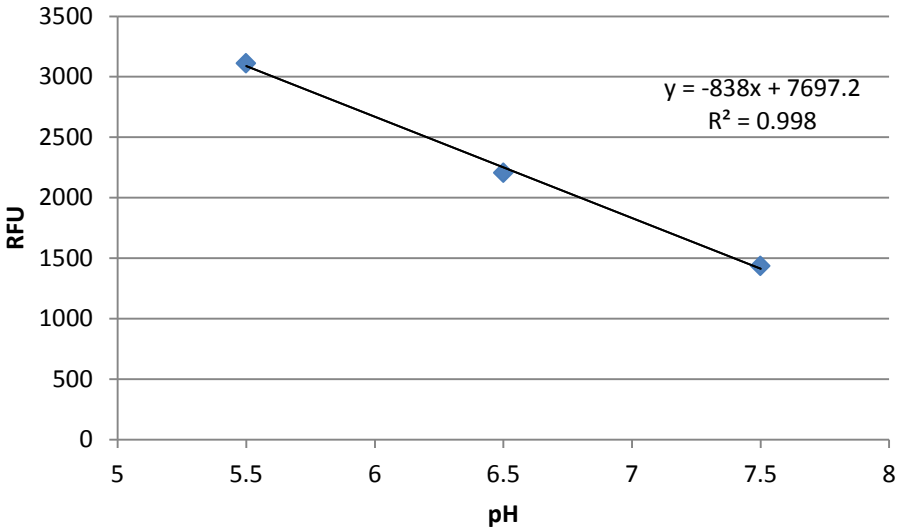

Figure 2- 2 Generation of standard curve for intracellular pH

NK cells were treated with Valinomycin/Nigericin (1µM each) and incubated with buffers at pH 5.5, 6.5 and 7.5. Cells were then stained with pHrodo and data acquired on LSR Fortessa. Relative fluorescence units (RFU) were plotted from the average of two replicates against pH of buffer to construct a standard curve. Equation: y=-838x+7697.2, R^2= 0.998. Standard curve was used to determine intracellular pH of experimental samples.

2.22 Apoptosis Assay

In normal viable cells, phosphatidylserine (PS) is located on the cytoplasmic surface of the cell membrane. However, in the intermediate stages of apoptosis, PS is translocated from the inner to the outer leaflet of the membrane, exposing PS to the external cellular environment where it can be detected. Annexin V conjugates provide quick and reliable detection method for identifying the externalization of phosphatidylserine. 7-Amino-Actinomycin D (7-AAD) is a nucleic acid dye that can be used for the exclusion of nonviable cells in flow cytometric assays. 7-AAD does not readily pass through intact cell membranes so is therefore excluded from live cells but enters and binds to DNA of apoptotic cells. Used in combination these two dyes can be used to identify apoptotic and pro-apoptotic cells in culture.

After treatment cells were removed from culture media and placed in Annexin V staining buffer. Staining buffer is prepared by adding the following to PBS: 140mM NaCl, 10mM HEPES, 2.5mM $CaCl_2$ (Sigma-Aldrich). 2µl Annexin V was added to each tube and incubated at RT for 30 mins. 1µl 7-AAD was added to each tube prior to running on LSR Fortessa. Apoptotic cells were identified as Annexin V^+ 7-AAD^+, while pro-apoptotic cells were Annexin V^+ 7-AAD^-. Live cells take up neither dye. Necrotic cells appear as Annexin V^- 7-AAD^+.

2.23 RNA extraction

Total RNA was extracted using a phenol-chloroform extraction protocol. RNA later frozen tissue samples (~50mg per extraction) were disrupted by placing the tissue in a 2mL microcentrifuge tube with 1mL of TRIzol and a 3mm stainless steel bead. The tubes were loaded into the Tissue Lyser II which was run at full speed for 1.5 mins, until the sample was completely broken down. All tubes were centrifuged at 12,000 x g for 10 mins at 4ºC to precipitate cell debris (and stainless steel bead). The supernatant was transferred to a clean tube and 200µL of chloroform added. The tubes were vigorously mixed for 15 seconds and

incubated for 3 mins at room temperature before centrifugation at 12,000 x g for 15 mins at 4ºC. At this point, the samples had separated into 3 phases: an upper aqueous phase containing RNA and some DNA, an interphase containing DNA and an organic phase containing proteins and lipids. 600µL of the upper aqueous phase were transferred into a new tube containing 500µL of isopropanol/2-propanol. Samples were then vortexed for 30 seconds and incubated at -20ºC for 30 mins. After incubation, samples were centrifuged at 12,000 x g for 10 mins at 4ºC. The supernatant was removed and discarded without disturbing the white gel-like RNA pellet. This was resuspended in 1mL of 75% ethanol, prepared with nuclease-free water. The samples were centrifuged at 7,600 x g for 5 minutes at 4ºC. The supernatant was removed and a second ethanol wash performed. The remaining pellet was air dried for 2 mins to evaporate residual ethanol before being dissolved in 35µL nuclease-free water. Samples were then incubated at 55ºC for 5 mins to dissolve RNA and stored at -80ºC. RNA quantity was determined by measurement of absorbance at 260nm using a NanoDrop spectrophotometer. A260/280nm and A260/230nm ratios were checked to assess presence of non-nucleic acid contaminants. RNA quality was evaluated by 2% agarose gel electrophoresis with SYBR SAFE staining, where the presence of 28S and 18S ribosomal RNAs as discrete bands, with minimal smearing indicative of RNA degradation, or high molecular weight products, indicative of DNA contamination, was assessed.

2.24 cDNA synthesis

1000ng of tissue RNA per sample was reversed transcribed using the Omniscript RT kit and oligo dT primers. A 20µL total reaction volume contained 1X reaction buffer, 16ng Oligo dT, 1µM dNTP solution, 1µL of Omniscript reverse transcriptase enzyme and 1000ng RNA, with nuclease-free water making up the remainder. Required RNA quantities were calculated using the RNA quantity determined by the NanoDrop. The reaction was carried out in a Techne

Prime thermocycler, incubating at 37°C for 1 hour before a 5 mins 95°C phase to denature the enzyme. cDNA solutions were diluted 1:10 in nuclease-free water before storage at -20°C.

2.25 Quantitative PCR primer design

Primer-BLAST (http://www.ncbi.nlm.nih.gov/tools/primer-blast/) was used to design qPCR primers, supplying the GenBank accession number and specifying a product of between 70 and 250bp in length, which spanned an exon-exon junction to avoid amplification of any contaminating genomic DNA and was gene-specific. All primers were synthesised by Integrated DNA Technologies in lyophilised form and resuspended in the lab in nuclease-free water. Primer solutions were aliquoted into working stocks to avoid excessive freeze-thaw.

2.26 Quantitative PCR

PowerUp SYBR Green Master Mix and StepOnePlus Real-time PCR System with StepOne Software v2.3 was used for endometrial stromal cell experiments. A 10µL reaction volume contained 8µL pre-made qPCR master mix, primers, 2µL cDNA and nuclease-free water. A non-template control was included in each gene assay to detect molecular contamination. All reactions were carried out in triplicate. The thermocycling program was: 10 min polymerase activation at 95°C, 40 cycles of 95°C for 30 sec, primer-specific annealing temperature for 1 min, 72°C for 30 sec; dissociation curve analysis at 95°C for 1 min, 55°C for 30 sec and 95°C for 30 sec.

After all qPCR assays, the absence of an amplification product within the non-template control was confirmed by absence of a plate Cq value and dissociation curves were checked for absence of non-specific amplification as determined by the presence of a single amplification peak.

Levels of gene of interest (GOI) expression were determined as a ratio of abundance compared with *B2M*, [ratio=2(-CtGOI)/2(-CtGAPDH)]. *B2M* has been selected as the most

stable gene across all samples from a panel of possible housekeeping genes (*GAPDH*, *B2M*, *HPRT*, and *RPS9*) and was analysed using geNorm software version 3.4 (Vandesompele et al., 2002). Raw Ct values were used for the geNorm analysis. geNorm calculates the gene expression stability measure (M) for a reference gene as the average pairwise variation for that gene with all other tested reference genes.

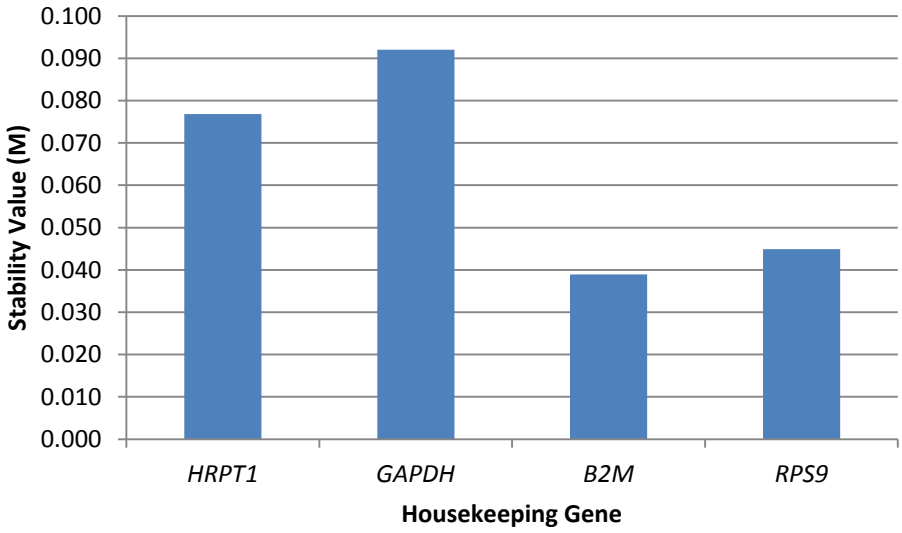

Figure 2- 3 GeNorm analysis of housekeeping genes in liver tissue samples

Healthy and tumour liver tissues were used to perform geNorm analysis. The housekeeping genes *HRPT1*, *GAPDH*, *B2M* and *RPS9* were used in this analysis, their M values are plotted above.

2.27 Quantitative PCR assay optimisation

The StepOnePlus machine was used to run a temperature gradient qPCR with annealing phase temperatures of 55-65°C. The optimal temperature was assessed via examination of dissociation curves for a single peak and via 2% gel electrophoresis, choosing a temperature which resulted in the brightest band of expected size.

Optimal primer concentration was determined by titration. The concentration which achieved the lowest Cq value while still generating a single product (single band after gel electrophoresis, single peak on dissociation curve) was selected.

The efficiency of each primer set with the specified reaction conditions was determined by running a reaction with 5 point 5-fold or 2-fold serial dilutions of the positive control cDNA, using the 2-fold series where the positive control Cq values were in high twenties and upwards. The standard curves were represented as the semi-log regression line plot of Cq value vs. log of the relative input cDNA concentration. The efficiencies were calculated using formula:

$E = 10(-1/Slope)-1;$

$\%E= (10(-1/Slope)-1) \times 100$

Efficiencies between 85% and 110% were considered acceptable. Where an efficiency of >100% was found, a 100% efficiency was used in calculations. The specificity of each primer set was determined by Sanger sequencing (GATC Biotech, Konstanz, Germany) of PCR products, examining electropherograms for single peaks at each position to confirm a single amplicon and running the returned sequence through BLAST (http://blast.ncbi.nlm.nih.gov/Blast.cgi) to ensure the desired gene target was amplified.

2.28 Generation of tissue conditioned media

Wedge biopsies taken at the time of transplantation or during surgical resection of hepatic malignancy were used to generate tissue conditioned media. Tissue samples were measured and weighed. Tissue was then cut into sections measuring approximately $5mm^3$. These were placed in a 24-well culture plate. 500µl of X-VIVO media (Lonza) was added to each well and tissue was incubated for 72 hours at 37°C. Supernatants were transferred to Eppendorf tubes and centrifuged at 500 x g for 5 mins. Pelleted debris was discarded and supernatants were stored at -80^{o}C for long term storage.

2.29 Treatment of natural killer cells with liver conditioned media

$1x10^5$ natural killer cells, isolated by negative selection, from peripheral blood or liver perfusate were cultured in round bottomed 96 well plates. Culture media was made up of RPMI+ L-glutamine, 10% v/v Human AB serum, 100U/ml penicillin and 100µg/ml streptomycin, with IL-15 (5ng/ml). Additionally liver conditioned media was added to appropriate wells at either 5 or 10% v/v. Cell phenotype and transcription factor expression was measured at 3, 5, or 7 days.

2.30 Treatment of natural killer cells with tumour conditioned media, sodium lactate and lactic acid

$CD56^{bright}$ and $CD56^{dim}$ NK cells were isolated from liver perfusate by FACS. Cells were plated at $1x10^4$/well in 96-well round bottom plates. Various treatments were used over the course of this project, including tumour conditioned media (50% v/v), sodium lactate (10-20mM), lactic acid (10-20mM) and media with adjusted pH (pH 6.4-7.4). Unless otherwise stated in the figure legend, samples were incubated for 24 hours with respective treatments at 37^{o}C. Samples were then harvested and apoptosis was assessed as described above (section 2.22).

2.31 Enzyme linked immunosorbent assay (ELISA)

ELISA is a commonly used immunoassay used to quantify the amount of antigen or antibody present in a sample. ELISA kits for IL-15, TGF-β, and IL-10 from Peprotech were used. The working concentrations for the antibodies and standards used were obtained from the manufacturer's instructions and varied depending on the cytokine being measured. Each kit consisted of a capture and detection (biotin conjugated) antibody specific for different epitopes of a particular cytokine as well as a known standard quantity of the cytokine being measured and a streptavidin-horseradish peroxidise (HRP) solution.

ELISA plates were coated with 50µl of capture antibody diluted in PBS and sealed with paraffin strips to be incubated overnight at room temperature (RT^{o}) protected from light. Excess capture antibody was then removed by submerging the plates in wash buffer (PBS containing 0.5% v/v Tween 20) and then emptying the plates, this was repeated three times and the plates were then thoroughly dried by blotting on tissue paper. A serial dilution of the provided standard was carried out in PBS to give an eight point standard curve. 50µl of standards and tissue conditioned media were then added to each well and the plates were sealed with paraffin strips and incubated at RT^{o} for 60 mins protected from light. Unbound antigen was then removed by repeating the washing step outlined above. 50µl of detection antibody, diluted in PBS, was then added to each well and the plates were sealed with paraffin strips and incubated at RT^{o} for 60 mins protected from light. Unbound detection antibody was then removed by repeating the washing step. Fifty microliters of streptavidin-HRP diluted in PBS was then added to each well and the plates were incubated at RT^{o} for 20 mins protected from the light. Any unbound streptavidin-HRP was removed by repeating the wash step. 50µl of 3, 3', 5, 5'–tetramethylbenzidine (TMB) substrate solution was then added to each well and the plates were incubated at RT^{o} protected from light. The plates were left until the colour of the unknown samples matched that of the middle of the known standard samples. At which point, 25µl of 1M sulphuric acid was added to stop the enzyme reaction. Dual wavelength absorbance from each well was read at the appropriate wavelength according to the

manufacturer's instructions by the microplate reader. Standard curves were drawn using Microsoft Excel to determine unknown cytokine concentrations.

2.32 ATP determination assay

The assay was performed as per the manufacturer's instructions (Invitrogen). Reagents were prepared as follows:

- 1x reaction buffer was prepared by diluting 20x buffer in dH_2O
- 1ml of 10mM D-Luciferin was prepared by adding 1ml 1x Reaction buffer to vial of D-Luciferin.
- 100mM DTT was prepared by adding 1.62ml dH_2O to bottle containing 25mg DTT.
- ATP standards were supplied at 5mM and serial dilution was performed to prepare standard curves.

Standard reaction solution was prepared by combining the reagents in the following volumes:

- 8.9ml dH_2O
- 0.5ml 20X Reaction buffer
- 0.1ml 0.1M DTT
- 0.5ml 10mM D-Luciferin
- 2.5µl firefly luciferase (5mg/ml stock solution)

Solution was gently mixed and protected from light on ice until ready for use. Standards were prepared in dH_2O at concentrations of 500, 250, 125, 62.5, 31.25, 15.6 pmol/well. $1x10^5$ cells were plated in white 96 well flat bottomed plates and required treatments performed. Plates were spun at 500 x g for 5 mins and supernatants aspirated. Standards were added to appropriate wells. 50µl reaction solution was added to each well. Plate was protected from light until reading. Luminescence was measured on Fluoroskan Ascent FL (Labsystems).

Standards were used to generate a standard curve (Microsoft Excel) and sample ATP levels were calculated.

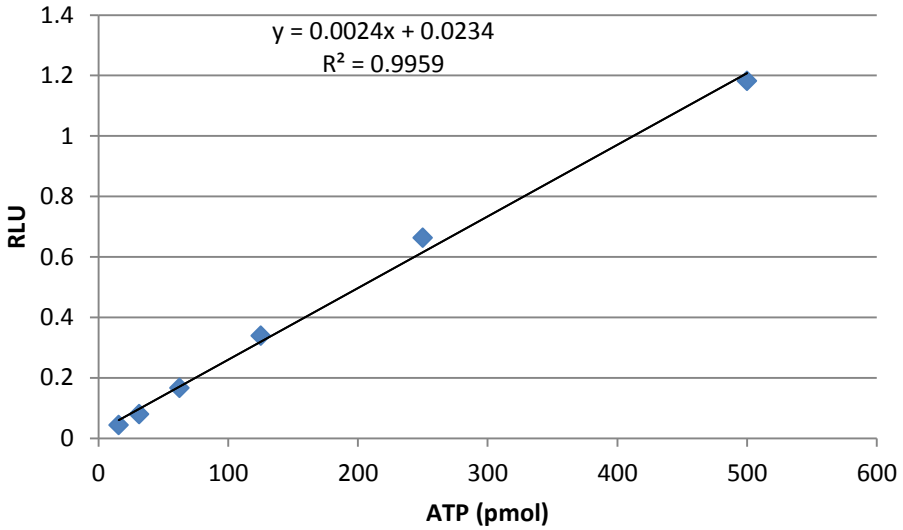

Figure 2- 4 Generation of standard curve for intracellular ATP levels.

ATP standards were provided by manufacturer and diluted in assay buffer to a top standard of 500pmol, serial dilution was performed to a lowest standard of 15.6pmol. Relative luminescence units (RLU) were plotted from the average of three replicates against ATP standard to construct a standard curve. Equation: y=-0.0024x+0.0234, R^2= 0.9959. Standard curve was used to determine intracellular ATP levels of experimental samples.

2.33 Glucose determination assay

This assay (Abcam) directly measures glucose levels in biological samples. The glucose enzyme mix specifically oxidizes glucose to generate a product which reacts with a dye to produce colorimetric and fluorometric signals. Reagents prepared as follows:

- Glucose Enzyme Mix- Reconstitute in 220µl Glucose assay buffer
- All other reagents provided ready to use

Standards were prepared by diluting 1nM glucose standard in glucose assay buffer to produce standards between 0-10nmol/well. 50µl/well of glucose reaction mix was prepared by combining 46µl glucose assay buffer, 2µl glucose probe, and 2µl glucose enzyme mix. 50µl reaction mix was added to each standard and sample well in 96 well ELISA plate. Plates were incubated at 37^{o}C for 30 mins. Colorimetric output was measured at OD 570nm. Standards were used to prepare a standard curve (Microsoft Excel) and sample absorbance were used to calculate amount of glucose per well. The following equation was used to calculate the concentration of glucose.

$$\text{Glucose concentration} = \left(\frac{Sa}{Sv}\right) * D$$

Where: Sa= amount of glucose calculated/well, Sv= Sample Volume, D=Dilution factor

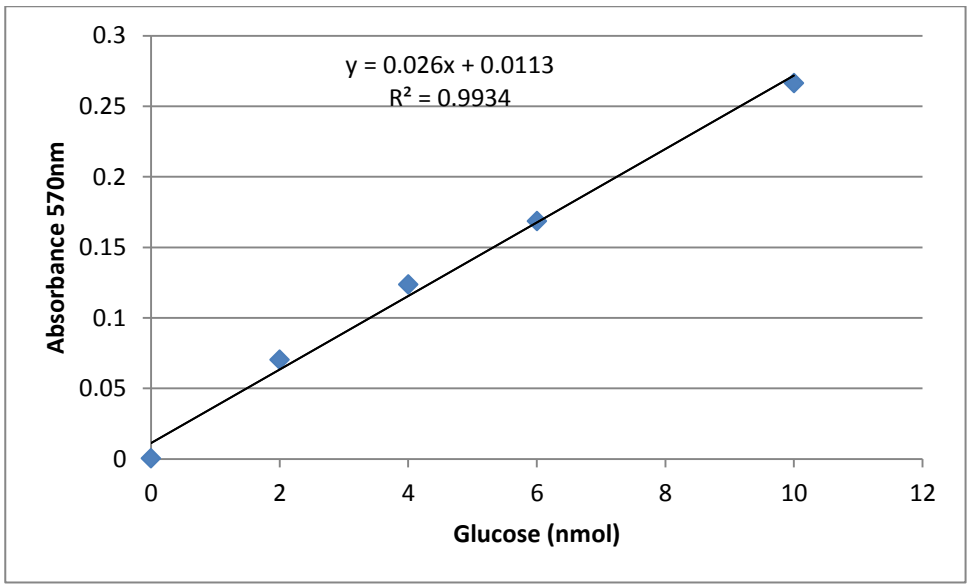

Figure 2- 5 Generation of standard curve for glucose levels

Glucose standards were provided by manufacturer and diluted in assay buffer to a top standard of 10 nmol, serial dilution was performed to a lowest standard of 2 nmol. Absorbance values (570nm) were plotted from the average of three replicates against Glucose standard to construct a standard curve. Equation: y=-0.026x+0.0113, R^2= 0.9934. Standard curve was used to determine glucose levels of experimental samples.

2.34 Lactate Assay

L(+)-Lactate is a metabolic compound formed in animals by the action of the enzyme Lactate Dehydrogenase (LDH). Lactate is produced in proliferating cells and during anaerobic conditions such as exercise. L(+)-Lactate is the major stereoisomer of lactate formed in human intermediary metabolism and is present in blood at levels of 1–2 mM. This kit (Sigma-Aldrich) provides a convenient means for detecting L(+)-Lactate in biological samples, lactate concentration is determined by enzymatic assay, which results in a colorimetric signal (570nm). The assay was carried out as per the manufacturer's instructions. Reagents were provided in a ready to use format. Lactate standard (100nmol/µl) was diluted 1:100 in lactate assay buffer to generate a 1nmol/ml standard. 2-10µl of standard was then added to respective wells to prepare 0-5 nmol/well standards. Lactate assay buffer was added to each well to bring the final volume to 50µl. Conditioned media was diluted 1:50 in lactate assay buffer. 50µl of diluted sample was applied to each well. Assay reaction buffer was prepared as follows: 46µl Lactate Assay buffer, 2µl lactate enzyme mix, 2µl lactate probe. 50µl of Assay reaction buffer was then added to each well and incubated at RT^{o} for 30 mins. Absorbance was then read at 570nm. Standards were used to generate a standard curve for the calculation of unknown samples (Microsoft Excel). The equation below was used to calculate the concentration of lactate in each sample.

Lactate concentration= $(\frac{Sa}{Sv}) * D$

Where: Sa= amount of lactate calculated/well, Sv= Sample Volume, D=Dilution factor

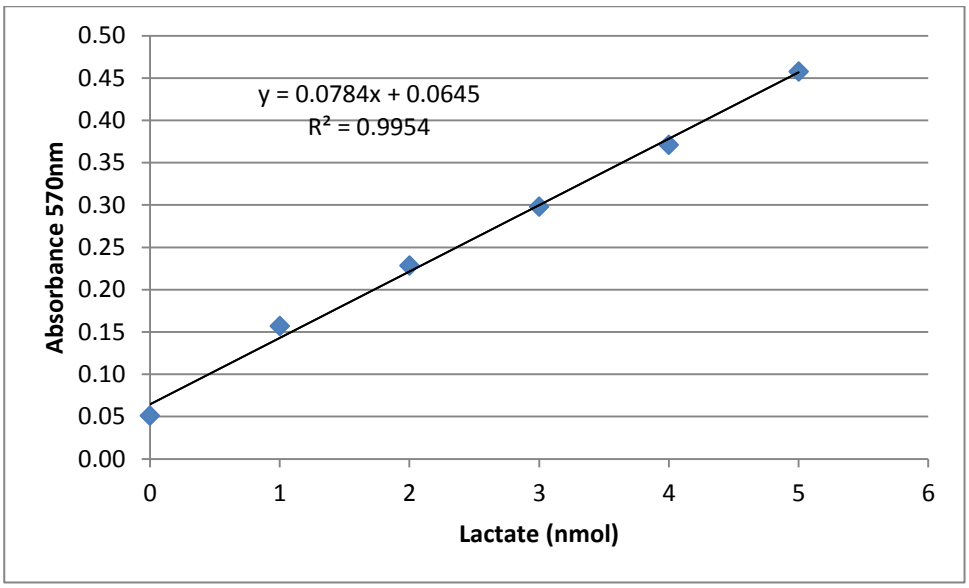

Figure 2- 6 Generation of standard curve for lactate levels

Lactate standards were provided by manufacturer and diluted in assay buffer to a top standard of 5 nmol, serial dilution was performed to a lowest standard of1 nmol. Absorbance values (570nm) were plotted from the average of three replicates against lactate standard to construct a standard curve. Equation: y=-0.0784x+0.0645, R^2= 0.9954. Standard curve was used to determine glucose levels of experimental samples.

2.35 Chemotaxis Assay

A transwell assay was used to determine the chemotactic properties of conditioned medias on liver NK cells (Conroy et al., 2016). An insert containing a 5µm polycarbonate membrane was inserted into a sterile 24-well plate, creating an upper and lower chamber. The lower chamber was filled with 600µl serum free RPMI supplemented with 10% healthy liver or tumour conditioned media. NK cells isolated from liver perfusate were serum starved for 2 hours in RPMI at 37^{o}C. NK cells were then transferred to fresh serum-free media and 1x10^{5} NK cells were applied to the upper chamber of the wells and incubated for 2 hours at 37^{o}C. Inserts were then removed and media from lower chamber was aspirated into FACS tubes. Samples were centrifuged at 500 x g for 5 mins and resuspended in FACS buffer. Cell counts were performed using 123Count eBeads on an LSR Fortessa. Cell count/ml was calculated based on counting beads collected (see section 2.15 for details).

2.36 Generation of humanized mice

Tg (PGK1-KITLG*220)441Daw/SzJ (hu-mSCF) mice were obtained from Jax (Bar Harbor, Maine, USA). All procedures involving mice were performed according to the Irish Health Products Regulatory Authority regulations. Humanized mice were generated by injecting of 1×10^{5} human cord blood CD34^{+} stem cells from two donors (Lonza, Slough, Berkshire, UK) into lateral tail veins of 10-14 week old mice approximately 24 hours post irradiation (2.4 Gy). Human cell reconstitution was assessed by flow cytometry 13 weeks post engraftment. Livers were excised, perfused and transported to the tissue culture facility in complete RPMI (with 10% FBS and 1% penstrep). The isolation of hepatic lymphocytes by mechanical dissection was carried out as follows: the liver was thoroughly dissected and gently passed through a 70µm filter using a syringe plunger. Filter was washed thoroughly in 10ml PBS. The filtrate was centrifuged at 50 x g for 1 min and the supernatant was collected. Resuspended cells were isolated by density centrifugation using Ficoll-Paque™ PLUS (GE

Healthcare, Uppsala, Sweden). After centrifugation with 2000 rpm for 20 mins, the interphase was collected. This cell suspension was then centrifuged at 1500 rpm for 5 mins. Cell numbers and viability were assessed by staining with trypan blue under light microscopy.

2.37 Statistical analysis

Statistical analysis was carried out using Prism GraphPad Version 5.0. Appropriate statistical tests were used to compare data in selected experiments. Comparison of more than two unmatched groups was performed using Kruskal-Wallis test, with Dunn's multiple comparison test. For paired comparisons, Friedman test with Dunns multiple comparison tests was used for more than two groups, Wilcoxon signed rank test was used for comparison of two matched groups. For comparison of two unmatched groups, Mann Whitney U test was used. Within an experiment, *, ** and *** represent $p<0.05$, $p<0.01$ and $p<0.001$ respectively.

CHAPTER 3:

Characterisation of hepatic natural killer cells in healthy donor liver

3.1 Introduction

The adult human liver is an organ of predominantly innate immunity with large populations of myeloid and innate lymphoid cells, particularly natural killer (NK) cells (Crispe, 2009; Doherty et al., 1999; Doherty and O'Farrelly, 2000; Hata et al., 1990). Indeed, over 40% of the hepatic lymphoid population are NK cells, making the liver the most 'NK populated' organ in the body. NK cells are group 1 innate lymphoid cells (ILC), important in anti-viral and tumour immunity (Spits and Di Santo, 2011). More recently, as the diversity of NK cell populations has become increasingly recognised, they have been attributed with additional functions including metabolic, immunoregulatory and tissue remodelling activities (Freud et al., 2017; Lynch et al., 2009; Maini and Peppa, 2013; Moffett-King, 2002).

Liver NK cell populations are likely to be important for viral and tumour surveillance, as well as tissue homeostasis and immune regulation. However, these divergent functions have yet to be attributed to distinct NK cell subsets. In human peripheral blood, subsets of NK cells are readily distinguished by the level of CD56 expression. $CD56^{bright}$ NK cells are potent producers of immunoregulatory cytokines, such as IFN-γ and TNF-α, while $CD56^{dim}$ NK cells are potent cytotoxic effector cells, and produce less cytokines than the $CD56^{bright}$ population (Cooper et al., 2001a). These functional distinctions have been ascribed to circulating NK cells; tissue resident NK cell populations have been less well characterised, although they have been shown to be phenotypically distinct from their peripheral blood counterparts, displaying markers of activation and enhanced cytotoxic functions (Hata et al., 1990; Moroso et al., 2010; Norris et al., 1998). It has been hypothesised that local development and the tissue microenvironment contribute to distinct tissue-specific subpopulations of NK cells (Golden-Mason et al., 2000; Lysakova-Devine and O'Farrelly, 2014; Shi et al., 2013).

Much of our knowledge of NK cell development comes from murine studies of bone marrow differentiation, which have identified several essential transcription factors which regulate each stage of maturation. Such studies have identified the transcription factors eomesodermin

(Eomes) and T-bet as essential for the final stages of maturation, regulating the transition from immature to mature NK cell (Daussy et al., 2014; Freud et al., 2006, 2005; Freud and Caligiuri, 2006; Gordon et al., 2012; Yu et al., 2013). Despite their similarity, they are thought to have both redundant and non-redundant roles in this process. T-bet is acquired during NK cell precursor differentiation and stabilizes the immature NK cell phenotype; Eomes is required for further differentiation and acquisition of effector function, including cytotoxicity. A population of murine hepatic NK cells, characterised as $CD49a^{+}$ $DX5^{-}$, have been shown to mature independently of Eomes, suggesting a new pathway of NK cell differentiation for this subpopulation. Expression of chemokine (C-X-C motif) receptor 6 (CXCR6) by these $CD49a^{+}$ $DX5^{-}$ NK cells is believed to be important for homing to and retention in the liver (Paust et al., 2011). Liver sinusoidal endothelial cells provide a constant source of CXCL16, the ligand for CXCR6, which retains NK cells in the sinusoidal space (Hudspeth et al., 2015; Parker et al., 2013). An $Eomes^{-}$ $CD49a^{+}$ population of NK cells was demonstrated in human liver tissue, accounting for a small proportion of hepatic NK cells (0.11-12.7%) and were only identifiable in around 40% of samples in this study (Marquardt et al., 2015). They did, however, display phenotypical and functional features in common with murine liver resident NK cells. These tissue resident NK cells account for only a fraction of the total pool of liver NK cells. This project aimed to characterise the full hepatic repertoire of NK cells in humans and identify other tissue resident populations.

We also aimed to assess what signals from the tissue microenvironment are required for the acquisition of tissue resident phenotype. The impact of the tissue microenvironment on the differentiation of immune cells has proven difficult to investigate, as significant differences arise between humans and mice in several organs including the liver and uterus. For example the immune repertoire of the liver differs significantly between humans and mice, with an enrichment of NK cells in humans compared to mice (Gao et al., 2008). Additionally, replicating the microenvironment of a complex organ such as the liver, which possesses

significant immune cell populations as well as immunologically active parenchymal cells, is equally difficult. However, it has become increasingly evident that tissue microenvironments play a substantial role in defining the phenotype and function of immune cells residing in it. Uterine NK cells are poorly cytotoxic but produce a range of cytokines and growth factors required for vascular remodelling (VEGF) and successful embryo implantation (Hanna et al., 2006). Alteration of the uterine microenvironment alters NK cell differentiation and drastically decreases fertility (Glover et al., 2018; Thiruchelvam et al., 2016). Here, we have developed an *in vitro* culture system which aims to replicate the hepatic microenvironment, with an aim to assess the effect of tissue signals on the maintenance of tissue resident NK cell populations.

Investigating human liver resident NK cells has previously proven difficult due in part to access to healthy human tissues. This project utilised donor liver perfusate as a source of unaltered hepatic leukocytes. Healthy liver tissue is difficult to obtain and requires enzymatic and mechanical dissociation to obtain a single cell suspension. This treatment can result in alterations in the phenotype of NK cells (Curry et al., 2000). Liver perfusate offers an easily accessible liquid starting material that does not require enzymatic treatment. Previous work by our group has shown no significant difference in the proportion of NK cell subsets in liver perfusate compared to biopsies (Fahey et al, unpublished). We have further compared perfusate and biopsy-acquired NK cells for phenotypic profiling of liver resident cells. Accurate functional assessment requires a pure population of unmodified NK cells. Using negatively selected hepatic NK cells, we have been able to assess the degranulation (CD107a expression (Alter et al., 2004)) and cytokine secretion of liver resident populations in response to tumour cells and cytokine stimulation. Using liver conditioned media, we have shown that hepatic NK cells require liver derived factors to maintain their phenotype and the function of peripheral blood NK cells is altered after culture in this microenvironment.

Hypothesis:
Hepatic NK cells are phenotypically and functionally distinct from peripheral blood NK cells.

Aims:

1. Characterise the diversity of NK cell populations in adult human liver.
2. Determine if the human liver contains populations of tissue resident NK cells.
3. Determine if hepatic NK cells are functionally distinct from peripheral blood NK cells.
4. Identify the factor(s) which causes changes in NK cell phenotype in the liver.

3.2 Results

3.2.1 Study samples

Samples from 62 transplant donors were collected. Organ donors ranged in age from 18-73 years (mean 43.3 years). Protocol requires that donor organs must be transplanted within 12 hours of retrieval from the donor. Variation in ischaemic time for each sample was due to transportation time from donor organ retrieval site to the transplant theatre. Samples transported from the United Kingdom had the longest transportation time to the SVUH operating theatre. The majority of cases provided matched donor resting transport medium (RTM) (n=57), donor liver flush (n=55), donor blood (n=50) and where possible a donor biopsy (n=40). In each case, samples were processed immediately upon retrieval from the transplant theatre. Previous work by our group demonstrated no significant differences in the populations isolated from RTM or flush fractions. Therefore RTM and flush samples were combined and are hence referred to liver perfusate.

Due to inter-individual variation in liver size and technical difficulties in collecting flush samples, considerable variation was seen in the amount of material collected from each procedure. On average 885ml (±28ml n=57) of RTM and 80.5ml (±2.85ml n=55) of liver flush was collected per transplant. In addition, a matching 5ml donor blood sample was received in most cases (n=50). 40 matched donor biopsies were also collected, these ranged in weight from 0.02-0.3g. Tissue samples were digested to produce single cell suspensions, stored in RNAlater & formalin, used for the generation of liver conditioned media or used for other on-going projects.

Table 3-3 Samples retrieved from liver transplants

Sample Source	Type of Sample	Number
Donor	Liver flush	55
	Resting Transport Medium	57
	Matched Blood	50
	Matched Liver biopsy	40

3.2.2 Isolation of hepatic mononuclear cells

Hepatic mononuclear cells (HMNC's) were isolated as previously described (Jonsson et al., 1997; Kelly et al., 2014). Significant variability was seen in the number of HMNCs isolated from both the RTM and liver flush. On average, 32.1 x 10^6 (±6 x 10^6, n=57) HMNCs were isolated from the RTM and 10.9 x 10^6 (±1.9 x 10^6, n=55) from the flush, the maximum counts of HMNCs were 183 x 10^6 and 53.2 x 10^6 respectively (**Figure 3-1B**). The RTM contained significantly more cells than the liver flush (p=0.016), this is likely due to the larger starting volume (**Figure 3-1A**). The liver flush contains significantly more cells/ml (0.14±0.02 x 10^6/ml) compared to the RTM (0.04±0.008 x 10^6/ml, **Figure 3-1C**). Cell viability was initially assessed by trypan exclusion, with all sample viabilities in excess of 96%.

3.2.3 Immunophenotyping of hepatic mononuclear cells

HMNCs or PBMCs, isolated from liver perfusate (LP), liver biopsy (LB) or donor peripheral blood (PB), were stained with fluorescently labelled monoclonal antibodies to characterise hepatic and peripheral NK cell phenotypes. HMNCs are highly enriched in NK cells accounting for 49.4±2.2% (n=62) of liver perfusate lymphocytes compared to 32.6±2.7% of lymphocytes from liver biopsies (n=31) and only 18.4±1.7% of lymphocytes in the donor blood (n=50) (**Figure 3-2C**). $CD56^{bright}$ NK cells were enriched in liver perfusate (47.5±2.2%) and biopsy (56.6±3.5%); while significantly fewer $CD56^{bright}$ NK cells were detected in peripheral blood (7.9±1%) (**Figure 3-2D**). The ratio of $CD56^{dim}$ $CD16^{+}$ to $CD56^{bright}$ $CD16^{+/-}$ NK cells in the perfusate varied between individuals from 0.3:1 to 4:1, and was distinct from peripheral blood where the ratio was usually greater than 10:1. The proportion of hepatic NK cells was not affected by age, sex or CMV status of donor (**Figure 3-3 A-C**). The variation in $CD56^{dim}$ $CD16^{+}$ to $CD56^{bright}$ $CD16^{+/-}$ hepatic NK cell ratios was not attributable to the age, sex or CMV status of the organ donor (**Figure 3-3 D-F**).

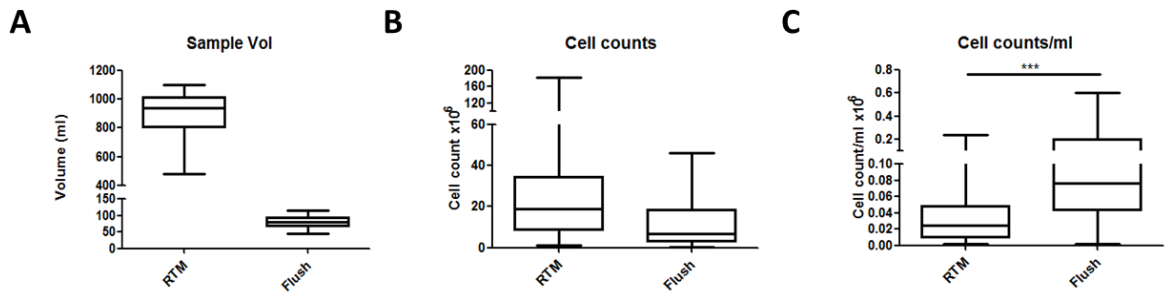

Figure 3- 1 Characterisation of transplant samples.

(A) Volume (ml) of resting transport media (RTM) (n=57) and liver flush (n=55) obtained during liver perfusion. **(B)** Total cell yield (x 10^6) from RTM and liver flush. **(C)** Cell yield as a proportion of starting volume (x10^6/ml). Data presented as mean ± SEM., ***, $p < 0.001$. Data was analysed using Wilcoxon matched pairs test.

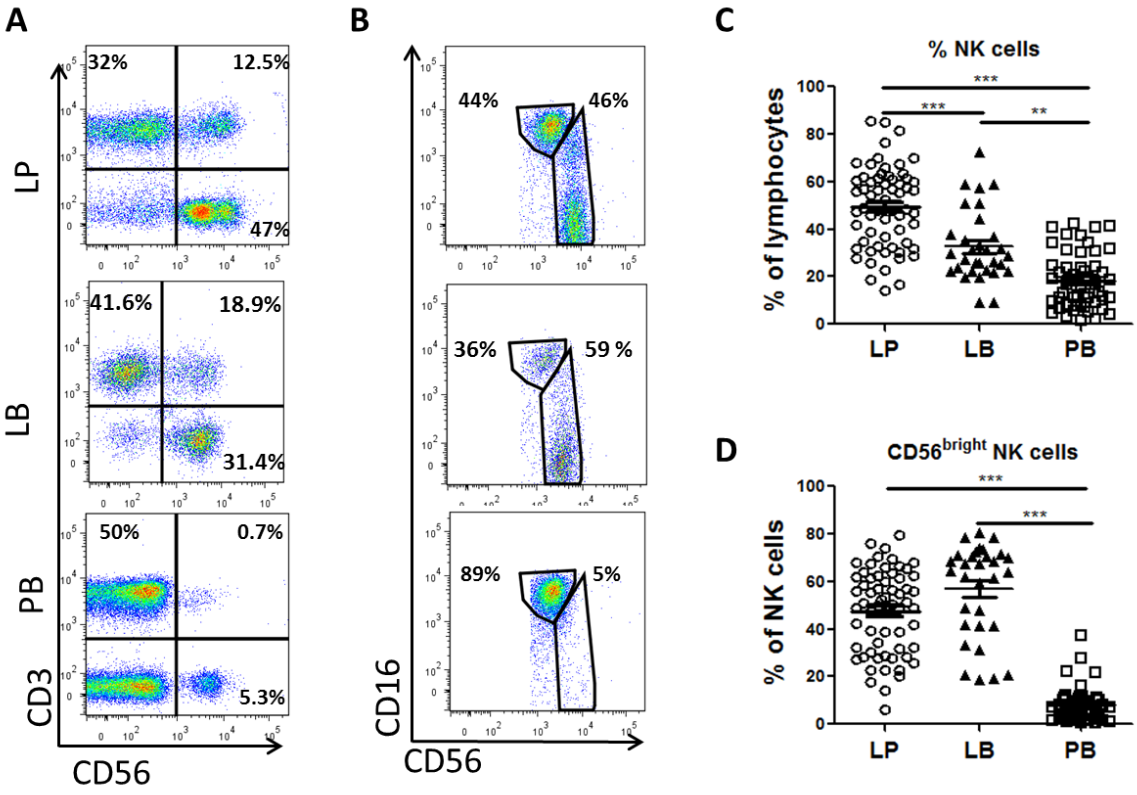

Figure 3- 2 Natural killer cell subsets in liver perfusate and peripheral blood

Mononuclear cells, isolated from liver perfusate (LP), liver biopsy (LB) and matched peripheral blood (PB), were stained with monoclonal antibodies Gating strategy: NK cells were identified from the $CD45^+$ lymphocyte gate as $CD56^+CD3^-$. $CD56^{bright}$ $CD16^{-/+}$ and $CD56^{dim}$ $CD16^+$ subsets were then gated on. Non-viable cells were excluded by FVS780 staining. **(A)** Representative gating strategy for liver perfusate (LP), donor liver biopsy (LB) and peripheral blood (PB). NK cells were identified from viable $CD45^+$ lymphocytes as $CD56^+CD3^-$. **(B)** NK cell subsets were identified as $CD56^{bright}$ $CD16^{-/+}$ and $CD56^{dim}$ $CD16^+$. **(C)** Total NK cells in LP (o), LB (▲) PB (□) as a percentage of $CD45^+$ lymphocytes. **(D)** $CD56^{bright}$ $CD16^{-/+}$ NK cell frequencies in LP (o), DB (▲) and PB (□) as a percentage of total NK cells. Data analysed using Kruskal-Wallis test, with Dunn's multiple comparison test. (LP n=62, LB n=31, PB n=50, **, $p<0.01$, ***, $p<0.001$).

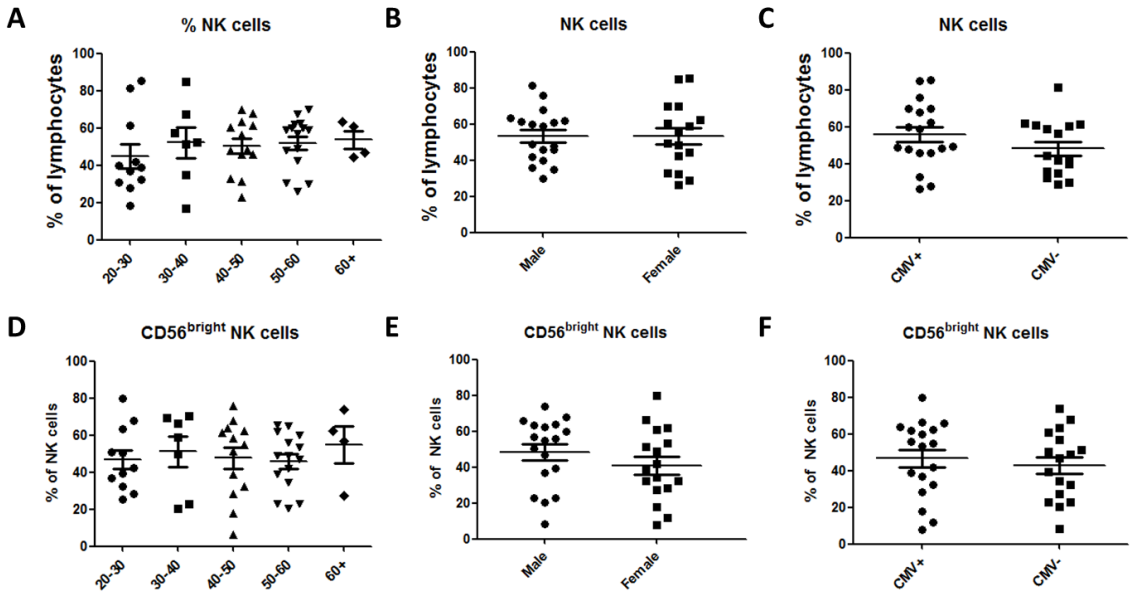

Figure 3- 3 The variability in NK cell heterogeneity is not related to age, sex or CMV status

The proportion of total natural killer (NK) cells and CD56^{bright} NK cells were analysed based on age, gender and CMV status of the donor. Donors were divided into five age groups; 20-30 (n=11), 30-40 (n=7), 40-50 (n=13), 50-60 (n=15) and 60+ (n=4), two gender groups; male (n=18) or female (n=16), and CMV positive (n=18) or CMV negative (n=16). The percentage of NK cells in liver perfusate from donors of different age groups **(A)**, in male and female donors **(B)** and in CMV positive and negative donors **(C)** The percentage of CD56^{bright} NK cells in liver perfusate from donors of different age groups **(D)**, in male and female donors **(E)** and in CMV positive and negative donors **(F).** Age group data was analysed using Kruskal-Wallis test, with Dunn's multiple comparison test. Sex and CMV status data was analysed using Mann-Whitney U test.

3.2.4 Expression of NKG cytotoxicity receptors on NK cell subsets

NKG2D, a C-type Lectin binding receptor which recognises stress induced ligands such as MIC-A, MIC-B and ULBPs, is expressed on the majority of both hepatic and peripheral blood NK cells, but is significantly increased in $CD56^{bright}$ hepatic NK cells (MFI 876.3±270 vs 518.4±111.3, p=0.0078, **Figure 3-4B**). The expression of the activatory receptor NKG2C, which recognises HLA-E molecules, was significantly lower in $CD56^{bright}$ hepatic NK cells (8.6±2.3%) compared to their blood counterparts (19.07±6.1%, p=0.0017) (**Figure 3-4C**). Expression of the related inhibitory receptor NKG2A, was higher in both $CD56^{bright}$ (13.2±10.5%, p=0.02) hepatic NK populations compared to matched peripheral blood NK cells (5.1±3.8%, **Figure 3-4D**).

NKG2D was similar in hepatic $CD56^{dim}$ NK cells compared to peripheral blood (MFI 561.7±192.7 vs 411.4±99.4, p=, **Figure 3-5B**). $CD56^{dim}$ hepatic NK cells also had lower expression of NKG2C compared to peripheral blood $CD56^{dim}$ NK cells (7.9±2.4% vs 13.4±4.2%, p=0.0018, **Figure 3-5C**). NKG2A was also differentially expressed between hepatic and peripheral $CD56^{dim}$ NK cells (9.0±5.6% vs 3.2±1.8%, p=0.009, **Figure 3-5D**).

3.2.5 Expression of NCR cytotoxicity receptors on NK cell subsets

Hepatic NK calls also have distinct expression of the natural cytotoxicity receptors NKp44 and NKp46. NKp46 is expressed on the majority of both peripheral and hepatic NK cells, although slightly more hepatic $CD56^{bright}$ NK cells express this receptor (MFI 1271±400) than peripheral cells (MFI 884±513, p=0.0313, **Figure 3-6C**). No differences were seen between natural cytotoxicity receptor expression on hepatic and peripheral $CD56^{dim}$ NK cells (**Figure 3-6D)**. NKp44 is an activatory receptor which is not expressed on resting NK cells.

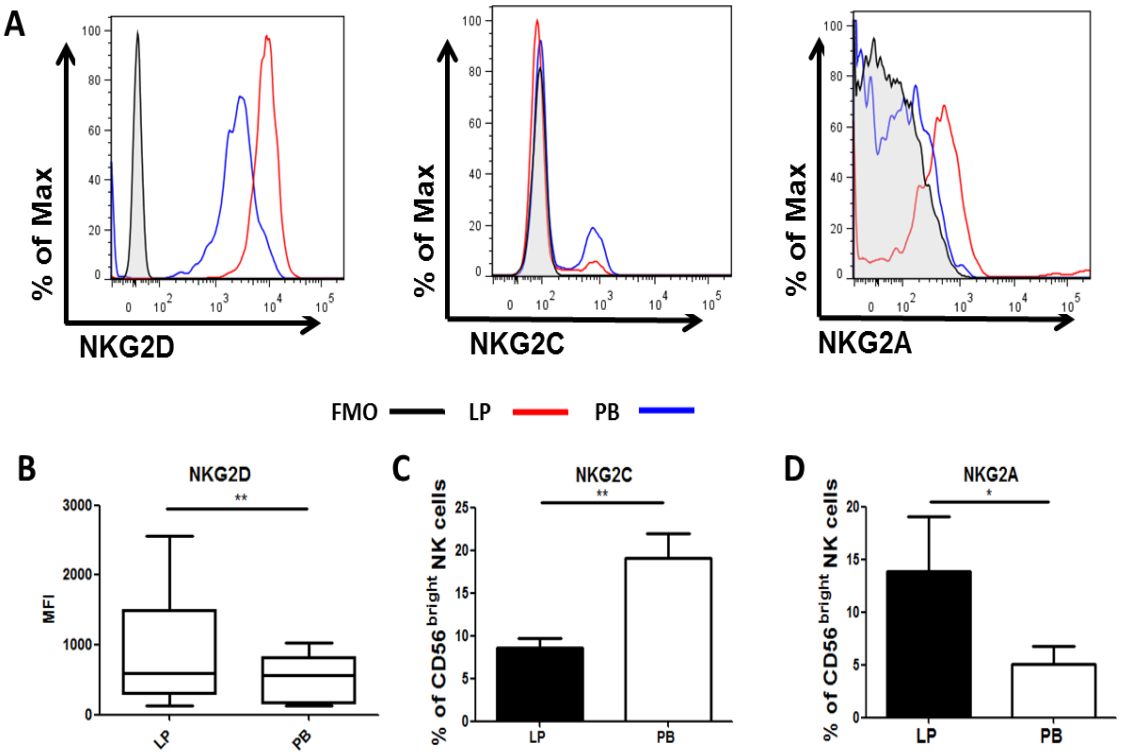

Figure 3- 4 Expression of NKG2 receptors by CD56^{bright} natural killer cell

Mononuclear cells isolated from liver perfusate (LP) and matched peripheral blood (PB), were stained with monoclonal antibodies. NK cells were identified from the CD45^{+} lymphocyte gate as CD56^{+}CD3^{-}. CD56^{bright} CD16$^{-/+}$ and CD56^{dim} CD16^{+} subsets were then gated on. Non-viable cells were excluded by FVS780 staining. **(A)** Representative histograms of NKG2D, NKG2C and NKG2A expression (LP-red, PB-blue, FMO-black). **(B-D)** Expression of NKG2D **(B)**, NKG2C **(C)**, and NKG2A **(D)** in CD56^{bright} NK cells from LP (black bars) and PB (white bars). Data presented as mean ± SEM. Data analysed using Wilcoxon matched pairs test. (n=18, * $p<0.05$, ** $p<0.01$)

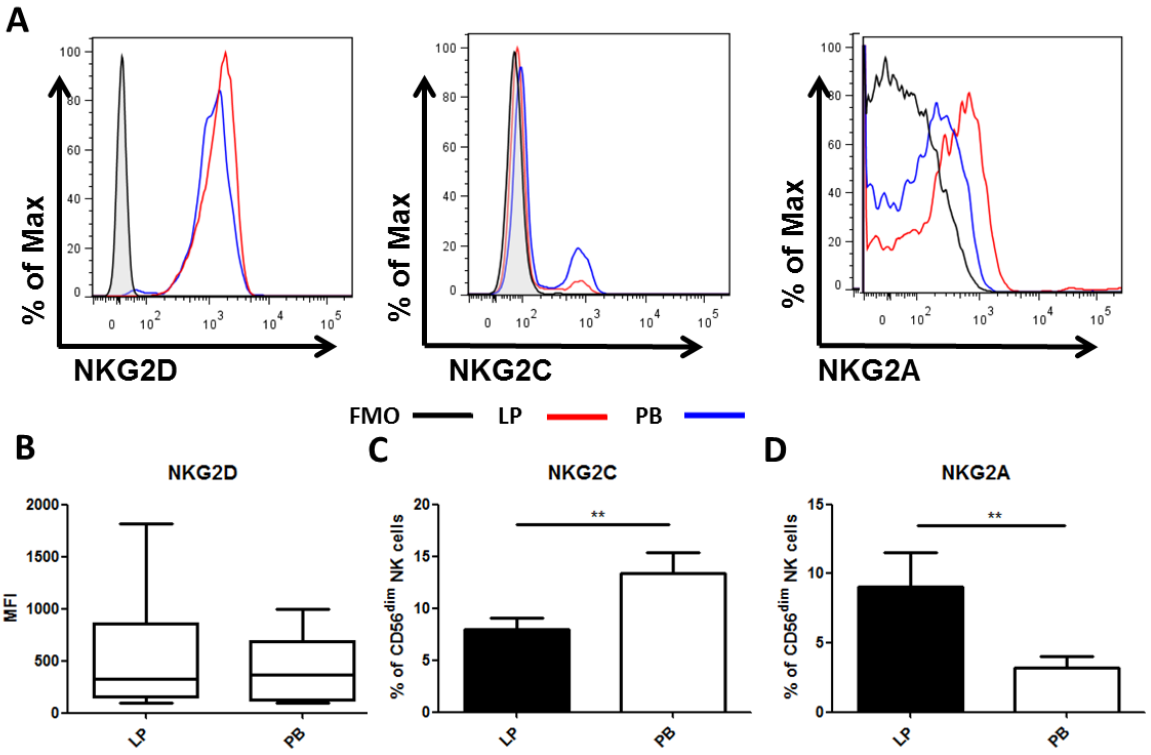

Figure 3- 5 Expression of NKG2 receptors by CD56^{dim} natural killer cell

Mononuclear cells isolated from liver perfusate (LP) and matched peripheral blood (PB), were stained with monoclonal antibodies. NK cells were identified from the CD45^{+} lymphocyte gate as CD56^{+}CD3^{-}. CD56^{bright} CD16$^{-/+}$ and CD56^{dim} CD16^{+} subsets were then gated on. Non-viable cells were excluded by FVS780 staining. **(A)** Representative histograms of NKG2D, NKG2C and NKG2A expression (LP-red, PB-blue, and FMO-black). **(B-D)** Expression of NKG2D **(B)**, NKG2C **(C)**, and NKG2A **(D)** in CD56^{dim} NK cells from LP (black bars) and PB (white bars). Data presented as mean ± SEM. Data analysed using Wilcoxon matched pairs test. (n=18, * $p<0.05$, ** $p<0.01$)

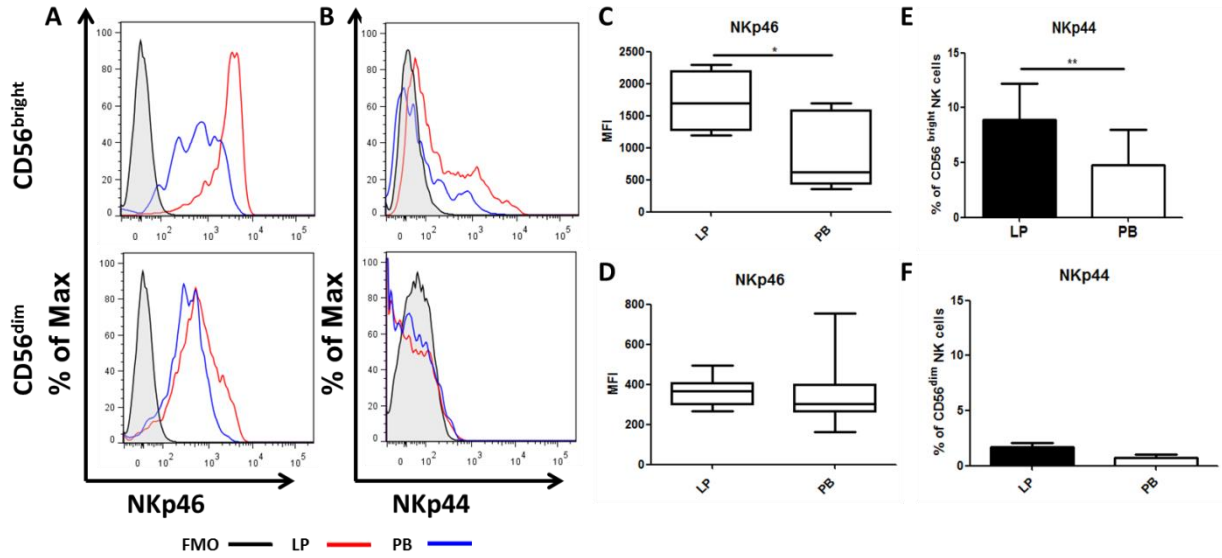

Figure 3- 6 Expression of NCRs by natural killer subsets

Mononuclear cells isolated from liver perfusate (LP) and matched peripheral blood (PB), were stained with monoclonal antibodies. NK cells were identified from the $CD45^{+}$ lymphocyte gate as $CD56^{+}CD3^{-}$. $CD56^{bright}$ $CD16^{-/+}$ and $CD56^{dim}$ $CD16^{+}$ subsets were then gated on. Non-viable cells were excluded by FVS780 staining. **(A)** Representative histograms of NKp46 expression in $CD56^{bright}$ and $CD56^{dim}$ NK cells (LP-red, PB-blue, and FMO-black). **(B)** Representative histograms of NKp44 expression in $CD56^{bright}$ and $CD56^{dim}$ NK cells (LP-red, PB-blue, and FMO-black). **(C, D)** Expression of NKp46 in $CD56^{bright}$ and $CD56^{dim}$ NK cells from LP (black bars) and PB (white bars). **(E, F)** Expression of NKp44 in $CD56^{bright}$ and $CD56^{dim}$ NK cells from LP (black bars) and PB (white bars). Data presented as mean ± SEM. Data analysed using Wilcoxon matched pairs test. (n=18, * $p<0.05$, ** $p<0.01$).

Not surprisingly NKp44 is low or absent on peripheral blood NK cells but the NKp44^{+} population is significantly increased in the hepatic CD56^{bright} NK cell population (5.7±3.6%, p=0.0029, **Figure 3-6E**) confirming the previously described activated phenotype of hepatic NK cells (Moroso et al., 2010). The receptor is not differentially expressed on CD56^{dim} NK cells from the liver or blood (**Figure 3-6F**).

3.2.6 Intracellular expression of cytotoxic molecules by NK cell subsets

To assess the cytotoxic potential of these hepatic NK cells, we examined expression of the cytotoxic molecules perforin, granzyme B, granzyme A and granzyme K. Hepatic CD56^{bright} NK cells have lower expression of granzyme B (MFI 678±306) compared to blood CD56^{bright} cells (MFI 2021±1258, p=0.0313, **Figure 3-7B**). However, it is unusual for CD56^{bright} NK cells in the peripheral blood to express granzyme B at rest. Due to the trauma suffered by organ donors prior to organ and blood donation, it is possible that peripheral and liver NK cells undergo activation *in vivo* (Sotosek Tokmadzic et al., 2012; Spitzer et al., 2017). Alternatively, long term storage of blood samples (up to 12 hours) and transport and handling may lead to the release of pro-inflammatory cytokines (Duffy et al., 2017) and activation of NK cells *ex vivo*. Granzyme B expression was not seen in CD56^{bright} NK cells from fresh healthy donors (Supplemental Figure 1). No significant difference was observed in the expression of perforin or granzyme A between hepatic and peripheral blood CD56 ^{bright} NK cells (**Figure 3-7C-D**). Granzyme K was significantly increased in hepatic CD56^{bright} NK cells compared to peripheral blood counterparts (MFI 422.5±51.7 vs 225.8±23.1, p=0.0381, **Figure 3-7E**). CD56^{dim} NK cells did not differ in their expression of granzyme A, granzyme B, granzyme K or perforin (**Figure 3-8B-E**).

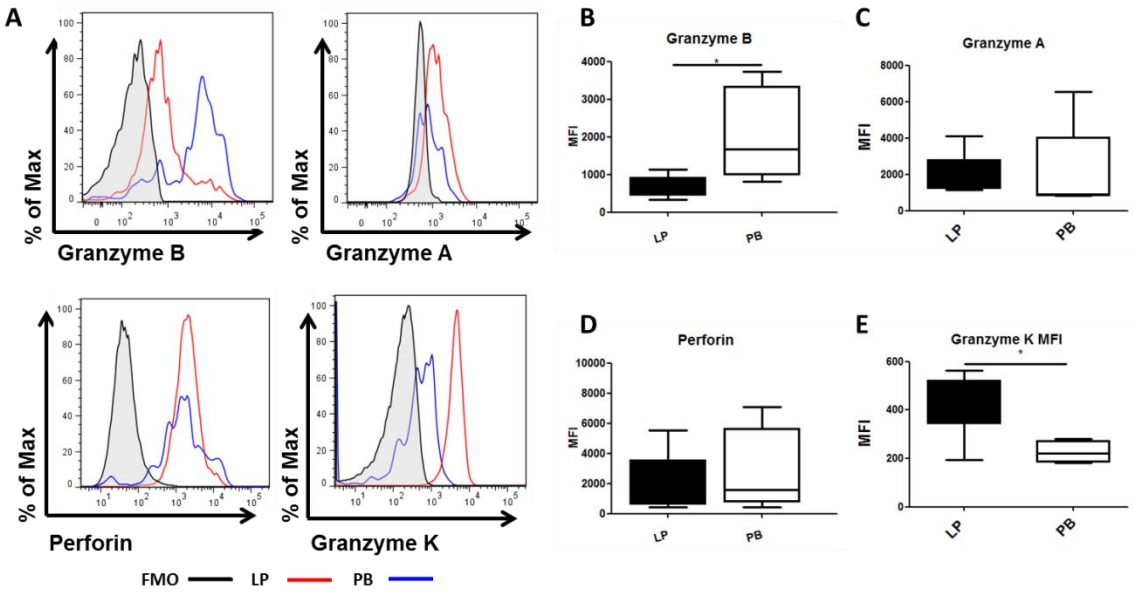

Figure 3- 7 Intracellular expression of cytotoxic molecules by CD56^{bright} natural killer cell

Mononuclear cells isolated from liver perfusate (LP) and matched peripheral blood (PB), were stained with monoclonal antibodies. NK cells were identified from the CD45^{+} lymphocyte gate as CD56^{+}CD3^{-}. CD56^{bright} CD16$^{-/+}$ and CD56^{dim} CD16^{+} subsets were then gated on. Non-viable cells were excluded by FVS780 staining **(A)** Representative histograms of granzyme B, granzyme A, granzyme K and perforin expression in CD56^{bright} NK cells (LP-red, PB-blue, and FMO-black). **(B-D)** MFI values of granzyme B **(B)**, granzyme A **(C)**, perforin **(D)**, and granzyme K **(E)** expression in CD56^{bright} NK cells from LP and PB. Data presented as mean ± SEM. Data analysed using Wilcoxon matched pairs test. (n=6, * $p<0.05$)

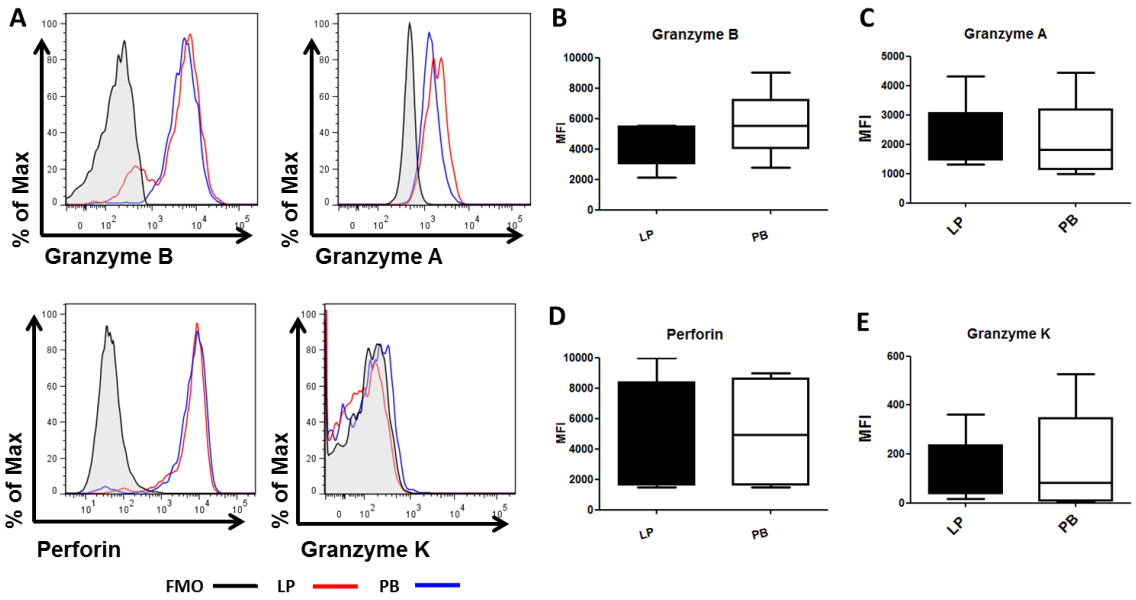

Figure 3- 8 Intracellular expression of cytotoxic molecules by CD56^{dim} natural killer cell

Mononuclear cells isolated from liver perfusate (LP) and matched peripheral blood (PB), were stained with monoclonal antibodies. NK cells were identified from the CD45^{+} lymphocyte gate as CD56^{+}CD3^{-}. CD56^{bright} CD16$^{-/+}$ and CD56^{dim} CD16^{+} subsets were then gated on. Non-viable cells were excluded by FVS780 staining **(A)** Representative histograms of granzyme B, granzyme A, granzyme K and perforin expression in CD56^{dim} NK cells (LP-red, PB-blue, and FMO-black). **(B-D)** MFI values of granzyme B **(B)**, granzyme A **(C)**, perforin **(D)**, and granzyme K **(E)** expression in CD56^{dim} NK cells from LP and PB. Data presented as mean ± SEM. Data analysed using Wilcoxon matched pairs test. (n=6, * $p<0.05$)

3.2.9 Degranulation and IFN-γ production of hepatic and peripheral blood NK cells

To examine cytotoxic function, NK cells were isolated by negative selection from donor perfusate and healthy donor blood. Viability of hepatic and peripheral blood NK cells was 98.6±0.7% and 96.3±0.5% respectively. NK cells were identified as $CD56^{+}$ $CD3^{-}$ lymphocytes. Purity of hepatic NK cells was 95.9±0.7% and 93.2±1.2% for peripheral blood NK cells. Hepatic and peripheral blood NK cells were incubated with MHC class I deficient K562 target cells in the presence or absence of IL-2. Degranulation was assessed by the expression of CD107a on the surface of NK cells (Alter et al., 2004). CD107a is found on the internal membrane of the lysosome, during degranulation the contents of the lysosome are excised and CD107a appears on the outer cell membrane. Hepatic NK cells display significantly higher CD107a expression compared to peripheral blood NK cells from healthy donors. This difference was most evident between $CD56^{bright}$ NK cells. In the absence of cytokine stimulation hepatic $CD56^{bright}$ NK cells display enhanced CD107a expression compared to peripheral blood counterparts (28.6±2.5% vs 9.3±1.3%, p=0.011, **Figure 3-9B**). No significant difference was seen between hepatic and peripheral blood $CD56^{dim}$ NK cells (13.5±2.7% vs 11.9±1.5%, p=0.8, **Figure 3-9C**). With the addition of IL-2, expression of CD107a increased in hepatic $CD56^{bright}$ NK cells (53.2±8.6%) and hepatic $CD56^{dim}$ cells (38.8±10.4%). These levels were not significantly different from peripheral blood subsets. This is in contrast to the peripheral blood where $CD56^{bright}$ NK cells are primarily cytokine producers and display low levels of cytotoxicity. $CD56^{bright}$ hepatic NK cells produced significantly less IFN-γ in response to IL-2 alone (3.2±1.7% vs 25.2±7.5%, p=0.02, **Figure 3-9D**) and in combination with target cells compared to peripheral blood $CD56^{bright}$ NK cells (21.4±7.5% vs 58.2±6.7%, p=0.01, **Figure 3-9D**). No significant differences were noted in IFN-γ production between $CD56^{dim}$ NK cells from liver or peripheral blood (**Figure 3-9E**).

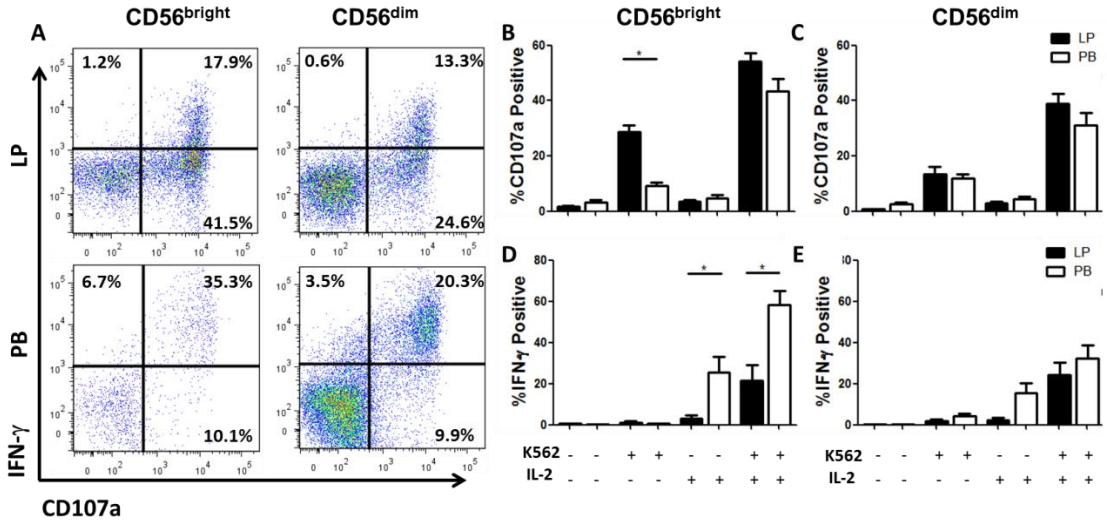

Figure 3- 9 Comparison of degranulation and IFN-γ production between hepatic and peripheral blood NK cells.

NK cells were isolated by negative selection by MACS from liver perfusate (LP) and healthy donor buffy coats (PB). Purified NK cells were untreated or stimulated with IL-2 (50ng/ml) for 18hrs. NK cells were then co-incubated with K562 cells (MHC Class I-deficient myeloid leukaemia cell line) for 4 hours. CD107a antibody was added simultaneously. After 1 hour, 4µg/ml of Golgi-stop (containing monensin) was added. NK cells were identified from the $CD45^{+}$ lymphocyte gate as $CD56^{+}CD3^{-}$. $CD56^{bright}$ $CD16^{-/+}$ and $CD56^{dim}$ $CD16^{+}$ subsets were then gated on. Non-viable cells were excluded by FVS780 staining **(A)** Representative flow plots of CD107a and IFN-γ expression from LP and PB NK cell subsets **(B)** Degranulation of $CD56^{bright}$ NK cells from liver perfusate (black bars) and peripheral blood (white bar) in response to target cells, IL-2 and combination. **(C)** Degranulation of $CD56^{dim}$ NK cells from liver perfusate (black bars) and peripheral blood (white bar) in response to target cells, IL-2 and combination. **(D)** Production of IFN-γ by $CD56^{bright}$ NK cells from liver perfusate (black bars) and peripheral blood (white bar) in response to target cells, IL-2 or combination **(E)** Production of IFN-γ by $CD56^{dim}$ NK cells from liver perfusate (black bars) and peripheral blood (white bar) in response to target cells, IL-2 or combination. Data presented as mean ± SEM. Data was analysed using Kruskal-Wallis test, with Dunn's multiple comparison test (LP n=7, PB n=5, *$p<0.05$).

3.2.10 Expression of transcription factors Eomes and Tbet

The transcription factors Eomes and T-bet are essential for normal NK cell differentiation in the bone marrow. A novel population of Eomes^{-} NK cells have been described in murine liver and more recently in human liver in both healthy and malignant tissue (Daussy et al., 2014; Marquardt et al., 2015). This Eomes^{-} NK cell population was not detectable in human liver perfusate, liver biopsy or peripheral blood, although a unique population of Eomes^{hi} T-bet^{lo} NK cells was identified in liver perfusate and liver biopsies from all donors. This population accounts for nearly 50% of liver perfusate NK cells (47.2±3.4%), and 61.7±2.8% of biopsy NK cells (**Figure 3-10B**). Less than 2% of peripheral blood NK cells express this phenotype (1.8±0.6%, **Figure 3-10B**). The Eomes^{lo} Tbet^{hi} population made up the remaining hepatic NK cell numbers and most of peripheral blood NK cells (**Figure 3-10C**). The Eomes^{hi} T-bet^{lo} phenotype is almost exclusively confined to the CD56^{bright} subset. In liver perfusate 89.5±1.8% of CD56^{bright} cells are Eomes^{hi} T-bet^{lo}, while only 7.5±1.5% of perfusate CD56^{dim} NK cells possesses this phenotype (**Figure 3-11B&D**). Similarly, 87.5±4% of biopsy CD56^{bright} NK cells were Eomes^{hi} Tbet^{lo}, with only 2.8±1% of CD56^{dim} NK cells sharing this phenotype (**Figure 3-11B&D**). Small proportions of blood CD56^{bright} and CD56^{dim} NK cells were also Eomes^{hi} T-bet^{lo} (10.4±2.3% and 1.8±0.5% respectively, **Figure 3-11B&D**). The majority of liver perfusate, biopsy and blood CD56^{dim} NK cells had an Eomes^{lo} Tbet^{hi} phenotype **(Figure 3-11C&E)**.

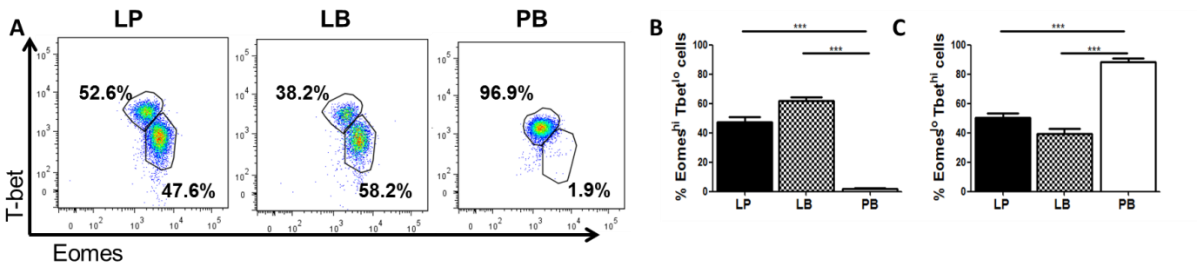

Figure 3- 10 Expression of transcription factors Eomes and Tbet in NK cells

Mononuclear cells isolated from liver perfusate (LP), liver biopsy (LB) and matched peripheral bloods (PB) were stained with monoclonal antibodies. NK cells were identified from the $CD45^{+}$ lymphocyte gate as $CD56^{+}CD3^{-}$. Non-viable cells were excluded by FVS780 staining **(A)** Representative plots of Eomes and Tbet expression from LP, LB and PB NK cells. **(B)** The percentage of NK cells from LP (black bars), LB (grey bars) and PB (white bar) with an $Eomes^{hi}$ $Tbet^{lo}$ phenotype **(C)** The percentage of NK cells from LP (black bars), LB (grey bars) and PB (white bar) with an $Eomes^{hi}$ $Tbet^{lo}$ phenotype. Data presented as mean ± SEM. Data was analysed using Kruskal-Wallis test, with Dunn's multiple comparison test (LP & PB n=21, LB=5 ***$p<0.001$).

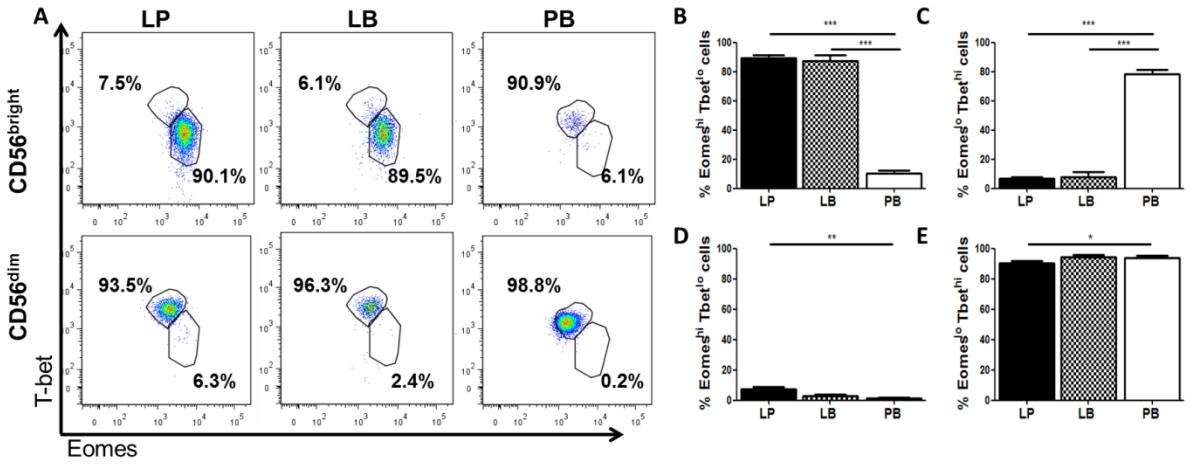

Figure 3- 11 Expression of transcription factors Eomes and Tbet in NK cell subsets

Mononuclear cells isolated from liver perfusate (LP), liver biopsy (LB) and matched peripheral bloods (PB) were stained with monoclonal antibodies. NK cells were identified from the $CD45^{+}$ lymphocyte gate as $CD56^{+}CD3^{-}$. $CD56^{bright}$ $CD16^{-/+}$ and $CD56^{dim}$ $CD16^{+}$ subsets were then gated on. Non-viable cells were excluded by FVS780 staining **(A)** Representative plots of Eomes and Tbet expression in liver perfusate (LP), liver biopsy (LB) and peripheral blood (PB) NK cell subsets. **(B)** The percentage of $CD56^{bright}$ NK cells from LP (black bars), LB (grey bars) and PB (white bar) with an $Eomes^{hi}$ $Tbet^{lo}$ phenotype **(C)** The percentage of $CD56^{bright}$ NK cells from LP (black bars), LB (grey bars) and PB (white bar) with an $Eomes^{lo}$ $Tbet^{hi}$ phenotype **(D)** The percentage of $CD56^{dim}$ NK cells from LP (black bars), LB (grey bars) and PB (white bar) with an $Eomes^{hi}$ $Tbet^{lo}$ phenotype **(E)** The percentage of $CD56^{bright}$ NK cells from LP (black bars), LB (grey bars) and PB (white bar) with an $Eomes^{lo}$ $Tbet^{hi}$ phenotype. Data presented as mean ± SEM. Data was analysed using Kruskal-Wallis test, with Dunn's multiple comparison test (LP & PB n=21, LB=5, *p<0.05, **p<0.01, ***p<0.001).

3.2.11 Functional comparison of Eomes^{hi} Tbet^{lo} and Eomes^{lo} Tbet^{hi} NK cells

Due to the enhanced degranulation of the hepatic CD56^{bright} NK cell population and the fact that the hepatic CD56^{bright} NK cell population is enriched for the Eomes^{hi} T-bet^{lo} phenotype, we examined the response of Eomes^{hi} T-bet^{lo} and Eomes^{lo} T-bet^{hi} subsets to target cell and cytokine stimulation. Hepatic NK cells were incubated with target cells, K562 cells, in the presence or absence of IL-2. Data from Figure 3-9 was reanalysed to identify CD56^{bright} subsets based on Eomes and T-bet expression two subsets were examined: Eomes^{hi} Tbet^{lo} and Eomes^{lo} T-bet^{hi}. No difference was seen in CD107a expression between Eomes^{hi} Tbet^{lo} and Eomes^{lo} T-bet^{hi} subsets from liver perfusate (26.7±3% vs 22.4±2.6%, p=0.08) regardless of cytokine stimulation (53.7±4.7% vs 50.6±4.3%, p=0.8, **Figure 3-12B**). However, a significantly lower proportion of Eomes^{hi} T-bet^{lo} NK cells express IFN-γ with cytokine stimulation (0.66±0.6% vs 2.4±1.1%, p=0.01) and cytokine target cell combination (13.8±6.7% vs 26.1±4.9%, p=0.02, **Figure 3-12D**).

3.2.12 Hepatic CD56^{bright} NK cells express markers of tissue residency

To assess whether these phenotypically distinct NK cells were indeed tissue resident, we measured the expression of CXCR6 a chemokine receptor which recognises CXCL16, a chemokine produced in large amounts by liver sinusoidal endothelial cells (Hudspeth et al., 2015; Parker et al., 2013), CD69 a marker of tissue residency (Mackay et al., 2015), CD49a and TRAIL (both markers associated with tissue resident murine NK cells (Daussy et al., 2014; Gordon et al., 2012; Paust et al., 2011)). In contrast to the peripheral blood (3.1±2.0%), the majority of hepatic CD56^{bright} NK cells express CXCR6 (LP 68.3±8.1%, LB 28.3±7.2%, p=0.0002, **Figure 3-13B**). This phenotype is not reflected in the CD56^{dim} population which do express low levels of CXCR6 in the liver perfusate (1.2±0.3%), liver biopsy (1.5±0.7%) or peripheral blood (0.13±0.1%, p=0.01, **Figure 3-13C**). CD69 was expressed on nearly all CD56^{bright} NK cells from liver perfusate (96.2±0.96%), liver biopsy (92.7±4.7%) but only a small proportion of peripheral blood cells (20.2±12.1%, p=0.04, **Figure 3-13D**). CD69 is

expressed by a small proportion of hepatic and peripheral blood $CD56^{dim}$ NK cells (LP 5.9±3.3%, LB 13.4±8.1%, PB 4.4±1.9%, p=0.73, **Figure 3-13E**).

CD49a has previously been shown, in murine and humans, to be expressed on a population of tissue resident NK cells (Daussy et al., 2014; Marquardt et al., 2015). $CD56^{bright}$ CD49a positive cells were only detectable in liver samples, with a higher proportion in liver biopsy compared to liver perfusate (LP 0.57±0.18%, LB 6.25±2.3%, PB 0%, p=0.1, **Figure 3-14B**). However, this population did not share the $Eomes^{-}$ phenotype previously described. Similarly, $CD56^{dim}$ NK cells only expressed CD49a in liver samples but at lower levels than $CD56^{bright}$ hepatic NK cells (LP 0.1±0.1%, LB 2.9±1.3%, PB 0.03±0.03, p=0.19, **Figure 3-14C**).

TRAIL expression has been shown in tissue resident NK cells in patients with HBV and murine hepatic NK cells (Gordon et al., 2012; Peppa et al., 2013; Stegmann et al., 2016). However, TRAIL does not appear to be highly expressed in healthy liver, at levels similar to peripheral blood. $CD56^{bright}$ NK cells from liver perfusate (3.8±0.9%), liver biopsy (4.3±1.3%), and peripheral blood (3.9±1.3%) showed no significant differences in TRAIL expression (p=0.93, **Figure 3-14D**). TRAIL was expressed at similar levels in $CD56^{dim}$ NK cells from liver perfusate (5.1±2.4%), liver biopsy (4.1±0.9%) and peripheral blood (2.0±0.8%, p=0.32, **Figure 3-14E**).

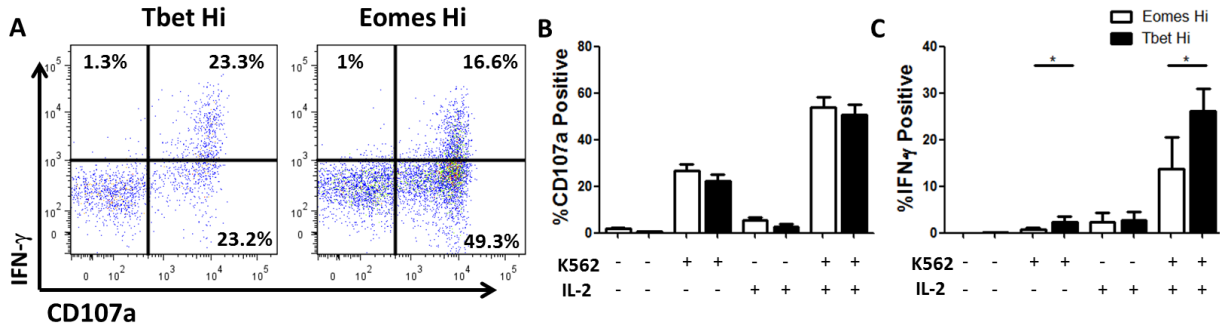

Figure 3- 12 Comparison of degranulation and IFN-γ production between hepatic NK cell subsets.

NK cells were isolated by negative selection by MACS from liver perfusate Purified NK cells were untreated or stimulated with IL-2 (50 ng/ml) for 18hrs. NK cells were then co-incubated with K562 cells (MHC Class I-deficient myeloid leukaemia cell line) for 4 hours. CD107a antibody was added simultaneously. After 1 hour, 4µg/ml of Golgi-stop (containing monensin) was added. NK cells were identified from the $CD45^{+}$ lymphocyte gate as $CD56^{bright}CD3^{-}$. $Eomes^{hi}$ $Tbet^{lo}$ and $Eomes^{lo}$ $Tbet^{hi}$ subsets were identified as before. Non-viable cells were excluded by FVS780 staining **(A)** Representative dot plots of CD107a and IFN-γ expression from $Eomes^{hi}$ $Tbet^{lo}$ and $Eomes^{lo}$ $Tbet^{hi}$ NK cell subsets **(B)** Degranulation of $Eomes^{hi}$ $Tbet^{lo}$ (white bar) and $Eomes^{lo}$ $Tbet^{hi}$ (black bars) NK cells from liver perfusate in response to target cells, IL-2 and combination. **(C)** Production of IFN-γ by $Eomes^{hi}$ $Tbet^{lo}$ (white bar) and $Eomes^{lo}$ $Tbet^{hi}$ (black bars) NK cells from liver perfusate in response to target cells, IL-2 and combination Data presented as mean ± SEM. Data was analysed using Friedman test, with Dunn's multiple comparison test (n=7, *$p<0.05$).

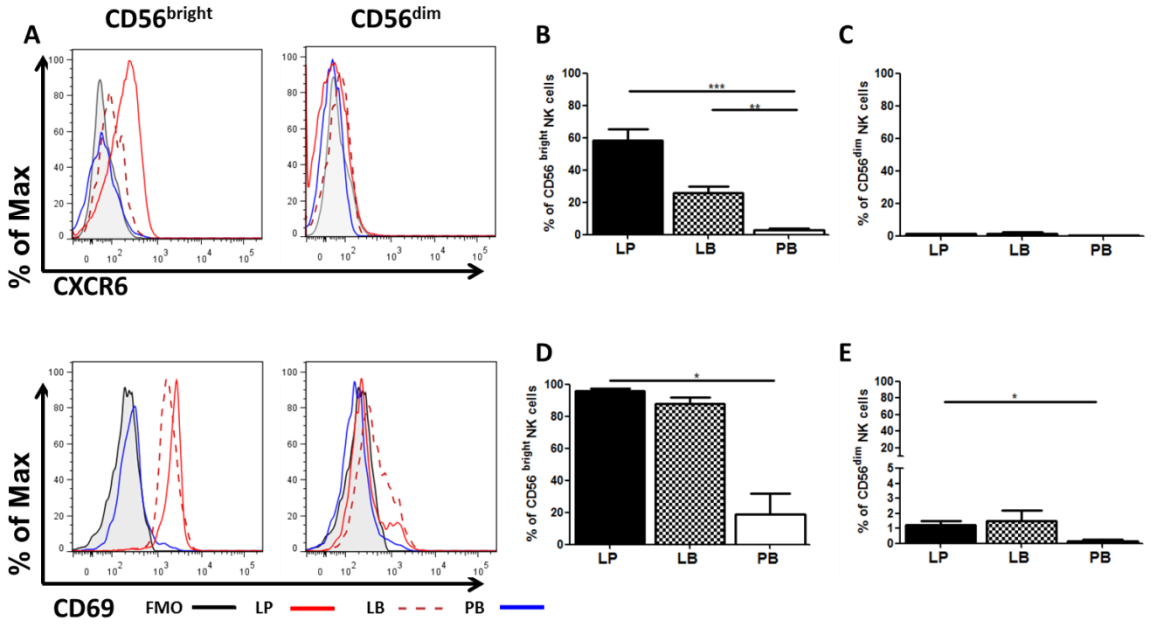

Figure 3- 13 Expression of tissue residency markers CXCR6 and CD69 on natural killer cell subsets

Mononuclear cells isolated from liver perfusate (LP), liver biopsy (LB) and matched peripheral bloods (PB) were stained with monoclonal antibodies. NK cells were identified from the $CD45^{+}$ lymphocyte gate as $CD56^{+}CD3^{-}$. $CD56^{bright}$ $CD16^{-/+}$ and $CD56^{dim}$ $CD16^{+}$ subsets were then gated on. Non-viable cells were excluded by FVS780 staining **(A)** Representative histograms of CXCR6 and CD69 expression in LP (solid red line), LB (dashed red line) and PB (blue line) NK cell subsets (FMO black) **(B)** Percentage of CXCR6 positive $CD56^{bright}$ NK cells in LP (black bar), LB (grey bar) and PB (white bar) **(C)** Percentage of CXCR6 positive $CD56^{dim}$ NK cells in LP (black bar), LB (grey bar) and PB (white bar) **(D)** Percentage of CD69 positive $CD56^{bright}$ NK cells in LP (black bar), LB (grey bar) and PB (white bar) **(E)** Percentage of CD69 positive $CD56^{dim}$ NK cells in LP (black bar), LB (grey bar) and PB (white bar). Data presented as mean ± SEM. Data was analysed using Kruskal-Wallis test, with Dunn's multiple comparison test (LP & PB n=8, LB=5 p*<0.05, p**<0.01, ***p<0.001).

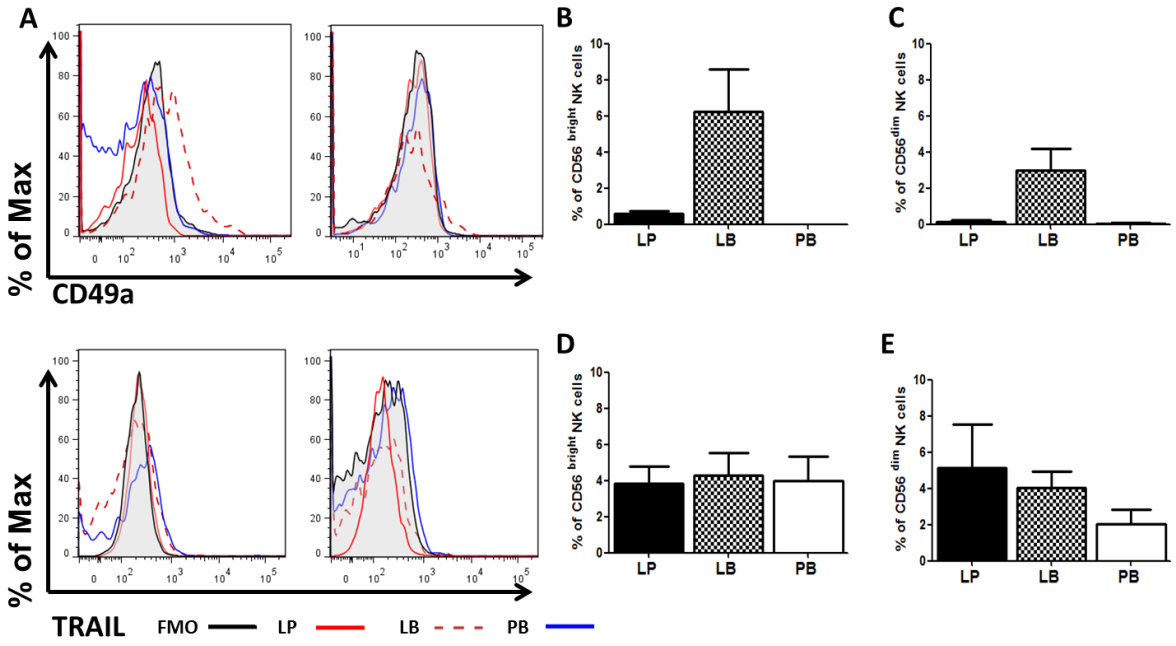

Figure 3- 14 Expression of tissue residency markers CD49a and TRAIL on natural killer cell subsets

Mononuclear cells isolated from liver perfusate (LP), liver biopsy (LB) and matched peripheral bloods (PB) were stained with monoclonal antibodies. NK cells were identified from the $CD45^{+}$ lymphocyte gate as $CD56^{+}CD3^{-}$. $CD56^{bright}$ $CD16^{-/+}$ and $CD56^{dim}$ $CD16^{+}$ subsets were then gated on. Non-viable cells were excluded by FVS780 staining **(A)** Representative histograms of CD49a and TRAIL expression in LP (solid red line), LB (dashed red line) and PB (blue line) NK cell subsets (FMO black) **(B)** Percentage of CD49a positive $CD56^{bright}$ NK cells in LP (black bar), LB (grey bar) and PB (white bar) **(C)** Percentage of CD49a positive $CD56^{dim}$ NK cells in LP (black bar), LB (grey bar) and PB (white bar) **(D)** Percentage of TRAIL positive $CD56^{bright}$ NK cells in LP (black bar), LB (grey bar) and PB (white bar) **(E)** Percentage of TRAIL positive $CD56^{dim}$ NK cells in LP (black bar), LB (grey bar) and PB (white bar). Data presented as mean ± SEM. Data was analysed using Kruskal-Wallis test, with Dunn's multiple comparison test (LP & PB n=8, LB=5).

3.2.13 Characteristic Eomes^{hi} Tbet^{lo} hepatic phenotype is lost in culture

In order to determine whether the phenotype of hepatic NK cells is permanently altered by residing within the liver microenvironment , NK cells were isolated from liver perfusate and cultured in RPMI supplemented with human AB serum, to more closely replicate the peripheral blood microenvironment. It was necessary to supplement this culture with IL-15 (5ng/ml) in order to maintain NK cell viability and expression of CD56 (Carson et al., 1997; Dunne et al., 2001). NK cells were cultured for 7 days with the culture media replaced every 2-3 days.

CD56^{bright} hepatic NK cells have a unique pattern of expression of these transcription factors, characterised by reduced expression of Tbet. In culture this phenotype is reversed, with Tbet increasing significantly between day 0 (MFI 461.5±255.5) and day 7 (MFI 1214±572, p=0.042, **Figure 3-15C**). At the same time Eomes expression increased slightly between day 0 and 7 (p=0.3, **Figure 3-15E**). In CD56^{dim} hepatic NK cells, Tbet remained stable throughout the experiment with the MFI ranging between 2007 MFI at day 0 and 1550 MFI at day 7 (p=0.69, **Figure 3-15D**). Eomes expression also increased between day 0 (MFI 1463±516) and day 7 (MFI 3364±1807, **Figure 3-15F**).

CXCR6 expression differentiated hepatic CD56^{bright} NK cells from their peripheral blood counterparts and CD56^{dim} hepatic cells. In culture, CXCR6 expression did not significantly differ between day 0 (71.8±10.2%) and day 7 (40.3±10.4%, p=0.052, **Figure 3-16B**). CXCR6 expression in CD56^{dim} hepatic NK cells increases marginally at the same, probably due to overlap of the two populations (Day 0 2.5±1.3%, day 7 6.6±2.4%, p=0.3, **Figure 3-16C).**

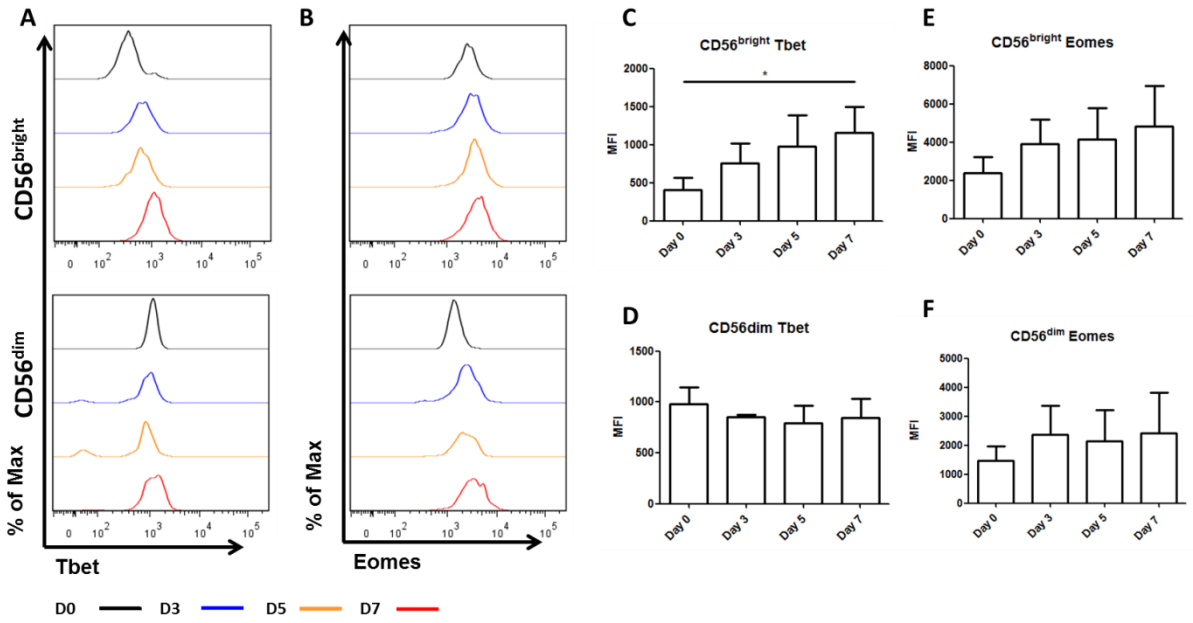

Figure 3- 15 Eomes^{hi} Tbet^{lo} phenotype is lost in culture

NK cells isolated from liver perfusate (LP) were cultured for 7 days. Cells were then stained with monoclonal antibodies to assess transcription factor expression. CD56^{bright} CD16$^{-/+}$ and CD56^{dim} CD16^{+} subsets were gated. Non-viable cells were excluded by FVS780 staining **(A)** Representative histograms of Tbet expression from cells at day 0 (black line), day 3 (blue line), day 5 (orange line), and day 7 (red line) **(B)** Representative histograms of Eomes expression from cells at day 0 (black line),day 3 (blue line), day 5 (orange line), and day 7 (red line) **(C)** Mean fluorescence intensity (MFI) of Tbet CD56^{bright} NK cells from LP at day 0, 3, 5, and 7. **(D)** Mean fluorescence intensity (MFI) of Tbet CD56^{dim} NK cells from LP at day 0, 3, 5, and 7. **(E)** Mean fluorescence intensity (MFI) of Eomes CD56^{bright}NK cells from LP at day 0, 3, 5, and 7. **(F)** Mean fluorescence intensity (MFI) of Eomes CD56^{dim} NK cells from LP at day 0, 3, 5, and 7. Data presented as mean ± SEM. Data was analysed using Friedman test, with Dunn's multiple comparison test (n=3, *p <0.05)

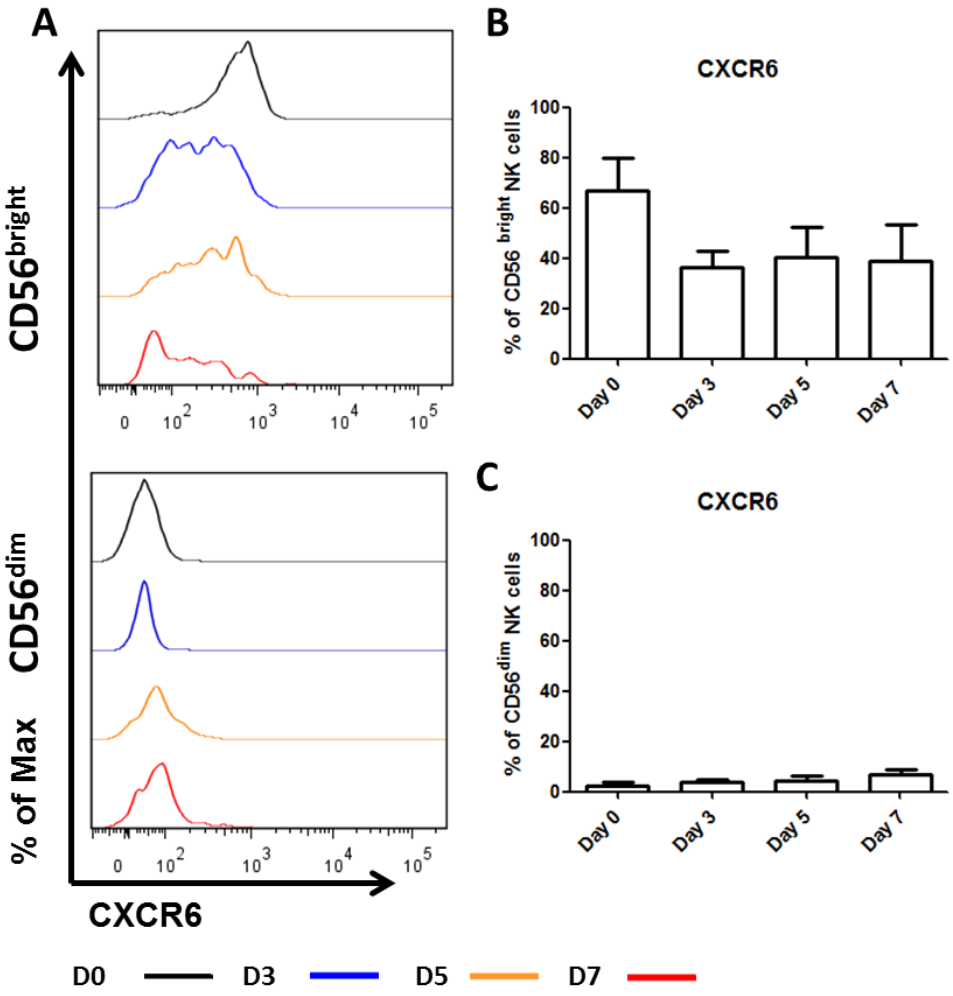

Figure 3- 16 CXCR6 expression is maintained in culture

NK cells isolated from liver perfusate (LP) were cultured for 7 days. Cells were then stained with monoclonal antibodies to assess CXCR6 expression. $CD56^{bright}$ $CD16^{-/+}$ and $CD56^{dim}$ $CD16^{+}$ subsets were then gated on. Non-viable cells were excluded by FVS780 staining **(A)** Representative histograms of CXCR6 expression from cells at day 0 (black line), day 3 (blue line), day 5 (orange line), and day 7 (red line) **(B)** Percentage of CXCR6 positive $CD56^{bright}$ NK cells from LP at day 0, 3, 5, and 7. **(C)** Percentage of CXCR6 positive $CD56^{dim}$ NK cells from LP at day 0, 3, 5, and 7. Data presented as mean ± SEM. Data was analysed using Friedman test, with Dunn's multiple comparison test (n=3).

3.2.14 Liver conditioned media is capable of maintaining Eomes^{hi} Tbet^{lo} phenotype in hepatic NK cells

Hepatic NK cells were isolated from liver perfusate by negative selection and cultured in RPMI supplemented with 10% human AB serum and IL-15 (5ng/ml) for 7 days (n=3). Liver conditioned media (LCM) was prepared using donor liver biopsies. Briefly, small tissue samples (~5mm^3) were placed into 500µl X-VIVO media for 72 hours, whereupon supernatants were collected. LCM added at 5 or 10% v/v. The media was replenished every 2-3 days.

Hepatic CD56^{bright} NK cells have a unique pattern of Eomes and Tbet expression, which is lost in long term culture. In order to determine the effect of the liver microenvironment on these transcription factors, we assessed Eomes and Tbet expression after culture supplemented with liver conditioned media (n=3). Tbet expression increases gradually in cultured CD56^{bright} NK cells. LCM significantly reduced the expression of Tbet in a dose dependent manner, to a level similar to that seen at day 0. At day 7, the MFI of Tbet in untreated CD56^{bright} NK cells was 724.3±170.4 MFI, rising from 323.7±34.3 MFI at day 0. This was reduced to 391.0±29.8 MFI with 5% LCM and further reduced to 261.7±11.9 with 10% LCM (p=0.017, **Figure 3-17C**). Similarly, Eomes expression increased in CD56^{bright} NK cells in culture. This was significantly reduced by treatment with LCM in a dose dependent manner. By day 7, Eomes MFI in untreated NK cells had risen to 3149±389.9 from 1343±204.4 MFI at day 0. Treatment with 5% LCM reduced the MFI to 1774±630.6, with a further reduction to 983.3±243.1 MFI with 10% LCM (p=0.0278, **Figure 3-17E**).

Hepatic CD56^{dim} NK cells behave in a similar manner when treated with LCM although the effect is not as significant as in CD56^{bright} NK cells. Tbet expression is reduced in a dose dependent manner (untreated MFI 789.7±171.8, 5% LCM MFI 720.7±19.7, 10% LCM MFI 553.2±7.8, p=0.18, **Figure 3-17D**). A dose dependent decrease in Eomes expression was also

seen, returning the MFI of Eomes to levels seen at day 0 (untreated MFI 2323±4336, 5% LCM MFI 1157±164.9, 10% LCM MFI 736±118, p=0.0331, **Figure 3-17F**).

CXCR6 is differentially expressed by hepatic $CD56^{bright}$ NK cells. In long term culture, this receptor is lost from many of these cells. We analysed the expression of CXCR6 on hepatic NK cells cultured with liver conditioned media (n=3). Treatment with LCM restored some expression of CXCR6 in hepatic $CD56^{bright}$ NK cells. At day 7, CXCR6 was expressed on 45.5±6.4% of $CD56^{bright}$ NK cells. This level increased to 58.0±15.5% and 65.3±10.8% with 5% and 10% LCM respectively (p=0.21, **Figure 3-18C**). No significant change was seen in $CD56^{dim}$ NK cells (untreated 6.6± 2.4%, 5% LCM 3.6±2.1%, 10% LCM 4.1±2.6, p=0.72, **Figure 3-18D**).

3.2.15 Liver conditioned media suppresses IFN-γ in peripheral blood NK cells

NK cells were isolated from peripheral blood by negative MACS selection (n=5). NK cells were incubated overnight in the presence of IL-2 (50ng/ml). In addition, 5% liver conditioned media was added to half of the wells. The following morning K562 target cells were added to the respective wells, while a CD107a antibody was simultaneously added. After 1 hour, GolgiStop was added to each well and incubated for a further 3 hrs. After 4 hours, cells were stained for IFN-γ production. No significant difference was observed in the expression of CD107a in either $CD56^{bright}$ (43.3±6.1% vs 34.9±9.9%, p=0.62) or $CD56^{dim}$ (36.0±10.5% vs 23.4±7.4%, p=0.25) populations after treatment with LCM (**Figure 3-19B&D**). Interestingly, production of IFN-γ was significantly reduced in $CD56^{bright}$ (47.6±0.9% vs 10.9±4.9%, p=0.01, **Figure 3-19C**) and $CD56^{dim}$ NK cells treated with LCM (25.7±1% vs 4.7±1.4%, p=0.005, **Figure 3-19E**).

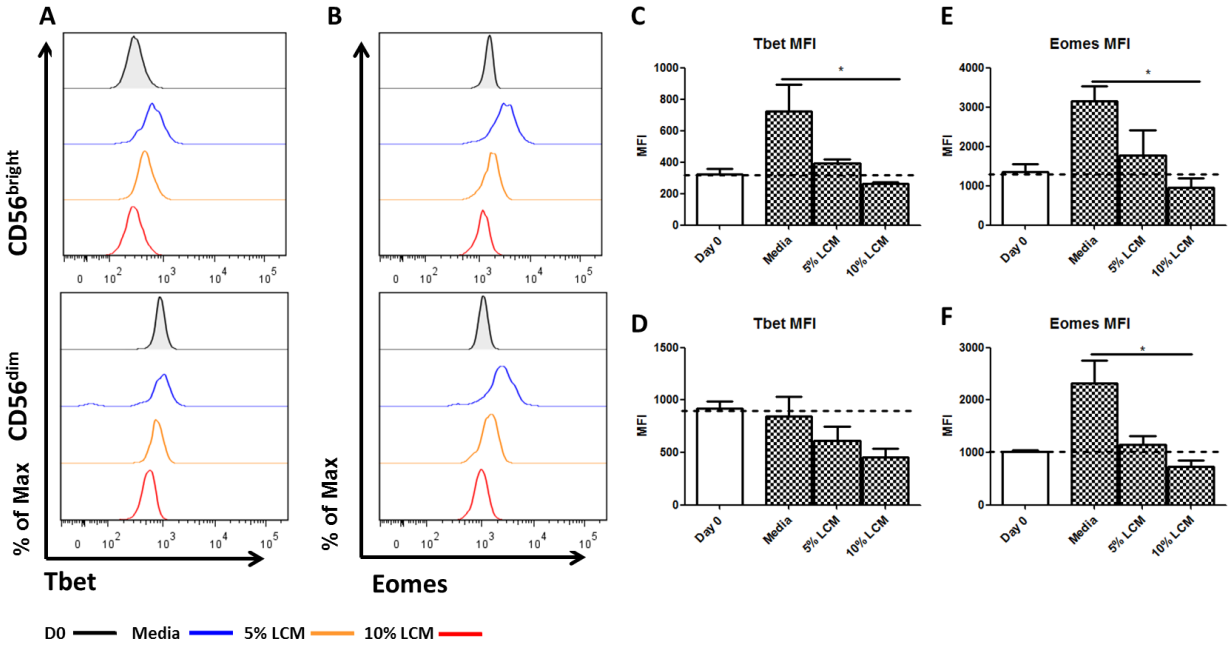

Figure 3- 17 Liver conditioned media regulates Eomes and Tbet expression

NK cells isolated from liver perfusate (LP) were cultured for 7 days, supplemented with 5 or 10% v/v liver conditioned media (LCM). Cells were then stained with monoclonal antibodies to assess transcription factor expression. $CD56^{bright}$ $CD16^{-/+}$ and $CD56^{dim}$ $CD16^{+}$ subsets were then gated on. Non-viable cells were excluded by FVS780 staining **(A)** Representative histograms of Tbet expression from cells at day 0 (black line), day 7 untreated (blue line), day 7 5% LCM (orange line), and day 7 10% LCM (red line) **(B)** Representative histograms of Eomes expression from cells at day 0 (black line), day 7 untreated (blue line), day 7 5% LCM (orange line), and day 7 10% LCM (red line) **(C)** Mean fluorescence intensity (MFI) of Tbet $CD56^{bright}$ NK cells from LP at day 0 & 7 with LCM treatments. **(D)** Mean fluorescence intensity (MFI) of Tbet $CD56^{dim}$ NK cells from LP at day 0 & 7 with LCM treatments. **(E)** Mean fluorescence intensity (MFI) of Eomes $CD56^{bright}$ NK cells from LP at day 0 & 7 with LCM treatments. **(F)** Mean fluorescence intensity (MFI) of Eomes $CD56^{dim}$ NK cells from LP at day 0 & 7 with LCM treatments. Data presented as mean ± SEM. Data was analysed using Friedman test, with Dunn's multiple comparison test (n=5, *p <0.05)

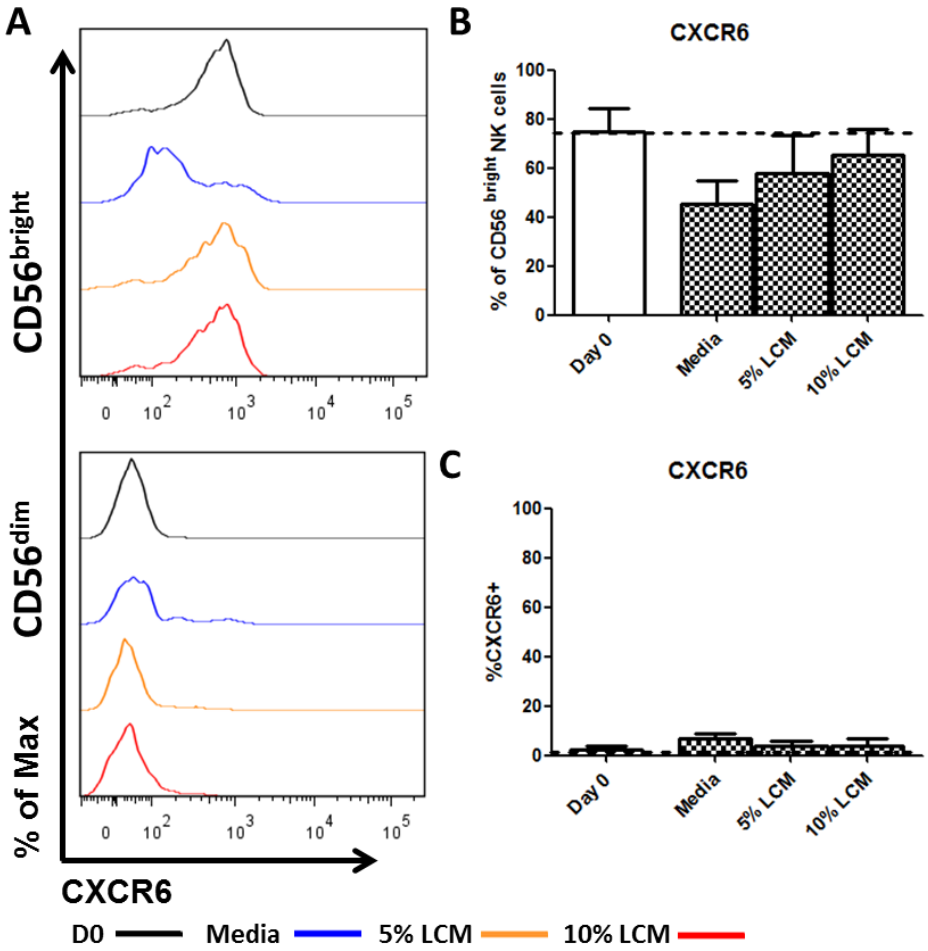

Figure 3- 18 CXCR6 expression is unchanged by liver conditioned media treatment

NK cells isolated from liver perfusate (LP) were cultured for 7 days supplemented with 5 or 10% v/v liver conditioned media (LCM). Cells were then stained with monoclonal antibodies to assess CXCR6 expression. $CD56^{bright}$ $CD16^{-/+}$ and $CD56^{dim}$ $CD16^{+}$ subsets were then gated on. Non-viable cells were excluded by FVS780 staining **(A)** Representative histograms of CXCR6 expression from cells at day 0 (black line), day 7 untreated (blue line), day 7 5% LCM (orange line), and day 7 10% LCM (red line) **(B)** Percentage of CXCR6 positive $CD56^{bright}$ NK cells from LP at day 0 & 7 with LCM treatments. **(C)** Percentage of CXCR6 positive $CD56^{dim}$ NK cells from LP at day 0 & 7 with LCM treatments. Data presented as mean ± SEM. Data was analysed using Friedman test, with Dunn's multiple comparison test (n=5).

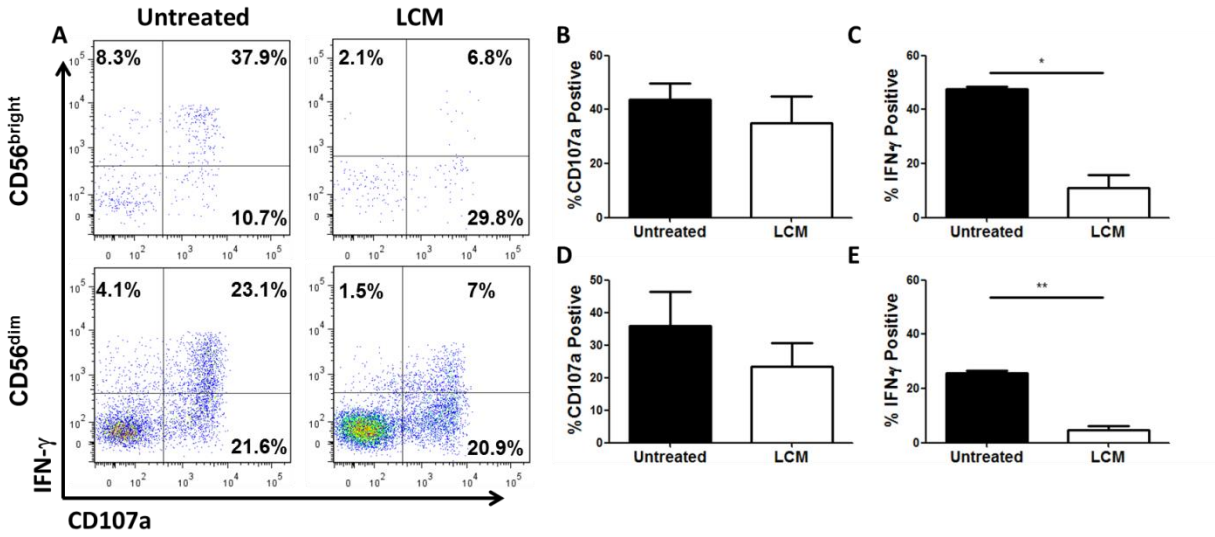

Figure 3- 19 Liver conditioned media inhibits IFN-γ in peripheral blood NK cells

NK cells isolated from peripheral blood (PB) were cultured for 24 hours supplemented with 10% v/v liver conditioned media (LCM). NK cells were then stimulated with IL-2 and K562 target cells. **(A)** Representative FACS plots of $CD56^{bright}$ and $CD56^{dim}$ NK cells treated with 10% LCM or untreated. **(B)** Percentage of $CD56^{bright}$ NK cells positive for CD107a **(C)** Percentage of $CD56^{bright}$ NK cells positive IFN-γ **(C)** in response to IL-2 and K562 target cell stimulation with/without 5% LCM. **(D)** Percentage of $CD56^{dim}$ NK cells positive for CD107a **(E)** Percentage of $CD56^{dim}$ NK cells positive for IFN-γ in response to IL-2 and K562 target cell stimulation with/without 5% LCM. Data are presented as mean ± SEM. Data was analysed using Wilcoxon matched pairs test. (n=5, *p <0.05; **p <0.01)

3.2.16 Liver conditioned media regulates Eomes and Tbet expression in peripheral blood NK cells

In order to determine if the liver microenvironment could convert peripheral blood NK cells to a liver-like phenotype, NK cells were isolated from healthy donor buffy coats and cultured for 7 days in the presence or absence of liver conditioned media. In culture untreated NK cells increase their expression of Eomes. Treatment with liver conditioned media reduces the expression of Eomes to basal level in both $CD56^{bright}$ and $CD56^{dim}$ NK cells. In contrast to hepatic NK cells, blood $CD56^{bright}$ NK cells do not significantly increase their expression of Tbet in culture (Day 0 954.7±47.5 MFI, Day 7 973.5±88.5 MFI). However, treatment with LCM induces reduced Tbet expression after 7 days of treatment, substantially lower than basal expression (Day 0 954.7±47.5 MFI, Day 7 5% LCM 443±91.2, 10% LCM 395.3±25.2 MFI, p=0.033, **Figure 3-20C**). At day 0 the MFI of Eomes was 1514±237.1 for $CD56^{bright}$ cells, by day 7 the MFI had increased to 2371±267. This was reduced by addition of LCM to 1177±209 MFI (5% LCM) and 927.7±34.2 MFI (10% LCM, **Figure 3-20E**). $CD56^{dim}$ NK cells also undergo a significant decrease in Tbet expression after LCM treatment (day 0 1198±72.8 MFI, Day 7 untreated 1012±99.1 MFI, 5% LCM 418±83.5 MFI, 10% LCM 464.7±21.5 MFI, p=0.017, **Figure 3-20D**).

At day 0 the MFI of Eomes was 1500±420.5 for $CD56^{dim}$ NK cells. At day 7 the MFI had increased to 2155±163.5, this was reduced to basal levels with the addition of LCM (5% LCM 1040±199.5 MFI, 10% LCM 859.9±41 MFI, **Figure 3-20F**). Peripheral blood NK cells do not basally express CXCR6 and the receptor was not detected at any point during the experiment. LCM is able to alter the expression of Tbet, mimicking a liver-resident phenotype in peripheral blood NK cells. However, it is not sufficient to induce expression of CXCR6, indicating a second signal is necessary for conversion of blood NK cells to liver resident phenotype.

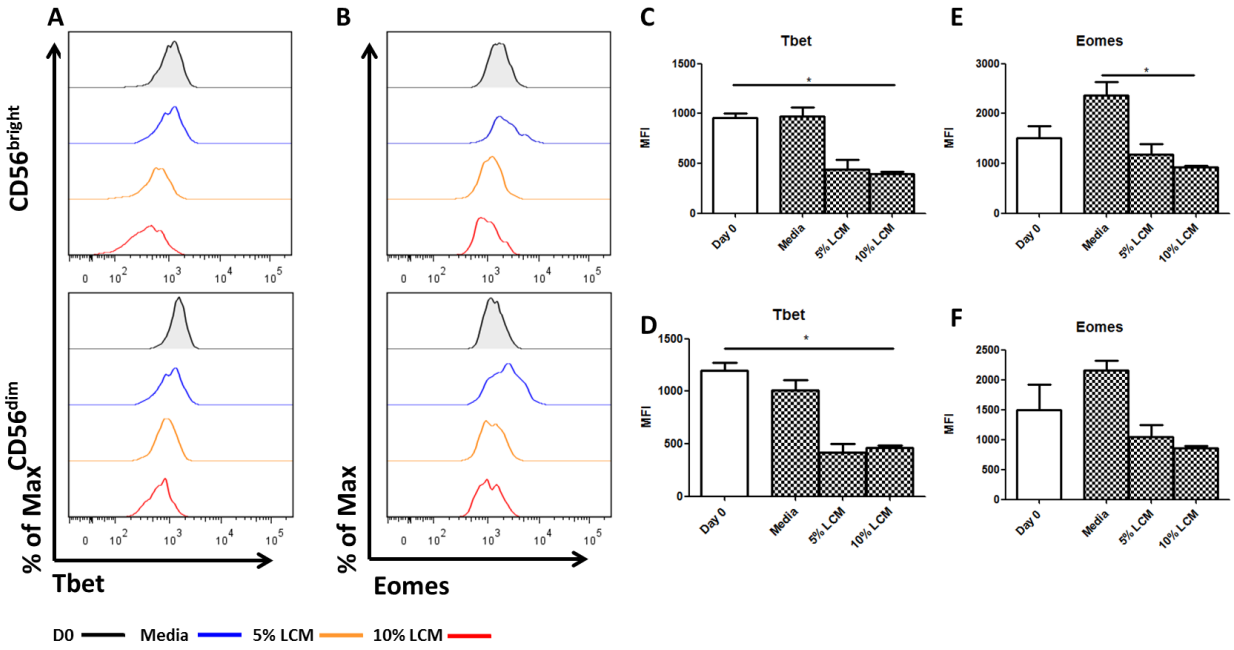

Figure 3- 20 Liver conditioned media regulates Tbet expression in peripheral blood NK cells

NK cells isolated from peripheral blood (PB) were cultured for 7 days, supplemented with 5 or 10% v/v liver conditioned media (LCM). Cells were then stained with monoclonal antibodies to assess transcription factor expression. $CD56^{bright}$ $CD16^{-/+}$ and $CD56^{dim}$ $CD16^{+}$ subsets were then gated on. Non-viable cells were excluded by FVS780 staining **(A)** Representative histograms of Tbet expression from cells at day 0 (black line), day 7 untreated (blue line), day 7 5% LCM (orange line), and day 7 10% LCM (red line) **(B)** Representative histograms of Eomes expression from cells at day 0 (black line), day 7 untreated (blue line), day 7 5% LCM (orange line), and day 7 10% LCM (red line) **(C)** Mean fluorescence intensity (MFI) of Tbet $CD56^{bright}$ NK cells from PB at day 0 & 7 with LCM treatments. **(D)** Mean fluorescence intensity (MFI) of Tbet $CD56^{dim}$ NK cells from PB at day 0 & 7 with LCM treatments. **(E)** Mean fluorescence intensity (MFI) of Eomes $CD56^{bright}$ NK cells from PB at day 0 & 7 with LCM treatments. **(F)** Mean fluorescence intensity (MFI) of Eomes $CD56^{dim}$ NK cells from PB at day 0 & 7 with LCM treatments. Data presented as mean ± SEM. Data was analysed using Friedman test, with Dunn's multiple comparison test. (n=3, *p <0.05)

3.2.17 The liver microenvironment is rich in immunomodulating cytokines IL-10 and TGF-β

We next attempted to identify the factor present in liver conditioned media (LCM) responsible for maintaining this liver resident phenotype. IL-10 and TFG-β are two immunosuppressive cytokines which can suppress IFN-γ production in NK cells and T cells (Groux et al., 1998; Knolle et al., 1998; Viel et al., 2016). Our lab group has previously reported the presence of several NK related cytokines including the essential IL-15, activatory IL-12 and IL-18, in addition to IL-10 and TGF-β in healthy tissue (Kelly et al., 2006). Here, we have measured the levels of secreted IL-15, IL-10 and TGF-β in liver conditioned media. IL-15 has previously been shown to be essential for NK survival and maintaining phenotype (Liu et al., 2000). IL-15 was detected in all LCM tested at an average concentration of 335.3±74.0pg/ml. TGF-β and IL-10 were also detected in all samples at concentrations of 270.3±63.1pg/ml and 124.3±22.3pg/ml respectively (**Figure 3-21**).

3.2.18 TGF-β but not IL-10 is capable of maintaining hepatic Eomes^{hi} Tbet^{lo} phenotype

Next we assessed the effect of IL-10 and TGF-β on the phenotype on hepatic NK cells in culture. CD56^{bright} Eomes^{hi} Tbet^{lo} NK cells were isolated by FACS sorting. They were cultured in RPMI supplemented with 10% human AB serum and IL-15 (5ng/ml) for 7 days with or without LCM (10% v/v), IL-10 (10ng/ml) or TGF-β (5ng/ml). Media was replenished ever 2-3 days. As before Tbet and Eomes expression increased during culture. LCM significantly reduced the expression of Tbet as previously described (**Figure 3-22B**). Similarly, TGF-β significantly reduced the expression of Tbet compared to untreated cells (untreated MFI 760.5±46.9, LCM 381.1± 78.2, TGF-β 385.2±79.8, p=0.0014, **Figure 3-22B**). IL-10 had no effect on Tbet expression (MFI 792.4±56.4).

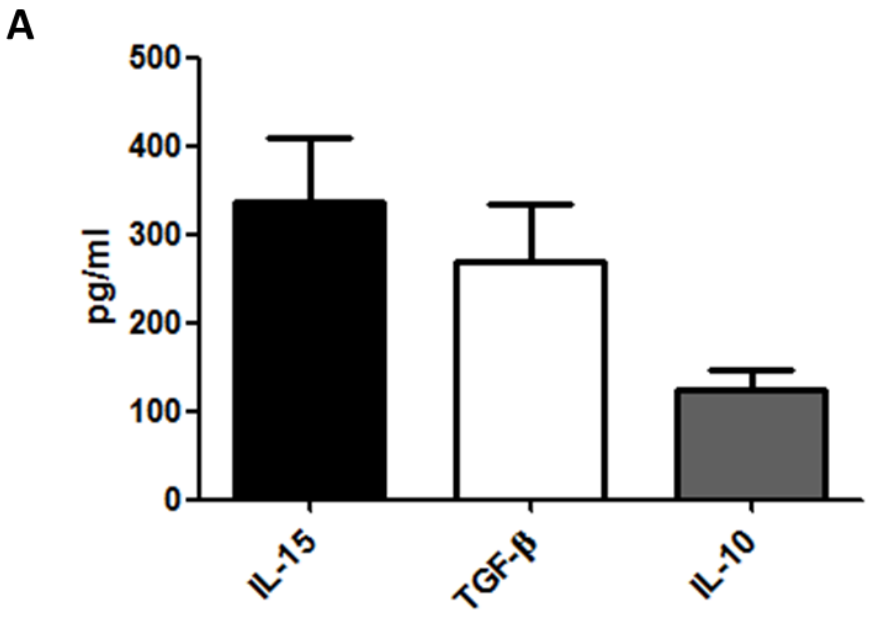

Figure 3- 21 The liver microenvironment contains cytokines IL-15, TGF-β and IL-10

Liver conditioned media (LCM) was generated from healthy donor liver biopsies. Tissue was cultured for 72hrs in X-VIVO media. Supernatants were then aspirated and used for analysis. ELISA was performed for the cytokines IL-15, TGF-β and IL-10 on matched LCM samples. **(A)** Concentration of cytokines IL-15, TGF-β and IL-10 from matched LCM samples. Data presented as mean ± SEM. (n=10)

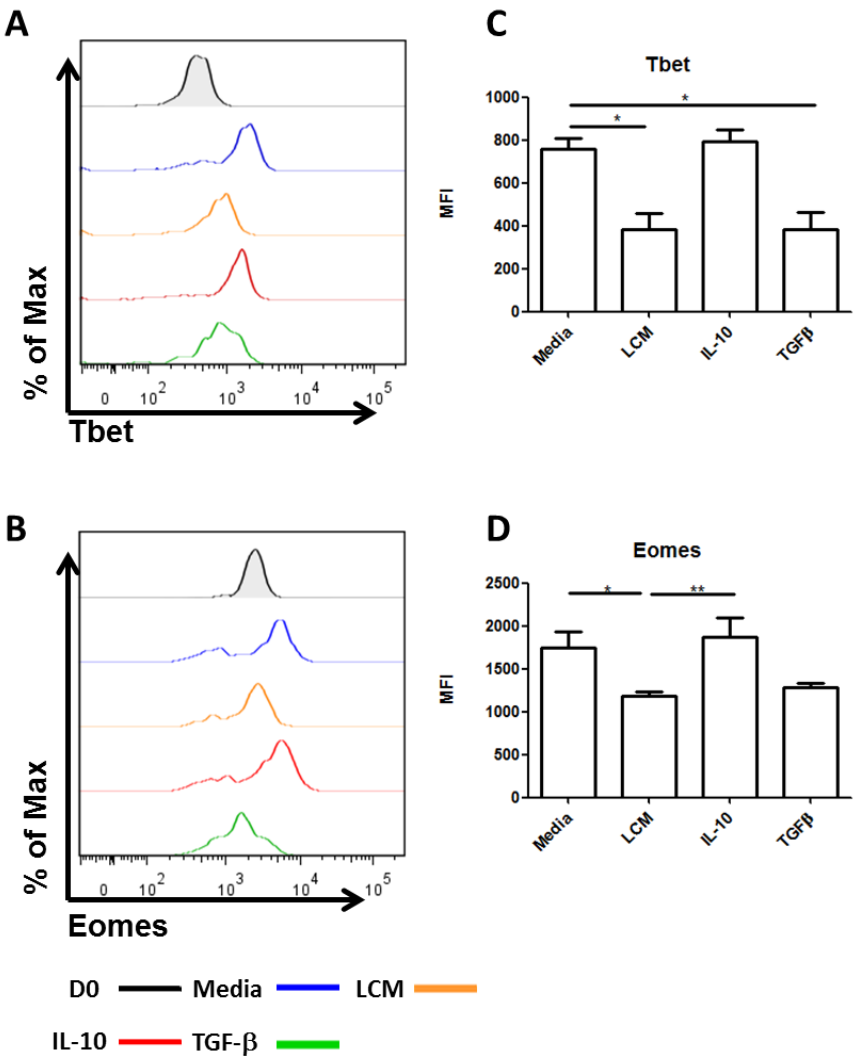

Figure 3- 22 TGF-β is capable of regulating Tbet expression in hepatic NK cells

CD56^{bright} Eomes^{hi} Tbet^{lo} NK cells isolated from liver perfusate (LP) were cultured for 7 days, supplemented with 10% v/v liver conditioned media (LCM), IL-10 (10ng/ml) or TGF-β (5ng/ml). Cells were then stained with monoclonal antibodies to assess transcription factor expression. Non-viable cells were excluded by FVS780 staining **(A)** Representative histograms of Tbet expression from cells at day 0 (black line), day 7 untreated (blue line), day 7 5% LCM (orange line), day 7 IL-10 (red line), and day 7 TGF-β (green line) **(B)** Representative histograms of Eomes expression from cells at day 0 (black line), day 7 untreated (blue line), day 7 5% LCM (orange line), day 7 IL-10 (red line), and day 7 TGF-β (green line) **(C)** Mean fluorescence intensity (MFI) of Tbet CD56^{bright} NK cells from LP at day 7 with LCM, IL-10 or TGF-β treatments. **(D)** Mean fluorescence intensity (MFI) of Eomes CD56^{bright} NK cells from LP at day 7 with LCM, IL-10 or TGF-β treatments. Data presented as mean ± SEM. Data was analysed using Friedman test, with Dunn's multiple comparison test. (n=5, *p <0.05, **p<0.01)

TGF-β reduced Eomes expression to a similar level, however this was not significant (MFI 1288±48.5, p=0.065). IL-10 induced a small increase in Eomes expression (untreated MFI 1740±196.9, IL-10 MFI 1873± 228.4, **Figure 3-22D**). Eomes expression was significantly reduced by LCM as before (MFI 1187±42.6, **Figure 3-22D**). In order to formally establish TGF-β as the factor responsible for inducing the liver-resident phenotype ($Eomes^{hi}$ $Tbet^{lo}$) further experiments will be required to block or deplete TFG-β signalling in conditioned media cultures.

3.3 Discussion

The study of human liver immunology has proven difficult, due in part to the availability of healthy human tissue for study. We have attempted to address this issue by using liver perfusate (a waste product of liver transplantation) and small biopsies from donor organs. While these materials are a step in the right direction there are caveats to their use that must be considered. Organs are obtained from brain stem dead patients, often after suffering significant head trauma, therefore donors cannot be considered truly "healthy". Once the organ retrieval process begins organs are exposed to both warm and cold ischaemia (loss of blood supply), transport in preservative solutions and the perfusion process, all of which can contribute to sterile inflammation and tissue damage (Chen and Nuñez, 2010; Zhai et al., 2013). Finally, enzymatic and mechanical digestion of biopsy material can effect NK cell phenotype (Curry et al., 2000). We have characterised the diverse NK repertoire of healthy human liver and have identified a novel subpopulation of liver resident NK cells with unique phenotypic features, effector function and transcriptional regulation. As previously described, we have shown that the liver is enriched with NK cells, accounting for more than half of hepatic lymphocytes. Over 40% of these were $CD56^{bright}$ NK cells. Hepatic NK cells have increased expression of activating receptors, such as NKG2D, NKp44 and NKp46, which recognise stress induced ligands and viral and tumour associated antigens. In line with this activated phenotype and increased cytotoxic molecule expression, hepatic NK cells display increased degranulation in response to target cell stimulation. Interestingly, the $CD56^{bright}$ subset which is significantly enriched in hepatic NK cells and is normally considered poorly cytotoxic, displayed the highest level of CD107a expression. While we have found that granzyme B expression is reduced in hepatic $CD56^{bright}$ NK cells, expression of granzyme A and perforin were similar to peripheral blood $CD56^{bright}$ NK cells. Hepatic $CD56^{bright}$ NK cells expressed significantly more granzyme K in addition, which has previously been demonstrated (Moroso et al., 2010).

In contrast to the peripheral blood, hepatic $CD56^{bright}$ NK cells display enhanced degranulation and significantly reduced IFN-γ production. Expression of IFN-γ is similar in $CD56^{bright}$ and $CD56^{dim}$ hepatic NK cells. This differs markedly from the prominent difference in IFN-γ production by peripheral blood $CD56^{bright}$ and $CD56^{dim}$ subsets. However, these results represent NK cells activated through target cell recognition with cytokine stimulation, hepatic NK cells may become activated through other pathways and produce pro-inflammatory cytokines.

Differentiation of precursor to mature NK cell requires the transcription factors Eomes and T-bet, which regulate acquisition of cytolytic function and IFN-γ production respectively (Daussy et al., 2014; Gordon et al., 2012; Montaldo et al., 2014). Murine studies have identified a liver resident NK cell population with altered transcription factor usage ($Eomes^{-}$ $T\text{-}bet^{+}$) (Daussy et al., 2014; Gordon et al., 2012). In human liver, these cells have been described as poorly cytotoxic $CD56^{bright}$ NK cells which are capable of enhanced pro-inflammatory cytokine production (Marquardt et al., 2015). While these cells appear to be liver resident, they account for only a small proportion of hepatic NK cells and are absent entirely from the majority of liver samples. No distinct $Eomes^{-}$ $T\text{-}bet^{+}$ populations were detectable in liver perfusate or liver biopsies in this study. However, we detected a small population of $CD49a^{+}$ NK cells in liver tissue alone. Interestingly, some innate immune populations appear resistant to perfusion (Kupffer cells, γδ T cells, iNKT cells, Fahey et al. unpublished, **Figure 1-1**). These populations may resist perfusion through adhesion to liver sinusoidal endothelium. Tissue processing procedures differed between previously published work and this study. Marquardt and colleagues made use of grafts unsuitable for transplantation and uninvolved tissue from liver resections from cancer patients. Due to the size of these tissues they required significant enzymatic and mechanical manipulation (up to one hour of tissue dissociation). In the current study, we have limited the tissue dissociation procedure to a maximum of 20 minutes to minimise the effect of manipulation artefacts.

Furthermore, analysis of cirrhotic livers has shown a distinct change in NK cell populations, a loss of Eomes^{hi} Tbet^{lo} NK cells and the expansion of CD49a^{+} cells (Lunemann et al., 2017; Martrus et al., 2017). This difference was attributed to the anti-fibrotic function of CD49a^{+} NK cells but equally may be due to the loss of tissue resident NK cells during chronic inflammation. We, and others, have identified a significant population of Eomes^{hi} T-bet^{lo} NK cells which are largely absent from the peripheral blood (Harmon et al., 2016; Stegmann et al., 2016; Aw Yeang et al., 2017). The majority of this population is made up of CD56^{bright} NK cells, with a small percentage of CD56^{dim} cells. These cells display enhanced degranulation and significantly reduced IFN-γ expression in response to cytokines (IL-2, IL-12/15) (Harmon et al., 2016; Stegmann et al., 2016). In addition, these cells express the chemokine receptor CXCR6, which recognises CXCL16 produced by liver sinusoidal endothelium (Hudspeth et al., 2015; Parker et al., 2013; Paust et al., 2011). In combination with CCR5, these receptors act to retain NK cells within the hepatic sinusoids (Hudspeth et al., 2015). These hepatic NK cells also expressed CD69, a marker of tissue residency.

The functional or phenotypic implications of increased expression of Eomes by hepatic CD56^{bright} NK cells are unclear. The origin of Eomes^{hi} T-bet^{lo} NK cells also remains to be established. We hypothesize that some hepatic NK cells differentiate locally from lymphoid progenitors, which have been previously described in the adult human liver (Crosbie et al., 1999; Golden-Mason et al., 2000; Shi et al., 2013). We have analysed the complex cytokine milieu present in healthy liver tissue. In these studies, we identified cytokines essential for progenitor differentiation and NK cell activation including IL-15, IL-12, IL-18 and IL-2 (Golden-Mason et al., 2001; Kelly et al., 2006, 2004). This local microenvironment may also induce liver specific phenotypical and functional changes in bone marrow derived NK cells which traffic to the liver. However, others have shown that in transplant recipients, donor NK cells are retained for many years, but NK cell progenitors of donor origin are not detectable (Cuff et al., 2016; Shi et al., 2013). Whether these represent long lived or "memory-like" cells

remains to be determined. They may also develop from single progenitor clones which are difficult to detect using current methods.

In this study, we have shown that the liver microenvironment is essential for maintaining the unique Eomes^{hi} Tbet^{lo} phenotype of liver resident NK cells. In culture, this phenotype is lost over time but can be maintained by supplementing cultures with liver tissue derived factors. We believe TGF-β is the main regulator of these transcription factors. Furthermore, Tbet expression in peripheral blood NK cells can be modulated by treatment with liver conditioned media. However, this treatment cannot induce the expression of CXCR6; therefore a second signal is required in order to acquire expression of this receptor. Hydes and colleagues have shown that CXCR6 and CD49a can be upregulated in cytokine activated peripheral blood NK cells (Hydes et al., 2018). This indicates that NK cells may migrate to the liver after activation and are retained through CXCR6 and CCR5 expression (Hudspeth et al., 2015); they then alter their transcription factor usage in a TGF-β rich liver microenvironment. However, humanised mice develop CD49a^{+} CXCR6^{+} hepatic NK cells in the absence of any exogenous stimulation (Aw Yeang et al., 2017). Our lab has further investigated this, and found that tissue resident NK cells develop poorly in humanised mice and only represent a small fraction of hepatic immune cells (**Appendix Figure 2**). Hepatic progenitors may give rise to a proportion of tissue resident NK cells (**Appendix Figure 3**). It seems likely that peripheral NK cells, activated through cytokine release, traffic to the liver, are retained in the sinusoids and differentiate into tissue resident cells.

The liver is a naturally tolerogenic environment, which maintains unique anti-inflammatory status even in the presence of immune activating dietary antigens and bacterial components. In this context, Eomes^{hi} T-bet^{lo} NK cells may provide a potent cytotoxic cellular response while minimising wider tissue inflammation through reduced pro-inflammatory cytokine

production. This would allow for a response to intracellular infection and malignant transformation while maintaining the overall tolerogenic environment in the liver.

The proportion and subset heterogeneity of hepatic NK cells varies greatly between individuals; while the clinical significance of this variation is largely unknown it is clear that differences in hepatic NK cell populations can influence an individual's response to liver diseases including malignancy, viral infection, autoimmunity, and transplantation. While increased intra-tumoural accumulation of NK cells in hepatocellular carcinoma correlates with increased survival (Cai et al., 2008; Jinushi et al., 2005), increased proportion of NK cells in the liver of patients with hepatic colorectal cancer metastasis can have a negative or positive impact on patient mortality (Donadon et al., 2017; Pugh et al., 2014). However, it was unclear from these studies whether distinct NK cell subsets were of benefit or the overall number of NK cells was of prognostic value. We know from a number of cancer types that the type of NK cell infiltrate is an important indicator of disease outcome (Stabile et al., 2017).

Chronic HCV infection is a leading cause of liver disease; however, the clinical and histological severity of HCV varies widely. The proportion of intrahepatic $CD56^{bright}$ NK cells has been demonstrated to strongly correlate with preserved graft function post-transplant in HCV recipients (Doyle et al., 2015). However, several studies have shown dysregulation of NK cells can contribute to viral replication and more severe tissue damage (Golden-Mason et al., 2008; Lunemann et al., 2014; Pembroke et al., 2014). There is also emerging data suggesting NK cells also have immunoregulatory roles in the liver, maintaining tissue homeostasis (Gao, Radaeva and Park, 2009; Radaeva et al., 2006; Robinson, Harmon and O'Farrelly, 2016) and minimising immune activation during viral infection (Huber et al., 2014; Peppa et al., 2013; Waggoner et al., 2012). It has been proposed that these regulatory roles may extend to transplantation tolerance, where NK cell numbers and related transcripts have been proposed as markers of operational tolerance (García de la Garza et al., 2015;

Harmon et al., 2016; Martinez-llordella et al., 2008). Inter-individual variation in levels of specific hepatic NK populations may help explain the spectrum in susceptibility to these pathologies and in some cases enhanced protection. The ability of hepatic NK cells to both regulate and drive liver disease highlights the importance of understanding tissue-resident immune cell populations and the need for further analysis of the impact of this important liver immune cell population.

Chapter 4:

The role of natural killer cells in colorectal liver metastasis

4.1 Introduction

Colorectal cancer is the third most common cancer worldwide, with approximately 1.3 million new cases per year (Ferlay et al., 2015). Up to 50% of CRC patients will go on to develop a metastatic tumour in the liver (CRLM) or other distant organ. If left untreated, the average survival is between 5-20 months (Arnaud et al., 1984; Simmonds, 2000). The only curative treatment is surgical removal of the tumour, usually in combination with chemotherapy or monoclonal antibody therapy (anti-VEGF) (Misiakos, 2011). However surgical resection is only possible in around 30% of patients with CRLM (De Greef et al., 2016). Up to 70% of resected patients will develop a recurrent liver tumour or metastasis of another organ (Tomlinson et al., 2007). Five year survival in resected patients can reach 40% with chemotherapy and a second resection procedure (Nathan et al., 2010). How these tumours evade the hepatic immune repertoire is unclear and may represent a novel treatment target. Despite the success of surgical resection in many patients, the majority are still unsuitable for surgery and no curative therapy is available. Understanding the mechanism by which CRLM tumours evade local immunity may provide a novel target for the treatment of all CRLM patients.

Considering the potent anti-tumour repertoire of the adult human liver, with an enrichment of cytotoxic $CD8^+$ T cells, NK cells, iNKT cells and γδ T cells (Doherty et al., 1999; Golden-Mason et al., 2004; Hata et al., 1990), it is surprising to find that many cancers metastasise to the liver. Apart from the lymphatic system, the liver is the most common site of cancer metastasis (Disibio and French, 2008). Previous work within our lab group has demonstrated that significant alterations to the hepatic immune system occur during colorectal metastatic disease. These include a redistribution of γδ T cell subsets (Kenna et al., 2004), a reduction in NKT cells and alteration of their phenotype (Kenna et al., 2003), a depletion of iNKT cells (Whelan et. al unpublished), while NK cells were found to be increased in tumour bearing liver and expressed lower levels of inhibitory KIRs (Norris et al., 2003). These changes were

accompanied by alterations in the hepatic microenvironment. Pro-inflammatory cytokines such as IFN-γ, IL-18, IL-12 and IL-2 were increased, while anti-inflammatory cytokine production was less clear. IL-10 levels were increased in tumour bearing liver, however TGF-β levels were significantly reduced (Kelly et al., 2006, 2004). More recent work from our group has further investigated the tumour microenvironment and extended our analysis to tissue at the distal resection margin (i.e. tissue considered macro- and microscopically healthy). Interestingly, the microenvironment of this tissue differs significantly from healthy donor tissue, with increases in myeloid growth factors and chemokines (GM-CSF, IL-6, and IL8), and a reduction in cytotoxic cell chemokines such as RANTES (Hand et al. 2018). The overall effect of this cytokine milieu on hepatic NK cells is unclear. We therefore will investigate the ability of liver resident NK cells to migrate toward CRLM tumours *in vitro*. The presence of NK cells in the tumour of patients with primary colorectal cancer and metastasis has been found to negatively correlate with patient survival (Galon et al., 2006; Halama et al., 2011; Pugh et al., 2014). However, in the periphery poor NK cell activity was associated with the development of metastases (Jobin et al., 2017). Furthermore, CXCL16 produced by tumour cells has been shown to prevent colorectal metastasis, possibly by drawing hepatic $CXCR6^+$ NK cells to the tumour site and preventing dissemination (Kee et al., 2014, 2013). Therefore it is important to ascertain the ability of liver resident NK cells to migrate toward CRLM tumours.

The high rate of tumour recurrence has led to the hypothesis that the immune repertoire of the remaining liver is somehow compromised making immunosurveillance ineffective. It is possible that intensive chemotherapy regimens, used to reduce tumour size and allow resection may reduce immune activity and increase the likelihood of recurrence (Nichols et al., 1994). However, some therapies have been shown to dramatically enhance NK cell function in cancer patients (Markasz et al., 2007). More likely is the possibility that tumour

intrinsic factors in the tumour microenvironment have selective effects on local tumour immunity.

When considering metastasis we must also consider the effect of the primary tumour. Recently it has become clear that not all tumour phenotypes have the same tendency to metastasise, subtypes with gene expression enriched in metabolic and epithelial-mesenchymal transition (EMT) related genes being much more likely to metastasise (Hugen et al., 2014; Riihimäki et al., 2016; Yaeger et al., 2018). These metabolically highly active tumours are capable of altering the microenvironment of organs they metastasise to through metabolic by-products and matrix remodelling (Balkwill et al., 2012; Carmona-Fontaine et al., 2017; Maley et al., 2017). For example, lactate has been shown to play a number of roles in reorganising the physical tumour architecture and the immune landscape of many tumour types (Romero-Garcia et al., 2016). It can act upon vascular endothelial cells to induce angiogenesis and tumour associated fibroblasts to produce MMPs and matrix degrading enzymes (Carmona-Fontaine et al., 2017; Hirschhaeuser et al., 2011; Sonveaux et al., 2012; Stern et al., 2002). Additionally lactate can alter innate immune cell phenotypes and promote an immunosuppressive environment through polarisation of tumour associated macrophages to M2-like cells and differentiation of myeloid derived suppressor cells (MDSCs) (Colegio et al., 2014; Goetze et al., 2011; Husain et al., 2013a). Antigen presentation by dendritic cells is also perturbed by high levels of lactic acid in the tumour microenvironment, resulting in poor T cell activation (Fischer et al., 2007; Gottfried, 2006). Furthermore, decreasing pH has been shown to result in apoptosis of T cells and NK cells in melanoma (Brand et al., 2016). Reversing tumour acidosis has also been shown to restore NK cell function and improve anti-tumour activity (Pötzl et al., 2017).

Apoptosis can occur as a result of a number of both intrinsic and extrinsic signals (**Figure 4-1**). Extrinsic signals are transmitted through "death receptors" such as TRAIL-R, TNFR1 and

FAS and is often used by NK cells to kill target cells (de Miguel et al., 2016; Peppa et al., 2013). This process recruits the death inducing signalling complex (DISC), containing the FAS associated death domain (FADD) which allows for the self-cleavage of pro-caspase 8 into its active form. Caspase-8 is released into the cytosol and converts pro-caspase 3 to its active form and initiates the execution pathway. This process can be blocked by association of c-FLIP with the FADD complex (Elmore, 2007; Taylor et al., 2008). The intrinsic pathway is regulated by mitochondrial BCL-2 family members, which regulate cytochrome C release. Cytochrome C activates pro-caspase 9, forming the apoptosome, which regulates caspase 3 activities and execution pathway activation. This process can be activated by loss of growth factors, metabolic stress, endoplasmic reticulum stress, DNA damage or hypoxia (Elmore, 2007; Taylor et al., 2008). In this study we have investigated the effect of the tumour microenvironment on liver resident NK cell viability, with particular interest in the pathways activated by tumour products.

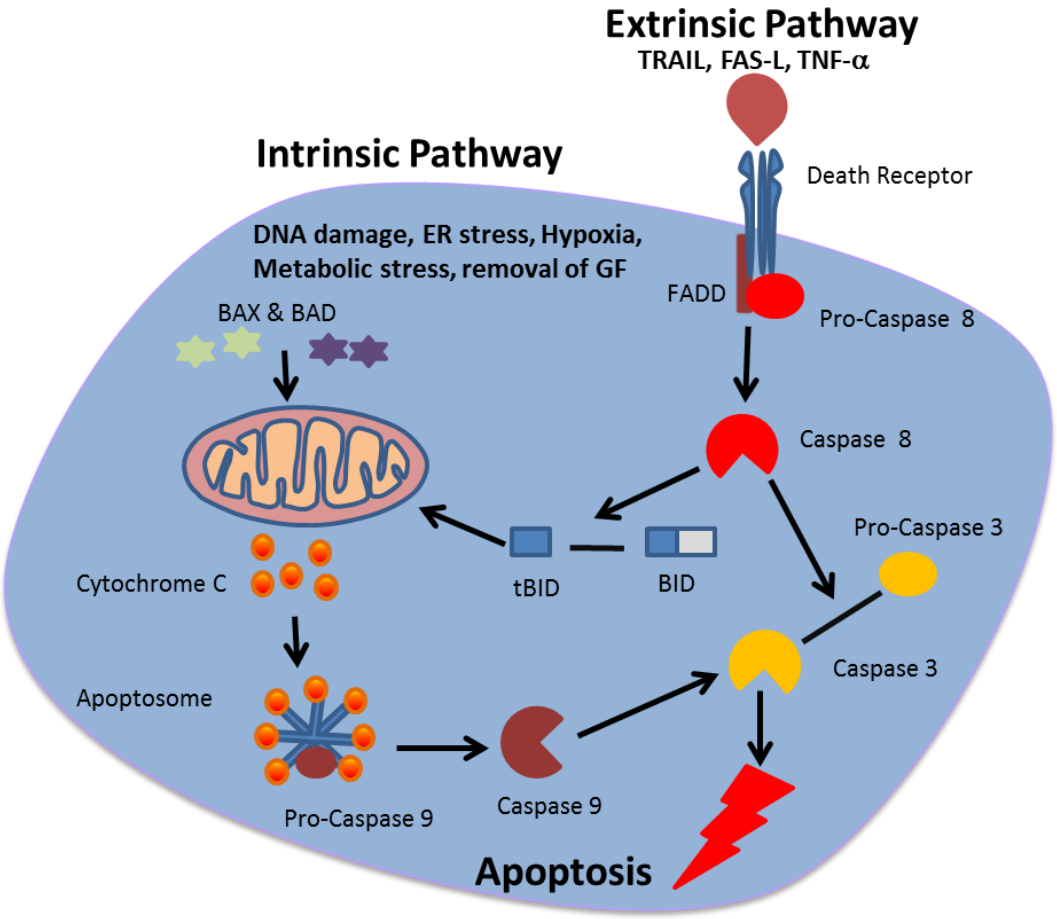

Figure 4- 1 Intrinsic and extrinsic pathways of apoptosis

Diagram shows the pathways leading to apoptosis, how they are activated and the effect of activation on downstream targets. The extrinsic pathway is activated by death receptor ligation, leading to activation of caspase 8 through FADD activity. Caspase 8 cleaves BID and pro-caspase 3 to initiate mitochondrial release of cytochrome c and activation of the execution pathway leading to apoptosis. The intrinsic pathway can be activated by a number of stimuli related to cellular stress or damage. This stimuli cause mitochondrial depolarisation and release of cytochrome c, which goes on to form the apoptosome and caspase-9 activation. This results in caspase 3 cleavage and activation of execution pathway. (FADD- FAS associated death domain, BID- BH3 interacting domain death agonist, GF- growth factor, BAX- BCL2 associated X, apoptosis regulator, BAD- BCL2 associated agonist of cell death, ER- endoplasmic reticulum, DNA- deoxyribonucleic acid).

It remains unclear whether liver resident NK cells are important in immunosurveillance in the liver or whether they perform non-classical functions such as tissue remodelling. In the first instance we have compared the cytotoxic ability of tissue resident and non-resident NK cells from healthy liver against metastatic colorectal cancer cell line (SW620). They appear particularly suited for tumour surveillance but this mechanism fails in many patients. Identifying the mechanism by which metastatic colorectal tumours subvert the innate cytotoxic response of the liver may uncover better therapeutic targets. We set out to establish whether tumour infiltrating liver resident NK cells were still capable of cytotoxicity, by analysing cytotoxicity receptor and effector molecule expression. In addition, we investigated the potential for changes in the cytokine milieu to prevent migration of liver resident NK cells to the tumour site. Finally we assessed the effect of the tumour microenvironment on the viability of liver resident NK cells. Using an *in vitro* model of the tumour microenvironment, developed by generating tissue conditioned media from CRLM tumours (Michielsen et al., 2011; O'Toole et al., 2014); we investigate the effect of this environment on liver resident NK cells.

Rationale:

- Up to 70% of patients with colorectal cancer metastasis to the liver will develop further tumours after surgical removal of the original tumour
- The liver is enriched with highly cytotoxic tissue resident natural killer cells
- There is a defective immune response to colorectal metastasis

Hypothesis:

Liver resident natural killer cells are depleted or functionally ineffective in the livers of patients with colorectal metastasis

Aims:

1. To determine if liver resident natural killer cells are capable of tumour immunosurveillance
2. To identify changes in liver resident natural killer cells in CRLM
3. To characterise phenotypic changes in hepatic natural killer cells in CRLM
4. To determine the mechanism by which liver resident natural killer cells are depleted from CRLM

4.2 Results

4.2.1 Study samples

During surgical resection tumour bearing tissue is removed along with a sufficient margin of healthy tissue to ensure no cancerous tissue remains. Resected tissue is histologically examined to determine if tissue margins are free of cancer cells. During histological examination, biopsies are taken from the tumour (n=18) (in large tumours samples are taken from tumour edge to avoid necrotic tissue), adjacent tissue (n=18) (macroscopically normal) and the distal margin (n=18) (as far from the tumour edge as possible). Single cell suspensions were prepared from each section by collagenase digestion and mechanical disruption. For comparison wedge biopsies, taken at the time of transplant, were also digested into single cell suspensions for analysis (n=10). Due to differences in the type of resection and variability in the size of tumour removed, significant variation in the size of tissue samples were encountered and therefore the number of cells recoverable. Tissue taken from tumours was generally the smaller samples (0.25±0.06g) but was not significantly different than adjacent (0.28±0.06g) or distal tissue samples (0.33±0.07g, **Table 4-1).** Patients undergoing resection were mainly men (12/18) with an average age of 64.9yrs. Liver donors were generally younger (mean 36yrs) and were made up of 6 males and 4 females.

Seven patients had solitary tumours resected, the remainder had multiple lesions removed (2-5 tumours/patient). Where possible multiple tumours were sampled. Tumours varied considerably in size, ranging from 7mm to 100mm in diameter (average 28mm). Adjacent tissue was sampled from within 5mm of the tumour invasive margin for all patients. Distal tissue was sampled from varying distance from the tumour edge depending on size of resection. The furthest sample taken was 75mm from the tumour edge and the closest 10mm (average 27.9mm).

Age (years)	64.9
Gender (M/F)	12/6
Number of tumours (n=)	
1	6
2	6
3	4
4	1
5	1
Tumour size (mm, range)	28(7-100)
Distal distance (mm, range)	27.9(10-75)
Sample weight (g ± SEM)	
Tumour	0.25±0.06
Adjacent	0.28±0.06
Distal	0.33±0.07

Table 4- 1 CRC patient demographics

Patient age and gender, number of tumours resected, size of tumours and distance to distal tissue. Weights of samples taken from tumour, adjacent and distal tissue.

4.2.2 Hepatic CD56^{bright} NK cells have increased cytotoxicity receptor expression

In order to determine the role of liver resident NK cells (CD56^{bright} CXCR6^{+} Eomes^{hi} Tbet^{lo}) in immunosurveillance we assessed their cytotoxic potential compared to conventional anti-tumour CD56^{dim} NK cells from liver perfusate. Data from Figure 3-4/5/6 was reanalysed to directly compare liver CD56^{bright} and liver CD56^{dim} NK cell subsets Firstly, liver resident NK cells display increased expression of several cytotoxicity receptors important in anti-tumour surveillance. NKG2D was expressed on significantly more tissue resident NK cells compared to matched CD56^{dim} cells (MFI 876.3±270.4 vs 422.3±148.6, p=0.0039, **Figure 4-2B**). NKp46 was also differentially expressed on tissue resident NK cells with compared to CD56^{dim} NK cells (1769±163.9 vs 364.6±28.3, p=0.015, **Figure 4-2C**). NKp44 is significantly increased in CD56^{bright} NK cells compared to matched CD56^{dim} cells (5.8±1.7% vs 1.7±0.4%, p=0.0009, **Figure 4-2D**). NKG2C did not differ between NK cells subsets (8.6±1.1%, vs 7.9±1.2%, p=0.177, **Figure 4-2E**). TRAIL was expressed at low levels on both subsets in healthy livers (4.3±1.2% vs 4.1±0.9%, p=0.9, **Figure 4-2F**). This pattern of receptor expression indicated that CD56^{bright} NK cells were capable of tumour cell recognition.

4.2.3 Cytotoxic molecules of differentially expressed between CD56^{bright} and CD56^{dim} hepatic NK cells

Next we assessed the expression of cytotoxic molecules by NK cell subsets in liver perfusate. Data from Figure 3-7/8 was reanalysed to compare liver CD56^{bright} and CD56^{dim} NK cell subsets. Perforin, a key molecule for the insertion of granzymes into the target cell cytoplasm, was expressed at significantly lower levels in tissue resident NK cells compared to non-resident CD56^{dim} cells (MFI 324.1±80.7 vs 1738±446.2, p=0.0078, **Figure 4-3B**). Similarly, Granzyme B was found to be expressed at a much lower level in CD56^{bright} compared to CD56^{dim} NK cells (MFI 824.5±209.5 vs 4315±646.1, p=0.006, **Figure 4-3C**). Granzyme A showed no variation between NK cell subsets in liver perfusate (MFI 1713±29.7 vs 1855±215.9, p=0.38, **Figure 4-3D**). However, granzyme K was significantly increased in

$CD56^{bright}$ NK cells compared to $CD56^{dim}$ counterparts (MFI 367.9±33.5 vs 198.7±39.4, p=0.0313, **Figure 4-3E**). Cytotoxic molecules were differentially expressed between NK cell subsets; therefore we attempted to resolve this question using measures of direct cytotoxicity and degranulation.

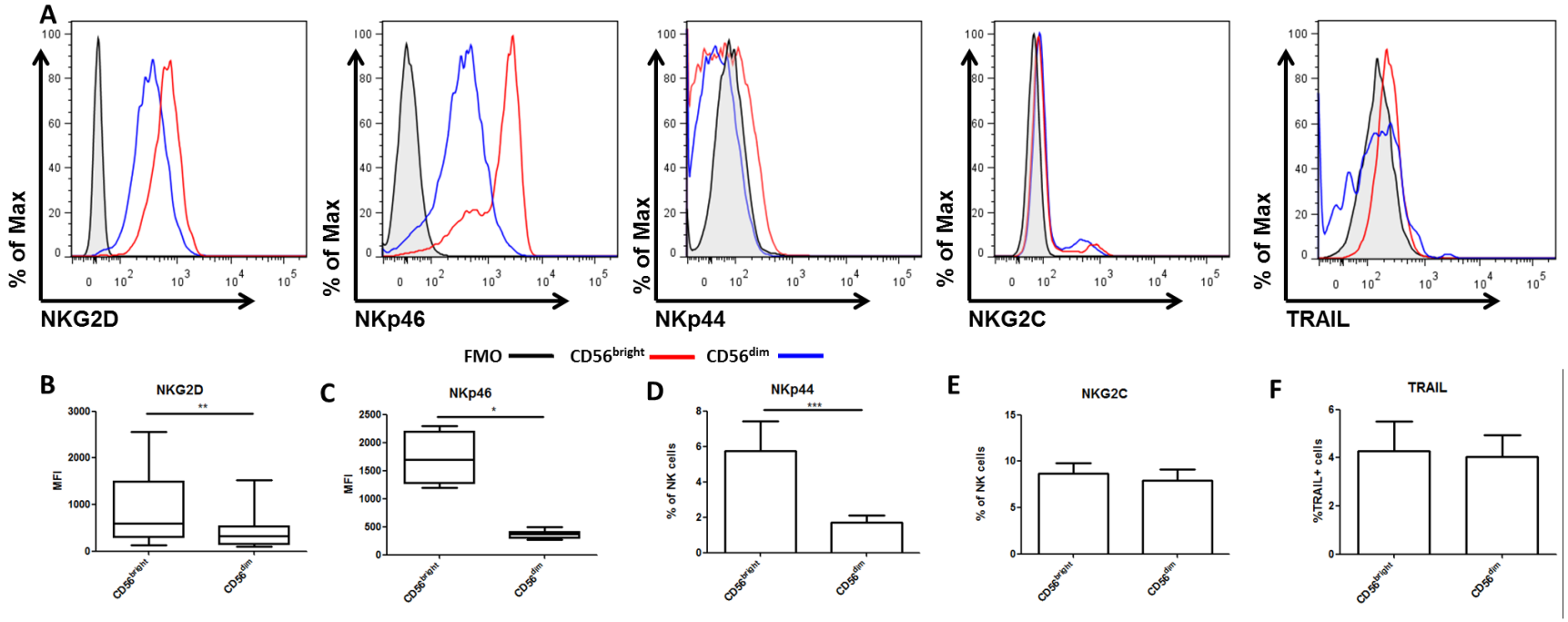

Figure 4- 2 CD56^{bright} hepatic NK cells have increased expression of cytotoxicity receptors

Mononuclear cells isolated from liver perfusate (LP), were stained with monoclonal antibodies. NK cells were identified from the CD45^{+} lymphocyte gate as CD56^{+}CD3^{-}. CD56^{bright} CD16$^{-/+}$ and CD56^{dim} CD16^{+} subsets were then gated on. Non-viable cells were excluded by FVS780 staining. **(A)** Representative histograms of NKG2D, NKp46, NKp44 NKG2C and TRAIL expression (CD56^{bright}-red, CD56^{dim} -blue, FMO-black). **(B)** Expression of NKG2D in NK cells from LP. **(C)** Expression of NKp46 in NK cells from LP **(D)** Expression of NKp44 in NK cells from LP. **(E)** Expression of NKG2C in NK cells from LP. **(F)** Expression of TRAIL in NK cells from LP. Data presented as mean ± SEM. Data analysed using Wilcoxon matched pairs test. (n=5-18, * $p<0.05$, ** $p<0.01$, ***$p<0.001$)

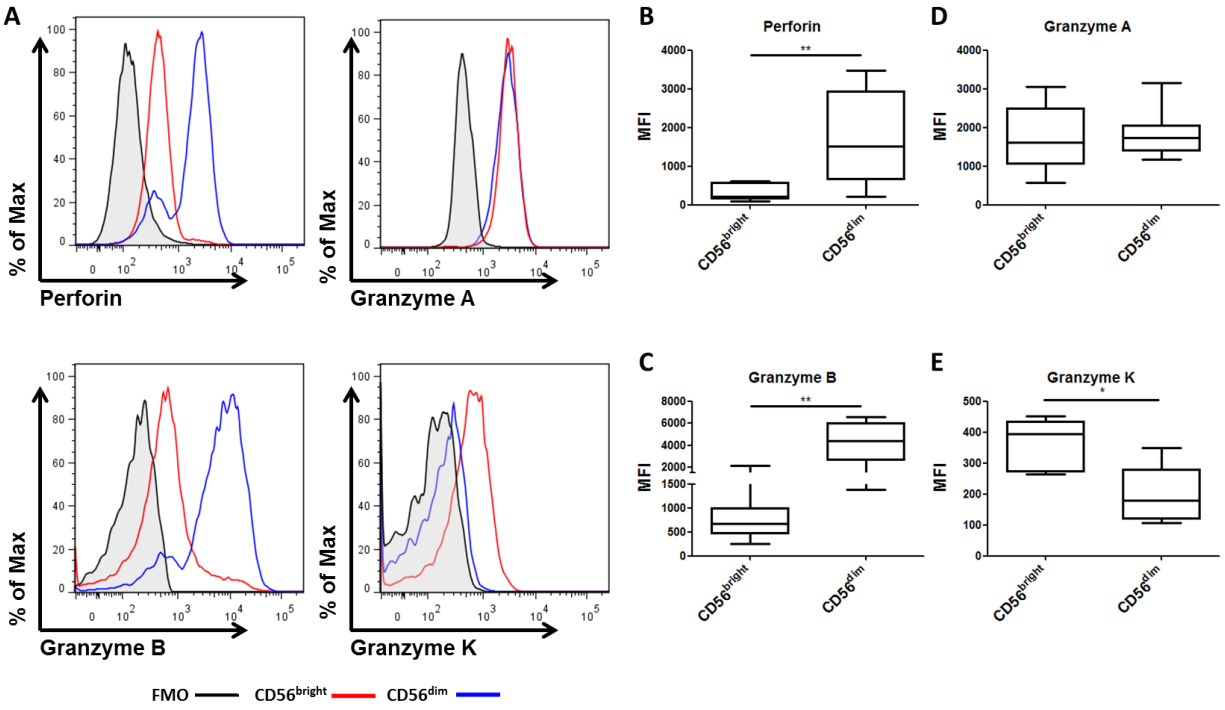

Figure 4- 3 Perforin and Granzyme molecules are differentially expressed by hepatic NK cell subsets

Mononuclear cells isolated from liver perfusate (LP), were stained with monoclonal antibodies. NK cells were identified from the $CD45^{+}$ lymphocyte gate as $CD56^{+}CD3^{-}$. $CD56^{bright}$ $CD16^{-/+}$ and $CD56^{dim}$ $CD16^{+}$ subsets were then gated on. Non-viable cells were excluded by FVS780 staining. **(A)** Representative histograms of perforin, granzyme B, granzyme A and granzyme K expression ($CD56^{bright}$-red, $CD56^{dim}$ -blue, FMO-black). **(B)** Expression of perforin in NK cells from LP. **(C)** Expression of granzyme B in NK cells from LP **(D)** Expression of granzyme A in NK cells from LP. **(E)** Expression of granzyme K in NK cells from LP. Data presented as mean ± SEM. Data analysed using Wilcoxon matched pairs test. (n=6, * $p<0.05$, ** $p<0.01$).

4.2.4 Hepatic CD56^{bright} NK cells are capable of direct cytotoxicity against colorectal cancer cell line SW620

CD56^{bright} NK cells have previously been described as poorly cytotoxic (Melsen et al., 2016). Due to the significant phenotypic differences between liver resident NK cells we compared their ability to degranulate and kill target cells to conventional anti-tumour CD56^{dim} NK cells. To examine cytotoxic function, NK cells were isolated by FACS sorting from donor perfusate. NK cell subsets were identified as CD56^{+} CD3^{-} lymphocytes, CD56^{bright} CD16$^{+/-}$ and CD56^{dim} CD16^{+}. Purity of hepatic NK cells was 95.9±0.7% and 93.2±1.2% for peripheral blood NK cells. Two target cell lines were used to assess degranulation and direct cytotoxicity, K562 (an MHC deficient leukaemia cells line) and SW620 (a metastatic colorectal cancer cell line isolated from lymph node). Target cells were labelled with cell trace violet (CTV) and stained with 7-AAD to assess cell death. Hepatic NK cells were incubated with either K562 or SW620 target cells for 4 hours at a ratio of 5:1 (effector: target). Degranulation was assessed by the expression of CD107a on the surface of NK cells.

CD56^{bright} NK cells displayed higher degranulation in response to K562 compared to CD56^{dim} cells (CD107a^{+} cells: 37.7±4.9% vs 17.8±1.4%, p=0.0169, **Figure 4-4C**). However this did not translate into increased cytotoxicity, with both subsets inducing cell death in a similar number of target cells (7-AAD^{+} target cells 21.2±4.6% vs 20.95±4.3%, p=0.37, **Figure 4-4E**). When challenged with SW620, CD56^{bright} NK cells degranulated more than CD56^{dim} cells (CD107a^{+} cells 12.2±2.0% vs 6.1±1.9%, p=0.109, **Figure 4-4D**). Both subsets were found to be capable of inducing cell death in SW620 cells (7-AAD $^{+}$ target cells 11.4±2.3% vs 13.3±2.4%, p=0.68, **Figure 4-4F).** Despite decreased expression of cytotoxic molecules, CD56^{bright} NK cells recognise and kill tumour cells at equal levels to CD56^{dim} NK cells.

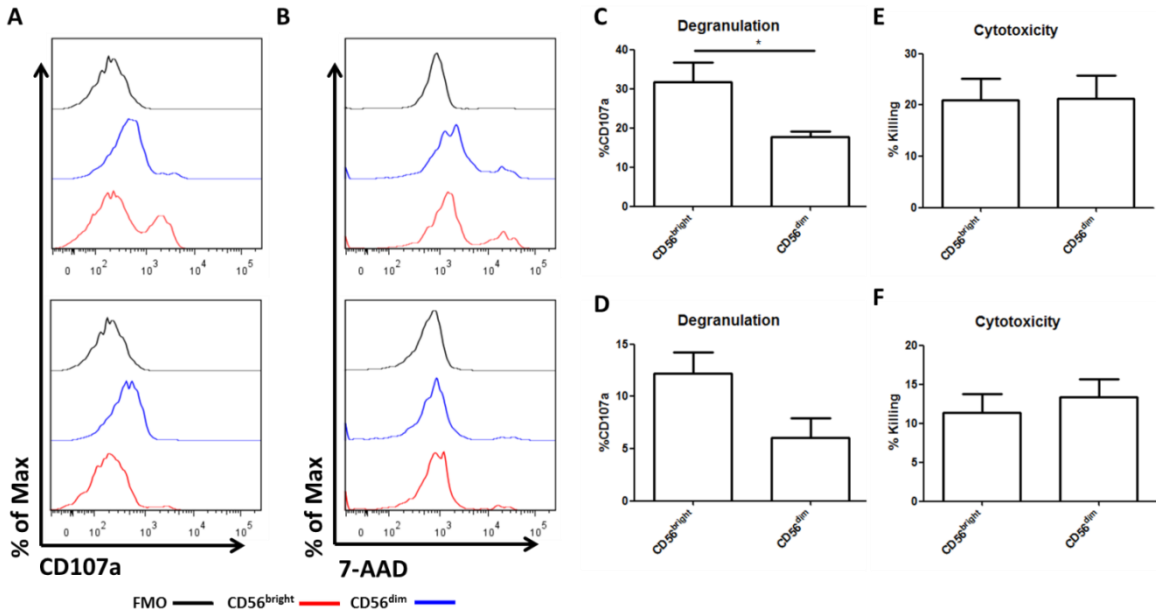

Figure 4- 4 Degranulation and direct cytotoxicity of hepatic NK cell subsets

$CD56^{bright}$ and $CD56^{dim}$ NK cells were isolated by FACS from liver perfusate (LP). Purified NK cells were then co-incubated with cell trace violet (CTV) labelled K562 or SW620 cells for 4 hours. CD107a antibody was added simultaneously. After 1 hour, 4µg/ml of Golgi-stop (containing monensin) was added. NK cells were identified as CTV negative cells, and CD107a expression was measured. Target cells were identified as CTV positive and cell death was measured by 7-AAD uptake. **(A)** Representative histograms of CD107a expression in response to K562 (top panel) and SW620 (bottom panel) (FMO-black, $CD56^{dim}$-blue, $CD56^{bright}$-red. **(B)** Representative histograms of 7-AAD uptake in response to K562 (top panel) and SW620 (bottom panel) (FMO-black, $CD56^{dim}$-blue, $CD56^{bright}$-red. **(C)** Expression of CD107a by NK cells from LP in response to K562 cells. **(D)** Expression of CD107a by NK cells from LP in response to SW620 cells. **(E)** Percentage of K562 cells killed by NK cells from liver perfusate. **(F)** Percentage of SW620 cells killed by NK cells from liver perfusate. Data presented as mean ± SEM. Data analysed using Wilcoxon matched pairs test.
(n=5, * $p<0.05$).

4.2.5 The proportion of natural killer subsets in tumour bearing liver

HMNC suspensions were prepared by enzymatically and mechanically disrupting tissue samples from the tumour, adjacent to the tumour and close to the resection margin (distal). These were stained with monoclonal antibodies and the proportion of lymphocyte subsets was analysed. NK cells are significantly depleted from the metastatic tumour itself, accounting for only 4.5±0.8% of intra-tumoural leukocytes ($CD45^+$). The proportion of NK cells gradually increases through the adjacent and distal tissue accounting for 13.6±1.9% and 15.6±2.2% of $CD45^+$ leukocytes respectively ($p<0.0001$, Figure 4-4B). This is similar to level seen in healthy donor liver (19.8±4.3%). This decrease in the proportion of NK cells is due to a drop in the absolute count of NK cells rather than increasing proportions of other cell types (absolute counts: tumour 320.9±143/mg, adjacent 1036±205.8/mg, distal 1310±283.6/mg, p=0.004, **Figure 4-5C**).

$CD56^{bright}$ NK cells are significantly reduced in the tumour compared to surrounding tissue accounting for 38.1±3.4% of hepatic NK cells. The proportion of $CD56^{bright}$ NK cells was significantly higher in the adjacent (50.±3.2%) and distal tissue (56.0±3.2%, p=0.0009, **Figure 4-5E**). This correlated with a decrease in the absolute count of $CD56^{bright}$ NK cells per milligram of tissue (absolute count: tumour 139.9±86.5/mg, adjacent 547.6±100.2/mg, distal 711.5±150.9/mg, p=0.003, **Figure 4-5F**).

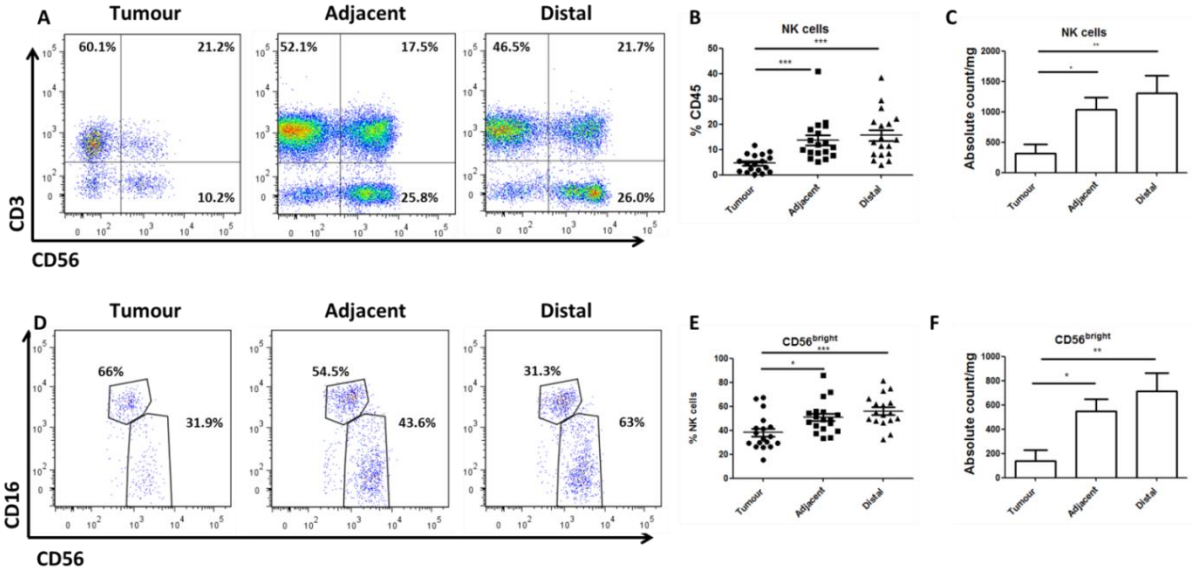

Figure 4- 5 Proportion of NK cell subsets in tumour bearing liver

Mononuclear cells isolated from tumour, adjacent, and distal tissue samples were stained with monoclonal antibodies**.** Gating strategy: NK cells were identified from the $CD45^{+}$ lymphocyte gate as $CD56^{+}CD3^{-}$. $CD56^{bright}$ $CD16^{-/+}$ and $CD56^{dim}$ $CD16^{+}$ subsets were then gated on. Non-viable cells were excluded by FVS780 staining. Absolute counts were established using 123Count eBeads. **(A)** Representative dot plots of lymphoid populations in samples from tumour, adjacent and distal tissue. **(B)** The percentage of NK cells in tumour, adjacent and distal tissue. **(C)** Absolute counts of NK cells per milligram of tissue from tumour, adjacent and distal samples **(D)** Representative dot plots of NK cell subsets in tumour, adjacent and distal tissue. **(E)** $CD56^{bright}$ $CD16^{-/+}$ NK cell frequencies in tumour, adjacent and distal tissue. **(F)** Absolute counts of $CD56^{bright}$ NK cells per milligram of tissue from tumour, adjacent and distal samples. Data presented as mean ± SEM. Data analysed using Friedman test, with Dunn's multiple comparison test. (n=18 *, $p<0.05$, **, $p<0.01$, ***, $p<0.001$)

4.2.6 The remaining CD56^{bright} NK cells display tissue resident phenotype

In order to determine if the NK cells present in tumour bearing liver are tissue resident or derived from peripheral blood we investigated the expression of the transcription factors Eomes and Tbet, and markers of tissue residency such as CXCR6, CD69, CD49a and TRAIL. No significant difference in the expression of Eomes or Tbet was observed in NK cells from resected liver compared to donor. The majority of CD56^{bright} NK cells are Eomes^{hi} Tbet^{lo} in all tissues analysed (tumour 86.1±2.3%, adjacent 87.1±2.9%, distal 90.2±2.5, p=0.29, **Figure 4-6B**). Similarly, CD56^{dim} NK cells remained Eomes^{lo} Tbet^{hi} in tumour bearing liver (tumour 97.5±1.2%, adjacent 95.7±1%, distal 95.9±1.2, p=0.23, **Figure 4-6C**).

We have previously shown that the majority of liver CD56^{bright} NK cells express CXCR6 (Chapter 3). CD56^{bright} NK cells from tumour bearing liver express CXCR6 at comparable levels (tumour 55.9±9.9%, adjacent 50.3±9.6%, distal 49.5±6.5, p=0.69, **Figure 4-7B**). Similarly, CD69 expression was not changed between CD56^{bright} NK cells in tumour or surrounding tissue (tumour 88.0±4.3%, adjacent 90.4±4.2%, distal 89.7±3.2%, p=0.83, **Figure 4-7C**). TRAIL expression did not differ significantly between cells from tumour bearing liver (tumour 12.8±4.4%, adjacent 16.9±6.9%, distal 12.4±4.7%, p=0.91, **Figure 4-7D**) but was found at higher levels compared to healthy NK cells from liver perfusate (4.3±1.2%). This may indicate activation of tissue resident NK cells throughout the tumour bearing liver tissue. Finally, CD49a expression was not significantly altered between tumour infiltrating NK cells and those from the surrounding tissue (tumour 9.9±4.9 %, adjacent 6.2±2.9%, distal 6.7±2.2%, p=0.97, **Figure 4-7E**). This was found to be similar to the level seen in healthy donor biopsies (6.3±2.4%). The remaining CD56^{bright} NK cells in the tumour appear to be tissue resident cells and not peripheral blood cells which have infiltrated the tumour.

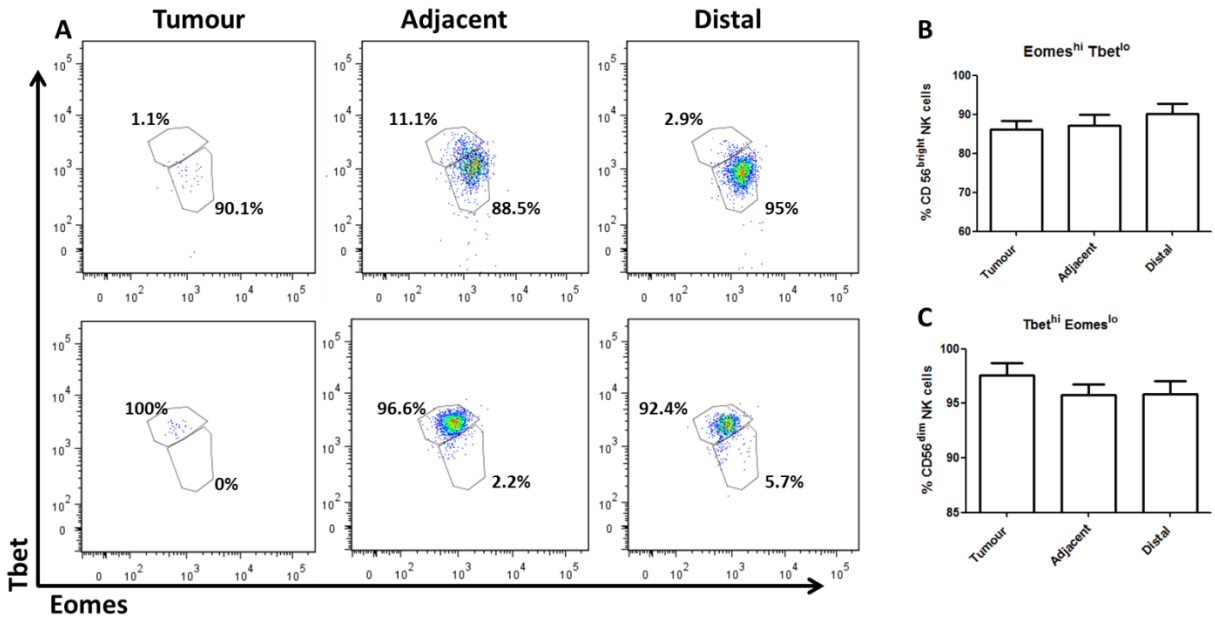

Figure 4- 6 Tumour infiltrating NK cells maintain their Eomes^{hi} Tbet^{lo} phenotype

Mononuclear cells isolated from tumour, adjacent, and distal tissue samples were stained with monoclonal antibodies**.** Gating strategy: NK cells were identified from the CD45^{+} lymphocyte gate as CD56^{+}CD3^{-}. CD56^{bright} CD16$^{-/+}$ and CD56^{dim} CD16^{+} subsets were then gated on. Non-viable cells were excluded by FVS780 staining. **(A)** Representative dot plots of Eomes and Tbet expression in CD56^{bright} (top line) and CD56^{dim} (bottom line) NK cells in samples from tumour, adjacent and distal tissue. **(B)** The percentage of Eomes^{hi} Tbet^{lo} CD56^{bright} NK cells in tumour, adjacent and distal tissue. **(C)** The percentage of Eomes^{lo} Tbet^{hi} CD56^{dim} NK cells in tumour, adjacent and distal tissue. Data presented as mean ± SEM. Data analysed using Friedman test, with Dunn's multiple comparison test. (n=6)

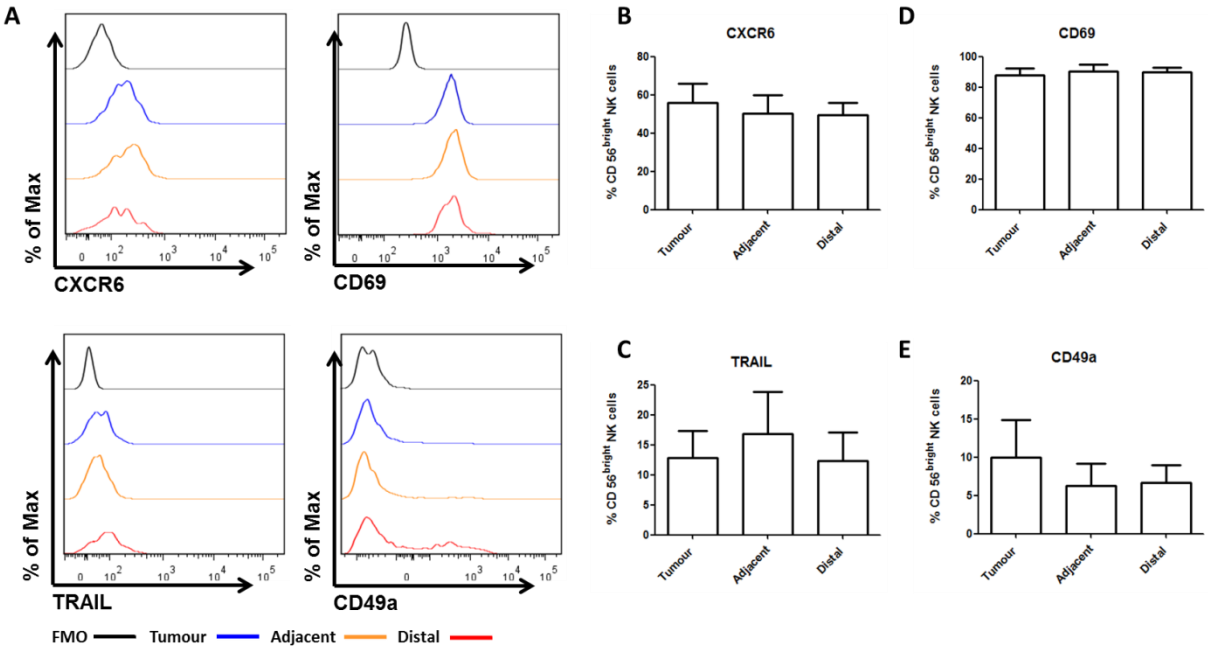

Figure 4- 7 Tumour infiltrating NK cells maintain expression of markers of tissue residency

Mononuclear cells isolated from tumour, adjacent, and distal tissue samples were stained with monoclonal antibodies**.** Gating strategy: NK cells were identified from the $CD45^{+}$ lymphocyte gate as $CD56^{+}CD3^{-}$. $CD56^{bright}$ $CD16^{-/+}$ and $CD56^{dim}$ $CD16^{+}$ subsets were then gated on. Non-viable cells were excluded by FVS780 staining. **(A)** Representative histograms of CXCR6, TRAIL, CD69 and CD49a in $CD56^{bright}$ NK cells in samples from tumour (red), adjacent (orange) and distal tissue (blue) (black-FMO). **(B)** The percentage of CXCR6 positive $CD56^{bright}$ NK cells in tumour, adjacent and distal tissue. **(C)** The percentage of TRAIL positive $CD56^{bright}$ NK cells in tumour, adjacent and distal tissue. **(D)** The percentage of CD69 positive $CD56^{bright}$ NK cells in tumour, adjacent and distal tissue. **(E)** The percentage of CD49a positive $CD56^{bright}$ NK cells in tumour, adjacent and distal tissue. Data presented as mean ± SEM. Data analysed using Friedman test, with Dunn's multiple comparison test. (n=5)

4.2.7 Tumour infiltrating CD56^{bright} NK cells maintain cytotoxicity receptor expression

Considering liver resident NK cells are capable of direct cytotoxicity against metastatic colorectal cancer cells and are still present in the tumour we next investigated if infiltration of the tumour effected cytotoxicity receptor expression, which would prevent tumour cell killing. NKG2D is an important receptor for recognising stressed or altered cells (Lanier, 2015) and was found to be increased in liver resident NK cells. No significant changes in NKG2D expression were noted in tumour infiltrating CD56^{bright} NK cells (tumour 93.0±4.2%, adjacent 98.2±1.0%, distal 97.6±1.1%, p=0.55, **Figure 4-8B**). Similarly, NKp46 was not significantly altered in liver resident NK cells from tumour compared to surrounding tissue (tumour 86.7±1.7%, adjacent 89.1±3.4%, distal 84.7±4.4%, p=0.47, **Figure 4-8C**). NKp44 was significantly increased on tumour infiltrating liver resident NK cells compared to those in the surrounding tissue (tumour 31.1±11.3%, adjacent 14.7±1.0%, distal 11.9±0.9%, p=0.039, **Figure 4-8D**). NKp44 was higher in all parts of the tumour bearing liver compared to the healthy donor liver (5.7±1.7%), indicating that throughout the organ tissue resident NK cells appear more highly activated. NKG2C was unchanged in NK cells infiltrating the tumour (tumour 17.2±7.5%, adjacent 7.5±1.2%, distal 5.8±1.1%, p=0.4, **Figure 4-8E**). Tumour infiltrating liver resident NK cell maintain cytotoxicity receptor expression and therefore ability to recognise tumour cells.

4.2.8 Tumour infiltrating CD56^{bright} NK cells maintain cytotoxic molecule expression

We next analysed expression of cytotoxic molecules in tumour infiltrating liver resident NK cells to determine if cytotoxicity was prevented by dysregulation of effector molecules. However, perforin, granzyme B, granzyme A and granzyme K expression was unchanged in CD56^{bright} NK cells from CRLM tumours compared to NK cells in the surrounding tissue. Granzyme B was expressed at similar levels in all samples tested (MFI tumour 447±114, adjacent 764±278, distal 867±410, p=0. 0625, **Figure 4-9B**). Perforin remained at a similar level in tumour (MFI 129±20), adjacent (MFI 117±15), and distal tissue (MFI 130±16, p=0.88, **Figure 4-8C**).

Similarly granzyme A was not affected by the tumour environment (MFI tumour 1276±145, adjacent 1361±269, distal 1512±275, p=0.87, **Figure 4-9D**). Granzyme K showed a small reduction in expression in tumour infiltrating CD56^{bright} NK cells but this was not significant (MFI tumour 133±26, adjacent 257±77, distal 304±103, p=0.79, **Figure 4-9E**). Tumour infiltrating liver resident NK cells maintains cytotoxic potential through cytotoxicity receptor and effecter molecule expression.

4.2.9 Hepatic CD56^{bright} NK cells migrate toward tumour conditioned media

In order to address the decreased numbers of liver resident CD56^{bright} NK cells in CRLM tumours, we first investigated whether these cells are capable of being chemotactically attracted to these tumours. Tumours were dissected and used to produce conditioned media. Healthy donor biopsies were used to generate liver conditioned media (LCM). CD56^{bright} and CD56^{dim} NK cells were FACS sorted from liver perfusate. A chemotaxis assay was then performed to assess cell migration. Briefly, NK cells were serum starved for 2 hours and placed in the upper chamber of a transwell insert. The bottom chamber was filled with serum free media supplemented with 10% v/v LCM or tumour conditioned media from CRLM. CD56^{bright} and CD56^{dim} NK cells showed no difference in migration toward LCM (p=0.31, **Figure 4-10A**). However, CD56^{bright} NK cells migrated significantly more toward CRLM conditioned media compared to CD56^{dim} NK cells (p=0.0156, Figure 4-10B). This appears to be due to reduced migration of CD56^{dim} NK cells, while CD56^{bright} NK cells have similar levels of migration to toward both LCM and CRLM conditioned media. Defects in migration do not appear to account for the depletion of CD56^{bright} NK cells in CRLM tumours.

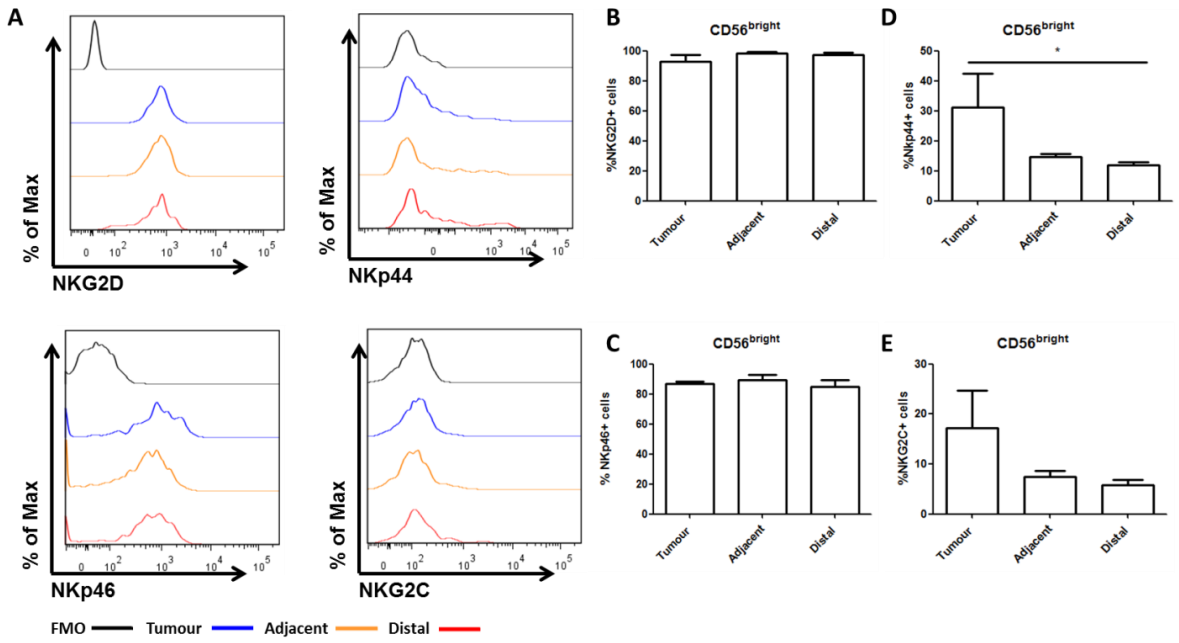

Figure 4- 8 Expression of cytotoxicity receptors in NK cell subsets in CRLM

Mononuclear cells isolated from tumour, adjacent, and distal tissue samples were stained with monoclonal antibodies**.** Gating strategy: NK cells were identified from the CD45+ lymphocyte gate as $CD56^{+}CD3^{-}$. $CD56^{bright}$ $CD16^{-/+}$ and $CD56^{dim}$ $CD16^{+}$ subsets were then gated on. Non-viable cells were excluded by FVS780 staining. **(A)** Representative histograms of NKG2D, NKp46, NKp44 and NKG2C in $CD56^{bright}$ NK cells in samples from tumour (red), adjacent (orange) and distal tissue (blue) (black-FMO). **(B)** The percentage of NKG2D positive $CD56^{bright}$ NK cells in tumour, adjacent and distal tissue. **(C)** The percentage of NKp46 positive $CD56^{bright}$ NK cells in tumour, adjacent and distal tissue. **(D)** The percentage of NKp44 positive $CD56^{bright}$ NK cells in tumour, adjacent and distal tissue. **(E)** The percentage of NKG2C positive $CD56^{bright}$ NK cells in tumour, adjacent and distal tissue. Data presented as mean ± SEM. Data analysed using Friedman test, with Dunn's multiple comparison test. (n=5,*, $p<0.05$)

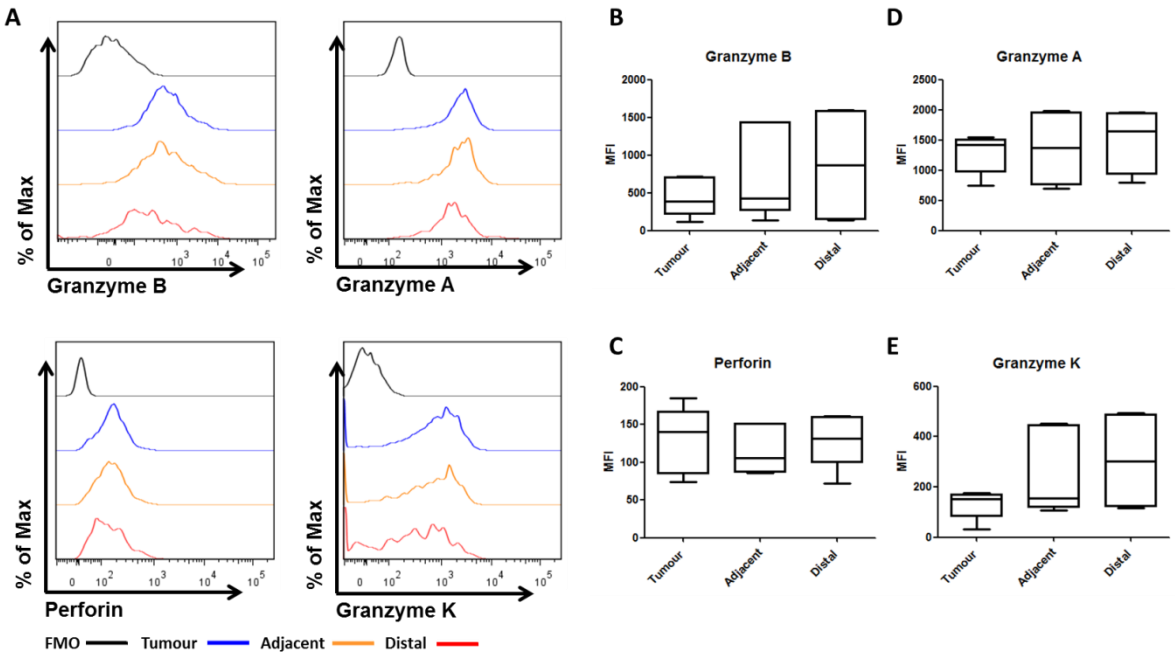

Figure 4- 9 Granzyme and perforin expression in tumour infiltrating NK cells

Mononuclear cells isolated from tumour, adjacent, and distal tissue samples were stained with monoclonal antibodies**.** Gating strategy: NK cells were identified from the CD45+ lymphocyte gate as $CD56^{+}CD3^{-}$. $CD56^{bright}$ $CD16^{-/+}$ and $CD56^{dim}$ $CD16^{+}$ subsets were then gated on. Non-viable cells were excluded by FVS780 staining. **(A)** Representative histograms of granzyme B, perforin, granzyme A and granzyme K in $CD56^{bright}$ NK cells in samples from tumour (red), adjacent (orange) and distal tissue (blue) (black-FMO). **(B)** The expression of granzyme B in $CD56^{bright}$ NK cells from tumour, adjacent and distal tissue. **(C)** The expression of perforin in $CD56^{bright}$ NK cells from tumour, adjacent and distal tissue. **(D)** The expression of granzyme A in $CD56^{bright}$ NK cells from tumour, adjacent and distal tissue. **(E)** The expression of granzyme K in $CD56^{bright}$ NK cells from tumour, adjacent and distal tissue. Data presented as mean ± SEM. Data analysed using Friedman test, with Dunn's multiple comparison test. (n=5)

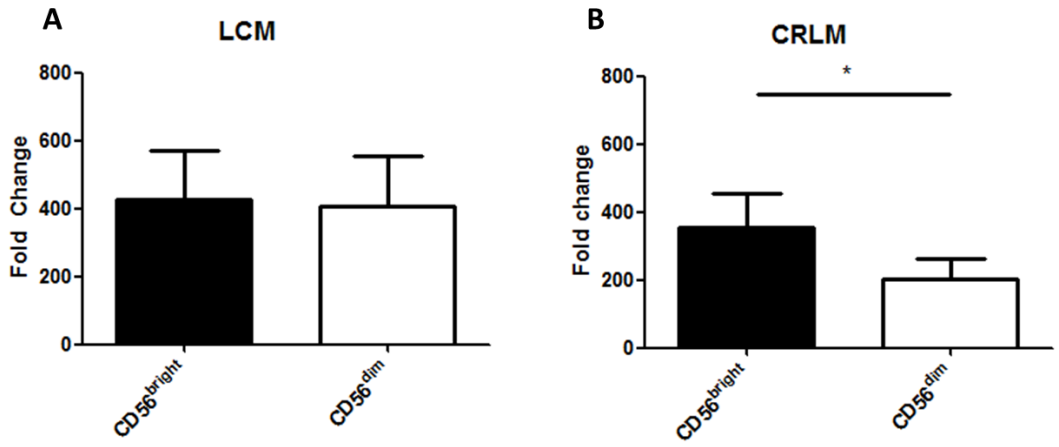

Figure 4- 10 CD56^{bright} hepatic NK cells are chemotactically attracted to CRLM tumours

CD56^{bright} and CD56^{dim} NK cells were isolated by FACS from liver perfusate (LP). Purified NK cells were then serum starved for two hours. Cells were then washed and media resuspended in fresh serum free media. 1x10^{5} cells were then placed in the upper chamber of a transwell insert. The lower chamber was filled with serum free media supplemented with/without 10% conditioned media from healthy donor tissue (LCM) or from colorectal liver metastasis tissue (CRLM). After two hours the media from the lower chamber was harvested and absolute cell counts were performed using 123Count eBeads by flow cytometry. Fold change over media alone was calculated. **(A)** Fold change in migration of NK cell subsets from LP in response to LCM. **(B)** Fold change in migration of NK cell subsets from LP in response to CRLM. Data presented as mean ± SEM. Data analysed using Wilcoxon matched pairs test. (n=5, * $p<0.05$).

4.2.10 Tumour conditioned media induces apoptosis in hepatic CD56^{bright} NK cells

Liver resident NK cells are chemotactically attracted to CRLM tumour supernatants but are significantly reduced in tumour samples. We therefore investigated whether the tumour microenvironment was resulting in the apoptosis of liver resident NK cells. Liver resident CD56^{bright} and non-resident CD56^{dim} NK cells were isolated by FACS sorting. Cells were then cultured for 24 hours in the presence or absence of 50% v/v, healthy liver conditioned media (LCM) or conditioned media from colorectal liver metastasis tumours (CRLM). A concentration of 50% was chosen after titration of CRLM conditioned media at a range of concentrations (**Appendix Figure 4**). Apoptosis was then assessed by annexin/7AAD staining. Apoptotic cells were identified by binding of annexin (bound to cell surface phosphatidylserine) and uptake of 7AAD (DNA binding dye). CD56^{bright} NK cells cultured in CRLM underwent significantly more apoptosis compared to matched cells treated with LCM (LCM- 21.1±2.8%, CRLM-39.2±8.1%, p=0.034, **Figure 4-11B**). In contrast, there was no significant change in apoptosis of CD56^{dim} NK cells treated with LCM or CRLM (LCM-18.9±6.8%, CRLM-20.0±10.5%, p=0.699, **Figure 4-11C**). There was no difference between CD56^{bright} and CD56^{dim} NK cells cultured with LCM (**Figure 4-11D**). However, when cultured with CRLM CD56^{bright} NK cells undergo significantly more apoptosis compared to CD56^{dim} cells (39.2±8.1% vs 20.0±10.5%, p=0.0313, **Figure 4-11E**). The proportion of pro-apoptotic cells (annexin^{+} 7-AAD^{-}) decreased in both CD56^{bright} (LCM 32.8±13.2%, CRLM 24.2±10.7%, p=0.98) and CD56^{dim} ((LCM 31.9±15.6%, CRLM 21.8±12.4%, p=0.87) NK cells between LCM and CRLM treatment (**Appendix Figure 5**).

4.2.11 Apoptosis induced by tumour conditioned media is not caspase 8 mediated

In order to determine the mechanism of apoptosis occurring in liver resident NK cells, caspase 8 (a mediator of extrinsic cell death) was inhibited using Z-IETD-FMK (BD Biosciences). Effective dosage of Z-IETD-FMK was determined using the Jurkat cell line and anti-FAS, which activates caspase 8 mediated apoptosis (**Appendix Figure 6**). FACS isolated CD56^{bright} NK cells from liver perfusate were treated with 50μM Z-IETD-FMK for two hours. Cells

were then treated CRLM conditioned media for 24 hours. No significant difference in annexin positive cells was seen (48.2±9.2% vs 46.7±1.3%, p=0.88, **Figure 4-12B**).

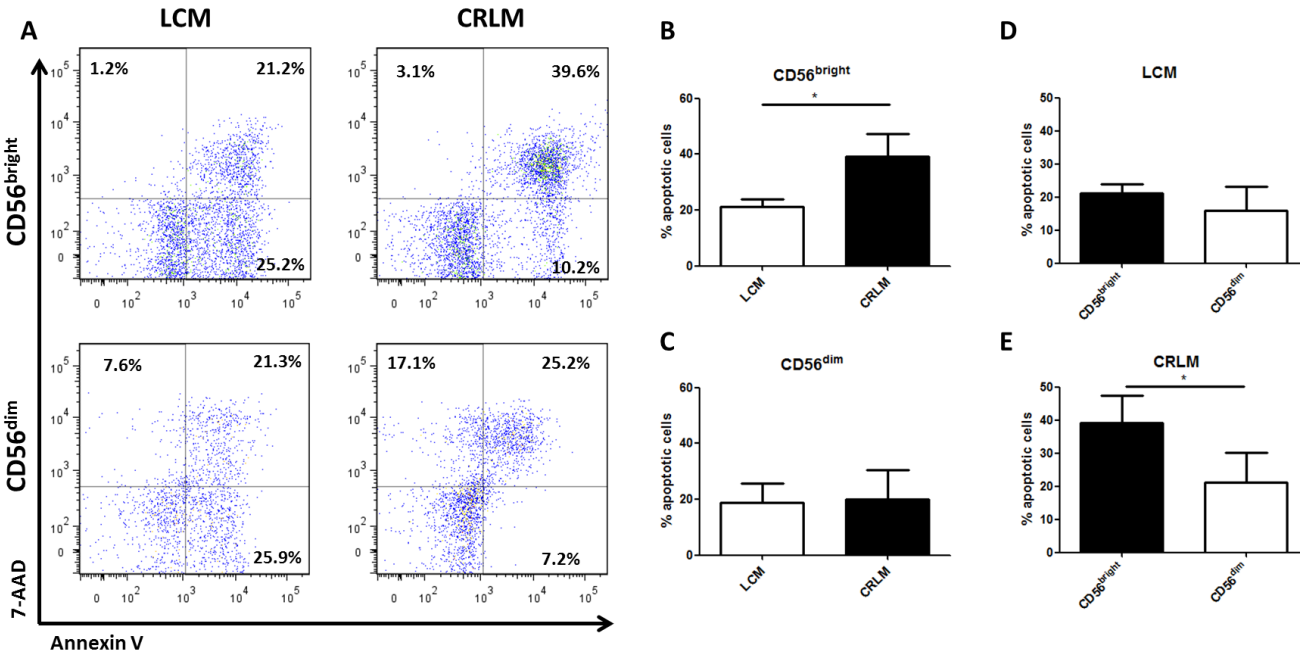

Figure 4- 11 Tumour conditioned media from CRLM induces apoptosis of CD56^{bright} hepatic NK cells

NK cell subsets were isolated from liver perfusate by FACS. Cells were cultured for 24 hours in the presence of 50% v/v healthy liver conditioned media (LCM) or conditioned media from colorectal liver metastasis tumours (CRLM). Apoptosis was assessed by annexin V and 7AAD staining. **(A)** Representative dot plots of annexin V/7AAD staining in CD56^{bright} and CD56^{dim} NK cells treated with LCM or CRLM. **(B)** Percentage of apoptotic CD56^{bright} NK cells after treatment with LCM or CRLM. **(C)** Percentage of apoptotic CD56^{dim} NK cells after treatment with LCM or CRLM. **(D)** Percentage of apoptotic NK cells after treatment with LCM. **(E)** Percentage of apoptotic NK cells after treatment with CRLM. Data presented as mean ± SEM. Data analysed using Wilcoxon matched pairs test. (n=5, * $p<0.05$).

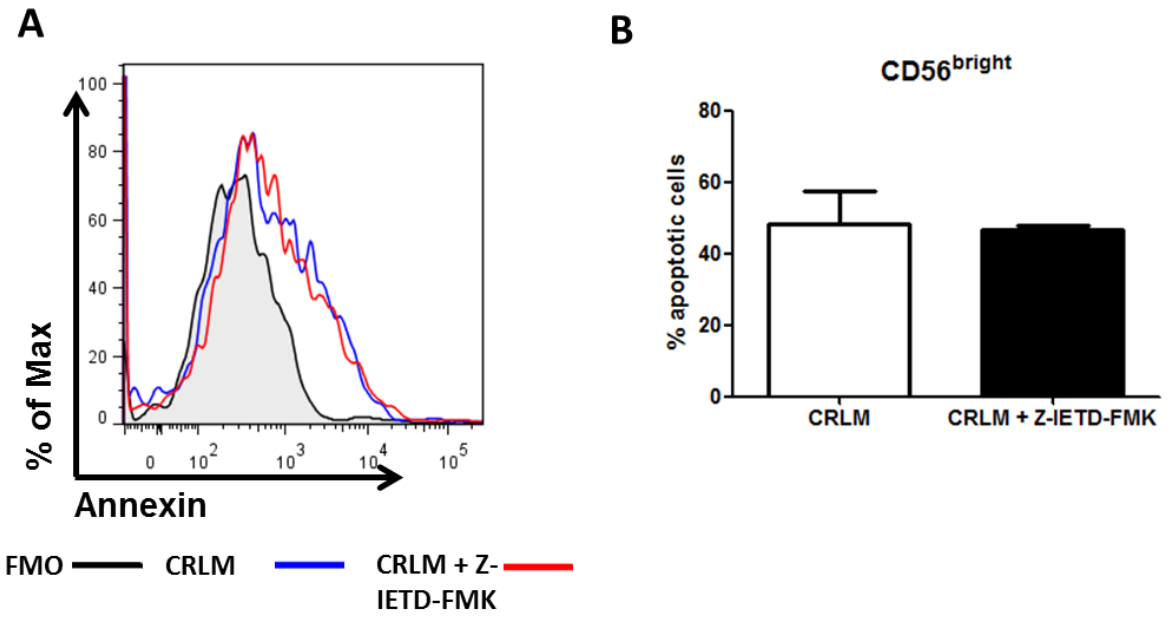

Figure 4- 12 Tumour conditioned media induced apoptosis is not caspase-8 mediated

CD56^{bright} NK cells were isolated from liver perfusate by FACS. Cells were treated with caspase 8 inhibitor Z-IETD-FMK for 2 hours. Cells were cultured for 24 hours in the presence of 50% v/v conditioned media from colorectal liver metastasis tumours (CRLM). Apoptosis was assessed by annexin V. **(A)** Representative histogram of annexin V staining in CD56^{bright} NK cells treated with CRLM with/without Z-IETD-FMK. **(B)** Percentage of apoptotic CD56^{bright} NK cells after treatment with CRLM with/without Z-IETD-FMK. Data presented as mean ± SEM. Data analysed using Wilcoxon matched pairs test. (n=5).

4.2.12 Characterisation of the CRLM microenvironment

Since apoptosis of liver resident NK cells was not mediated by death signalling acting through the extrinsic pathway, we next analysed the tumour microenvironment for potential targets which may induce intrinsic or mitochondrial mediated apoptosis. The intrinsic pathway can be activated as a result of the loss of growth factors, metabolic starvation, DNA damage or ER stress (Elmore, 2007; Taylor et al., 2008). NK cells are reliant on IL-15 for cell survival (Liu et al., 2000). These 24 hour cultures contained no exogenous source of IL-15 so endogenous levels were measured by ELISA. No significant difference was seen in the levels of IL-15 in healthy liver conditioned media (LCM) and those from CRLM (LCM-335.6±74pg/ml, CRLM-300±15.4pg/ml, p=0.84, **Figure 4-13A**). In our previous experiments we identified TGF-β as an essential cytokine that maintains liver resident NK cell homeostasis. While TGF-β levels were increased in CRLM compared to LCM, These differences were not significant (LCM-222.7±68.2pg/ml, CRLM-331.0±134.7pg/ml, p=0.67, **Figure 4-13B**).

We next investigated whether glucose deprivation was inducing apoptosis in the CRLM treated cells. It is well established that tumour cells consume larger amounts of glucose than healthy cells (Pavlova and Thompson, 2016). In our *ex vivo* cultures, glucose was provided at high non-biological levels in cell culture media, therefore it was not surprising that levels did not differ between LCM and CRLM (LCM- 17.1±3.6mM, CRLM- 17.2±1.5mM, p=0.49, **Figure 4-14A**). As an alternative method of measuring glycolysis in these cultures, lactate levels were measured. CRLM conditioned media contained significantly higher levels of lactate compared to LCM (LCM- 1.7±0.3mM, CRLM-11.5±2.8mM, p=0.002, **Figure 4-14B**).

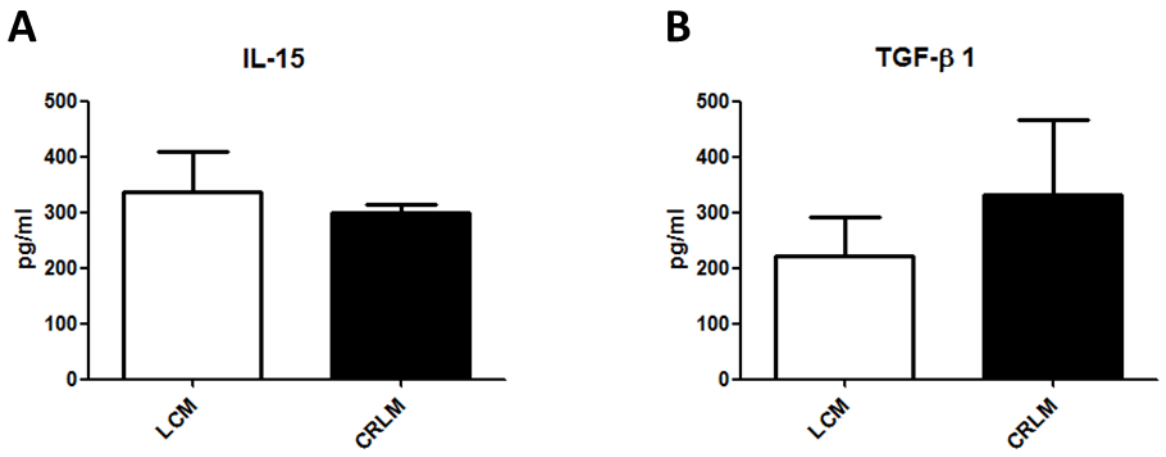

Figure 4- 13 NK cell related cytokines unchanged in CRLM tumours

Conditioned media from healthy livers (LCM) and colorectal liver metastasis (CRLM) were generated and analysed for cytokine levels by ELISA. **(A)** IL-15 concentration in LCM and CRLM. **(B)** TGF-β1 concentration in LCM and CRLM. Data presented as mean ± SEM. Data analysed using Wilcoxon matched pairs test. (n=10).

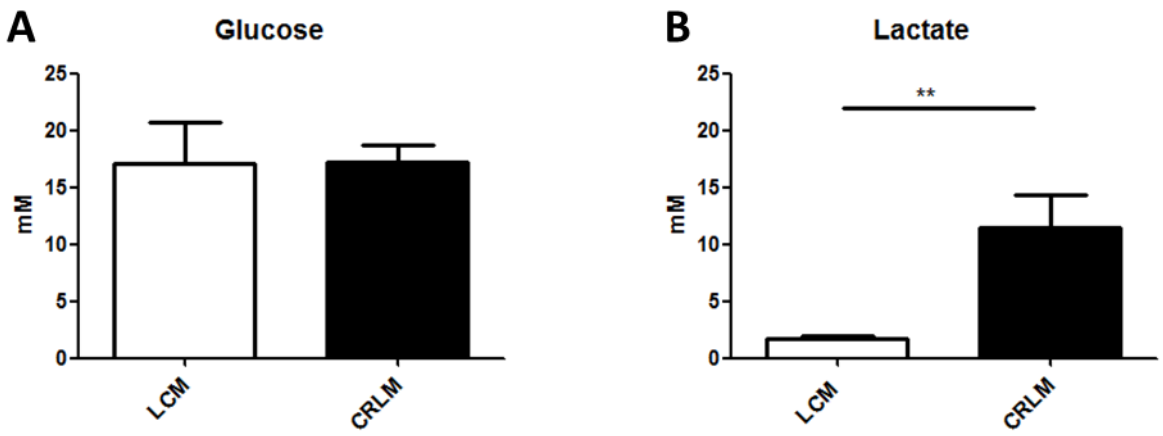

Figure 4- 14 CRLM tumours produce significantly more lactate than healthy liver tissue

Conditioned media from healthy livers (LCM) and colorectal liver metastasis (CRLM) were generated and analysed for metabolite levels by biochemical assays. **(A)** Glucose concentration in LCM and CRLM. **(B)** Lactate concentration in LCM and CRLM. Data presented as mean ± SEM. Data analysed using Wilcoxon matched pairs test. (n=10, **p<0.01).

4.2.13 CRLM tumours have increased expression of GLUT1 and lactate transporters

CRLM tumours were examined for expression of GLUT1, a major glucose transporter and MCT1 and MCT4 (the main lactate transporting molecules). Gene expression of these three receptors was analysed in tissue from tumour and adjacent tissue. *SLC16A1* (MCT-1 gene) was not differentially expressed between tumour and adjacent tissue (p=0.37, **Figure 4-15A**). *SLC16A3* or MCT-4, the main lactate exporter, was highly expressed in tumour compared to adjacent tissue (p=0.0391, **Figure 4-15B**). CRLM tumours also showed increased expression of *SLC2A1* (GLUT1, p=0.0469, **Figure 4-15C**). These results, in combination with lactate levels in conditioned media, indicate that CRLM tumours are highly glycolytic.

4.2.14 Metabolic receptors and mitochondrial mass in NK cell subsets

In order to determine if liver resident NK cells are more susceptible to nutrient deprivation in the tumour environment, we analysed expression of nutrient transporters and mitochondrial mass. GLUT1 is the main receptor associated with glucose transport in immune cells (MacIver et al., 2008). However, GLUT1 was not differentially expressed between $CD56^{bright}$ and $CD56^{dim}$ NK cells from liver perfusate (MFI 147.7±47.9 vs MFI 215.5±69.6, p=0.125, **Figure 4-16B**). Similarly, expression of the amino acid transporter CD98 was unchanged ($CD56^{bright}$- MFI 1695±97.2, $CD56^{dim}$- MFI 967.8±297.1, p=0.315, **Figure 4-16C**). Likewise, the transferrin receptor (CD71) was not differentially expressed between NK cell subsets from liver perfusate ($CD56^{bright}$- MFI 131.1±24.8, $CD56^{dim}$- MFI 118.3±23.5, p=0.625, **Figure 4-16D**). We also measured mitochondrial mass, as a surrogate marker of potential ATP generation, using a mitochondrial dye that binds independently of mitochondrial membrane potential (MitoTracker dye (Agnello et al., 2008)). Liver resident NK cells displayed significantly lower mitochondrial mass compared to $CD56^{dim}$ NK cells from liver perfusate (MFI 1606±437.7 vs MFI 6917±1976, p=0.046, **Figure 4-16E**).Whether this is due to increased mitochondrial number or size in $CD56^{dim}$ NK cells remains to be determined and will require further experimentation using confocal or electron microscopy.

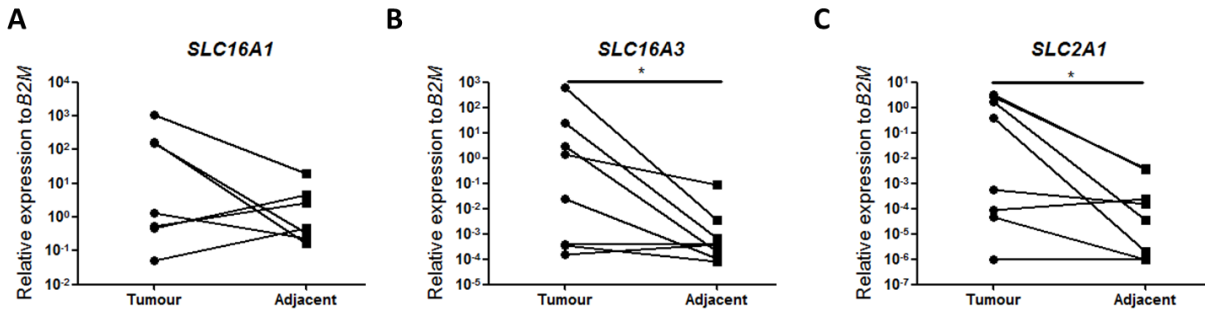

Figure 4- 15 Expression of *SCL16A1, SLC16A3* and *SLC2A1* mRNA in CRLM tumour and adjacent tissue

Biopsies were taken from tumour and adjacent liver tissue from patients undergoing liver resection for colorectal metastases. RNA was extracted; reverse transcribed into cDNA and real time PCR was performed. Gene expression was normalised to internal control *B2M*. **(A)** Expression of *SLC16A1* (MCT1) in tumour and adjacent tissue. **(B)** Expression of *SLC16A3* (MCT4) in tumour and adjacent tissue. **(C)** Expression of *SLC2A1* (GLUT1) in tumour and adjacent tissue. Data presented as mean ± SEM. Data analysed using Wilcoxon matched pairs test. (n=6-7, *p<0.05).

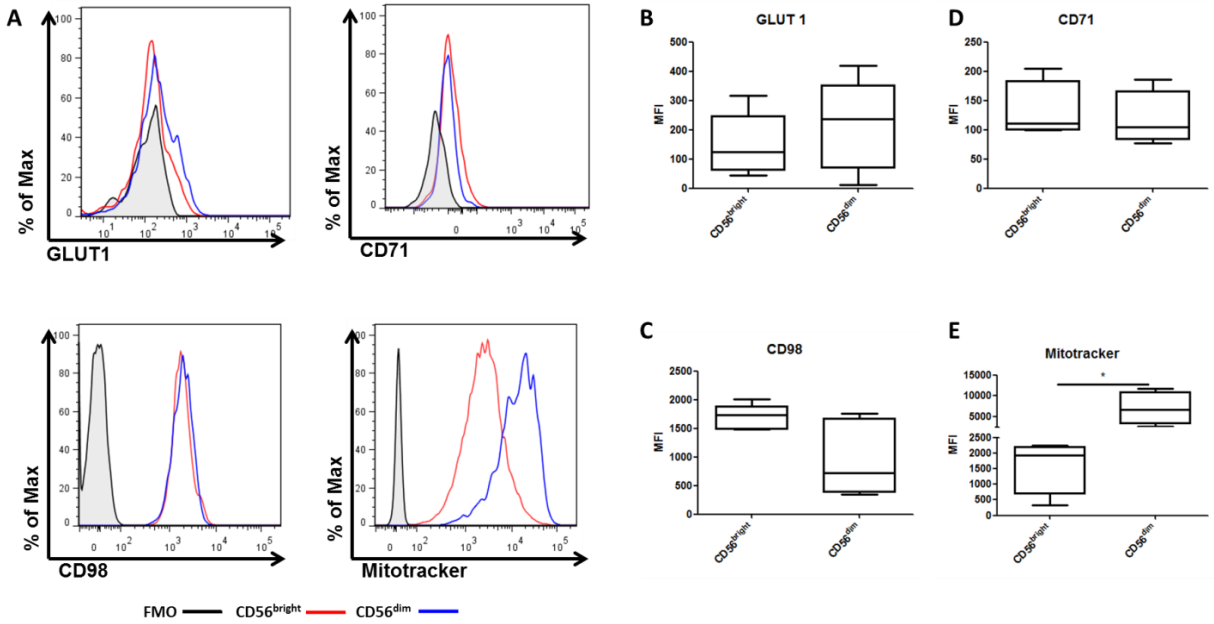

Figure 4- 16 Expression of nutrient transporters and mitochondrial mass of hepatic NK cell subsets

Mononuclear cells isolated liver perfusate were stained with monoclonal antibodies**.** Gating strategy: NK cells were identified from the $CD45^{+}$ lymphocyte gate as $CD56^{+}CD3^{-}$. $CD56^{bright}$ $CD16^{-/+}$ and $CD56^{dim}$ $CD16^{+}$ subsets were then gated on. Non-viable cells were excluded by FVS780 staining. **(A)** Representative histograms of GLUT1, CD98, CD71 and Mitotracker Deep Red in $CD56^{bright}$ (red line) and $CD56^{dim}$ (blue line) NK cells in liver perfusate samples (black-FMO). **(B)** The expression of GLUT1 in NK cell subsets from liver perfusate. **(C)** The expression of CD98 in NK cell subsets from liver perfusate. **(D)** The expression of CD71 in NK cell subsets from liver perfusate. **(E)** The level of Mitotracker Deep Red uptake in NK cell subsets from liver perfusate. Data presented as mean ± SEM. Data analysed using Wilcoxon matched pairs test. (n=6, * $p<0.05$)

4.2.15 Metabolic receptor expression in CD56^{bright} NK cells in CRLM tumours

Nutrient receptors are often upregulated in incidences of nutrient deprivation (Aft et al., 2002; Jensen et al., 2017). Therefore, expression of GLUT1, CD98, and CD71 were analysed in tumour infiltrating liver resident NK cells. GLUT1 showed no variation in expression between CD56^{bright} NK cells from tumour, adjacent or distal tissue (MFI tumour 307.8±131.4, adjacent 203.8±41.4, distal 257.4±40.4, p=0.18, **Figure 4-17B**). CD98 was also unchanged in tissue resident NK cells from tumour, adjacent or distal tissue (MFI tumour 3430±967, adjacent 2949±726, distal 3406±958, p=0.69, **Figure 4-17C**). Similarly, CD71 was not found to be significantly changed in tumour infiltrating CD56^{bright} NK cells compared to adjacent or distal cells (MFI tumour 39.6±8.7, adjacent 41.8±12.6, distal 58.8±10.1, p=0.125, **Figure 4-17D**). Tumour infiltrating NK cells do not upregulate nutrient transporters compared to the surrounding tissue, indicating nutrient deprivation may not be the cause of apoptosis.

4.2.16 Tumour infiltrating CD56^{bright} hepatic NK cells display mitochondrial stress

Despite phenotypic similarities between tumour infiltrating CD56^{bright} NK cells and those in surrounding tissue, they differ significantly in their mitochondrial function. Mitochondrial mass and dysfunction were measured using Mitotracker and the mitochondrial reactive oxygen species (ROS) specific dye MitoSox. Tumour infiltrating CD56^{bright} NK cells expressed significantly more ROS than liver resident NK cells in the surrounding tissue (tumour 19.9±5.6%, adjacent 10.9±5.4%, distal 8.9±4.2%, p=0.0085, **Figure 4-18B**). No change in MitoSox positive cells was observed in CD56^{dim} NK cells from tumour, adjacent or distal tissue (tumour 2.1±1.3%, adjacent 1.5±0.7%, distal 1.9±0.6%, p=0.74, **Figure 4-18C**). This increased mitochondrial ROS was accompanied by a decrease in mitochondrial mass in CD56^{bright} NK cells (MFI tumour 1463±527, adjacent 1727±557, distal 2791±874, p=0.0356, **Figure 4-18D**). No significant change in mitochondrial mass was seen in CD56^{dim} cells MFI (MFI tumour 6146±536, adjacent 5812±748, distal 5687±464, p=0.95, **Figure 4-18E**).

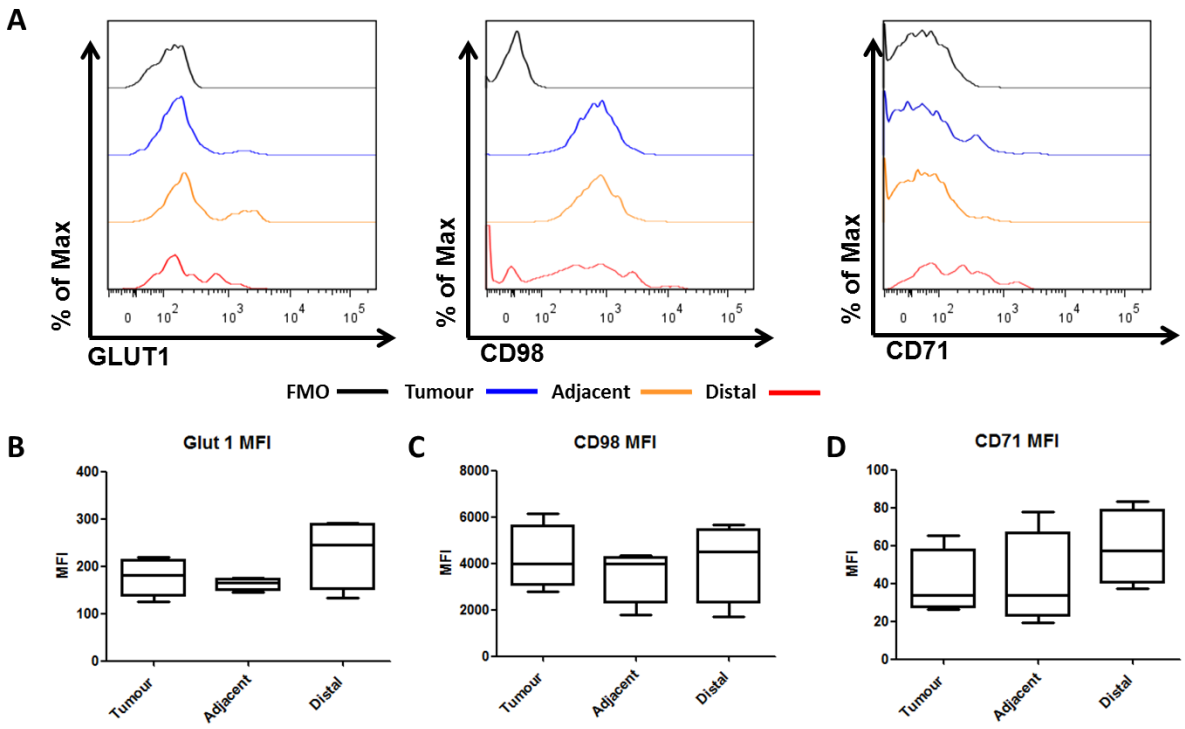

Figure 4- 17 Expression of nutrient transporters in CD56^{bright} hepatic NK cells from CRLM

Mononuclear cells isolated from tumour, adjacent, and distal tissue samples were stained with monoclonal antibodies**.** Gating strategy: NK cells were identified from the CD45^{+} lymphocyte gate as CD56^{+}CD3^{-}. CD56^{bright} CD16$^{-/+}$ NK cells were then gated on. Non-viable cells were excluded by FVS780 staining. **(A)** Representative histograms of GLUT1, CD98, and CD71 in CD56^{bright} NK cells in samples from tumour (red), adjacent (orange) and distal tissue (blue) (black-FMO). **(B)** The expression of GLUT1 on CD56^{bright} NK cells in tumour, adjacent and distal tissue. **(C)** The expression of CD98 on CD56^{bright} NK cells in tumour, adjacent and distal tissue. **(D)** The expression of CD71 on CD56^{bright} NK cells in tumour, adjacent and distal tissue. Data presented as mean ± SEM. Data analysed using Friedman test, with Dunn's multiple comparison test. (n=5)

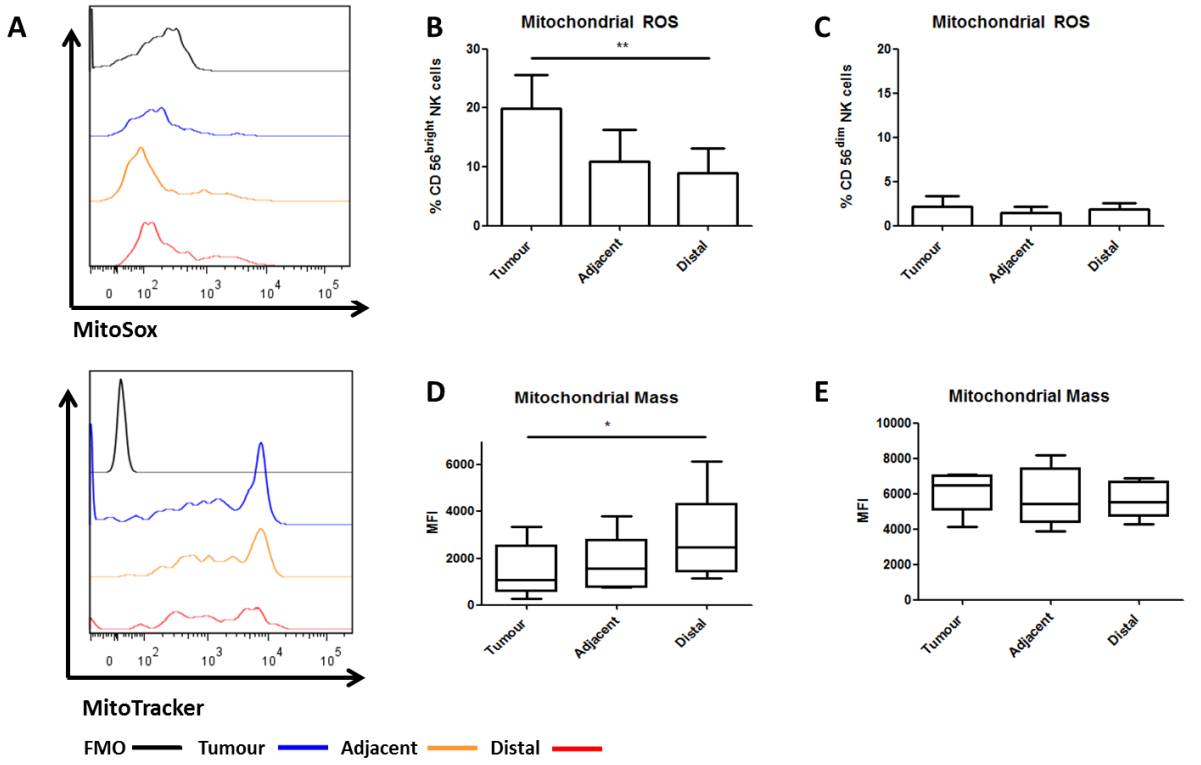

Figure 4- 18 Production of mitochondrial ROS and mitochondrial mass of NK cells in CRLM

Mononuclear cells isolated from tumour, adjacent, and distal tissue samples were stained with monoclonal antibodies and mitochondrial specific dyes to measure mitochondrial ROS (MitoSox) and mitochondrial mass (Mitotracker)**.** Gating strategy: NK cells were identified from the $CD45^{+}$ lymphocyte gate as $CD56^{+}CD3^{-}$. $CD56^{bright}$ $CD16^{-/+}$ and $CD56^{dim}$ $CD16^{+}$ NK cells were then gated on. Non-viable cells were excluded by FVS780 staining. **(A)** Representative histograms of MitoSox and Mitotracker in $CD56^{bright}$ NK cells in samples from tumour (red), adjacent (orange) and distal tissue (blue) (black-FMO). **(B)** The percentage of MitoSox positive $CD56^{bright}$ NK cells in tumour, adjacent and distal tissue. **(C)** The percentage of MitoSox positive $CD56^{dim}$ NK cells in tumour, adjacent and distal tissue. **(D)** The level of Mitotracker staining in $CD56^{bright}$ NK cells in tumour, adjacent and distal tissue. **(D)** The level of Mitotracker staining in $CD56^{dim}$ NK cells in tumour, adjacent and distal tissue. Data presented as mean ± SEM. Data analysed using Friedman test, with Dunn's multiple comparison test. (n=5, *, $p<0.05$, **, $p<0.01$)

4.2.17 Effect of lactate on CD56^{bright} liver resident NK cells

The production of lactate in the tumour microenvironment has previously been shown to effect NK cell function and viability (Brand et al., 2016; Husain et al., 2013a). We therefore investigated the effects of lactate on liver resident NK cells. From our analysis of lactate in CRLM conditioned media we identified the physiological range of lactate produced by CRLM tumours (mean 11.5mM, range 1.5-24.8mM). Using sodium lactate and lactic acid the effect of lactate on cell viability was assessed as before. In addition, pH stabilised media was used to determine whether effects were specific to lactate. CD56^{bright} and CD56^{dim} NK cells were FACS isolated from liver perfusate. There were then treated with sodium lactate (10 or 20mM), lactic acid (10 or 20mM), pH stabilised media (pH 7.4 or pH 6.4) or untreated media for 24 hours.

Sodium lactate showed little effect on apoptosis in either NK cell subsets. Liver resident NK cells showed a small increase in apoptosis after treatment with sodium lactate (media 16.2±2.8%, 10mM 19.7±3.8, 20mM 23.3±4.5, p=0.28, **Figure 4-19B**). Similar results were observed in CD56^{dim} NK cells from liver perfusate (media 10.0±2.9%, 10mM 13.8±4.1%, 20mM 16.6±3.1%, p=0.34, **Figure 4-19C**). In contrast, lactic acid induced significantly higher levels of apoptosis in liver resident CD56^{bright} NK cells (media 13.5±2.9%, 10mM 20.7±4.6%, 20mM 43.4±9.1%, p=0.011, **Figure 4-20B**). CD56^{dim} NK cells did not appear as susceptible to lactic acid mediated apoptosis (media 11.2±3.0%, 10mM 21.1±3.6%, 20mM 30.9±5.8%, p=0.066, **Figure 4-20C**). Finally, the pH of normal media was altered to reflect the pH produced by 20mM lactic acid. Reducing the pH to 6.4 induced significant apoptosis in liver resident CD56^{bright} NK cells (media 11.5±2.7%, pH7.4 23.9±6.5%, pH6.4 32.9±5.9%, p=0.042, **Figure 4-21B**). This effect was not replicated in CD56^{dim} NK cells (media 13.3±4.6%, pH7.4 17.9±3.4%, pH6.4 29.8±5.6%, p=0.19, **Figure 4-21C**). It appears that pH change caused by the addition of lactic acid is contributing to the apoptosis of liver resident NK cells in CRLM.

4.2.18 Lactic acid induces changes in intracellular pH, mitochondrial ROS production and decreased ATP generation

Having identified lactic acid and low pH as a potent inducer of apoptosis in liver resident NK cells, we next investigated the mechanism by which this apoptosis is induced. The acidity of the tumour microenvironment has previously been shown to cause decreases in the intracellular pH of T and NK cells, resulting in mitochondrial dysfunction and cell death (Brand et al., 2016). Liver resident $CD56^{bright}$ NK cells were isolated from liver perfusate by FACS. These cells were cultured with and without lactic acid at 10 or 20mM for 2 hours to identify early intracellular changes causing apoptosis. The intracellular pH was analysed using pHrodo, a pH sensitive dye which freely diffuses into the cell cytosol. As a control NK cells, stained with pHrodo, were incubated with buffers at pH 5.5, 6.5 and 7.5. Standard curves were generated and intracellular pH associated with lactic acid treatment calculated. A dose dependent decrease in intracellular pH was observed in $CD56^{bright}$ NK cells cultured with lactic acid (Media- pH7.4±0.15, 10mM lactic acid- pH6.9±0.2, 20mM lactic acid-pH6.5±0.4, p=0.0046, **Figure 4-21C**).

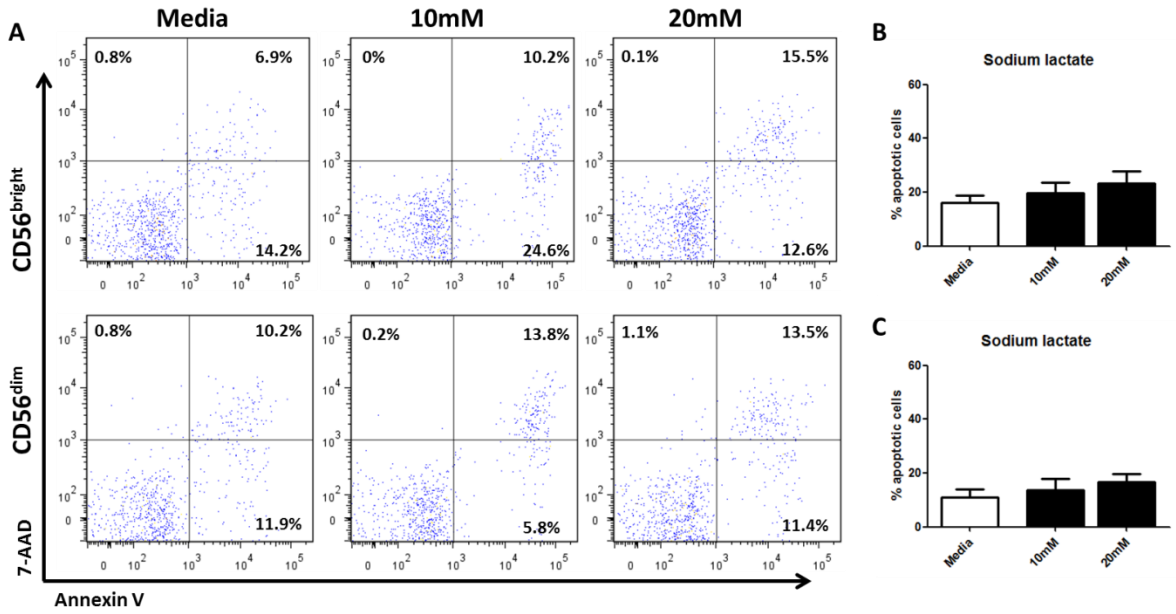

Figure 4- 19 Effect of sodium lactate on hepatic NK cell viability

NK cell subsets were isolated from liver perfusate by FACS. Cells were cultured for 24 hours in the presence of 10 or 20mM sodium lactate. Apoptosis was assessed by annexin V and 7AAD staining. **(A)** Representative dot plots of annexin V/7AAD staining in $CD56^{bright}$ and $CD56^{dim}$ NK cells treated with 10 or 20mM sodium lactate. **(B)** Percentage of apoptotic $CD56^{bright}$ NK cells after treatment with sodium lactate. **(C)** Percentage of apoptotic $CD56^{dim}$ NK cells after treatment with sodium lactate. Data presented as mean ± SEM. Data analysed using Friedman test, with Dunn's multiple comparison test. (n=5).

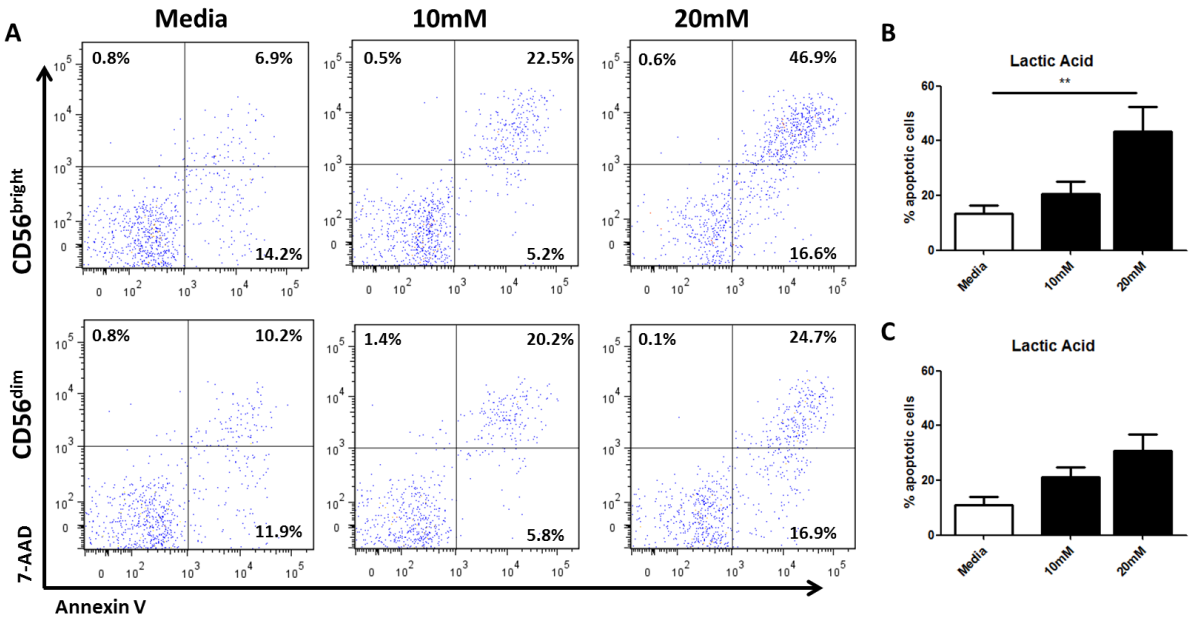

Figure 4- 20 Effect of lactic acid on hepatic NK cell viability

NK cell subsets were isolated from liver perfusate by FACS. Cells were cultured for 24 hours in the presence of 10 or 20mM lactic acid. Apoptosis was assessed by annexin V and 7AAD staining. **(A)** Representative dot plots of annexin V/7AAD staining in $CD56^{bright}$ and $CD56^{dim}$ NK cells treated with 10 or 20mM lactic acid. **(B)** Percentage of apoptotic $CD56^{bright}$ NK cells after treatment with lactic acid. **(C)** Percentage of apoptotic $CD56^{dim}$ NK cells after treatment with lactic acid. Data presented as mean ± SEM. Data analysed using Friedman test, with Dunn's multiple comparison test. (n=5, **, $p<0.01$).

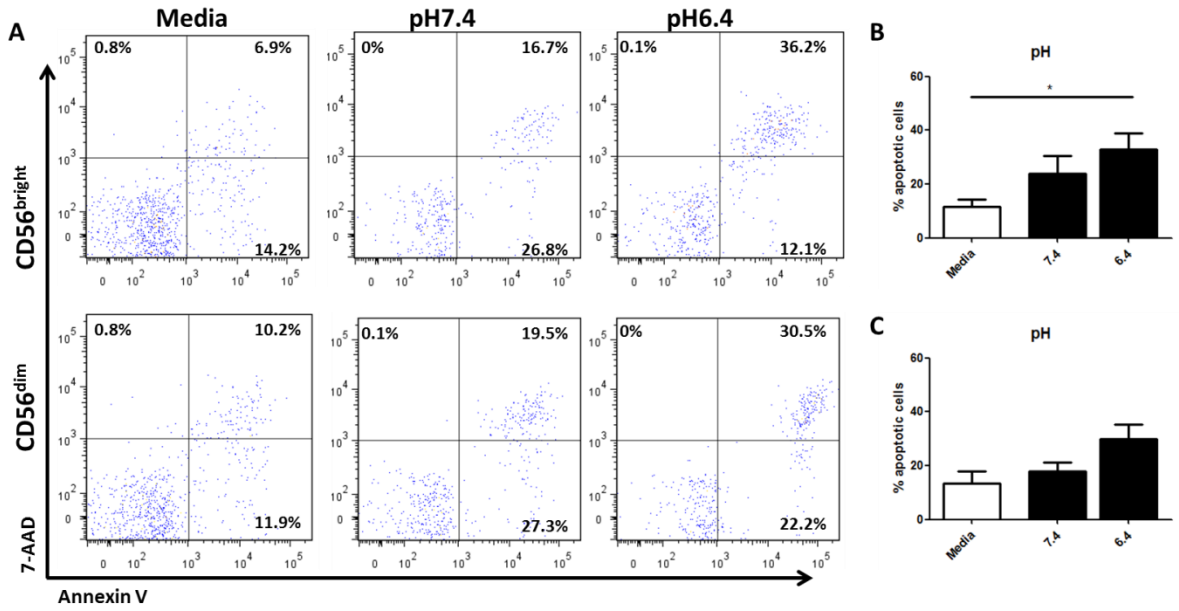

Figure 4- 19 Effect of altering pH on hepatic NK cell viability

NK cell subsets were isolated from liver perfusate by FACS. Cells were cultured for 24 hours in media with pH adjusted to 7.4 or 6.4. Apoptosis was assessed by annexin V and 7AAD staining. **(A)** Representative dot plots of annexin V/7AAD staining in $CD56^{bright}$ and $CD56^{dim}$ NK cells cultured in media pH 7.4 or 6.4. **(B)** Percentage of apoptotic $CD56^{bright}$ NK cells after culture in media pH 7.4 or 6.4. **(C)** Percentage of apoptotic $CD56^{dim}$ NK cells after culture in media pH 7.4 or 6.4. Data presented as mean ± SEM. Data analysed using Friedman test, with Dunn's multiple comparison test. (n=5, *, $p<0.05$).

This decrease in intracellular pH was accompanied by evidence of mitochondrial dysfunction and the release of mitochondrial ROS. MitoSox staining was used to measure mitochondrial ROS production in NK cells cultured with lactic acid. $CD56^{bright}$ NK cells showed a dose dependent increase in MitoSox positive cells (Media- 10.4±1.9%, 10mM lactic acid- 13.3±2.6%, 20mM lactic acid-20.0±0.9%, p=0.021, **Figure 4-21D**). We next analysed intracellular ATP levels, to determine if mitochondrial dysfunction caused a functional defect in energy production.

As before, a dose dependent decrease in ATP was observed in $CD56^{bright}$ NK cells treated with lactic acid (Media- 1070±334pmol/10^5 cells, 10mM lactic acid- 688±230pmol/10^5 cells 20mM lactic acid-589±178pmol/10^5 cells p=0.008, **Figure 4-22A**).

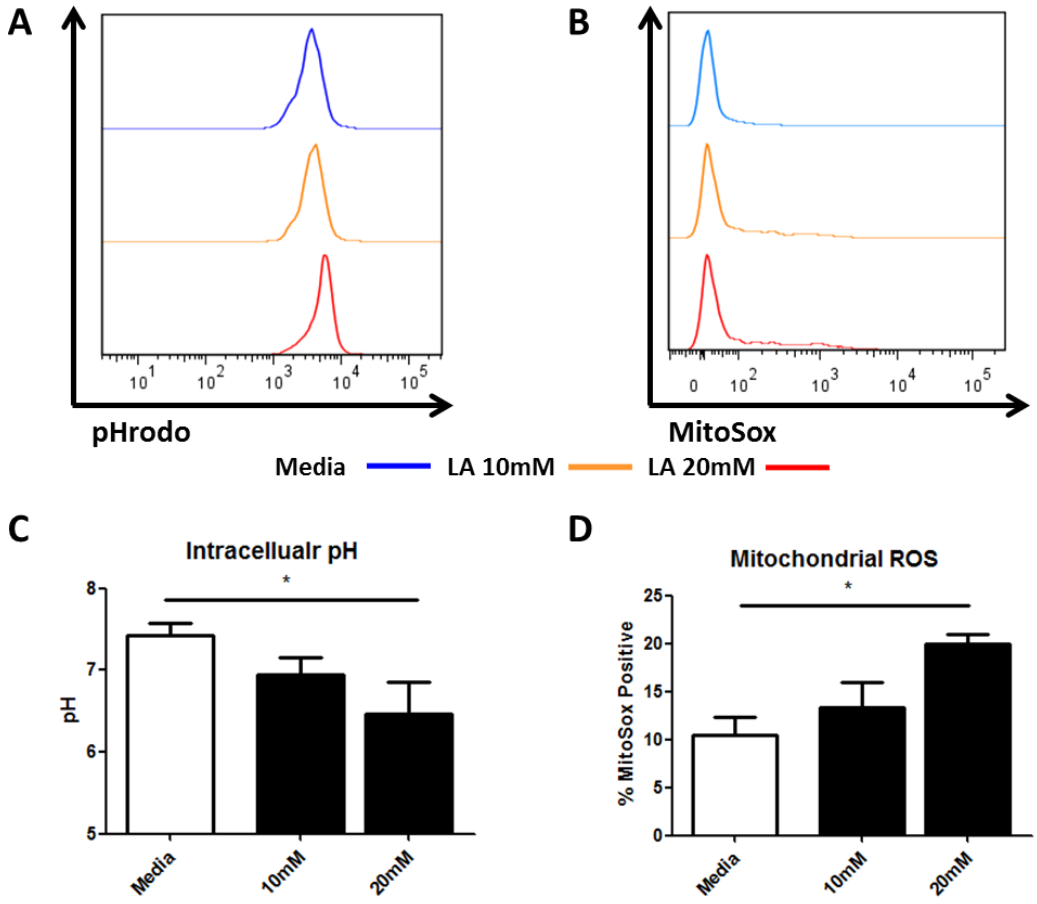

Figure 4- 21 Lactic acid treatment induces altered intracellular pH and ROS production

CD56^{bright} NK cells were isolated from liver perfusate by FACS. Cells were cultured for 2 hours in the presence of lactic acid (10 or 20mM). Intracellular pH was assessed by measuring fluorescence of pH sensitive dye pHrodo. Mitochondrial ROS was measured by fluorescence of MitoSox staining **(A)** Representative histogram of pHrodo staining in CD56^{bright} cultured in media (blue line), 10mM lactic acid (orange line) or 20mM lactic acid (red line). **(B)** Representative histogram of MitoSox staining in CD56^{bright} cultured media (blue line), 10mM lactic acid (orange line) or 20mM lactic acid (red line). **(C)** Intracellular pH of CD56^{bright} cells cultured in media, 10mM lactic acid or 20mM lactic acid. **(C)** Percentage of MitoSox positive CD56^{bright} cells cultured in media, 10mM lactic acid or 20mM lactic acid. Data presented as mean ± SEM. Data analysed using Friedman test, with Dunn's multiple comparison test. (n=5, *, $p<0.05$).

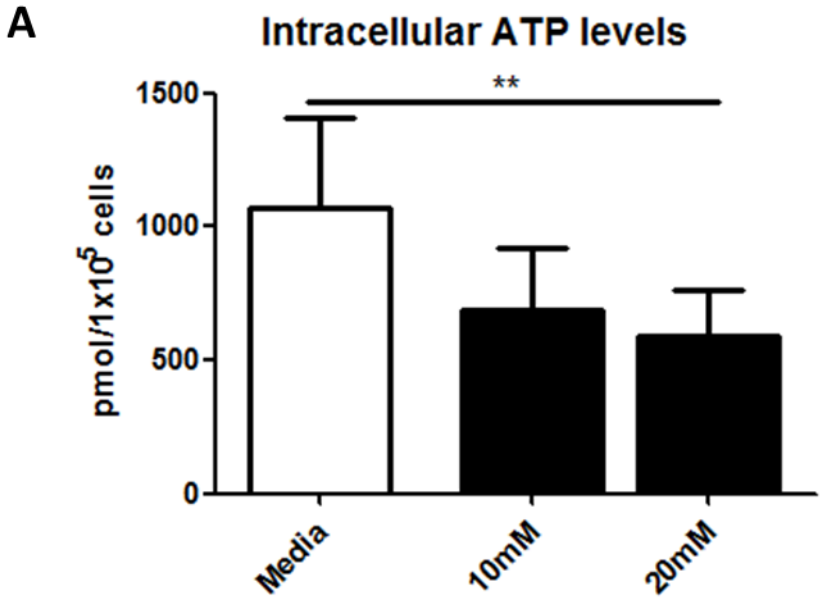

Figure 4- 22 effect of lactic acid on intracellular ATP production

CD56^{bright} NK cells were isolated from liver perfusate by FACS. Cells were cultured for 2 hours in the presence of lactic acid (10 or 20mM). Cells were pelleted, wash and resuspended in lysis buffer containing DTT. ATP levels were determined by an ATP dependent luciferase assay. ATP levels were calculated by luminescence produced by converted luciferin-D relative to the number of cells plated (1x10^5). **(A)** Concentration of ATP in CD56^{bright} NK cells cultured in media, 10mM lactic acid or 20mM lactic acid. Data presented as mean ± SEM. Data analysed using Friedman test, with Dunn's multiple comparison test. (n=5, **, $p<0.01$).

4.2.19 GLUT1 and lactate transporters are not differentially expressed between hepatic NK subsets

Liver resident $CD56^{bright}$ and non-resident $CD56^{dim}$ NK cells display different susceptibilities to lactic acid induced apoptosis. We therefore analysed their expression of lactate transporters as a possible cause of this disparity. NK cell subsets were isolated from liver perfusate by FACS. mRNA was isolated from separated subsets and reverse transcribed to cDNA. qPCR was performed to determine expression of MCT-1 (*SLC16A1*) and MCT-4 (*SLC16A3*). No significant difference in gene expression was observed between NK cells subsets for *SLC16A1* ($p=0.625$) or *SLC16A3* ($p=0.31$) (**Figure 4-22A&B**). Although there was no difference in mRNA levels, this did not exclude the possibility of differences at a protein level.

4.2.20 Blocking lactate transport does not prevent mitochondrial ROS production

In order to determine whether these changes in mitochondrial function were a direct result of lactate entering the cell or a side effect of pH dysregulation, we investigated the effect of blocking MCT transporters. α-cyano-4-hydroxycinnamic acid (αCHC) has been identified as an inhibitor of MCT transporters and was used to block lactate uptake in liver resident NK cells treated with lactic acid. $CD56^{bright}$ NK cells were isolated from liver perfusate by FACS, treated for two hours with αCHC (500μM), and then incubated with lactic acid (20mM) for a further two hours. Cells were then stained with MitoSox to measure mitochondrial ROS production. αCHC treatment showed no significant decrease in MitoSox positive cells (media 5.2±2.3%, αCHC 8.8±0.2%, lactic acid 20.2±1.4%, lactic acid & αCHC 20.1±3.6%, $p=0.17$, **Figure 4-23B**). While blocking lactate transport showed no effect on mitochondrial ROS production, αCHC is also acidic and may amplify the effect of any pH related cellular stress.

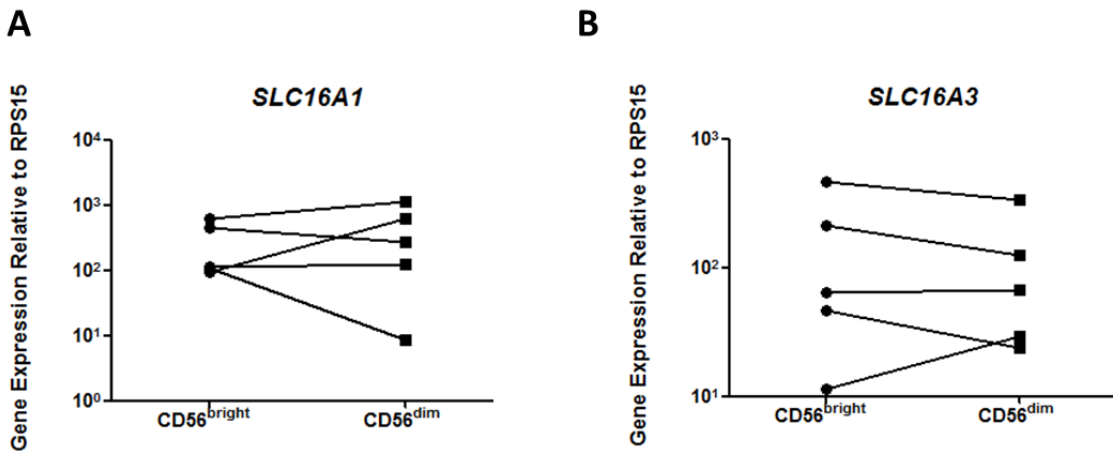

Figure 4- 23 Expression of *SLC16A1 and SLC16A3* in hepatic NK cell subsets

NK cell subsets were isolated from liver perfusate by FACS. RNA was extracted; reverse transcribed into cDNA and real time PCR was performed. Gene expression was normalised to internal control *RPS15*. **(A)** Expression of *SLC16A1* (MCT1) in $CD56^{bright}$ and $CD56^{dim}$ NK cells from liver perfusate. **(B)** Expression of *SLC16A3* (MCT4) in $CD56^{bright}$ and $CD56^{dim}$ NK cells from liver perfusate Data presented as mean ± SEM. Data analysed using Wilcoxon matched pairs test. (n=5).

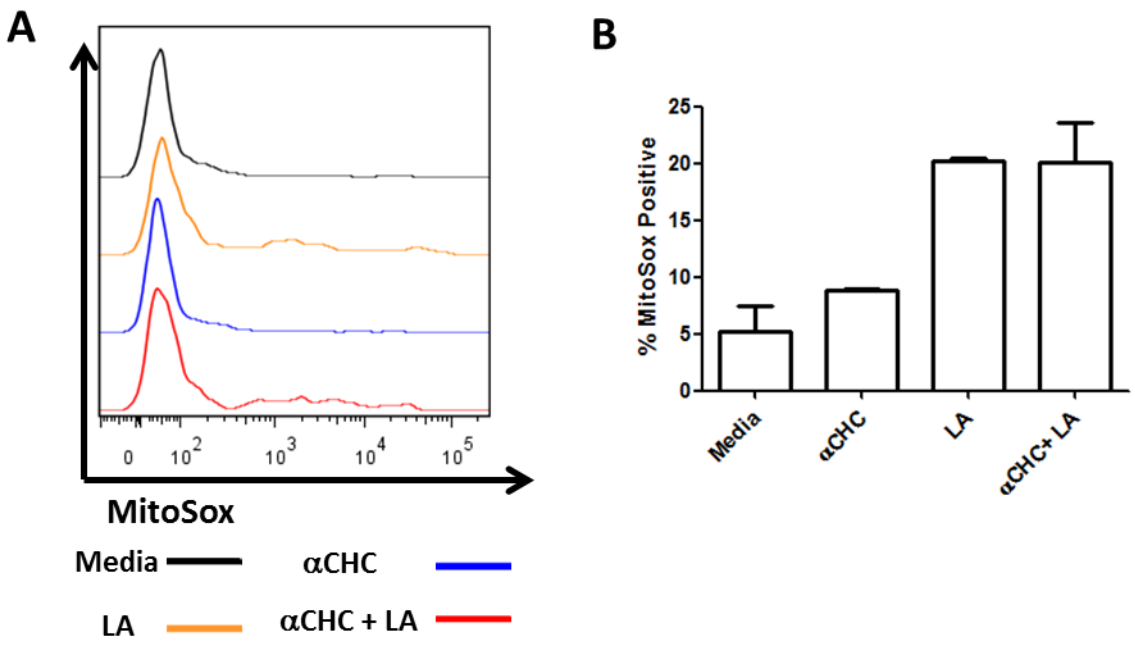

Figure 4- 24 Effect of blocking lactate transport on lactic acid induced ROS production

CD56^{bright} NK cells were isolated from liver perfusate by FACS. Cells were pre-treated with αCHC (500μM) for 2 hours, and cultured for a further 2 hours in the presence of lactic acid (20mM). Mitochondrial ROS was measured by fluorescence of MitoSox staining **(A)** Representative histogram of MitoSox staining in CD56^{bright} cultured media (black line), lactic acid 20mM (orange line), αCHC (blue line) or αCHC & 20mM lactic acid (red line). **(B)** Percentage of MitoSox positive CD56^{bright} cells cultured in media, αCHC, 20mM lactic acid or αCHC & 20mM lactic acid. Data presented as mean ± SEM. Data analysed using Friedman test, with Dunn's multiple comparison test. (n=3).

4.2.21 Treatment with MitoTempo rescues CD56^{bright} hepatic NK cells from apoptosis

While lactate transport does not appear to be necessary for the induction of apoptosis in liver resident NK cells, changes in pH remain essential to induce apoptosis. It remains unclear what the mechanism of cell death in these conditions is. We therefore investigated whether mitochondrial ROS was necessary for the induction of apoptosis, or simply a side effect of oxidative stress. ROS has been implicated in many pathologies as a potent inducer of apoptosis (Circu and Aw, 2010; Simon et al., 2000). MitoTempo is a mitochondria-targeted superoxide dismutase mimetic that possesses superoxide and alkyl radical scavenging properties which been shown to efficiently scavenge mitochondrial ROS (McCarthy and Kenny, 2016; Porporato et al., 2014). CD56^{bright} NK cells were isolated from liver perfusate by FACS. Cells were pre-treated with MitoTempo (50μM) for two hours. Cells were subsequently treated with lactic acid (20mM) for either two hours (MitoSox analysis) or 24 hours (apoptosis analysis). After two hours, cells treated with MitoTempo had produced significantly less mitochondrial ROS (lactic acid- 47.1±11.3%, lactic acid & MitoTempo- 25.6±12.9%, p=0.011, **Figure 4-24B**). Similarly, at 24 hours post lactic acid treatment, liver resident NK cells treated with MitoTempo displayed significantly lower levels of apoptosis compared to untreated controls (lactic acid- 33.5±2.3%, lactic acid & MitoTempo- 20.4±2.5%, p=0.001, **Figure 4-25B**). This data suggests that lactic acid induced apoptosis is mediated by the release of mitochondrial ROS.

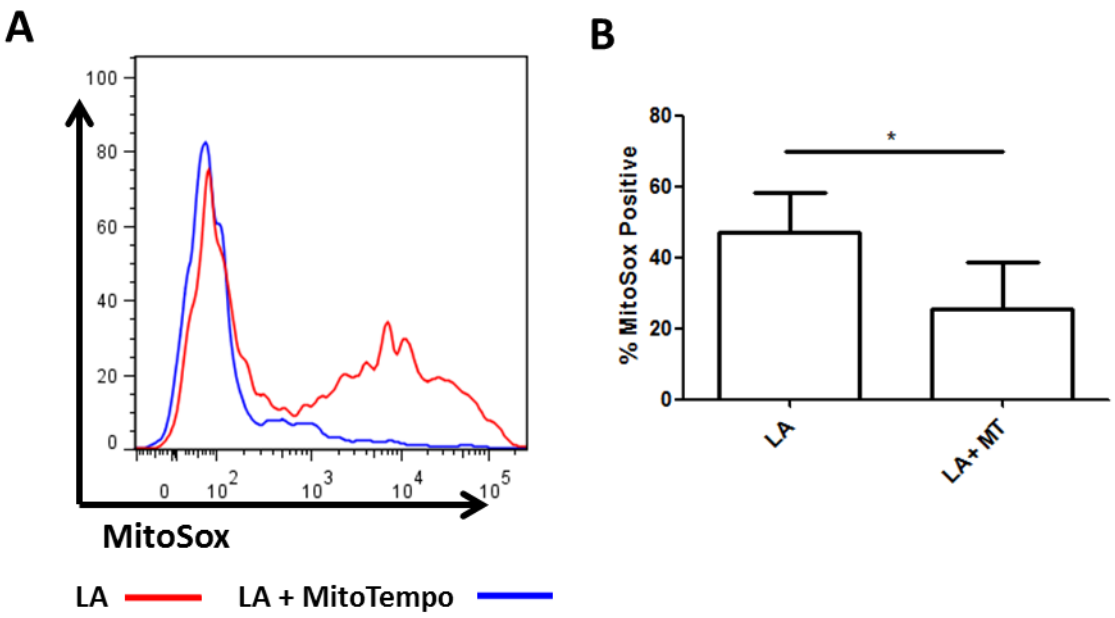

Figure 4- 25 MitoTempo reduces mitochondrial ROS production

CD56^{bright} NK cells were isolated from liver perfusate by FACS. Cells were pre-treated with MitoTempo (50μM) for 2 hours, and cultured for a further 2 hours in the presence of lactic acid (20mM). Mitochondrial ROS was measured by fluorescence of MitoSox staining **(A)** Representative histogram of MitoSox staining in CD56^{bright} lactic acid 20mM (red line) or MitoTempo & 20mM lactic acid (blue line). **(B)** Percentage of MitoSox positive CD56^{bright} cells cultured in lactic acid 20mM or MitoTempo & 20mM lactic acid. Data presented as mean ± SEM. Data analysed using Wilcoxon matched pairs test. (n=3, *, $p<0.05$).

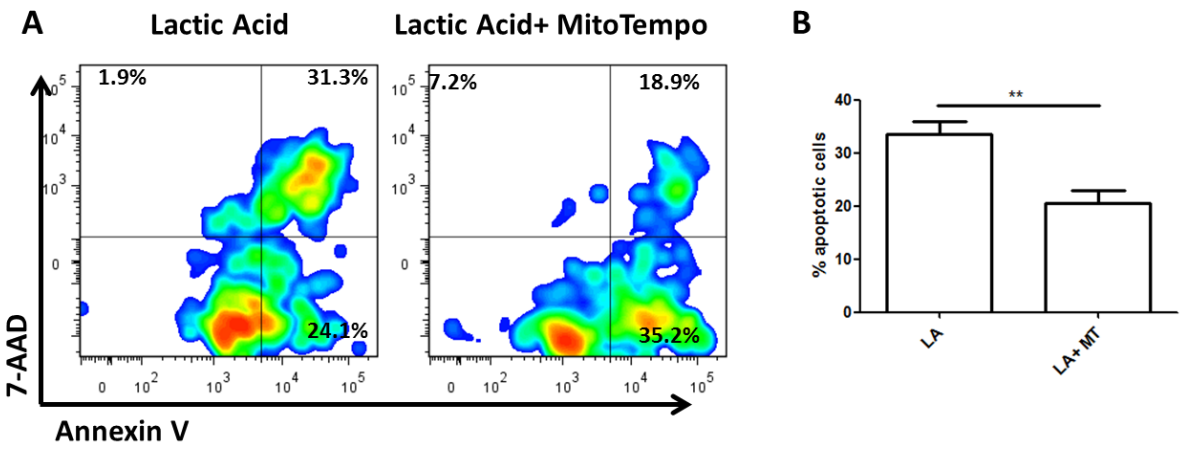

Figure 4- 26 MitoTempo reduces apoptosis in response to lactic acid

CD56^{bright} NK cells were isolated from liver perfusate by FACS. Cells were pre-treated with MitoTempo (50μM) for 2 hours, and cultured for a further 24 hours in the presence of lactic acid (20mM). Apoptosis was assessed by annexin V and 7AAD staining. **(A)** Representative dot plot of annexin V/7-AAD staining in CD56^{bright} NK cells treated with lactic acid 20mM or MitoTempo & 20mM lactic acid. **(B)** Percentage of apoptotic CD56^{bright} cells cultured in lactic acid 20mM or MitoTempo & 20mM lactic acid. Data presented as mean ± SEM. Data analysed using Wilcoxon matched pairs test. (n=3, **, $p<0.01$).

4.3 Discussion

Natural killer cells are an essential component of the anti-tumour immune repertoire. This importance stems from their ability to recognise tumour cells without prior antigen sensitisation. This is achieved through recognition of stress induced and tumour associated antigens, as well as loss of MHC expression (Kruse et al., 2014). Hepatic NK cells appear particularly adept at targeting tumours that would be otherwise escape immune recognition (Ishiyama et al., 2006; Vermijlen et al., 2002). The majority of research has focused on the role of NK cells in HCC, the primary cancer affecting the liver. In this disease, the number of tumour infiltrating NK cells is strongly associated with improved clinical outcome (Chew et al., 2012). The pathogenesis of HCC is markedly different from CRC metastasis. HCC develops on the back of fibrosis and cirrhosis of the liver which disrupts the normal hepatic immune surveillance (Sun et al., 2015; Zhang and Friedman, 2012). CRC tumours which metastasise to an otherwise healthy liver do not have the benefit of a dysfunctional hepatic immune landscape as in the case of HCC. CRC tumours must overcome a repertoire of anti-tumour cells, of which NK cell are the most prominent. Despite this, liver metastasis is twenty times more common than primary tumours of the liver. However, in CRC liver metastasis, the presence NK cells has been correlated with both a reduced life expectancy and improved disease outcome (Donadon et al., 2017; Pugh et al., 2014), although it was unclear whether this difference was due to changes in specific subsets or NK cell phenotype. The authors hypothesised that the CRC tumour was able to evade the local immune repertoire. In the case of reduced life expectancy the authors further hypothesised that hepatic NK cells may disrupt an effective T cell response through "fratricide" of antigen specific T cells, as has been described in viral infection (Peppa et al., 2013; Waggoner et al., 2012). Our identification of a liver resident NK cells population has added another layer of complexity to this scenario. We therefore sought to establish whether liver resident NK cells are important in immunosurveillance against metastatic tumours.

Compared to non-resident CD56^{dim} NK cells, which are classically considered cytotoxic and anti-tumour, liver resident CD56^{bright} NK cells display several common features characteristic of cytotoxic NK cells. CD56^{bright} NK cells show increased expression of several cytotoxicity receptors capable of tumour recognition, including NKG2D, NKp46 and NKp44. CD56^{bright} NK cells displayed lower levels of important cytotoxic molecules, with lower expression of granzyme B and perforin. However, this was accompanied by significantly higher expression of granzyme K. While granzyme B has classically been considered the most important granzyme that mediates tumour cell death (Rousalova and Krepela, 2010), there is increasing evidence from tumour transcriptomics that granzyme K is a positive prognostic in many cancers, most prominently breast cancer (Uhlen et al., 2017). Granzyme K is most commonly found in innate cytotoxic cells such as MAIT cells and CD56^{bright} NK cells (Jiang et al., 2011; Kurioka et al., 2015). When co-incubated with metastatic colorectal cancer cell line (SW620) CD56^{bright} NK cells from the liver showed equal levels of cytotoxicity compared to non-resident cytotoxic CD56^{dim} cells, classically considered the most potent anti-tumour NK cell subset. These findings are similar to those of peripheral blood CD56^{bright} NK cells which, after activation through IL-15, display enhanced cytotoxicity (Wagner et al., 2017). In addition, it has been shown that activation by IL-12 and IL-15 increases expression of markers of tissue residency, CXCR6 and CD49a, which may indicate that liver resident NK cells have previously been activated by cytokines (Hydes et al., 2018). Whether the cell death induced by liver resident NK cells is mediated through granzyme K is currently under investigation by our group. Alternatively this cell death could be mediated by death receptor signalling. TRAIL is only expressed on small proportion of liver resident NK cells in healthy liver, in tumour bearing and HBV infected liver this level rises dramatically (**Figure 4-6**, Stegmann *et al.*, 2016). Also worth noting is the significantly higher proportion of CD56^{bright} NK cells that degranulate in response to target cells. While granzyme K may not be as efficient as other cytotoxic molecules (Voskoboinik et al., 2015), this may be compensated for by an increase in

the number of NK cells activated by tumour cells, increasing the effective ratio of effectors to targets.

Liver resident NK cells are competent anti-tumour cells and should provide the liver with ample anti-tumour immunity. However, in many cancers the liver becomes the main site of metastases (Ferlay et al., 2015). How these tumours evade the local NK cell immunity remains to be resolved. As previously reported, we have confirmed that NK cells are depleted from metastatic CRC tumours (Pugh et al., 2014). We have further identified that tissue resident $CD56^{bright}$ NK cells are preferentially depleted. The remaining tumour infiltrating $CD56^{bright}$ NK cells appear to be tissue resident, with a distinctive $Eomes^{hi}$ $Tbet^{lo}$ phenotype and expression of CXCR6 and CD69, and are not thought to be infiltrating peripheral blood cells.

Primary CRC tumours are relatively devoid of NK cells, with surrounding tissue containing normal levels (Halama et al., 2011). This is assumed to be due to ineffective infiltration into the tumour mass. The relative depletion of NK cells from the CRLM tumour may therefore be due to an inability to migrate to the tumour site or the induction of NK cell death (similar to iNKT cells, Whelan et al. unpublished). We have addressed this question using chemotactic assays employing liver NK cells and tumour conditioned media from CRLM. Counterintuitively, $CD56^{bright}$ NK cells actually migrated toward CRLM tumour conditioned media significantly more than $CD56^{dim}$ cells, which make up the majority of tumour infiltrating NK cells. This may be due to the production of CXCL16 by colorectal cancer cells (Kee et al., 2014, 2013), which has previously been shown to limit metastases of primary colorectal tumours, possibly by recruiting NK cells from the liver. With no defect in chemotaxis, we therefore investigated the effect of the tumour microenvironment on liver resident NK cell viability and phenotypes. Many tumour types have been shown to alter NK cells through the production of anti-inflammatory mediators (IL-10, TGF-β, IDO, Arg1) or

metabolic dysregulation of the surrounding tissue (Cortez et al., 2017; Husain et al., 2013a; Lassen et al., 2010; Mamessier et al., 2011; Pietra et al., 2012; Pötzl et al., 2017; Viel et al., 2016). Using tumour conditioned media we have shown that NK cells undergo apoptosis in the tumour microenvironment. This process is not mediated by extrinsic death receptor signalling, as shown by continued apoptosis in the presence of a caspase-8 inhibitor. Alternatively apoptosis can be triggered by intrinsic cell signals. This process is mediated by release of cytochrome c from the mitochondria. This process is commonly induced by loss of a growth factor, DNA damage, nutrient deprivation, endoplasmic reticulum stress, or mitochondrial stress (Elmore, 2007; Taylor et al., 2008). *Ex vivo* liver resident NK cells isolated from CRLM tumours displayed mitochondrial stress (increased mitochondrial ROS production) and decreasing mitochondrial mass compared to cells from surrounding tissue. Non-resident $CD56^{dim}$ NK cells did not display these features of mitochondrial stress. We therefore began by investigating changes in growth factors known to regulate NK cell homeostasis. IL-15 levels were unchanged between healthy liver and CRLM. IL-2 likewise was not altered between healthy and tumour bearing tissue (Hand et al, 2018). We have shown that tissue resident NK cells require TGF-β to maintain their phenotype, but this was not significantly changed between healthy and CRLM tissue.

Nutrient deprivation was not considered a cause of apoptosis as glucose levels were equivalent in healthy and CRLM conditioned media. This is probably due to the use of culture media which has an excess of glucose and does not accurately reflect glucose availability in the tumour microenvironment. In order to address this, alternative culture methods are being developed in the lab to more closely mimic the tumour microenvironment (low glucose, low glutamine, pH controlled media, addition of tumour cell lines etc.). In order to identify metabolic differences between tumour and healthy liver tissue we examined lactate levels as a readout of glycolysis. Lactate was significantly increased in CRLM tumours compared to healthy tissue, unsurprising given the increased metabolic activity of tumour cells (Jiang,

2017; Pavlova and Thompson, 2016). Lactate has previously been described as a potent immune modulator in the tumour microenvironment, polarising macrophages and neutrophils, suppressing DC activity, dysregulating and killing T and NK cells (Brand et al., 2016; Colegio et al., 2014; Fischer et al., 2007; Gottfried, 2006; Husain et al., 2013a, 2013b).

We therefore investigated the effect of lactate on liver resident NK cell viability. While sodium lactate showed little effect on NK cell survival, lactic acid induced significant apoptosis *in vitro.* Altering the pH of media using hydrochloric acid displayed a similar effect. The effect was not abrogated by blocking lactate transporters, using αCHC, indicating that the effect was mediated by altering pH rather than a direct effect of lactate uptake. This acidic environment induced a change in the intracellular pH of liver resident NK cells, leading to mitochondrial dysfunction, production of mitochondrial ROS and reduced ATP generation. pH dependent apoptosis was reversed by pre-treatment with MitoTempo, a selective mitochondrial ROS scavenger. In order to confirm this mechanism further experiments will be required using MitoTempo and tumour conditioned media from CRLM tumours. Furthermore, using a humanised mouse model, MitoTempo could be tested as an immunotherapy in a metastatic CRC model such as HT-29 or HCT-116 (McIntyre et al., 2015).

We therefore believe that apoptosis of liver resident NK cells is as a result of decreasing pH in the tumour microenvironment, mediated by lactate production, which results in mitochondrial stress and ROS dependent apoptosis. Why liver resident NK cells are more susceptible to pH induced cellular stress compared to $CD56^{dim}$ NK cells remains unclear. Lymphocytes have been shown to be able to maintain intracellular pH in acidic conditions to a certain point (~pH6.8) (Deutsch et al., 1982). This process is maintained by the buffering capacity of the cell, a combination of intrinsic (various weak bases and amino acid groups) and the conversion of CO_2 to HCO^-. HCO^- provides most of the buffering capacity in the cell

and is produced from CO_2 generated from mitochondrial respiration (Casey et al., 2010). Therefore cells with greater mitochondrial mass and active TCA cycle will produce more CO_2 and have greater buffering capacity. Liver resident NK cells have significantly lower mitochondrial mass compared to $CD56^{dim}$ NK cells, making them more susceptible to extracellular pH changes. This hypothesis will require further investigation. Whether this decreased mitochondrial mass is indicative of loss of defective mitochondria through autophagy after activation remains to be elucidated (Westermann, 2010). Driving mitochondrial biogenesis through peroxisome-proliferator-activated receptor γ co-activator-1α (PGC-1α) may protect against pH induced changes, as it does in tumour cells (LeBleu et al., 2014). There is some evidence that biogenesis can be driven pharmacologically however these treatments require substantial research before entering the clinic (Chowanadisai et al., 2010). Alternatively, intracellular pH can be maintained by the activity of carbonic anhydrases (which convert CO_2 to bicarbonate), sodium/chloride HCO^- exchangers, vacuolor ATPase (pumps H^+ out of the cytosol into intracellular vesicles), and MCT lactate transporters (Casey et al., 2010; Damaghi et al., 2013). While we have not identified differences in MCT expression between $CD56^{bright}$ and $CD56^{dim}$ NK cells from liver, further work is required to address the expression and activity of these other targets. To that end, we have performed RNA-seq on NK cells isolated from liver perfusate in order to identify changes in pH sensors and regulators between liver resident and non-resident NK cells. The results of these studies will inform future functional analysis of the activity of targets of interest.

This lactate mediated mechanism, by which CRLM subverts local innate anti-tumour immunity, provides opportunities for therapies that target metabolic pathways and mitochondrial regulation. At the tumour level, the production and export of lactate could be targeted through regulation of glycolysis through inhibition of enzymes involved in that pathway, through drugs such as 2-DG, bromopyruvic acid, lonidamine (Hexokinase targeted), GAPDH inhibitors, pyruvate kinase inhibitors (TLN-22), or lactate dehydrogenase inhibitors

(Ganapathy-Kanniappan and Geschwind, 2013; Pelicano et al., 2006; Scatena et al., 2008). Alternatively lactate transport can be targeted to prevent release of lactate from tumour cells, increasing it to toxic levels (Payen et al., 2017; Sonveaux et al., 2012, 2008). Significant clinical improvement has been reported with the use of systemic bicarbonate buffering, which neutralises tumour acidity, reduces tumour invasiveness and improves immune response (Ibrahim-Hashim et al., 2017; Pötzl et al., 2017; Silva et al., 2009). Despite these positive results, patient adherence to treatment is difficult as large quantities of sodium bicarbonate must be consumed which proves difficult for many patients. An alternative approach would be to develop treatment which targets immune cells and prevents ROS induced apoptosis. The use of mitochondria targeted scavengers has shown some efficacy in murine models of cancer and other inflammatory diseases, maintaining immune activity and clearing tumour cells (Li et al., 2013; Nazarewicz et al., 2013; Porporato et al., 2014). MitoQ, a mitochondrial ROS scavenger, is available as an over the counter food supplement, purported to reduce mitochondrial stress and improve metabolic health, however no substantial studies of this effect have been published.

The recurrence of CRC liver metastasis after successful resection occurs in up to 70% of patients. It is clear from this that the immune surveillance mechanisms of the liver remain compromised after removal of the tumour. It remains unclear how these tumours reappear, whether from microscopic deposits present before resection or migration from the primary or another secondary site. Either way, treatment targeting lactate production may benefit these patients, improving immune surveillance, reducing the invasiveness of metastatic tumours and limiting tumour growth. Further characterisation of the tumour microenvironment in CRLM is essential in order to identify therapeutic targets specific to tumour cells and restore local innate immune function. We believe this approach will substantially reduce the recurrence rate after surgical resection. In addition this treatment will benefit patients with inoperable CRLM, reducing tumour growth and restoring local tumour immunity.

Chapter 5: General Discussion

The adult human liver is an organ of predominately innate immunity. It has evolved to tolerate a large antigenic load from the gastrointestinal tract. This is achieved through a unique population of tissue resident macrophages, Kupffer cells, which sample portal blood contents, remove antigenic molecules and maintain organ tolerance rather than initiating a systemic adaptive response. This tolerogenic environment, while necessary, presents some difficulty in the setting of hepatotrophic viral infection and malignancy. In the absence of efficient antigen presentation, T cell activation becomes problematic, and there is a body of literature describing these difficulties (Bowen et al., 2004; Crispe, 2003; Crispe and Metz, 2000; Huang et al., 1994; Mehal et al., 1999; Shuai et al., 2016). In chronic liver inflammation, these tolerogenic mechanisms breakdown and pathology ensues (Heymann et al., 2015; Robinson et al., 2016). In the setting of CRLM, the otherwise healthy liver into which the CRC tumour metastasises may remain tolerogenic and prevent T cell activation.

To complement this tight regulation of essential anti-tumour and anti-viral immunity, the liver is densely populated with cytotoxic innate lymphocytes including NK cells, γδ T cells, MAIT cells and iNKT cells (Doherty et al., 1999; Hata et al., 1991, 1990; Kenna et al., 2004; Norris et al., 1999). Hepatic NK cells have been characterised by their enhanced cytotoxicity and ability to clear tumour cells, regulate stellate cells and prevent fibrosis (Bahjat et al., 2007; Moroso et al., 2010; Peng et al., 2016; Sojka et al., 2014b; Zhang et al., 2011). It has become increasingly evident that NK cells isolated from tissues throughout the body differ from those of the peripheral blood (Freud et al., 2017; Sojka et al., 2014b; Tang et al., 2016). We therefore set out to examine the diversity of NK cells in the adult human liver and identify key features of liver resident NK cells.

Much work has been carried out in murine models to identify liver resident NK cells (Daussy et al., 2014; Gordon et al., 2012; Peng et al., 2013). These cells were characterised by poor

cytotoxicity and increased pro-inflammatory cytokine production. This population was identified by their lack of Eomes expression, a transcription factor necessary for the differentiation and acquisition of effector function of NK cells, and the expression of the integrin CD49a. Furthermore these cells were identified in humans, but was only present in a minority of livers studied and only accounted for a tiny proportion of hepatic NK cells (~1%) (Marquardt et al., 2015; Martrus et al., 2017). It is now becoming clear that this population is in fact a non-NK cell ILC1 type cell (Marotel et al., 2016). Accounting for only a small number of hepatic ILC cells, we hypothesised, that in humans, multiple tissue resident populations of NK cells may exist.

Here, we have characterised the diverse NK cell repertoire of healthy human liver and have identified a novel subpopulation of hepatic NK cells with unique phenotypic features, effector function and transcriptional regulation. These $CD56^{bright}$ NK cells are characterised by an $Eomes^{hi}$ $Tbet^{lo}$ phenotype, have increased degranulation in response to target cells and produce significantly less IFN-γ. This population also had increased expression of NCRs and NKG2D, receptors which recognise stress induced ligands (expressed by tumour and virally infected cells). In addition, $Eomes^{hi}$ $Tbet^{lo}$ NK cells express markers of tissue residency including the chemokine receptor CXCR6, and the C-type lectin CD69 previously described in liver sinusoidal NK cells and tissue resident T cells (Hudspeth et al., 2015; Mackay et al., 2015). A small population of $CD49a^{+}$ $CD56^{bright}$ NK cells was detected in liver biopsies but not liver perfusate or peripheral blood. Unlike the population described by Marquardt and colleagues, these cells were not $Eomes^{-}$. Their absence from liver perfusate may indicate that they are resistant to perfusion or may reside outside of the liver sinusoids, similar to Kupffer cells whose cellular projections cross into in the Space of Disse (Wardle, 1987). This population has been further characterised in cirrhosis where it does not possess an $Eomes^{-}$ phenotype (Lunemann et al., 2017). Alternatively, NK cell phenotype may be altered by shear

stress during removal of preservative fluid from donor liver ("flushing"), or migration into the transport media may alter expression of adhesion molecules.

During the course of this work, the Eomes^{hi} Tbet^{lo} Liver NK cell has been described by several groups (Aw Yeang et al., 2017; Cuff et al., 2016; Harmon et al., 2016a; Hudspeth et al., 2016; Hydes et al., 2017; Lunemann et al., 2017; Stegmann et al., 2016). From this series of studies much has been discovered about these liver resident NK cells. They appear unchanged phenotypically and functionally in chronic hepatitis B infection (Stegmann et al., 2016). They display reduced IFN-γ production in response to cytokine stimulation but not when treated with PMA (Aw Yeang et al., 2017; Harmon et al., 2016; Stegmann et al., 2016). This may be due to the differences in signalling pathways activated by PMA (NFAT) and pro-inflammatory cytokines (JAK-STAT). They degranulate at greater levels than non-resident NK cells (Harmon et al., 2016; Stegmann et al., 2016). They appear long-lived, as donor liver resident NK cells are detectable in transplanted organs years after transplantation (Cuff et al., 2016). In cirrhotic liver, their phenotype appears altered, with a loss of Eomes^{hi} Tbet^{lo} NK cells and expansion of CD49a^{+} NK cells characterised by increased Hobit expression, a transcription factor associated with T cell tissue residence (Lunemann et al., 2017; Mackay et al., 2016). Whether this is an expansion of a distinct CD49a^{+} population or a shift in the phenotype and function of liver resident NK cells remains unclear. It will be necessary to develop mouse models of liver disease in order to investigate this process. Normal mouse models have not shown the presence of any equivalent of the human Eomes^{hi} Tbet^{lo} NK cell. However, humanised mice, immunodeficient mice transplanted with human haematopoietic stem cells, show the presence of CD49e^{-} NK cells as described in humans (Aw Yeang et al., 2017). We have further investigated the phenotype of these NK cells in an NSG mouse transplanted with adult human stem cells. We have found the presence of CXCR6^{+}, CD49a^{+} and CD69^{+} CD56^{bright} NK cells (**Appendix Figure 2**). These cells have reduced Tbet expression but did not possess the increased Eomes expression characteristic of human liver

resident NK cells. This may be in part due to differences between human and murine liver microenvironments (Robinson et al., 2016). With the advent of CRISPR technology, next generation humanised mouse models may be able to more accurately reflect human hepatic immune repertoires. It appears human hepatocytes may be essential for the development of human-like immune populations in murine models (Billerbeck et al., 2016; Dorner et al., 2011; Guo et al., 2018). Furthermore if an activation signal is required to recruit NK cells to the liver to become resident populations, then a systemic treatment may be necessary to drive this recruitment (Hydes et al., 2018).

They were also only present in small numbers (~2.5% of $CD45^+$ cells) making the study of their function difficult when compared to their numbers in humans. In the absence of an efficient murine model, it will prove difficult to determine the ontogeny of human liver resident NK cells and their shifting phenotypes.

In order to address this, we have developed a rudimentary culture system to mimic the hepatic microenvironment. By culturing liver tissue ex vivo and collecting these supernatants, we can establish culture conditions with biologically relevant concentration of hepatic cytokines and growth factors produced by human hepatocytes stromal and immune cells (O'Toole et al., 2014). However, it must be noted that surgical stress, ischemia and reperfusion can cause damage to tissue and may altered their production of cytokines and growth factors (Chen and Nuñez, 2010; Zhai et al., 2013). This is unavoidable even in murine models and is a caveat to microenvironmental research. Using this system, we have determined that liver resident NK cells rely on soluble factors present in the liver microenvironment to maintain their unique phenotype.

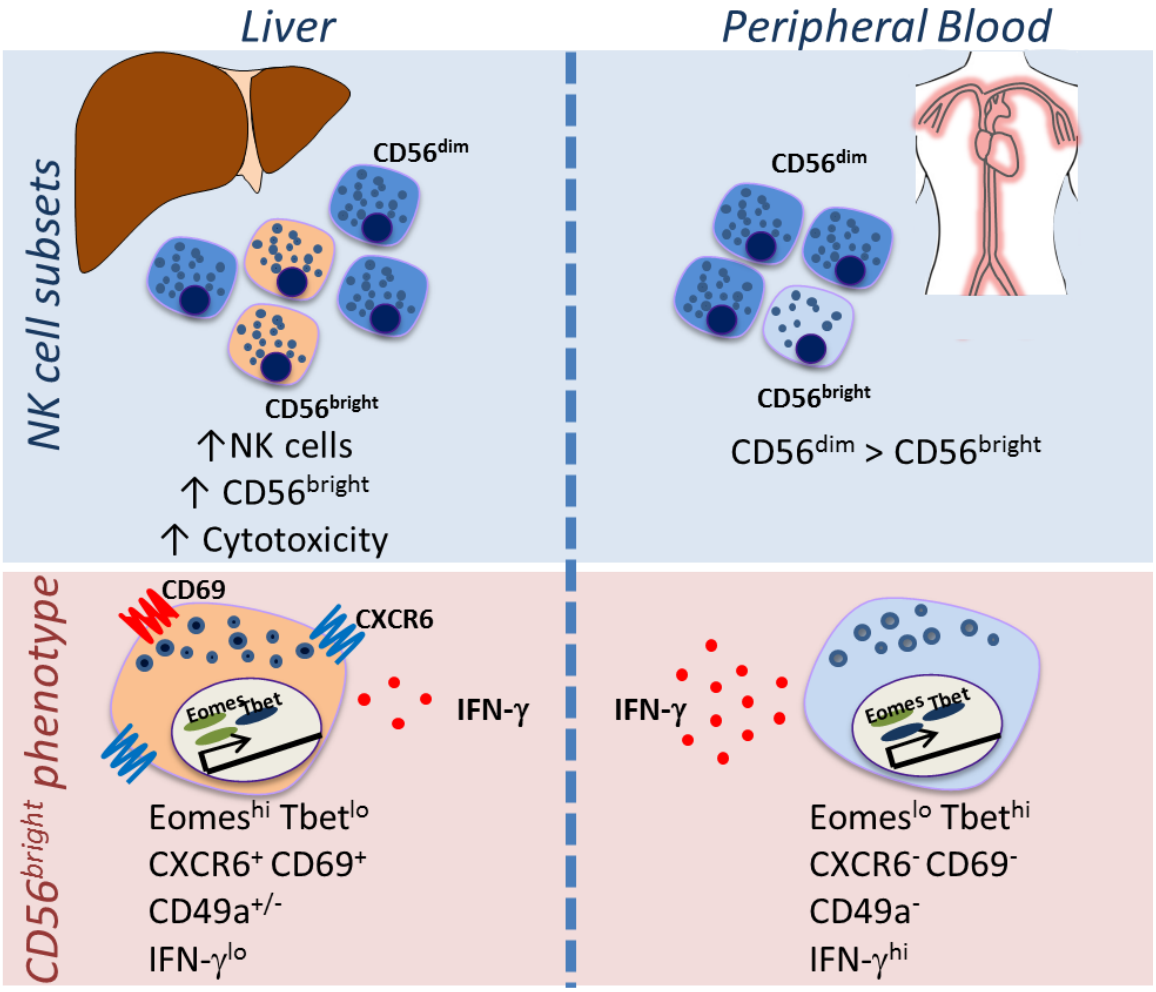

Figure 5- 1 Characteristics of liver resident NK cells

Population dynamics of liver NK cells compared to the peripheral blood. Functional and phenotypic characteristics which differentiate liver resident NK cells from peripheral blood NK cells. (Figure adapted from Harmon et al 2016 *EJI*)

NK cells isolated from liver perfusate lose their unique Eomes^{hi} Tbet^{lo} phenotype when cultured but this can be reversed by addition of liver conditioned media. Liver conditioned media suppresses Tbet expression in cultured hepatic and peripheral blood NK cells. The liver is rich in immunoregulatory cytokines, including TGF-β and IL-10, produced by Kupffer cells and immature dendritic cells (Bamboat et al., 2009; Kelly et al., 2006; Knolle et al., 1995; Robinson et al., 2016). Liver resident NK cells cultured with TGF-β but not IL-10 maintain their unique phenotype, indicating that TGF−β is essential for maintaining liver resident populations in the liver. Further experiments are required to confirm this mechanism, including blocking TGF-β signalling in liver resident NK cells and peripheral blood NK cells cultured with LCM, using the small molecule inhibitor SB431542 (Inman et al., 2002). Culture with LCM can maintain CXCR6 expression, but it does not appear to induce expression of CXCR6 on peripheral blood NK cells. Peripheral blood NK cells require stimulation with cytokine (IL-12, IL-15) in order to express CXCR6 or CD49a (Hydes et al., 2018). Therefore, liver resident NK cells probably acquire CXCR6 expression in the periphery, through cytokine activation, migrate to the liver, where CXCL16, RANTES and CCL3 present in the liver sinusoid retain activated NK cells (Hudspeth et al., 2015; Paust et al., 2011). TGF-β (produced by resident macrophages and dendritic cells) alters transcription factor expression, repressing the production of pro-inflammatory cytokines (IFN-γ). Significant work has been performed investigating the effect of TGF-β on NK cells, and it has been shown to have potent immunosuppressive effects and alters NK cell development (Allan et al., 2010; Viel et al., 2016). Furthermore, TGF-β has been shown to suppress glycolysis and inhibit the pro-inflammatory effector functions of CD56^{bright} NK cells, such as IFN−γ production (Zaiatz-Bittencourt et al., 2018) Recently, TGF-β has been shown to be involved in the conversion of NK cells to ILC1-like cells with reduced cytotoxicity in tumour models (Cortez et al., 2017; Gao et al., 2017). This process does not appear to occur in liver resident NK cells but may be worth further investigation in peripheral blood or other tissue resident

populations. Use of a strong pro-inflammatory signal, such as PMA, appears to overcome this TGF-β mediated repression and restore IFN-γ production (Aw Yeang et al., 2017; Stegmann et al., 2016). From RNA-seq analysis we have identified changes in several signalling pathways involved in TGF-b signalling and repression of JAK-STAT signalling necessary for cytokine activation. This suppression did not extend to T cell related signalling pathways such as NFAT, which is activated by PMA treatment (Robinson et al. unpublished). So while in healthy liver these resident NK cells have suppressed pro-inflammatory function, this can be overcome with sufficient stimulation.

The role of liver resident NK cells in local immunity is unclear. They were found to be unchanged in chronic HBV infection, but had increased expression of TRAIL (Stegmann et al., 2016). In previous studies, $CD56^{bright}$ NK cells had been shown to be important in controlling HCV infection and preventing fibrosis (Doyle et al., 2015). Much work has been done by our group and others, characterising the dysfunctional nature of NK cells in chronic hepatitis (Eisenhardt et al., 2012; Golden-Mason and Rosen, 2013; Lunemann et al., 2014; Nel et al., 2016). In light of the discovery of liver resident NK cells these studies will need to be repeated to determine whether loss of liver resident NK cells is responsible for the severe pathology seen in some HCV patients. Liver NK cells have previously been shown to promote immune regulation through deletion of virus specific and autoimmune T cells (Huber et al., 2014; Peppa et al., 2013; Su et al., 2001; Waggoner et al., 2012), whether this function is carried out by liver resident NK cells remains to be elucidated. Hepatic NK cells have been demonstrated to be essential for controlling liver fibrosis in alcoholic liver disease, NAFLD/NASH and autoimmunity (Abu-Tair et al., 2013; Heymann and Tacke, 2016; Il-Jeong et al., 2008; Notas et al., 2009; Radaeva et al., 2006). It remains to be seen if this function is attributable to this $Eomes^{hi}$ $Tbet^{lo}$ subset of NK cells. The loss of this subset in advanced cirrhosis indicates that this population may be essential for control of fibrosis (Lunemann et al., 2017).

Finally, NK cells are essential for the control of tumour metastasis (Krasnova et al., 2015; López-Soto et al., 2017). Hepatic NK cells have been characterised by their enhanced cytotoxicity and have been isolated from liver perfusate for use as immunotherapy in recurrent HCC after liver transplantation (Bahjat et al., 2007; Moroso et al., 2010; Nishida et al., 2013; Ohira et al., 2012). In this study, we have demonstrated that liver resident $CD56^{bright}$ NK cells display comparable levels of cytotoxicity compared to $CD56^{dim}$ cells (against colorectal and leukemic cell lines), despite their reduced expression of granzyme B and perforin. This is similar to the cytotoxic profile displayed by IL-15 activated $CD56^{bright}$ NK cells and correlate with the requirement of cytokine activation to acquire CXCR6 (Hydes et al., 2018; Wagner et al., 2017). This deficiency may be overcome using other granzymes (K or A), or death receptor ligation (FAS-FASL, TRAIL-TRAIL-R). TRAIL expression has been shown to be increased in liver-resident NK cells in HBV infection (Stegmann et al., 2016). Alternatively, the increased proportion of degranulating $CD56^{bright}$ cells may provide an increased effective effector to target ratio. Depletion of NK cells has previously been shown in metastatic liver tumours but high T and NK cell infiltration of tumours are a positive prognostic for patient survival (Donadon et al., 2017; Pugh et al., 2014). Work from our group has previously shown that NK cells in the CRLM tumour bearing tissue are still functional and have reduced expression of inhibitory receptors (Norris et al., 2003).

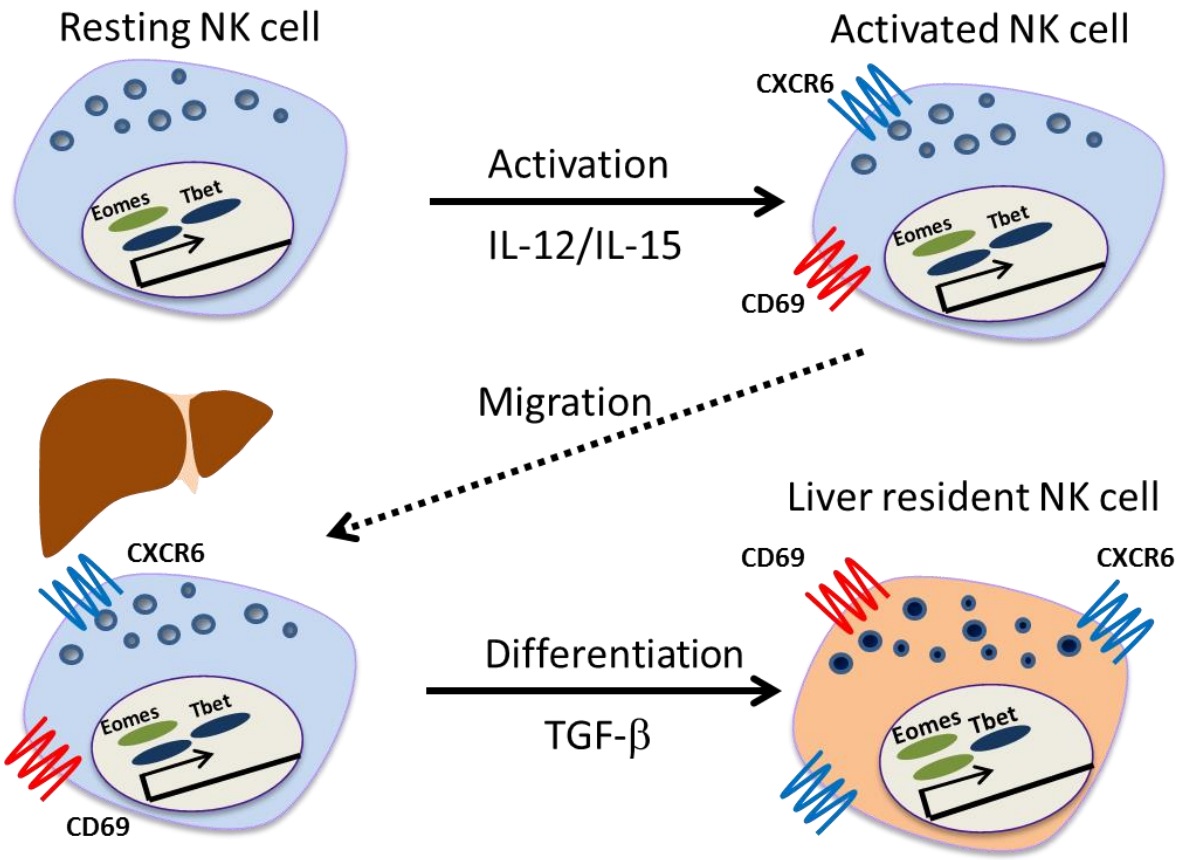

Figure 5- 2 Proposed pathway of liver resident NK cell differentiation

Resting NK cells acquire CXCR6 and CD69 expression after activation by cytokine (IL-12/IL-15). CXCR6+ NK cells are chemotactically attracted to liver sinusoids where they are retained by expression of CXCL16. TGF-β, produced in the liver sinusoid, suppresses Tbet expression in NK cells and a liver resident phenotype develops.

Therefore we further analysed the composition of tumour infiltrating NK cells and those of the surrounding tissue. NK cells are significantly depleted from the tumour compared to adjacent and distal tissue. Upon further phenotyping, it was determined that this depletion was mainly from the liver resident $CD56^{bright}$ NK cells.

The remaining tumour infiltrating $CD56^{bright}$ NK cells maintained their tissue resident phenotype, expressing CXCR6, CD69 and $Eomes^{hi}$ $Tbet^{lo}$. As in healthy liver, a small population of $CD49a^{+}$ NK cells was also detected but these were not $Eomes^{-}$ as described by Marquardt and colleagues (Marquardt et al., 2015). Furthermore, expression of cytotoxicity receptors and cytotoxic molecules was unchanged in tumour infiltrating cells compared to NK cells in the adjacent and distal tissue, indicating retention of cytotoxic capabilities. Unfortunately, low cell numbers precluded us from performing functional analysis of tumour infiltrating cells. A previous study by our group demonstrated that NK cells isolated from adjacent tissue were capable of cytotoxicity at similar levels to cells from healthy liver tissue (Norris et al., 2003). Using tumour conditioned media from CRLM tissue, we performed functional and viability assays to assess this mechanism of depletion. Liver resident $CD56^{bright}$ NK cells were chemotactically attracted to CRLM conditioned media, significantly more than $CD56^{dim}$ cells. *In vivo*, this should have correlated with an increased proportion of liver resident NK cells in CRLM tumours; however this was not the case. We therefore investigated the effect of tumour conditioned media (TCM) on NK cell viability and determined that liver resident NK cells undergo apoptosis in TCM, more so than $CD56^{dim}$ NK cells.

Apoptosis can be induced in a number of ways, through two distinct pathways; the intrinsic (mitochondrial mediated) or extrinsic (death receptor mediated) (Circu and Aw, 2010; Elmore, 2007; Taylor et al., 2008). We first investigated the extrinsic pathway, as colon cancer cells have previously been shown to release soluble death receptor ligands and NK

cells induce apoptosis of other immune cells through death receptor ligation (Nielsen et al., 2012; Peppa et al., 2013; Song et al., 2001). Blocking caspase-8 activity renders the extrinsic pathway inoperable, however inhibition of caspase-8 using z-IETD-FMK did not affect TCM induced apoptosis in our model (Guo et al., 2004). Next, we attempted to identify evidence of mitochondrial stress in tumour infiltrating NK cells. Indeed, liver resident NK cells from CRLM tumours displayed increased levels of mitochondrial ROS and reduced mitochondrial mass compared to NK cells in surrounding tissue, indicating increased mitochondrial stress. These results were similar to the effect of lactate on T and NK cells in metastatic melanoma models recently described (Brand et al., 2016).

Mitochondrial stress can be caused by a number of triggers, including loss of growth factors, metabolic deprivation, DNA damage, ER stress or dysregulation of metabolism (Circu and Aw, 2010; McCarthy and Kenny, 2016; Simon et al., 2000). NK cells are dependent on IL-15 for survival and homeostasis, we therefore measured levels of secreted IL-15 in healthy liver and CRLM tumour supernatants (Budagian et al., 2006; Ranson et al., 2003). However, there was no significant change in IL-15 or other NK cell related cytokines (Hand et al 2018).

Tumours often deprive immune cells of sources of essential energy sources such as glucose and glutamine (Pavlova and Thompson, 2016; Renner et al., 2017), however in our culture system, both are present in excess in culture media. While depletion of these factors *in vivo* may contribute to the loss of tumour infiltrating NK cells, in this system they were not affected by the presence of tumour tissue. The effects of glucose deprivation and reduced glutamine availability on liver resident NK cells are currently under investigation in our lab. While tumour glycolysis was not depriving NK cells of glucose in our system, there was an accumulation of lactate, the main "waste" product of glycolysis.

Lactate is of increasing interest in tumour immunity due to its profound effect on stromal cells, immune cells and tumour cells themselves (Dart, 2016; Hirschhaeuser et al., 2011; Xie

et al., 2015). In the context of tumour heterogeneity, highly glycolytic tumours have been shown to share space with low glycolytic neighbouring tumours, that use lactate as a fuel source for mitochondrial respiration (Hui et al., 2017). Lactate promotes tumour vascularisation through production of VEG-F by endothelial cells and induction of angiogenesis (Vegran et al., 2011). VEG-F was found to be significantly increased in supernatants from our CRLM cohort (Hand et al. 2018). Furthermore, in primary tumours lactate induces matrix degradation and the migration and metastases of tumour cells (Goetze et al., 2011; Payen et al., 2017; Romero-Garcia et al., 2016; Stern et al., 2002). In addition, lactate contributes to the polarisation of the innate immune system toward tolerance and immunosuppression. This is achieved through promotion of "M2" macrophages, differentiation of MDSCs, and inhibition of dendritic cell activity (Colegio et al., 2014; Goetze et al., 2011; Gottfried, 2006; Husain et al., 2013b). Finally, lactate has been shown to inhibit T and NK cell functions and, at high concentrations, induces apoptosis of these essential anti-tumour cells (Brand et al., 2016; Fischer et al., 2007; Husain et al., 2013a; Pötzl et al., 2017). Whether these effects are due to accumulation of acid (reducing pH) or a direct effect of lactate uptake remains unclear.

In vitro lactic acid induced the apoptosis of liver resident NK cells but not $CD56^{dim}$ cells. After treatment with sodium lactate and lactic acid, it became clear that the proton donating acidic form was a much more potent stimulus of apoptosis. Treatment with physiologically relevant levels of lactic acid induced a decrease in intracellular pH, increased mitochondrial ROS production and decreased ATP production, resulting in cell death. A similar affect was observed when media pH was altered using hydrochloric acid. This indicated that pH change rather than a direct effect of the lactate molecule was causing the observed apoptosis. Furthermore, blocking lactate transport, through αCHC, did not affect mitochondrial ROS production. ROS production has complex consequences for immune cells. It is essential for phagocytosis and is often observed in activation of immune cells (LeBleu et al., 2014; Mehta

et al., 2017; Mills et al., 2017). On the other hand, ROS accumulation causes extensive cellular damage to organelles and DNA when released in an uncontrolled manner, resulting in apoptosis (Holze et al., 2017; Kesavardhana and Kanneganti, 2018; Simon et al., 2000).

Therefore, blocking the accumulation of ROS could protect immune cells from pH induced apoptosis. Treatment with MitoTempo, a mitochondria specific ROS scavenger, reduced the accumulation of ROS and inhibited apoptosis in liver resident NK cells treated with lactic acid. It remains unclear why liver resident $CD56^{bright}$ NK cells are more sensitive to this form of apoptosis compared to $CD56^{dim}$ NK cells. One explanation may be the difference in mitochondrial mass we observed in healthy NK cells from liver perfusate. While all cells can regulate intracellular pH to a certain extent through intrinsic buffering capacity (amino acids, phosphates etc.), the largest contributor to pH regulation is the release of CO_2 from mitochondria and its conversion to bicarbonate (Casey et al., 2010; Damaghi et al., 2013; Deutsch et al., 1982). Therefore, the greater mitochondrial mass of $CD56^{dim}$ NK cells may provide them with a larger store of bicarbonate to counter the acidic environment; further experiments will be required to confirm this hypothesis. Alternatively, phenotypic differences between liver resident and $CD56^{dim}$ NK cells in terms of ion transporters may regulate the accumulation of hydrogen ions within the cell (Casey et al., 2010). To address this, we have performed RNA-Seq analysis of $CD56^{bright}$ and $CD56^{dim}$ NK cells from liver perfusate in order to identify differences in gene expression of these transporters, however no significant differences have been observed in genes associated with pH maintenance (Robinson et al. unpublished).

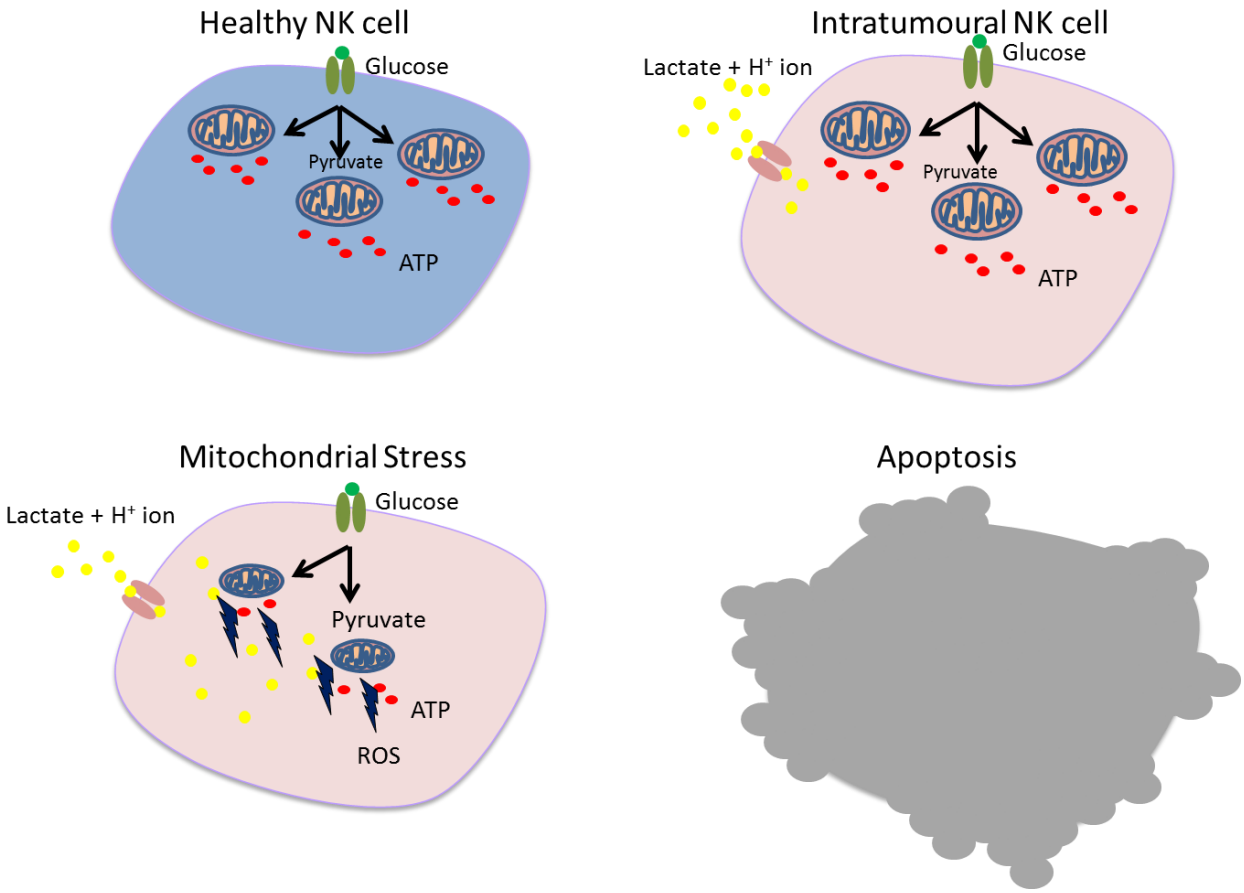

Figure 5- 3 Mechanism of liver resident NK cell apoptosis

Liver resident NK cells undergo apoptosis in the tumour microenvironment. At normal pH (blue cytoplasm) NK cells can metabolise glucose to pyruvate via glycolysis and produce ATP through mitochondrial respiration. Lactate produced by tumour glycolysis permeates the microenvironment where it releases a hydrogen ion (H^+) and becomes lactic acid. This acidic environment lowers the intracellular pH of intratumoural NK cells (pink cytoplasm). This decrease in pH induces mitochondrial stress resulting in decreased mitochondrial mass, the production of reactive oxygen species (ROS) and loss of ATP generation. ROS production induces apoptosis of tumour infiltrating liver resident NK cells.

The glycolysis pathway is an attractive target for cancer therapy. It provides the biochemical intermediates for several essential processes required for cell growth and division (Xie et al., 2015). However, our immune response is also dependent on glycolysis for acquisition of effector functions, especially T and NK cells which are the main mediators of tumour immunity (Assmann et al., 2017; Buck et al., 2015; Keating et al., 2016; MacIver et al., 2008; Mehta et al., 2017). Therefore, therapeutically targeting this pathway will require precision and specificity. Simple treatments such as systemic buffering with sodium bicarbonate have been surprisingly effective, however the practicality of such a treatment is questionable (Hu et al., 2017; Ibrahim-Hashim et al., 2017; Pötzl et al., 2017; Silva et al., 2009). Perhaps with more direct delivery systems this process could be harnessed on a larger scale. Partial inhibition of GAPDH, using koningic acid, has been shown to significantly inhibit tumour growth without impacting on tumour immunity (Liberti et al., 2017). Similarly, blocking lactate transporters specifically upregulated in tumour cells prevents tumour metastases and maintains NK cell function (Noble et al., 2017; Payen et al., 2017; Sonveaux et al., 2012). Metabolic therapies are in early stages of clinical trials and more research is required before they are seen commonly in clinical use (Altman et al., 2016; Doherty and Cleveland, 2013; Ganapathy-Kanniappan and Geschwind, 2013). In the context of CRLM, any new treatment approach would be most welcome. Current therapy has limited success, with up to 70% of patients developing a recurrence after surgical removal of the tumour, while more than half of patients are completely unsuitable for surgery. In addition, treatment with anti-VEGF therapy while reducing nutrient supply to these tumours, cuts off essential fuel and nutrients for immune cells and prevents the removal of lactate from the microenvironment, compromising local anti-tumour immunity (Patel et al., 2014).

In conclusion, the human liver is host to a variety of NK cell subsets. We have identified a population of liver resident NK cells specific to humans. These cells are characterised as $CD56^{bright}$ $Eomes^{hi}$ $Tbet^{lo}$ $CXCR6^{+}$ $CD69^{+}$, they display enhanced cytotoxic capabilities and

reduced pro-inflammatory cytokine production(Cuff et al., 2016; Harmon et al., 2016; Hudspeth et al., 2015; Hydes et al., 2017; Stegmann et al., 2016). In addition, we have also confirmed the presence of a $CD56^{bright}$ $CD49a^{+}$ previously described in humans and mice (Daussy et al., 2014; Marquardt et al., 2015). The immunosurveillance functions of liver resident NK cells are compromised in CRLM. We have identified a significant depletion of liver resident NK cells from CRLM tumours compared to surrounding tissue. This absence is not due to defects in chemotaxis but the induction of apoptosis through the release of lactate from tumour cells. We propose that CRLM tumours are highly glycolytic, producing large amounts of lactate (Holroyde et al., 1979; Xie et al., 2015). This lactate is converted to lactic acid, reducing the pH of the tumour microenvironment. This affects liver resident NK cells by reducing intracellular pH, either through the uptake of hydrogen ions or an inability to export endogenously produced hydrogen ions. This leads to mitochondrial stress and reduced ATP generation. The release of mitochondrial ROS activates the intrinsic apoptosis pathway and liver resident NK cells become depleted from the tumour.

We believe this process provides an ideal opportunity to develop new metabolic targeted therapies for the treatment of CRLM. With the success of immunotherapy in recent years, this approach may complement immune activating therapies and produce a synergistic anti-tumour effect by not only relieving the detrimental effects of lactate but by also augmenting local NK cells and driving tumour eradication.

References

Abu-Tair, L., Axelrod, J.H., Doron, S., Ovadya, Y., Krizhanovsky, V., Galun, E., Amer, J., Safadi, R., 2013. Natural Killer Cell-Dependent Anti-Fibrotic Pathway in Liver Injury via Toll-Like Receptor-9. PLoS One 8, e82571.

Adenugba, A., 2017. NK Cells in Transplantation. Transplantation 101, 2262–2264.

Adotevi, O., Godet, Y., Galaine, J., Lakkis, Z., Idirene, I., Certoux, J.M., Jary, M., Loyon, R., Laheurte, C., Kim, S., Dormoy, A., Pouthier, F., Barisien, C., Fein, F., Tiberghien, P., Pivot, X., Valmary-Degano, S., Ferrand, C., Morel, P., Delabrousse, E., Borg, C., 2018. In situ delivery of allogeneic natural killer cell (NK) combined with Cetuximab in liver metastases of gastrointestinal carcinoma: A phase I clinical trial. Oncoimmunology 7, e1424673.

Aft, R.L., Zhang, F.W., Gius, D., 2002. Evaluation of 2-deoxy-D-glucose as a chemotherapeutic agent: mechanism of cell death. Br. J. Cancer 87, 805–812.

Agnello, M., Morici, G., Rinaldi, A.M., 2008. A method for measuring mitochondrial mass and activity. Cytotechnology 56, 145–149.

Allan, D.S.J., Rybalov, B., Awong, G., Zúñiga-Pflücker, J.C., Kopcow, H.D., Carlyle, J.R., Strominger, J.L., 2010. TGF-β affects development and differentiation of human natural killer cell subsets. Eur. J. Immunol. 40, 2289–95.

Alter, G., Malenfant, J.M., Altfeld, M., 2004. CD107a as a functional marker for the identification of natural killer cell activity. J. Immunol. Methods 294, 15–22.

Altman, B.J., Stine, Z.E., Dang, C. V., 2016. From Krebs to clinic: glutamine metabolism to cancer therapy. Nat. Rev. Cancer 16, 619–634.

Arase, H., Arase, N., Saito, T., 1996. Interferon gamma production by natural killer (NK) cells and NK1.1+ T cells upon NKR-P1 cross-linking. J. Exp. Med. 183, 2391–6.

Arase, H., Mocarski, E.S., Campbell, A.E., Hill, A.B., Lanier, L.L., 2002. Direct recognition of cytomegalovirus by activating and inhibitory NK cell receptors. Science 296, 1323–6.

Arnaud, J.P., Dumont, P., Adloff, M., Leguillou, A., Py, J.M., 1984. Natural history of colorectal carcinoma with untreated liver metastases. Surg. Gastroenterol. 3, 37–42.

Assmann, N., O'Brien, K.L., Donnelly, R.P., Dyck, L., Zaiatz-Bittencourt, V., Loftus, R.M., Heinrich, P., Oefner, P.J., Lynch, L., Gardiner, C.M., Dettmer, K., Finlay, D.K., 2017. Srebp-controlled glucose metabolism is essential for NK cell functional responses. Nat. Immunol. 18, 1197–1206.

Atkins, M.B., Lotze, M.T., Dutcher, J.P., Fisher, R.I., Weiss, G., Margolin, K., Abrams, J., Sznol, M., Parkinson, D., Hawkins, M., Paradise, C., Kunkel, L., Rosenberg, S.A., 1999. High-dose recombinant interleukin 2 therapy for patients with metastatic melanoma: analysis of 270 patients treated between 1985 and 1993. J. Clin. Oncol. 17, 2105–16.

Aw Yeang, H.X., Piersma, S.J., Lin, Y., Yang, L., Malkova, O.N., Miner, C., Krupnick, A.S., Chapman, W.C., Yokoyama, W.M., 2017a. Cutting Edge: Human CD49e- NK Cells Are Tissue Resident in the Liver. J. Immunol. 198, 1417–1422.

Bahjat, K.S., Prell, R.A., Allen, H.E., Liu, W., Lemmens, E.E., Leong, M.L., Portnoy, D.A., Dubensky, T.W., Brockstedt, D.G., Giedlin, M.A., 2007. Activation of immature hepatic NK cells as immunotherapy for liver metastatic disease. J. Immunol. 179, 7376–84.

Balkwill, F.R., Capasso, M., Hagemann, T., 2012. The tumor microenvironment at a glance. J. Cell Sci. 125, 5591–5596.

Bamboat, Z.M., Stableford, J.A., Plitas, G., Burt, B.M., Nguyen, H.M., Welles, A.P., Gonen, M., Young, J.W., DeMatteo, R.P., 2009. Human Liver Dendritic Cells Promote T Cell Hyporesponsiveness. J. Immunol. 182, 1901–1911.

Bancroft, G.J., Shellam, G.R., Chalmer, J.E., 1981. Genetic influences on the augmentation of natural killer (NK) cells during murine cytomegalovirus infection: correlation with patterns of resistance. J. Immunol. 126, 988–94.

Barlozzari, T., Reynolds, C.W., Herberman, R.B., 1983. In vivo role of natural killer cells: involvement of large granular lymphocytes in the clearance of tumor cells in anti-asialo GM1-treated rats. J. Immunol. 131, 1024–7.

Barrow, A.D., Edeling, M.A., Trifonov, V., Luo, J., Goyal, P., Bohl, B., Bando, J.K., Kim, A.H., Walker, J., Andahazy, M., Bugatti, M., Melocchi, L., Vermi, W., Fremont, D.H., Cox, S., Cella, M., Schmedt, C., Colonna, M., 2017. Natural Killer Cells Control Tumor Growth by Sensing a Growth Factor. Cell 172, 534–540.e19.

Barthel, A., Okino, S.T., Liao, J., Nakatani, K., Li, J., Whitlock, J.P., Roth, R.A., 1999. Regulation of GLUT1 Gene Transcription by the Serine/Threonine Kinase Akt1. J. Biol. Chem. 274, 20281–20286.

Bauer, S., Groh, V., Wu, J., Steinle, A., Phillips, J.H., Lanier, L.L., Spies, T., 1999. Activation of NK cells and T cells by NKG2D, a receptor for stress-inducible MICA. Science 285, 727–9.

Becht, E., De Reyniès, A., Giraldo, N.A., Pilati, C., Buttard, B., Lacroix, L., Selves, J., Sautès-Fridman, C., Laurent-Puig, P., Fridman, W.H., 2016. Immune and stromal classification of Colorectal cancer is associated with molecular subtypes and relevant for precision immunotherapy. Clin. Cancer Res. 22, 4057–4066.

Benitez, C., Londono, M.-C., Miquel, R., Manzia, T.-M., Abraldes, J.G., Lozano, J.-J., Martinez-llordella, M., Marta, L., Angelico, R., Bohne, F., Sese, P., Daoud, F., Larcier, P., Roelen, D.L., Claas, F., Whitehouse, G., Lerut, J., Pirenne, J., Rimola, A., Tisone, G., Sanchez-Fueyo, A., 2013. Prospective Multicenter Clinical Trial of Immunosuppressive Drug Withdrawal in Stable Adult Liver Transplant Recipients. Hepatology 58, 1824–1835.

Beziat, V., Hervier, B., Achour, A., Boutolleau, D., Marfain-Koka, A., Vieillard, V., 2011. Human NKG2A overrides NKG2C effector functions to prevent autoreactivity of NK cells. Blood 117, 4394–4397.

Billerbeck, E., Mommersteeg, M.C., Shlomai, A., Xiao, J.W., Andrus, L., Bhatta, A., Vercauteren, K., Michailidis, E., Dorner, M., Krishnan, A., Charlton, M.R., Chiriboga, L., Rice, C.M., Jong, Y.P. De, 2016. Humanized mice efficiently engrafted with fetal hepatoblasts and syngeneic immune cells develop human monocytes and NK cells. J. Hepatol. 65, 334–343.

Biron, C.A., Byron, K.S., Sullivan, J.L., 1989. Severe herpesvirus infections in an adolescent without natural killer cells. N. Engl. J. Med. 320, 1731–5.

Björkström, N.K., Ljunggren, H.-G., Michaëlsson, J., 2016. Emerging insights into natural killer cells in human peripheral tissues. Nat. Rev. Immunol. 16, 310–320.

Björkström, N.K., Ljunggren, H.-G., Sandberg, J.K., 2010. CD56 negative NK cells: origin, function, and role in chronic viral disease. Trends Immunol. 31, 401–6.

Borrego, F., Masilamani, M., Marusina, A.I., Tang, X., Coligan, J.E., 2006. The CD94/NKG2 family of receptors: From molecules and cells to clinical relevance. Immunol. Res. 35, 263–277.

Bottino, C., Castriconi, R., Pende, D., Rivera, P., Nanni, M., Carnemolla, B., Cantoni, C., Grassi, J., Marcenaro, S., Reymond, N., Vitale, M., Moretta, L., Lopez, M., Moretta, A., 2003. Identification of PVR (CD155) and Nectin-2 (CD112) as cell surface ligands for the human DNAM-1 (CD226) activating molecule. J. Exp. Med. 198, 557–67.

Bottino, C., Falco, M., Parolini, S., Marcenaro, E., Augugliaro, R., Sivori, S., Landi, E., Biassoni, R., Notarangelo, L.D., Moretta, L., Moretta, A., 2001. Gntb-A, a Novel Sh2d1a-Associated Surface Molecule Contributing to the Inability of Natural Killer Cells to Kill Epstein-Barr Virus–Infected B Cells in X-Linked Lymphoproliferative Disease. J. Exp. Med. 194, 235–246.

Bouwens, L., Wisse, E., 1992. Pit cells in the liver. Liver Int. 12, 3–9.

Bowen, D.G., Zen, M., Holz, L., Davis, T., McCaughan, G.W., Bertolino, P., 2004. The site of primary T cell activation is a determinant of the balance between intrahepatic tolerance and immunity. J. Clin. Invest. 114, 701–12.

Boya, P., Reggiori, F., Codogno, P., 2013. Emerging regulation and functions of autophagy. Nat. Cell Biol. 15, 713–720.

Brand, A., Singer, K., Koehl, G.E., Kolitzus, M., Schoenhammer, G., Thiel, A., Matos, C., Bruss, C., Klobuch, S., Peter, K., Kastenberger, M., Bogdan, C., Schleicher, U., Mackensen, A., Ullrich, E., Fichtner-Feigl, S., Kesselring, R., Mack, M., Ritter, U., Schmid, M., Blank, C., Dettmer, K., Oefner, P.J., Hoffmann, P., Walenta, S., Geissler, E.K., Pouyssegur, J., Villunger, A., Steven, A., Seliger, B., Schreml, S., Haferkamp, S., Kohl, E., Karrer, S., Berneburg, M., Herr, W., Mueller-Klieser, W., Renner, K., Kreutz, M., 2016. LDHA-Associated Lactic Acid Production Blunts Tumor Immunosurveillance by T and NK Cells. Cell Metab. 24, 657–671.

Brodbeck, T., Nehmann, N., Bethge, A., Wedemann, G., Schumacher, U., 2014. Perforin-dependent direct cytotoxicity in natural killer cells induces considerable knockdown of spontaneous lung metastases and computer modelling-proven tumor cell dormancy in a HT29 human colon cancer xenograft mouse model. Mol. Cancer 13, 244.

Bronte, V., Serafini, P., Mazzoni, A., Segal, D.M., Zanovello, P., 2003. L-arginine metabolism in myeloid cells controls T-lymphocyte functions. Trends Immunol. 24, 301–305.

Brown, M.H., Boles, K., van der Merwe, P.A., Kumar, V., Mathew, P.A., Barclay, A.N., 1998. 2B4, the natural killer and T cell immunoglobulin superfamily surface protein, is a ligand for CD48. J. Exp. Med. 188, 2083–90.

Bryceson, Y.T., March, M.E., Ljunggren, H.-G., Long, E.O., 2006. Synergy among receptors on resting NK cells for the activation of natural cytotoxicity and cytokine secretion. Blood 107, 159–66.

Buck, M.D., O'Sullivan, D., Pearce, E.L., 2015. T cell metabolism drives immunity. J. Exp. Med. 212, 1345–1360.

Budagian, V., Bulanova, E., Paus, R., Bulfone-paus, S., Lu, D.-, 2006. IL-15 / IL-15 receptor biology : A guided tour through an expanding universe. Cytokine Growth Factor Rev. 17, 259–280.

Bukowski, J.F., Woda, B.A., Habu, S., Okumura, K., Welsh, R.M., 1983. Natural killer cell depletion enhances virus synthesis and virus-induced hepatitis in vivo. J. Immunol. 131, 1531–8.

Burt, B.M., Plitas, G., Zhao, Z., Bamboat, Z.M., Nguyen, H.M., Dupont, B., DeMatteo, R.P., 2009. The Lytic Potential of Human Liver NK Cells Is Restricted by Their Limited Expression of Inhibitory Killer Ig-Like Receptors. J. Immunol. 183, 1789–1796.

Cabestre, F.A., Lefebvre, S., Moreau, P., Rouas-Friess, N., Dausset, J., Carosella, E.D., Paul, P., 1999. HLA-G expression: immune privilege for tumour cells? Semin. Cancer Biol. 9, 27–36.

Cai, L., Zhang, Z., Zhou, L., Wang, H., Fu, J., Zhang, S., Shi, M., Zhang, H., Yang, Y., Wu, H., Tien, P., Wang, F.-S., 2008. Functional impairment in circulating and intrahepatic NK cells and relative mechanism in hepatocellular carcinoma patients. Clin. Immunol. 129, 428–37.

Caligiuri, M.A., 2008. Human natural killer cells. Blood 112, 461–469.

Callery, M.P., Mangino, M.J., Flye, M.W., 1991. Kupffer cell prostaglandin-E2 production is amplified during hepatic regeneration. Hepatology 14, 368–72.

Calne, R., Sells, R., Pena, J., Davis, D., Millard, P., Herberton, B., Binns, R., Davies, D., 1969. Induction of Immunological tolerance by porcine liver allografts. Nature 223, 472–476.

Cannons, J.L., Tangye, S.G., Schwartzberg, P.L., 2011. SLAM Family Receptors and SAP Adaptors in Immunity. Annu. Rev. Immunol. 29, 665–705.

Cantor, H., Dumont, A., 1967. Hepatic suppression of sensitization to antigen absorbed into the portal system. Nature 215, 744–745.

Carmona-Fontaine, C., Deforet, M., Akkari, L., Thompson, C.B., Joyce, J.A., Xavier, J.B., 2017. Metabolic origins of spatial organization in the tumor microenvironment. Proc. Natl. Acad. Sci. 114, 2934–2939.

Carrega, P., Morandi, B., Costa, R., Frumento, G., Forte, G., Altavilla, G., Ratto, G.B., Mingari, M.C., Moretta, L., Ferlazzo, G., 2008. Natural killer cells infiltrating human nonsmall-cell lung cancer are enriched in CD56brightCD16− cells and display an impaired capability to kill tumor cells. Cancer 112, 863–875.

Carson, W.E., Fehniger, T.A., Haldar, S., Eckhert, K., Lindemann, M.J., Lai, C.F., Croce, C.M., Baumann, H., Caligiuri, M.A., 1997. A potential role for interleukin-15 in the regulation of human natural killer cell survival. J. Clin. Invest. 99, 937–943.

Casey, J.R., Grinstein, S., Orlowski, J., 2010. Sensors and regulators of intracellular pH. Nat. Rev. Mol. Cell Biol. 11, 50–61.

Cerboni, C., Zingoni, A., Cippitelli, M., Piccoli, M., Frati, L., Santoni, A., 2007. Antigen-activated human T lymphocytes express cell-surface NKG2D ligands via an ATM/ATR-dependent mechanism and become susceptible to autologous NK- cell lysis. Blood 110, 606–15.

Chambers, A.F., Groom, A.C., MacDonald, I.C., 2002. Dissemination and growth of cancer cells in metastatic sites. Nat. Rev. Cancer 2, 563–72.

Chen, G.Y., Nuñez, G., 2010. Sterile inflammation : sensing and reacting to damage. Nat. Rev. Gr. 10, 826–837.

Chen, S., Yang, M., Du, J., Zhang, L., Chen, S., Yang, M., Du, J., Li, D., Li, Z., Cai, C., Ma, Y., Zhang, L., 2016. The Self-Specific Activation Receptor SLAM Family Is Critical for NK Cell Education Article The Self-Specific Activation Receptor SLAM Family Is Critical for NK Cell Education. Immunity 45, 1–13.

Chen, W., Ten Dijke, P., 2016. Immunoregulation by members of the TGFβ superfamily. Nat. Rev. Immunol. 16, 723–740.

Cheung-Ong, K., Giaever, G., Nislow, C., 2013. DNA-Damaging Agents in Cancer Chemotherapy: Serendipity and Chemical Biology. Chem. Biol. 20, 648–659.

Chew, V., Chen, J., Lee, D., Loh, E., Lee, J., Lim, K.H., Weber, A., Slankamenac, K., Poon, R.T.P., Yang, H., Ooi, L.L.P.J., Toh, H.C., Heikenwalder, M., Ng, I.O.L., Nardin, A., Abastado, J.-P., 2012. Chemokine-driven lymphocyte infiltration: an early intratumoural event determining long-term survival in resectable hepatocellular carcinoma. Gut 61, 427–38.

Childs, R.W., Carlsten, M., 2015. Therapeutic approaches to enhance natural killer cell cytotoxicity against cancer: the force awakens. Nat Rev Drug Discov 14, 487–498.

Chiossone, L., Vacca, P., Orecchia, P., Croxatto, D., Damonte, P., Astigiano, S., Barbieri, O., Bottino, C., Moretta, L., Mingari, M.C., 2014. In vivo generation of decidual natural killer cells from resident hematopoietic progenitors. Haematologica 99, 448–57.

Chiossone, L., Vivier, E., 2017. Immune checkpoints on innate lymphoid cells. J. Exp. Med. 214, 1561–1563.

Chowanadisai, W., Bauerly, K.A., Tchaparian, E., Wong, A., Cortopassi, G.A., Rucker, R.B., 2010. Pyrroloquinoline Quinone Stimulates Mitochondrial Biogenesis through cAMP Response Element-binding Protein Phosphorylation and Increased PGC-1α Expression. J. Biol. Chem. 285, 142–152.

Circu, M.L., Aw, T.Y., 2010. Reactive oxygen species, cellular redox systems, and apoptosis. Free Radic. Biol. Med. 48, 749–762.

Coca, S., Perez-Piqueras, J., Martinez, D., Colmenarejo, A., Saez, M.A., Vallejo, C., Martos, J.A., Moreno, M., 1997. The prognostic significance of intratumoral natural killer cells in patients with colorectal carcinoma. Cancer 79, 2320–8.

Colegio, O.R., Chu, N.-Q., Szabo, A.L., Chu, T., Rhebergen, A.M., Jairam, V., Cyrus, N., Brokowski, C.E., Eisenbarth, S.C., Phillips, G.M., Cline, G.W., Phillips, A.J., Medzhitov, R., 2014. Functional polarization of tumour-associated macrophages by tumour-derived lactic acid. Nature 513, 559–563.

Colucci, F., Santo, J.P. Di, Leibson, P.J., Medawar, P.B., 2002. Natural killer cell activation in mice and men : different triggers for similar weapons ? lymphocytes are remarkably conserved between. Nat. Immunol. 3, 807–813.

Commisso, C., Davidson, S.M., Soydaner-Azeloglu, R.G., Parker, S.J., Kamphorst, J.J., Hackett, S., Grabocka, E., Nofal, M., Drebin, J.A., Thompson, C.B., Rabinowitz, J.D., Metallo, C.M., Vander Heiden, M.G., Bar-Sagi, D., 2013. Macropinocytosis of protein is an amino acid supply route in Ras-transformed cells. Nature 497, 633–637.

Conroy, M.J., Fitzgerald, V., Doyle, S.L., Channon, S., Useckaite, Z., Gilmartin, N., OFarrelly, C., Ravi, N., Reynolds, J. V., Lysaght, J., 2016. The microenvironment of visceral adipose tissue and liver alter natural killer cell viability and function. J. Leukoc. Biol. 100, 1–8.

Constantinides, M.G., McDonald, B.D., Verhoef, P. a, Bendelac, A., 2014. A committed precursor to innate lymphoid cells. Nature 508, 397–401.

Cooper, M.A., Fehniger, T.A., Caligiuri, M.A., 2001a. The biology of human natural killer-cell subsets. Trends Immunol. 22, 633–640.

Cooper, M.A., Fehniger, T.A., Fuchs, A., Colonna, M., Caligiuri, M.A., 2004. NK cell and DC interactions. Trends Immunol. 25, 47–52.

Cooper, M.A., Fehniger, T.A., Turner, S.C., Chen, K.S., Ghaheri, B.A., Ghayur, T., Carson, W.E., Caligiuri, M.A., 2001b. Human natural killer cells: a unique innate immunoregulatory role for the CD56bright subset. Blood 97, 3146–3151.

Corbet, C., Feron, O., 2017. Tumour acidosis: from the passenger to the driver's seat. Nat. Rev. Cancer 17, 577–593.

Cortez, V.S., Ulland, T.K., Cervantes-Barragan, L., Bando, J.K., Robinette, M.L., Wang, Q., White, A.J., Gilfillan, S., Cella, M., Colonna, M., 2017. SMAD4 impedes the conversion of NK cells into ILC1-like cells by curtailing non-canonical TGF-β signaling. Nat. Immunol. 18, 995–1003.

Cosman, D., Müllberg, J., Sutherland, C.L., Chin, W., Armitage, R., Fanslow, W., Kubin, M., Chalupny, N.J., 2001. ULBPs, Novel MHC Class I–Related Molecules, Bind to CMV Glycoprotein UL16 and Stimulate NK Cytotoxicity through the NKG2D Receptor. Immunity 14, 123–133.

Crispe, I.N., 2003. Hepatic T cells and liver tolerance. Nat. Rev. Immunol. 3, 51–62.

Crispe, I.N., 2009. The liver as a lymphoid organ. Annu. Rev. Immunol. 27, 147–163.

Crispe, I.N., Metz, D.P., 2000. The liver as a site of T-cell apoptosis : graveyard , or killing field ? Immunol. Rev. 174, 47–62.

Crosbie, O.M., Reynolds, M., McEntee, G., Traynor, O., Hegarty, J.E., O'Farrelly, C., 1999. In vitro evidence for the presence of hematopoietic stem cells in the adult human liver. Hepatology 29, 1193–8.

Cruz-Munoz, M.E., Dong, Z., Shi, X., Zhang, S., Veillette, A., 2009. Influence of CRACC, a SLAM family receptor coupled to the adaptor EAT-2, on natural killer cell function. Nat. Immunol. 10, 297–305.

Cuff, A.O., Male, V., 2017. Conventional NK cells and ILC1 are partially ablated in the livers of Ncr1iCreTbx21fl/fl mice. Wellcome Open Res. 2, 39.

Cuff, A.O., Robertson, F.P., Stegmann, K.A., Pallett, L.J., Maini, M.K., Davidson, B.R., Male, V., 2016. Eomes hi NK Cells in Human Liver Are Long-Lived and Do Not Recirculate but Can Be Replenished from the Circulation. J. Immunol. 197, 4283–4291.

Curry, M.P., Golden-mason, L., Doherty, D.G., Deignan, T., Norris, S., Duffy, M., Nolan, N., Hall, W., Hegarty, J.E., O'Farrelly, C., 2003. Expansion of innate CD5 pos B cells expressing high levels of CD81 in hepatitis C virus infected liver. J. Hepatol. 38, 642–650.

Curry, M.P., Norris, S., Golden-Mason, L., Doherty, D.G., Deignan, T., Collins, C., Traynor, O., McEntee, G., Hegarty, J.E., O'Farrelly, C., 2000. Isolation of lymphocytes from normal adult human liver suitable for phenotypic and functional characterisation. J. Immunol. Methods 242, 21–31.

Damaghi, M., Wojtkowiak, J.W., Gillies, R.J., 2013. pH sensing and regulation in cancer. Front. Physiol. 4, 370.

Dart, A., 2016. Tumour metabolism: Lactic acid: Not just a waste product? Nat. Rev. Cancer 16, 676–677.

Dasari, S., Bernard Tchounwou, P., 2014. Cisplatin in cancer therapy: Molecular mechanisms of action. Eur. J. Pharmacol. 740, 364–378.

Daussy, C., Faure, F., Mayol, K., Viel, S., Gasteiger, G., Charrier, E., Bienvenu, J., Henry, T., Debien, E., Hasan, U.A., Marvel, J., Yoh, K., Takahashi, S., Prinz, I., de Bernard, S., Buffat, L., Walzer, T., 2014. T-bet and Eomes instruct the development of two distinct natural killer cell lineages in the liver and in the bone marrow. J. Exp. Med. 211, 563–577.

De Creus, A., Abe, M., Lau, A.H., Hackstein, H., Raimondi, G., Thomson, A.W., 2005. Low TLR4 expression by liver dendritic cells correlates with reduced capacity to activate allogeneic T cells in response to endotoxin. J. Immunol. 174, 2037–45.

De Greef, K., Rolfo, C., Russo, A., Chapelle, T., Bronte, G., Passiglia, F., Coelho, A., Papadimitriou, K., Peeters, M., 2016. Multisciplinary management of patients with liver metastasis from colorectal cancer. World J. Gastroenterol. 22, 7215–25.

De Maria, A., Bozzano, F., Cantoni, C., Moretta, L., 2011. Revisiting human natural killer cell subset function revealed cytolytic CD56dimCD16+ NK cells as rapid producers of abundant IFN- on activation. Proc. Natl. Acad. Sci. 108, 728–732.

de Miguel, D., Lemke, J., Anel, A., Walczak, H., Martinez-Lostao, L., 2016. Onto better TRAILs for cancer treatment. Cell Death Differ. 23, 733–747.

DeBerardinis, R.J., Chandel, N.S., 2016. Fundamentals of cancer metabolism. Sci. Adv. 2, e1600200–e1600200.

Deutsch, C., Taylor, J.S., Wilson, D.F., 1982. Regulation of intracellular pH by human peripheral blood lymphocytes as measured by 19F NMR. Proc. Natl. Acad. Sci. U. S. A. 79, 7944–8.

Diefenbach, A., Jamieson, A.M., Liu, S.D., Shastri, N., Raulet, D.H., 2000. Ligands for the murine NKG2D receptor: expression by tumor cells and activation of NK cells and macrophages. Nat. Immunol. 1, 119–26.

Disibio, G., French, S.W., 2008. Metastatic patterns of cancers: results from a large autopsy study. Arch. Pathol. Lab. Med. 132, 931–9.

Doherty, D.G., Norris, S., Madrigal-estebas, L., McEntee, G., Traynor, O., Hegarty, J.E., O'Farrelly, C., 1999. The human liver contains multiple populations of NK cells, T cells, and CD3+CD56+ natural T cells with distinct cytotoxic activities and Th1, Th2, and Th0 cytokine secretion patterns. J. Immunol. 163, 2314–21.

Doherty, D.G., O'Farrelly, C., 2000. Innate and adaptive lymphoid cells in the human liver. Immunol. Rev. 174, 5–20.

Doherty, J., Cleveland, J., 2013. Targeting lactate metabolism for cancer therapeutics. J. Clin. Invest. 123, 3685–3692.

Donadon, M., Hudspeth, K., Cimino, M., Di Tommaso, L., Preti, M., Tentorio, P., Roncalli, M., Mavilio, D., Torzilli, G., 2017. Increased Infiltration of Natural Killer and T Cells in Colorectal Liver Metastases Improves Patient Overall Survival. J. Gastrointest. Surg. 21, 1226–1236.

Dong, Z., Cruz-Munoz, M.-E., Zhong, M.-C., Chen, R., Latour, S., Veillette, A.A., 2009. Essential function for SAP family adaptors in the surveillance of hematopoietic cells by natural killer cells. Nat Immunol 10, 973–980.

Dorner, M., Horwitz, J.A., Robbins, J.B., Barry, W.T., Feng, Q., Mu, K., Jones, C.T., Schoggins, J.W., Catanese, M.T., Burton, D.R., Law, M., Rice, C.M., Ploss, A., 2011. A genetically humanized mouse model for hepatitis C virus infection. Nature 474, 208–211.

Doubrovina, E.S., Doubrovin, M.M., Vider, E., Sisson, R.B., O'Reilly, R.J., Dupont, B., Vyas, Y.M., 2003. Evasion from NK Cell Immunity by MHC Class I Chain-Related Molecules Expressing Colon Adenocarcinoma. J. Immunol. 171, 6891–6899.

Doyle, E.H., Rahman, A., Klepper, A.L., Kim, S., Haydel, B.M., Florman, S.S., Field, M.I., Schiano, T.D., Branch, A.D., 2015. Proportion of Intrahepatic CD56Bright Natural Killer Cells Correlates with Well-preserved Liver Function Erin. Hepatology 62, 845A.

Dragovich, M.A., Mor, A., 2018. The SLAM family receptors: Potential therapeutic targets for inflammatory and autoimmune diseases. Autoimmun. Rev. 17, 674–682.

Drucker, C., Parzefall, W., Teufelhofer, O., Grusch, M., Ellinger, A., Schulte-Hermann, R., Grasl-Kraupp, B., 2005. Non-parenchymal liver cells support the growth advantage in the first stages of hepatocarcinogenesis. Carcinogenesis 27, 152–161.

Duffy, D., Rouilly, V., Braudeau, C., Corbière, V., Djebali, R., Ungeheuer, M.-N., Josien, R., LaBrie, S.T., Lantz, O., Louis, D., Martinez-Caceres, E., Mascart, F., Ruiz de Morales, J.G., Ottone, C., Redjah, L., Guen, N.S.-L., Savenay, A., Schmolz, M., Toubert, A., Albert, M.L., 2017. Standardized whole blood stimulation improves immunomonitoring of induced immune responses in multi-center study. Clin. Immunol. 183, 325–335.

Dunne, J., Lynch, S., O'Farrelly, C., Todryk, S., Hegarty, J.E., Feighery, C., Doherty, D.G., 2001. Selective Expansion and Partial Activation of Human NK Cells and NK Receptor-Positive T Cells by IL-2 and IL-15. J. Immunol. 167, 3129–3138.

Dusseaux, M., Martin, E., Serriari, N., Péguillet, I., Premel, V., Louis, D., Milder, M., Le Bourhis, L., Soudais, C., Treiner, E., Lantz, O., 2011. Human MAIT cells are xenobiotic-resistant, tissue-targeted, CD161hi IL-17-secreting T cells. Blood 117, 1250–9.

Eagle, H., 1955. The minimum vitamin requirements of the l and hela cells in tissue culture, the production of specific vitamin deficiencies, and their cure. J. Exp. Med. 102, 595–600.

Eisenhardt, M., Glässner, A., Krämer, B., Körner, C., Sibbing, B., Kokordelis, P., Nischalke, H.D., Sauerbruch, T., Spengler, U., Nattermann, J., 2012. The CXCR3(+)CD56Bright Phenotype Characterizes a Distinct NK Cell Subset with Anti-Fibrotic Potential That Shows Dys-Regulated Activity in Hepatitis C. PLoS One 7, e38846.

Elboim, M., Gazit, R., Gur, C., Ghadially, H., Betser-Cohen, G., Mandelboim, O., 2010. Tumor immunoediting by NKp46. J. Immunol. 184, 5637–44.

Elmore, S., 2007. Apoptosis: A Review of Programmed Cell Death. Toxicol. Pathol. 35, 495–516.

El-Serag, H.B., 2012. Epidemiology of viral hepatitis and hepatocellular carcinoma. Gastroenterology 142, 1264–1273.e1.

Esendagli, G., Bruderek, K., Goldmann, T., Busche, A., Branscheid, D., Vollmer, E., Brandau, S., 2008. Malignant and non-malignant lung tissue areas are differentially populated by natural killer cells and regulatory T cells in non-small cell lung cancer. Lung Cancer 59, 32–40.

Esin, S., Counoupas, C., Aulicino, A., Brancatisano, F.L., Maisetta, G., Bottai, D., Di Luca, M., Florio, W., Campa, M., Batoni, G., 2013. Interaction of *Mycobacterium tuberculosis* Cell Wall Components with the Human Natural Killer Cell Receptors NKp44 and Toll-Like Receptor 2. Scand. J. Immunol. 77, 460–469.

Evans, J.M.M., 2005. Metformin and reduced risk of cancer in diabetic patients. BMJ 330, 1304–1305.

Fan, Z., Beresford, P.J., Zhang, D., Lieberman, J., 2002. HMG2 interacts with the nucleosome assembly protein SET and is a target of the cytotoxic T-lymphocyte protease granzyme A. Mol. Cell. Biol. 22, 2810–20.

Farag, S.S., Caligiuri, M.A., 2006. Human natural killer cell development and biology. Blood Rev. 20, 123–137.

Fehniger, T.A., Cooper, M.A., Nuovo, G.J., Cella, M., Facchetti, F., Colonna, M., Caligiuri, M.A., 2003. CD56bright natural killer cells are present in human lymph nodes and are activated by T cell-derived IL-2: a potential new link between adaptive and innate immunity. Blood 101, 3052–3057.

Feldstein, A.E., Canbay, A., Angulo, P., Taniai, M., Burgart, L.J., Lindor, K.D., Gores, G.J., 2003. Hepatocyte apoptosis and fas expression are prominent features of human nonalcoholic steatohepatitis. Gastroenterology 125, 437–43.

Ferlay, J., Soerjomataram, I., Dikshit, R., Eser, S., Mathers, C., Rebelo, M., Parkin, D.M., Forman, D., Bray, F., 2015. Cancer incidence and mortality worldwide: sources, methods and major patterns in GLOBOCAN 2012. Int. J. cancer 136, E359-86.

Ferlazzo, G., Thomas, D., Lin, S.-L., Goodman, K., Morandi, B., Muller, W.A., Moretta, A., Münz, C., 2004. The abundant NK cells in human secondary lymphoid tissues require activation to express killer cell Ig-like receptors and become cytolytic. J. Immunol. 172, 1455–62.

Fischer, K., Hoffmann, P., Voelkl, S., Meidenbauer, N., Ammer, J., Edinger, M., Gottfried, E., Schwarz, S., Rothe, G., Hoves, S., Renner, K., Timischl, B., Mackensen, A., Kunz-Schughart, L., Andreesen, R., Krause, S.W., Kreutz, M., 2007. Inhibitory effect of tumor cell-derived lactic acid on human T cells. Blood 109, 3812–3819.

Flier, J.S., Underhill, L.H., Dvorak, H.F., 1986. Tumors: Wounds That Do Not Heal. N. Engl. J. Med. 315, 1650–1659.

Forkel, M., Berglin, L., Kekäläinen, E., Carlsson, A., Svedin, E., Michaëlsson, J., Nagasawa, M., Erjefält, J.S., Mori, M., Flodström-Tullberg, M., Bergquist, A., Ljunggren, H.G., Westgren, M., Lindforss, U., Friberg, D., Jorns, C., Ellis, E., Björkström, N.K., Mjösberg, J., 2017. Composition and functionality of the intrahepatic innate lymphoid cell-compartment in human nonfibrotic and fibrotic livers. Eur. J. Immunol. 47, 1280–1294.

Fox, C.J., Hammerman, P.S., Thompson, C.B., 2005. Fuel feeds function: energy metabolism and the T-cell response. Nat. Rev. Immunol. 5, 844–852.

Freshney, R.I., 2011. Culture of Animal Cells: A Manual of Basic Technique and Specialized Applications, 6th ed. John Wiley & Sons, Inc., Hoboken, NJ, USA.

Freud, A.G., Becknell, B., Roychowdhury, S., Mao, H.C., Ferketich, A.K., Nuovo, G.J., Hughes, T.L., Marburger, T.B., Sung, J., Baiocchi, R. a, Guimond, M., Caligiuri, M. a, 2005. A human CD34(+) subset resides in lymph nodes and differentiates into CD56bright natural killer cells. Immunity 22, 295–304.

Freud, A.G., Caligiuri, M. a., 2006. Human natural killer cell development. Immunol. Rev. 214, 56–72.

Freud, A.G., Mundy-Bosse, B.L., Yu, J., Caligiuri, M.A., 2017. The Broad Spectrum of Human Natural Killer Cell Diversity. Immunity 47, 820–833.

Freud, A.G., Yokohama, A., Becknell, B., Lee, M.T., Mao, H.C., Ferketich, A.K., Caligiuri, M. a, 2006. Evidence for discrete stages of human natural killer cell differentiation in vivo. J. Exp. Med. 203, 1033–43.

Fridlender, Z.G., Sun, J., Kim, S., Kapoor, V., Cheng, G., Ling, L., Worthen, G.S., Albelda, S.M., 2009. Polarization of Tumor-Associated Neutrophil Phenotype by TGF-β: "N1" versus "N2" TAN. Cancer Cell 16, 183–194.

Fu, B., Zhou, Y., Ni, X., Tong, X., Xu, X., Dong, Z., Sun, R., Tian, Z., Wei, H., 2017. Natural Killer Cells Promote Fetal Development through the Secretion of Growth-Promoting Factors. Immunity 47, 1100–1113.e6.

Funke, J., Dürr, R., Dietrich, U., Koch, J., 2011. Natural killer cells in HIV-1 infection: a double-edged sword. AIDS Rev. 13, 67–76.

Gaglio, D., Soldati, C., Vanoni, M., Alberghina, L., Chiaradonna, F., 2009. Glutamine Deprivation Induces Abortive S-Phase Rescued by Deoxyribonucleotides in K-Ras Transformed Fibroblasts. PLoS One 4, e4715.

Galluzzi, L., Kepp, O., Heiden, M.G. Vander, Kroemer, G., 2013. Metabolic targets for cancer therapy. Nat. Rev. Drug Discov. 12, 829–846.

Galon, J., Costes, A., Sanchez-Cabo, F., Kirilovsky, A., Mlecnik, B., Lagorce-Pagès, C., Tosolini, M., Camus, M., Berger, A., Wind, P., Zinzindohoué, F., Bruneval, P., Cugnenc, P.-H., Trajanoski, Z., Fridman, W.-H., Pagès, F., 2006. Type, density, and location of immune cells within human colorectal tumors predict clinical outcome. Science 313, 1960–4.

Ganapathy-Kanniappan, S., Geschwind, J.-F.H., 2013. Tumor glycolysis as a target for cancer therapy: progress and prospects. Mol. Cancer 12, 152.

Gandhi, A.K., Shi, T., Li, M., Jungnelius, U., Romano, A., Tabernero, J., Siena, S., Schafer, P.H., Chopra, R., 2013. Immunomodulatory Effects in a Phase II Study of Lenalidomide Combined with Cetuximab in Refractory KRAS-Mutant Metastatic Colorectal Cancer Patients. PLoS One 8, e80437.

Gao, B., 2010. Natural Killer Group 2 Member D, Its Ligands, and Liver Disease: Good or Bad? Hepatology 51, 8–11.

Gao, B., Jeong, W.-I., Tian, Z., 2008. Liver: An organ with predominant innate immunity. Hepatology 47, 729–36.

Gao, B., Radaeva, S., 2013. Natural killer and natural killer T cells in liver fibrosis. Biochim. Biophys. Acta - Mol. Basis Dis. 1832, 1061–1069.

Gao, B., Radaeva, S., Park, O., 2009. Liver natural killer and natural killer T cells : immunobiology and emerging roles in liver diseases. J. Leukoc. Biol. 86, 513–528.

Gao, Y., Souza-Fonseca-Guimaraes, F., Bald, T., Ng, S.S., Young, A., Ngiow, S.F., Rautela, J., Straube, J., Waddell, N., Blake, S.J., Yan, J., Bartholin, L., Lee, J.S., Vivier, E., Takeda, K., Messaoudene, M., Zitvogel, L., Teng, M.W.L., Belz, G.T., Engwerda, C.R., Huntington, N.D., Nakamura, K., Hölzel, M., Smyth, M.J., 2017. Tumor immunoevasion by the conversion of effector NK cells into type 1 innate lymphoid cells. Nat. Immunol. 18, 1004–1015.

García de la Garza, R., Sarobe, P., Merino, J., Lasarte, J.J., D'Avola, D., Belsue, V., Delgado, J. a., Silva, L., Iñarrairaegui, M., Sangro, B., Sola, I., Pardo, F., Quiroga, J., Ignacio Herrero, J., 2015. Immune monitoring of immunosuppression withdrawal of liver transplant recipients. Transpl. Immunol. 33, 110–116.

Garza, R., Sarobe, P., Merino, J., 2013. Trial of complete weaning from immunosuppression for liver transplant recipients: Factors predictive of tolerance. Liver Transplant. 19, 937–944.

Geissler, E.K., Schlitt, H.J., 2009. Immunosuppression for liver transplantation. Gut 58, 452–63.

Glasner, A., Levi, A., Enk, J., Isaacson, B., Viukov, S., Orlanski, S., Scope, A., Neuman, T., Enk, C.D., Hanna, J.H., Sexl, V., Jonjic, S., Seliger, B., Zitvogel, L., Mandelboim, O., 2018. NKp46 Receptor-Mediated Interferon-γ Production by Natural Killer Cells Increases Fibronectin 1 to Alter Tumor Architecture and Control Metastasis. Immunity 48, 107–119.e4.

Glässner, A., Eisenhardt, M., Krämer, B., Körner, C., Coenen, M., Sauerbruch, T., Spengler, U., Nattermann, J., 2012. NK cells from HCV-infected patients effectively induce apoptosis of activated primary human hepatic stellate cells in a TRAIL-, FasL- and NKG2D-dependent manner. Lab. Invest. 92, 967–77.

Glienke, W., Esser, R., Priesner, C., Suerth, J.D., Schambach, A., Wels, W.S., Grez, M., Kloess, S., Arseniev, L., Koehl, U., 2015. Advantages and applications of CAR-expressing natural killer cells. Front. Pharmacol. 6, 21.

Glover, L.E.L.E., Crosby, D., Thiruchelvam, U., Harmon, C., Chorcora, C.N.C.N., Wingfield, M.B.M.B., O'Farrelly, C., 2018. Uterine natural killer cell progenitor populations predict successful implantation in women with endometriosis-associated infertility. Am. J. Reprod. Immunol. e12817.

Goddard, S., Youster, J., Morgan, E., Adams, D.H., 2004. Interleukin-10 Secretion Differentiates Dendritic Cells from Human Liver and Skin. Am. J. Pathol. 164, 511–519.

Goetze, K., Walenta, S., Ksiazkiewicz, M., Kunz-Schughart, L.A., Mueller-Klieser, W., 2011. Lactate enhances motility of tumor cells and inhibits monocyte migration and cytokine release. Int. J. Oncol. 39, 453–63.

Golden-Mason, L., Curry, M.P., Nolan, N., Traynor, O., McEntee, G., Kelly, J., Hegarty, J.E., O'Farrelly, C., 2000. Differential expression of lymphoid and myeloid markers on differentiating hematopoietic stem cells in normal and tumor-bearing adult human liver. Hepatology 31, 1251–6.

Golden-Mason, L., Douek, D.C., Koup, R. a, Kelly, J., Hegarty, J.E., O'Farrelly, C., 2004. Adult human liver contains CD8pos T cells with naive phenotype, but is not a site for conventional alpha beta T cell development. J. Immunol. 172, 5980–5.

Golden-Mason, L., Kelly, A.M., Traynor, O., McEntee, G., Kelly, J., Hegarty, J.E., O'Farrelly, C., 2001. Expression of interleukin 7 (IL-7) mRNA and protein in the normal adult human liver: implications for extrathymic T cell development. Cytokine 14, 143–51.

Golden-Mason, L., Madrigal-Estebas, L., McGrath, E., Conroy, M.J., Ryan, E.J., Hegarty, J.E., O'Farrelly, C., Doherty, D.G., 2008. Altered natural killer cell subset distributions in resolved and persistent hepatitis C virus infection following single source exposure. Gut 57, 1121–8.

Golden-Mason, L., O'Farrelly, C., 2002. Having it all? Stem cells, haematopoiesis and lymphopoiesis in adult human liver. Immunol. Cell Biol. 80, 45–51.

Golden-Mason, L., Rosen, H.R., 2013. Natural killer cells: multifaceted players with key roles in hepatitis C immunity. Immunol. Rev. 255, 68–81.

Gomez Perdiguero, E., Klapproth, K., Schulz, C., Busch, K., Azzoni, E., Crozet, L., Garner, H., Trouillet, C., de Bruijn, M.F., Geissmann, F., Rodewald, H.-R., 2014. Tissue-resident macrophages originate from yolk-sac-derived erythro-myeloid progenitors. Nature 518, 547–551.

Gordon, S.M., Chaix, J., Rupp, L.J., Wu, J., Madera, S., Sun, J.C., Lindsten, T., Reiner, S.L., 2012. The transcription factors T-bet and Eomes control key checkpoints of natural killer cell maturation. Immunity 36, 55–67.

Gorelik, E., Herberman, R., 1986. Natural killer cells: role in local tumor growth and metastasis. In: Cancer Immunology: Innovative Approaches to Therapy. pp. 151–176.

Gottfried, E., 2006. Tumor-derived lactic acid modulates dendritic cell activation and antigen expression. Blood 107, 2013–2021.

Grimm, E.A., Mazumder, A., Zhang, H.Z., Rosenberg, S.A., 1982. Lymphokine-activated killer cell phenomenon. Lysis of natural killer-resistant fresh solid tumor cells by interleukin 2-activated autologous human peripheral blood lymphocytes. J. Exp. Med. 155, 1823–41.

Groux, H., Bigler, M., de Vries, J.E., Roncarolo, M.G., 1996. Interleukin-10 induces a long-term antigen-specific anergic state in human CD4+ T cells. J. Exp. Med. 184, 19–29.

Groux, H., Bigler, M., Vries, J.E. De, Roncarolo, M., 1998. Inhibitory and Stimulatory Effects of IL-10 on Human CD8 + T Cells. J. Immunol. 160, 3188–3193.

Guerra, N., Tan, Y.X., Joncker, N.T., Choy, A., Gallardo, F., Xiong, N., Knoblaugh, S., Cado, D., Greenberg, N.M., Greenberg, N.R., Raulet, D.H., 2008. NKG2D-deficient mice are defective in tumor surveillance in models of spontaneous malignancy. Immunity 28, 571–80.

Guo, H., Liu, D., Gelbard, H., Cheng, T., Insalaco, R., Fernández, J.A., Griffin, J.H., Zlokovic, B. V, 2004. Activated Protein C Prevents Neuronal Apoptosis via Protease Activated Receptors 1 and 3. Neuron 41, 563–572.

Guo, J., Li, Y., Shan, Y., Shu, C., Wang, F., Wang, X., Zheng, G., He, J., Hu, Z., Yang, Y.-G., 2018. Humanized mice reveal an essential role for human hepatocytes in the development of the liver immune system. Cell Death Dis. 9, 667.

Halama, N., Braun, M., Kahlert, C., Spille, A., Quack, C., Rahbari, N., Koch, M., Weitz, J., Kloor, M., Zoernig, I., Schirmacher, P., Brand, K., Grabe, N., Falk, C.S., 2011. Natural killer cells are scarce in colorectal carcinoma tissue despite high levels of chemokines and cytokines. Clin. Cancer Res. 17, 678–89.

Hamann, J.C., Surcel, A., Chen, R., Teragawa, C., Albeck, J.G., Robinson, D.N., Overholtzer, M., 2017. Entosis Is Induced by Glucose Starvation. Cell Rep. 20, 201–210.

Hammerich, L., Tacke, F., 2014. Role of gamma-delta T cells in liver inflammation and fibrosis. World J. Gastrointest. Pathophysiol. 5, 107.

Hanahan, D., Coussens, L.M., 2012. Accessories to the Crime: Functions of Cells Recruited to the Tumor Microenvironment. Cancer Cell 21, 309–322.

Hanahan, D., Weinberg, R.A., 2011. Hallmarks of Cancer: The Next Generation. Cell 144, 646–674.

Hanna, J., Goldman-Wohl, D., Hamani, Y., Avraham, I., Greenfield, C., Natanson-Yaron, S., Prus, D., Cohen-Daniel, L., Arnon, T.I., Manaster, I., Gazit, R., Yutkin, V., Benharroch, D., Porgador, A., Keshet, E., Yagel, S., Mandelboim, O., 2006. Decidual NK cells regulate key developmental processes at the human fetal-maternal interface. Nat. Med. 12, 1065–74.

Harmon, C., Robinson, M.W., Fahey, R., Whelan, S., Houlihan, D.D., Geoghegan, J., O'Farrelly, C., 2016. Tissue-resident Eomes hi T-bet lo CD56 bright NK cells with reduced proinflammatory potential are enriched in the adult human liver. Eur. J. Immunol. 46, 2111–2120.

Harmon, C., Sanchez-Fueyo, A., O'Farrelly, C., Houlihan, D.D.D., 2016. Natural Killer Cells and Liver Transplantation: Orchestrators of Rejection or Tolerance? Am. J. Transplant 16, 751–7.

Hata, K., Van Thiel, D.H., Herberman, R.B., Whiteside, T.L., 1991. Natural killer activity of human liver-derived lymphocytes in various liver diseases. Hepatology 14, 495–503.

Hata, K., Zhang, X.R., Iwatsuki, S., Van Thiel, D.H., Herberman, R.B., Whiteside, T.L., 1990. Isolation, phenotyping, and functional analysis of lymphocytes from human liver. Clin Immunol Immunopathol 56, 401–19.

He, Y., Tian, Z., 2017. NK cell education via nonclassical MHC and non-MHC ligands. Cell. Mol. Immunol. 14, 321–330.

Heldin, C.-H., 2013. Targeting the PDGF signaling pathway in tumor treatment. Cell Commun. Signal. 11, 97.

Hellerbrand, C., Stefanovic, B., Giordano, F., Burchardt, E.R., Brenner, D.A., 1999. The role of TGFbeta1 in initiating hepatic stellate cell activation in vivo. J. Hepatol. 30, 77–87.

Hensley, C.T., Wasti, A.T., DeBerardinis, R.J., 2013. Glutamine and cancer: cell biology, physiology, and clinical opportunities. J. Clin. Invest. 123, 3678–3684.

Herberman, R.B., Nunn, M.E., Holden, H.T., Lavrin, D.H., 1975a. Natural cytotoxic reactivity of mouse lymphoid cells against syngeneic and allogeneic tumors. II. Characterization of effector cells. Int. J. cancer 16, 230–9.

Herberman, R.B., Nunn, M.E., Lavrin, D.H., 1975b. Natural cytotoxic reactivity of mouse lymphoid cells against syngeneic acid allogeneic tumors. I. Distribution of reactivity and specificity. Int. J. cancer 16, 216–29.

Heymann, F., Peusquens, J., Ludwig-Portugall, I., Kohlhepp, M., Ergen, C., Niemietz, P., Martin, C., van Rooijen, N., Ochando, J.C., Randolph, G.J., Luedde, T., Ginhoux, F., Kurts, C., Trautwein, C., Tacke, F., 2015. Liver inflammation abrogates immunological tolerance induced by Kupffer cells. Hepatology 62, 279–91.

Heymann, F., Tacke, F., 2016. Immunology in the liver [mdash] from homeostasis to disease. Nat Rev Gastroenterol Hepatol 13, 88–110.

Hirschhaeuser, F., Sattler, U.G.A., Mueller-Klieser, W., 2011. Lactate: A metabolic key player in cancer. Cancer Res. 71, 6921–6925.

Holroyde, C.P., Axelrod, R.S., Skutches, C.L., 1979. Lactate metabolism in patients with metastatic colorectal cancer. Cancer Res. 4900–4904.

Holze, C., Michaudel, C., Mackowiak, C., Haas, D.A., Benda, C., Hubel, P., Pennemann, F.L., Schnepf, D., Wettmarshausen, J., Braun, M., Leung, D.W., Amarasinghe, G.K., Perocchi, F., Staeheli, P., Ryffel, B., Pichlmair, A., 2017. Oxeiptosis, a ROS-induced caspase-independent apoptosis-like cell-death pathway. Nat. Immunol. 19, 1–11.

Horowitz, A., Strauss-Albee, D.M., Leipold, M., Kubo, J., Nemat-Gorgani, N., Dogan, O.C., Dekker, C.L., Mackey, S., Maecker, H., Swan, G.E., Davis, M.M., Norman, P.J., Guethlein, L.A., Desai, M., Parham, P., Blish, C.A., 2013. Genetic and environmental determinants of human NK cell diversity revealed by mass cytometry. Sci. Transl. Med. 5, 208ra145.

Hu, X., Chao, M., Wu, H., 2017. Central role of lactate and proton in cancer cell resistance to glucose deprivation and its clinical translation. Signal Transduct. Target. Ther. 2, 16047.

Huang, L., Soldevila, G., Leeker, M., Flavell, R., Crispe, I.N., 1994. The liver eliminates T cells undergoing antigen-triggered apoptosis in vivo. Immunity 1, 741–9.

Huber, A.M., Mamyrova, G., Lachenbruch, P.A., Lee, J.A., Katz, J.D., Targoff, I.N., Miller, F.W., Rider, L.G., Childhood Myositis Heterogeneity Collaborative Study Group, 2014. Early illness features associated with mortality in the juvenile idiopathic inflammatory myopathies. Arthritis Care Res. (Hoboken). 66, 732–40.

Hudspeth, K., Donadon, M., Cimino, M., Pontarini, E., Tentorio, P., Preti, M., Hong, M., Bertoletti, A., Bicciato, S., Invernizzi, P., Lugli, E., Torzilli, G., Eric Gershwin, M., Mavilio, D., Gershwin, M.E., Mavilio, D., Eric Gershwin, M., Mavilio, D., 2015. Human liver-resident CD56bright/CD16neg NK cells are retained within hepatic sinusoids via the engagement of CCR5 and CXCR6 pathways. J. Autoimmun. 66, 40–50.

Hugen, N., van de Velde, C.J.H., de Wilt, J.H.W., Nagtegaal, I.D., 2014. Metastatic pattern in colorectal cancer is strongly influenced by histological subtype. Ann. Oncol. Off. J. Eur. Soc. Med. Oncol. 25, 651–7.

Hui, S., Ghergurovich, J.M., Morscher, R.J., Jang, C., Teng, X., Lu, W., Esparza, L.A., Reya, T., Le Zhan, Yanxiang Guo, J., White, E., Rabinowitz, J.D., 2017. Glucose feeds the TCA cycle via circulating lactate. Nature 551, 115–118.

Husain, Z., Huang, Y., Seth, P., Sukhatme, V.P., 2013a. Tumor-Derived Lactate Modifies Antitumor Immune Response: Effect on Myeloid-Derived Suppressor Cells and NK Cells. J. Immunol. 191, 1486–1495.

Husain, Z., Seth, P., Sukhatme, V., 2013b. Tumor-derived lactate and myeloid-derived suppressor cells: Linking metabolism to cancer immunology. Oncoimmunology 2, e26383.

Hydes, T., Abuhilal, M., Armstrong, T., Primrose, J., Takhar, A., Khakoo, S., 2015. Natural killer cell maturation markers in the human liver and expansion of an NKG2C+KIR+ population. Lancet 385, S45.

Hydes, T., Noll, A., Salinas-Riester, G., Abuhilal, M., Armstrong, T., Hamady, Z., Primrose, J., Takhar, A., Walter, L., Khakoo, S.I., 2018. IL-12 and IL-15 induce the expression of CXCR6 and CD49a on peripheral natural killer cells. Immunity, Inflamm. Dis. 6, 34–46.

Ibrahim-Hashim, A., Abrahams, D., Enriquez-Navas, P.M., Luddy, K., Gatenby, R.A., Gillies, R.J., 2017. Tris-base buffer: a promising new inhibitor for cancer progression and metastasis. Cancer Med. 6, 1720–1729.

Il-Jeong, W., Park, O., Gao, B., Jeong, W.-I., Park, O., Gao, B., 2008. Abrogation of the antifibrotic effects of natural killer cells/interferon-gamma contributes to alcohol acceleration of liver fibrosis. Gastroenterology 134, 248–58.

Imai, K., Matsuyama, S., Miyake, S., Suga, K., Nakachi, K., 2000. Natural cytotoxic activity of peripheral-blood lymphocytes and cancer incidence: an 11-year follow-up study of a general population. Lancet (London, England) 356, 1795–9.

Inman, G.J., Nicolás, F.J., Callahan, J.F., Harling, J.D., Gaster, L.M., Reith, A.D., Laping, N.J., Hill, C.S., 2002. SB-431542 is a potent and specific inhibitor of transforming growth factor-beta superfamily type I activin receptor-like kinase (ALK) receptors ALK4, ALK5, and ALK7. Mol. Pharmacol. 62, 65–74.

Introna, M., Mantovani, A., 1983. Natural killer cells in human solid tumors. Cancer Metastasis Rev. 2, 337–50.

Ishigami, S., Natsugoe, S., Tokuda, K., Nakajo, A., Che, X., Iwashige, H., Aridome, K., Hokita, S., Aikou, T., 2000. Prognostic value of intratumoral natural killer cells in gastric carcinoma. Cancer 88, 577–83.

Ishiyama, K., Ohdan, H., Ohira, M., Mitsuta, H., Arihiro, K., Asahara, T., 2006. Difference in cytotoxicity against hepatocellular carcinoma between liver and periphery natural killer cells in humans. Hepatology 43, 362–72.

Ito, M., Maruyama, T., Saito, N., Koganei, S., Yamamoto, K., Matsumoto, N., 2006. Killer cell lectin-like receptor G1 binds three members of the classical cadherin family to inhibit NK cell cytotoxicity. J. Exp. Med. 203, 289–95.

Iwai, Y., Ishida, M., Tanaka, Y., Okazaki, T., Honjo, T., Minato, N., 2002. Involvement of PD-L1 on tumor cells in the escape from host immune system and tumor immunotherapy by PD-L1 blockade. Proc. Natl. Acad. Sci. 99, 12293–12297.

Jacobs, J., Smits, E., Lardon, F., Pauwels, P., Deschoolmeester, V., 2015. Immune Checkpoint Modulation in Colorectal Cancer: What's New and What to Expect. J. Immunol. Res. 2015, 1–16.

Janeway, C.A., 1992. The immune system evolved to discriminate infectious nonself from noninfectious self. Immunol. Today 13, 11–6.

Jenne, C.N., Kubes, P., 2013. Immune surveillance by the liver. Nat. Immunol. 14, 996–1006.

Jensen, H., Potempa, M., Gotthardt, D., Lanier, L.L., 2017. Cutting Edge: IL-2-Induced Expression of the Amino Acid Transporters SLC1A5 and CD98 Is a Prerequisite for NKG2D-Mediated Activation of Human NK Cells. J. Immunol. 199, 1967–1972.

Jiang, B., 2017. Aerobic glycolysis and high level of lactate in cancer metabolism and microenvironment. Genes Dis. 4, 25–27.

Jiang, W., Chai, N.R., Maric, D., Bielekova, B., 2011. Unexpected Role for Granzyme K in CD56bright NK Cell-Mediated Immunoregulation of Multiple Sclerosis. J. Immunol. 187, 781–790.

Jinushi, M., Takehara, T., Tatsumi, T., Hiramatsu, N., Sakamori, R., Yamaguchi, S., Hayashi, N., 2005. Impairment of natural killer cell and dendritic cell functions by the soluble form of MHC class I-related chain A in advanced human hepatocellular carcinomas. J. Hepatol. 43, 1013–1020.

Jo, J., Tan, A.T., Ussher, J.E., Sandalova, E., Tang, X.-Z.Z., Tan-Garcia, A., To, N., Hong, M., Chia, A., Gill, U.S., Kennedy, P.T., Tan, K.C., Lee, K.H., De Libero, G., Gehring, A.J., Willberg, C.B., Klenerman, P., Bertoletti, A., 2014. Toll-Like Receptor 8 Agonist and Bacteria Trigger Potent Activation of Innate Immune Cells in Human Liver. PLoS Pathog. 10, e1004210.

Jobin, G., Rodriguez-Suarez, R., Betito, K., 2017. Association Between Natural Killer Cell Activity and Colorectal Cancer in High-Risk Subjects Undergoing Colonoscopy. Gastroenterology 153, 980–987.

Jonsson, J.R., Hogan, P.G., Balderson, G. a, Ooi, L.L., Lynch, S. V, Strong, R.W., Powell, E.E., Bosma, B.M., Metselaar, H.J., Mancham, S., Boor, P.P.C., Kusters, J.G., Kazemier, G., Tilanus, H.W., Kuipers, E.J., Kwekkeboom, J., Jonsson, J.R., Hogan, P.G., Balderson, G. a, Ooi, L.L., Lynch, S. V, Strong, R.W., Powell, E.E., 1997. Human liver transplant perfusate: an abundant source of donor liver-associated leukocytes. Hepatology 26, 1111–4.

Juelke, K., Killig, M., Luetke-eversloh, M., Parente, E., Gruen, J., Ferlazzo, G., Thiel, A., Schmitt-knosalla, I., Romagnani, C., Morandi, B., 2010. CD62L expression identifies a unique subset of polyfunctional CD56 dim NK cells. Blood 116, 1299–1307.

Kamphorst, J.J., Cross, J.R., Fan, J., de Stanchina, E., Mathew, R., White, E.P., Thompson, C.B., Rabinowitz, J.D., 2013. Hypoxic and Ras-transformed cells support growth by scavenging unsaturated fatty acids from lysophospholipids. Proc. Natl. Acad. Sci. 110, 8882–8887.

Karlsen, T.H., Boberg, K.M., Olsson, M., Sun, J.-Y., Senitzer, D., Bergquist, A., Schrumpf, E., Thorsby, E., Lie, B.A., 2007. Particular genetic variants of ligands for natural killer cell receptors may contribute to the HLA associated risk of primary sclerosing cholangitis. J. Hepatol. 46, 899–906.

Kärre, K., Ljunggren, H.G., Piontek, G., Kiessling, R., 1985. Selective rejection of H-2-deficient lymphoma variants suggests alternative immune defence strategy. Nature 319, 675–8.

Kawarabayashi, N., 2000. Decrease of CD56+T Cells and Natural Killer Cells in Cirrhotic Livers With Hepatitis C May Be Involved in Their Susceptibility to Hepatocellular Carcinoma. Hepatology 32, 962–969.

Keating, S.E., Zaiatz-Bittencourt, V., Loftus, R.M., Keane, C., Brennan, K., Finlay, D.K., Gardiner, C.M., 2016. Metabolic Reprogramming Supports IFN- Production by CD56bright NK Cells. J. Immunol. 196, 2552–2560.

Kee, J.-Y., Ito, A., Hojo, S., Hashimoto, I., Igarashi, Y., Tsukada, K., Irimura, T., Shibahara, N., Nakayama, T., Yoshie, O., Sakurai, H., Saiki, I., Koizumi, K., 2013. Chemokine CXCL16 suppresses liver metastasis of colorectal cancer via augmentation of tumor-infiltrating natural killer T cells in a murine model. Oncol. Rep. 29, 975–82.

Kee, J.-Y., Ito, A., Hojo, S., Hashimoto, I., Igarashi, Y., Tsuneyama, K., Tsukada, K., Irimura, T., Shibahara, N., Takasaki, I., Inujima, A., Nakayama, T., Yoshie, O., Sakurai, H., Saiki, I., Koizumi, K., 2014. CXCL16 suppresses liver metastasis of colorectal cancer by promoting TNF-α-induced apoptosis by tumor-associated macrophages. BMC Cancer 14, 949.

Keefe, D., Shi, L., Feske, S., Massol, R., Navarro, F., Kirchhausen, T., Lieberman, J., 2005. Perforin triggers a plasma membrane-repair response that facilitates CTL induction of apoptosis. Immunity 23, 249–62.

Kelly, A., Fahey, R., Fletcher, J.M., Keogh, C., Carroll, A.G., Siddachari, R., Geoghegan, J., Hegarty, J.E., Ryan, E.J., O'Farrelly, C., 2014. CD141 + myeloid dendritic cells are enriched in healthy human liver. J. Hepatol. 60, 135–142.

Kelly, A.M., Golden-Mason, L., McEntee, G., Traynor, O., Doherty, D.G., Hegarty, J.E., O'Farrelly, C., 2004. Interleukin 12 (IL-12) is increased in tumour bearing human liver and expands CD8(+) and CD56(+) T cells in vitro but not in vivo. Cytokine 25, 273–82.

Kelly, A.M., Golden-Mason, L., Traynor, O., Geoghegan, J., McEntee, G., Hegarty, J.E., O'Farrelly, C., 2006. Changes in hepatic immunoregulatory cytokines in patients with metastatic colorectal carcinoma: implications for hepatic anti-tumour immunity. Cytokine 35, 171–9.

Kenna, T., Golden-Mason, L., Norris, S., Hegarty, J.E., O'Farrelly, C., Doherty, D.G., 2004. Distinct subpopulations of gamma delta T cells are present in normal and tumor-bearing human liver. Clin. Immunol. 113, 56–63.

Kenna, T., Golden-Mason, L., Porcelli, S. a, Koezuka, Y., Hegarty, J.E., O'Farrelly, C., Doherty, D.G., Mason, L.G., 2003. NKT cells from normal and tumor-bearing human livers are phenotypically and functionally distinct from murine NKT cells. J. Immunol. 171, 1775–9.

Kesavardhana, S., Kanneganti, T.-D., 2018. Stressed-out ROS take a silent death route. Nat. Immunol. 19, 103–105.

Kiessling, R., Klein, E., Pross, H., Wigzell, H., 1975a. "Natural" killer cells in the mouse. II. Cytotoxic cells with specificity for mouse Moloney leukemia cells. Characteristics of the killer cell. Eur. J. Immunol. 5, 117–21.

Kiessling, R., Klein, E., Wigzell, H., 1975b. "Natural" killer cells in the mouse. I. Cytotoxic cells with specificity for mouse Moloney leukemia cells. Specificity and distribution according to genotype. Eur. J. Immunol. 5, 112–7.

Kingham, T.P., Chaudhry, U.I., Plitas, G., Katz, S.C., Raab, J., DeMatteo, R.P., 2007. Murine liver plasmacytoid dendritic cells become potent immunostimulatory cells after Flt-3 ligand expansion. Hepatology 45, 445–54.

Klingemann, H., 2014. Are natural killer cells superior CAR drivers? Oncoimmunology 3, e28147.

Knolle, P.A., Uhrig, A., Hegenbarth, S., Löser, E., Schmitt, E., Gerken, G., Lohse, A.W., 1998. IL-10 down-regulates T cell activation by antigen-presenting liver sinusoidal endothelial cells through decreased antigen uptake via the mannose receptor and lowered surface expression of accessory molecules. Clin. Exp. Immunol. 114, 427–33.

Knolle, P.A., Wohlleber, D., 2016. Immunological functions of liver sinusoidal endothelial cells. Cell. Mol. Immunol. 13, 347–353.

Knolle, P., Schlaak, J., Uhrig, A., Kempf, P., Meyer zum Büschenfelde, K.H., Gerken, G., 1995. Human Kupffer cells secrete IL-10 in response to lipopolysaccharide (LPS) challenge. J. Hepatol. 22, 226–9.

Koopman, L.A., Kopcow, H.D., Rybalov, B., Boyson, J.E., Orange, J.S., Schatz, F., Masch, R., Lockwood, C.J., Schachter, A.D., Park, P.J., Strominger, J.L., 2003. Human decidual natural killer cells are a unique NK cell subset with immunomodulatory potential. J. Exp. Med. 198, 1201–12.

Krajcovic, M., Krishna, S., Akkari, L., Joyce, J.A., Overholtzer, M., 2013. mTOR regulates phagosome and entotic vacuole fission. Mol. Biol. Cell 24, 3736–3745.

Krasnova, Y., Putz, E.M., Smyth, M.J., Souza-Fonseca-Guimaraes, F., 2015. Bench to bedside: NK cells and control of metastasis. Clin. Immunol. 177, 50–59.

Krneta, T., Gillgrass, A., Chew, M., Ashkar, A. a, 2016. The breast tumor microenvironment alters the phenotype and function of natural killer cells. Cell. Mol. Immunol. 13, 1–12.

Kroemer, G., Perfettini, J.-L., 2014. Entosis, a key player in cancer cell competition. Cell Res. 24, 1280–1281.

Krummel, M.F., Allison, J.P., 1995. CD28 and CTLA-4 have opposing effects on the response of T cells to stimulation. J. Exp. Med. 182, 459–465.

Kruse, P.H., Matta, J., Ugolini, S., Vivier, E., 2014. Natural cytotoxicity receptors and their ligands. Immunol. Cell Biol. 92, 221–9.

Kurioka, A., Ussher, J.E., Cosgrove, C., Clough, C., Fergusson, J.R., Smith, K., Kang, Y.-H., Walker, L.J., Hansen, T.H., Willberg, C.B., Klenerman, P., 2015. MAIT cells are licensed through granzyme exchange to kill bacterially sensitized targets. Mucosal Immunol. 8, 429–440.

Kurioka, A., Walker, L.J., Klenerman, P., Willberg, C.B., 2016. MAIT cells: new guardians of the liver. Clin. Transl. Immunol. 5, e98.

Lamas, O., Martínez, J.A., Marti, A., 2004. Energy restriction restores the impaired immune response in overweight (cafeteria) rats. J. Nutr. Biochem. 15, 418–25.

Lanier, L.L., 2015. NKG2D Receptor and Its Ligands in Host Defense. Cancer Immunol. Res. 3, 575–582.

Lanier, L.L., Le, A.M., Civin, C.I., Loken, M.R., Phillips, J.H., 1986. The relationship of CD16 (Leu-11) and Leu-19 (NKH-1) antigen expression on human peripheral blood NK cells and cytotoxic T lymphocytes. J. Immunol. 136, 4480–4486.

Laouar, Y., Sutterwala, F.S., Gorelik, L., Flavell, R.A., 2005. Transforming growth factor-beta controls T helper type 1 cell development through regulation of natural killer cell interferon-gamma. Nat Immunol 6, 600–607.

Lassen, M.G., Lukens, J.R., Dolina, J.S., Brown, M.G., Hahn, Y.S., 2010. Intrahepatic IL-10 Maintains NKG2A + Ly49 − Liver NK Cells in a Functionally Hyporesponsive State. J. Immunol. 184, 2693–2701.

Latour, S., Veillette, A., 2003. Molecular and immunological basis of X-linked lymphoproliferative disease. Immunol. Rev. 192, 212–24.

Law, R.H.P., Lukoyanova, N., Voskoboinik, I., Caradoc-Davies, T.T., Baran, K., Dunstone, M.A., D'Angelo, M.E., Orlova, E. V, Coulibaly, F., Verschoor, S., Browne, K.A., Ciccone, A., Kuiper, M.J., Bird, P.I., Trapani, J.A., Saibil, H.R., Whisstock, J.C., 2010. The structural basis for membrane binding and pore formation by lymphocyte perforin. Nature 468, 447–51.

Lazo, M., Hernaez, R., Eberhardt, M.S., Bonekamp, S., Kamel, I., Guallar, E., Koteish, A., Brancati, F.L., Clark, J.M., 2013. Prevalence of nonalcoholic fatty liver disease in the United States: the Third National Health and Nutrition Examination Survey, 1988-1994. Am. J. Epidemiol. 178, 38–45.

Le, D.T., Durham, J.N., Smith, K.N., Wang, H., Bartlett, B.R., Aulakh, L.K., Lu, S., Kemberling, H., Wilt, C., Luber, B.S., Wong, F., Azad, N.S., Rucki, A.A., Laheru, D., Donehower, R., Zaheer, A., Fisher, G.A., Crocenzi, T.S., Lee, J.J., Greten, T.F., Duffy, A.G., Ciombor, K.K., Eyring, A.D., Lam, B.H., Joe, A., Kang, S.P., Holdhoff, M., Danilova, L., Cope, L., Meyer, C., Zhou, S., Goldberg, R.M., Armstrong, D.K., Bever, K.M., Fader, A.N., Taube, J., Housseau, F., Spetzler, D., Xiao, N., Pardoll, D.M., Papadopoulos, N., Kinzler, K.W., Eshleman, J.R., Vogelstein, B., Anders, R.A., Diaz, L.A., 2017. Mismatch repair deficiency predicts response of solid tumors to PD-1 blockade. Science (80-.). 357, 409–413.

LeBleu, V.S., O'Connell, J.T., Gonzalez Herrera, K.N., Wikman, H., Pantel, K., Haigis, M.C., de Carvalho, F.M., Damascena, A., Domingos Chinen, L.T., Rocha, R.M., Asara, J.M., Kalluri, R., 2014. PGC-1α mediates mitochondrial biogenesis and oxidative phosphorylation in cancer cells to promote metastasis. Nat. Cell Biol. 16, 992–1003.

Li, X., Fang, P., Mai, J., Choi, E.T., Wang, H., Yang, X., 2013. Targeting mitochondrial reactive oxygen species as novel therapy for inflammatory diseases and cancers. J. Hematol. Oncol. 6, 19.

Li, Y., Koshiba, T., Yoshizawa, A., Yonekawa, Y., Masuda, K., Ito, A., Ueda, M., Mori, T., Kawamoto, H., Tanaka, Y., Sakaguchi, S., Minato, N., Wood, K., Tanaka, K., 2004. Analyses of peripheral blood mononuclear cells in operational tolerance after pediatric living donor liver transplantation. Am. J. Transplant 4, 2118–25.

Liberti, M. V., Dai, Z., Wardell, S.E., Baccile, J.A., Liu, X., Gao, X., Baldi, R., Mehrmohamadi, M., Johnson, M.O., Madhukar, N.S., Shestov, A.A., Chio, I.I.C., Elemento, O., Rathmell, J.C., Schroeder, F.C., McDonnell, D.P., Locasale, J.W., 2017. A Predictive Model for Selective Targeting of the Warburg Effect through GAPDH Inhibition with a Natural Product. Cell Metab. 26, 648–659.e8.

Liew, P.X., Lee, W.-Y., Kubes, P., 2017. iNKT Cells Orchestrate a Switch from Inflammation to Resolution of Sterile Liver Injury. Immunity 47, 752–765.e5.

Liotta, L.A., Kohn, E.C., 2001. The microenvironment of the tumour-host interface. Nature 411, 375–9.

Liu, C., Perussia, B., Young, J.D., 2000. The emerging role of IL-15 in NK-cell development. Trends Immunol. 121, 113–116.

Liu, Q., Luo, Q., Halim, A., Song, G., 2017. Targeting lipid metabolism of cancer cells: A promising therapeutic strategy for cancer. Cancer Lett. 401, 39–45.

Ljunggren, H.G., Kärre, K., 1990. In search of the "missing self": MHC molecules and NK cell recognition. Immunol. Today 11, 237–44.

López-Soto, A., Gonzalez, S., Smyth, M.J., Galluzzi, L., 2017. Control of Metastasis by NK Cells. Cancer Cell 32, 135–154.

Love, R.R., Leventhal, H., Easterling, D. V., Nerenz, D.R., 1989. Side effects and emotional distress during cancer chemotherapy. Cancer 63, 604–612.

Lugli, E., Lugli, E., Hudspeth, K., Roberto, A., 2016. Tissue-resident and memory properties of human T-cell and NK-cell subsets. Eur. J. Immunol. 46, 1809–1817.

Lugthart, G., Melsen, J.E., Vervat, C., Dam, M.V.O., Corver, W.E., Dave, L., Bergen, J. Van, Tol, M.J.D. Van, Arjan, C., Schilham, M.W., 2016. Human Lymphoid Tissues Harbor a Distinct CD69 + CXCR6 + NK Cell Population. J. Immunol. 197, 78–84.

Lunemann, S., Malone, D.F.G., Hengst, J., Port, K., Grabowski, J., Deterding, K., Markova, A., Bremer, B., Schlaphoff, V., Cornberg, M., Manns, M.P., Sandberg, J.K., Ljunggren, H.-G., Björkström, N.K., Wedemeyer, H., 2014. Compromised function of natural killer cells in acute and chronic viral hepatitis. J. Infect. Dis. 209, 1362–73.

Lunemann, S., Martrus, G., Goebels, H., Kautz, T., Langeneckert, A., Salzberger, W., Koch, M., J. Bunders, M., Nashan, B., van Gisbergen, K.P.J.M., Altfeld, M., 2017. Hobit expression by a subset of human liver-resident CD56bright Natural Killer cells. Sci. Rep. 7, 6676.

Lunt, S.Y., Vander Heiden, M.G., 2011. Aerobic glycolysis: meeting the metabolic requirements of cell proliferation. Annu. Rev. Cell Dev. Biol. 27, 441–64.

Lynch, L. a, O'Connell, J.M., Kwasnik, A.K., Cawood, T.J., O'Farrelly, C., O'Shea, D.B., 2009. Are natural killer cells protecting the metabolically healthy obese patient? Obesity (Silver Spring). 17, 601–605.

Lynch, L., O'Donoghue, D., Dean, J., O'Sullivan, J., O'Farrelly, C., Golden-Mason, L., 2006. Detection and characterization of hemopoietic stem cells in the adult human small intestine. J. Immunol. 176, 5199–204.

Lysakova-Devine, T., O'Farrelly, C., 2014. Tissue-specific NK cell populations and their origin. J. Leukoc. Biol. 96, 981–90.

MacDonald, G., Shi, L., Vande Velde, C., Lieberman, J., Greenberg, A.H., 1999. Mitochondria-dependent and -independent regulation of Granzyme B-induced apoptosis. J. Exp. Med. 189, 131–44.

MacIver, N.J., Jacobs, S.R., Wieman, H.L., Wofford, J.A., Coloff, J.L., Rathmell, J.C., 2008. Glucose metabolism in lymphocytes is a regulated process with significant effects on immune cell function and survival. J. Leukoc. Biol. 84, 949–957.

Mackay, L.K., Braun, A., Macleod, B.L., Collins, N., Tebartz, C., Bedoui, S., Carbone, F.R., Gebhardt, T., 2015. Cutting edge: CD69 interference with sphingosine-1-phosphate receptor function regulates peripheral T cell retention. J. Immunol. 194, 2059–63.

Mackay, L.K., Minnich, M., Kragten, N.A.M., Liao, Y., Freestone, D., Braun, A., Wynne-jones, E., Behr, F.M., Stark, R., 2016. Hobit and Blimp1 instruct a universal transcriptional program of tissue residency in lymphocytes. Science (80-.). 352, 459–463.

Maini, M.K., Peppa, D., 2013. NK cells: a double-edged sword in chronic hepatitis B virus infection. Front. Immunol. 4, 57.

Maley, C.C., Aktipis, A., Graham, T.A., Sottoriva, A., Boddy, A.M., Janiszewska, M., Silva, A.S., Gerlinger, M., Yuan, Y., Pienta, K.J., Anderson, K.S., Gatenby, R., Swanton, C., Posada, D., Wu, C.-I., Schiffman, J.D., Hwang, E.S., Polyak, K., Anderson, A.R.A., Brown, J.S., Greaves, M., Shibata, D., 2017. Classifying the evolutionary and ecological features of neoplasms. Nat. Rev. Cancer 17, 605–619.

Mamessier, E., Sylvain, A., Thibult, M.-L., Houvenaeghel, G., Jacquemier, J., Castellano, R., Gonçalves, A., André, P., Romagné, F., Thibault, G., Viens, P., Birnbaum, D., Bertucci, F., Moretta, A., Olive, D., 2011. Human breast cancer cells enhance self tolerance by promoting evasion from NK cell antitumor immunity. J. Clin. Invest. 121, 3609–22.

Manaster, I., Mizrahi, S., Goldman-Wohl, D., Sela, H.Y., Stern-Ginossar, N., Lankry, D., Gruda, R., Hurwitz, A., Bdolah, Y., Haimov-Kochman, R., Yagel, S., Mandelboim, O., 2008. Endometrial NK cells are special immature cells that await pregnancy. J. Immunol. 181, 1869–76.

Mandelboim, O., Lieberman, N., Lev, M., Paul, L., Arnon, T.I., Bushkin, Y., Davis, D.M., Strominger, J.L., Yewdell, J.W., Porgador, a, 2001. Recognition of haemagglutinins on virus-infected cells by NKp46 activates lysis by human NK cells. Nature 409, 1055–1060.

Maria, A. De, Bozzano, F., Cantoni, C., Moretta, L., De Maria, A., Bozzano, F., Cantoni, C., Moretta, L., Maria, A. De, Bozzano, F., Cantoni, C., Moretta, L., 2011. Revisiting human natural killer cell subset function revealed cytolytic CD56 dim CD16 + NK cells as rapid producers of abundant IFN- γ on activation. Proc. Natl. Acad. Sci. U. S. A. 108, 728–732.

Markasz, L., Stuber, G., Vanherberghen, B., Flaberg, E., Olah, E., Carbone, E., Eksborg, S., Klein, E., Skribek, H., Szekely, L., 2007. Effect of frequently used chemotherapeutic drugs on the cytotoxic activity of human natural killer cells. Mol. Cancer Ther. 6, 644–654.

Markman, J.L., Shiao, S.L., 2015. Impact of the immune system and immunotherapy in colorectal cancer. J. Gastrointest. Oncol. 6, 208–223.

Marotel, M., Marotel, M., Hasan, U., Marc, A., Lyon, B., Lyon, C. De, 2016. Back to the drawing board : Understanding the complexity of hepatic innate lymphoid cells. Eur. J. Immunol. 46, 2095–2098.

Marquardt, N., Beziat, V., Nystrom, S., Hengst, J., Ivarsson, M. a., Kekalainen, E., Johansson, H., Mjosberg, J., Westgren, M., Lankisch, T.O., Wedemeyer, H., Ellis, E.C., Ljunggren, H.-G., Michaelsson, J., Bjorkstrom, N.K., 2015. Identification and Characterization of Human Intrahepatic CD49a+ NK Cells. J. Immunol. 194, 2467–2471.

Marquardt, N., Kekäläinen, E., Chen, P., Kvedaraite, E., Wilson, J.N., Ivarsson, M.A., Mjösberg, J., Berglin, L., Säfholm, J., Manson, M.L., Adner, M., Al-Ameri, M., Bergman, P., Orre, A.-C., Svensson, M., Dahlén, B., Dahlén, S.-E., Ljunggren, H.-G., Michaëlsson, J., 2017. Human lung natural killer cells are predominantly comprised of highly differentiated hypofunctional CD69 − CD56 dim cells. J. Allergy Clin. Immunol. 139, 1321–1330.e4.

Martinet, L., Ferrari De Andrade, L., Guillerey, C., Lee, J.S., Liu, J., Souza-Fonseca-Guimaraes, F., Hutchinson, D.S., Kolesnik, T.B., Nicholson, S.E., Huntington, N.D., Smyth, M.J., 2015. DNAM-1 expression marks an alternative program of NK cell maturation. Cell Rep. 11, 85–97.

Martinez-llordella, M., 2006. Immune Profiling of Operational tolerance in Liver transplantation 2004–2006.

Martinez-llordella, M., Lozano, J.-J., Puig-pey, I., Orlando, G., Tisone, G., Lerut, J., Benitez, C., Pons, J.A., Parrilla, P., Ramírez, P., Bruguera, M., Rimola, A., Sánchez-fueyo, A., 2008. Using transcriptional profiling to develop a diagnostic test of operational tolerance in liver transplant recipients. J. Clin. Invest. 118, 2845–2857.

Martinez-llordella, M., Puig-pey, I., Orlando, G., Ramoni, M., Tisone, G., Rimola, A., Lerut, J., Latinne, D., Margarit, C., Bilbao, I., Brouard, S., Hernández-Fuentes, M., Soulillou, J.-P., Sánchez-fueyo, A., 2007. Multiparameter immune profiling of operational tolerance in liver transplantation. Am. J. Transplant 7, 309–19.

Martínez-Reyes, I., Chandel, N.S., 2017. Waste Not, Want Not: Lactate Oxidation Fuels the TCA Cycle. Cell Metab. 26, 803–804.

Martínez-Zaguilán, R., Seftor, E.A., Seftor, R.E., Chu, Y.W., Gillies, R.J., Hendrix, M.J., 1996. Acidic pH enhances the invasive behavior of human melanoma cells. Clin. Exp. Metastasis 14, 176–86.

Martrus, G., Kautz, T., Lunemann, S., Richert, L., Glau, L., Salzberger, W., Goebels, H., Langeneckert, A., Hess, L., Poch, T., Schramm, C., Oldhafer, K.J., Koch, M., Tolosa, E., Nashan, B., Altfeld, M., 2017. Proliferative capacity exhibited by human liver-resident CD49a+CD25+ NK cells. PLoS One 12, e0182532.

Mason, E.F., Rathmell, J.C., 2011. Cell metabolism: An essential link between cell growth and apoptosis. Biochim. Biophys. Acta - Mol. Cell Res. 1813, 645–654.

Mavoungou, E., Held, J., Mewono, L., Kremsner, P.G., 2007. A Duffy binding-like domain is involved in the NKp30-mediated recognition of Plasmodium falciparum-parasitized erythrocytes by natural killer cells. J Infect Dis 195, 1521–1531.

McCarthy, C., Kenny, L.C., 2016. Therapeutically targeting mitochondrial redox signalling alleviates endothelial dysfunction in preeclampsia. Sci. Rep. 6, 32683.

McGlynn, K.A., Petrick, J.L., London, W.T., 2015. Global Epidemiology of Hepatocellular Carcinoma. Clin. Liver Dis. 19, 223–238.

McIntyre, R.E., Buczacki, S.J.A., Arends, M.J., Adams, D.J., 2015. Mouse models of colorectal cancer as preclinical models. Bioessays 37, 909–20.

Mehal, W.Z., Juedes, A.E., Crispe, I.N., 1999. Selective retention of activated CD8+ T cells by the normal liver. J. Immunol. 163, 3202–10.

Mehta, M.M., Weinberg, S.E., Chandel, N.S., 2017. Mitochondrial control of immunity: beyond ATP. Nat. Rev. Immunol. 17, 608–620.

Melsen, J.E., Lugthart, G., Lankester, A.C., Schilham, M.W., 2016. Human Circulating and Tissue-Resident CD56bright Natural Killer Cell Populations. Front. Immunol. 7, 1–10.

Mezrich, J.D., Fechner, J.H., Zhang, X., Johnson, B.P., Burlingham, W.J., Bradfield, C.A., 2010. An Interaction between Kynurenine and the Aryl Hydrocarbon Receptor Can Generate Regulatory T Cells. J. Immunol. 185, 3190–3198.

Michielsen, A.J., Hogan, A.E., Marry, J., Tosetto, M., Cox, F., Hyland, J.M., Sheahan, K.D., O'Donoghue, D.P., Mulcahy, H.E., Ryan, E.J., O'Sullivan, J.N., 2011. Tumour tissue microenvironment can inhibit dendritic cell maturation in colorectal cancer. PLoS One 6, e27944.

Middleton, D., Gonzelez, F., 2010. The extensive polymorphism of KIR genes. Immunology 129, 8–19.

Mills, E.L., Kelly, B., O'Neill, L.A.J., 2017. Mitochondria are the powerhouses of immunity. Nat. Immunol. 18, 488–498.

Misiakos, E.P., 2011. Current treatment for colorectal liver metastases. World J. Gastroenterol. 17, 4067.

Moffett-King, A., 2002. Natural killer cells and pregnancy. Nat. Rev. Immunol. 2, 656–63.

Montaldo, E., Juelke, K., Romagnani, C., 2015. Group 3 innate lymphoid cells (ILC3s): Origin, differentiation, and plasticity in humans and mice. Eur. J. Immunol. 45, 2171–2182.

Montaldo, E., Vacca, P., Moretta, L., Mingari, M.C., 2014. Development of human natural killer cells and other innate lymphoid cells. Semin. Immunol. 1–7.

Moroso, V., Famili, F., Papazian, N., Cupedo, T., van der Laan, L.J.W., Kazemier, G., Metselaar, H.J., Kwekkeboom, J., 2011. NK cells can generate from precursors in the adult human liver. Eur. J. Immunol. 41, 3340–50.

Moroso, V., Metselaar, H.J., Mancham, S., Tilanus, H.W., Eissens, D., van der Meer, A., van der Laan, L.J.W., Kuipers, E.J., Joosten, I., Kwekkeboom, J., 2010. Liver grafts contain a unique subset of natural killer cells that are transferred into the recipient after liver transplantation. Liver Transpl. 16, 895–908.

Narni-Mancinelli, E., Gauthier, L., Baratin, M., Guia, S., Fenis, A., Deghmane, A.-E., Rossi, B., Fourquet, P., Escalière, B., Kerdiles, Y.M., Ugolini, S., Taha, M.-K., Vivier, E., 2017. Complement factor P is a ligand for the natural killer cell-activating receptor NKp46. Sci. Immunol. 2.

Nathan, H., de Jong, M.C., Pulitano, C., Ribero, D., Strub, J., Mentha, G., Gigot, J.-F., Schulick, R.D., Choti, M.A., Aldrighetti, L., Capussotti, L., Pawlik, T.M., 2010. Conditional survival after surgical resection of colorectal liver metastasis: an international multi-institutional analysis of 949 patients. J. Am. Coll. Surg. 210, 755–64, 764–6.

Nausch, N., Cerwenka, A., 2008. NKG2D ligands in tumor immunity. Oncogene 27, 5944–5958.

Nazarewicz, R.R., Dikalova, A., Bikineyeva, A., Ivanov, S., Kirilyuk, I.A., Grigor'ev, I.A., Dikalov, S.I., 2013. Does Scavenging of Mitochondrial Superoxide Attenuate Cancer Prosurvival Signaling Pathways? Antioxid. Redox Signal. 19, 344–349.

Nel, I., Lucar, O., Petitdemange, C., Béziat, V., Lapalus, M., 2016. Accumulation of Intrahepatic TNF-α-Producing NKp44+ NK Cells Correlates With Liver Fibrosis and Viral Load in Chronic HCV Infection. Medicine (Baltimore). 95, 1–9.

Nichols, P.H., Ward, U., Ramsden, C.W., Primrose, J.N., 1994. The effect of 5-fluorouracil and alpha interferon and 5-fluorouracil and leucovorin on cellular anti-tumour immune responses in patients with advanced colorectal cancer. Br J Cancer 70, 946–949.

Nielsen, N., Ødum, N., Ursø, B., Lanier, L.L., Spee, P., 2012. Cytotoxicity of CD56(bright) NK cells towards autologous activated CD4+ T cells is mediated through NKG2D, LFA-1 and TRAIL and dampened via CD94/NKG2A. PLoS One 7, e31959.

Nishida, S., Levi, D.M., Tzakis, A.G., 2013. Liver natural killer cell inoculum for liver transplantation with hepatocellular carcinoma. Curr. Opin. Organ Transplant. 18, 690–4.

Noble, R.A., Bell, N., Blair, H., Sikka, A., Thomas, H., Phillips, N., Nakjang, S., Miwa, S., Crossland, R., Rand, V., Televantou, D., Long, A., Keun, H.C., Bacon, C.M., Bomken, S., Critchlow, S.E., Wedge, S.R., 2017. Inhibition of monocarboxyate transporter 1 by AZD3965 as a novel therapeutic approach for diffuse large B-cell lymphoma and burkitt lymphoma. Haematologica 102, 1247–1257.

Norris, S., Collins, C., Doherty, D.G., Smith, F., McEntee, G., Traynor, O., Nolan, N., Hegarty, J.E., O'Farrelly, C., 1998. Resident human hepatic lymphocytes are phenotypically different from circulating lymphocytes. J. Hepatol. 28, 84–90.

Norris, S., Doherty, D.G., Collins, C., McEntee, G., Traynor, O., Hegarty, J.E., O'Farrelly, C., 1999. Natural T cells in the human liver: cytotoxic lymphocytes with dual T cell and natural killer cell phenotype and function are phenotypically heterogenous and include Valpha24-JalphaQ and gammadelta T cell receptor bearing cells. Hum. Immunol. 60, 20–31.

Norris, S., Doherty, D.G., Curry, M.P., McEntee, G., Traynor, O., Hegarty, J.E., O'Farrelly, C., 2003. Selective reduction of natural killer cells and T cells expressing inhibitory receptors for MHC class I in the livers of patients with hepatic malignancy. Cancer Immunol. Immunother. 52, 53–8.

Notas, G., Kisseleva, T., Brenner, D., 2009. NK and NKT cells in liver injury and fibrosis. Clin. Immunol. 130, 16–26.

O'Farrelly, C., Crispe, I.N., 2002. Prometheus throught the looking glass: reflections on the hepatic immune system. Crit. Rev. Immunol. 22, 47–103.

O'Farrelly, C., Pierce, R.H., Crispe, I.N., 2005. Hepatic immunology. In: Thomas, H., Lemon, S., Zuckerman, A. (Eds.), Viral Hepatitis. Blackwell Publishing, Oxford, pp. 15–29.

O'Neill, L.A.J., Kishton, R.J., Rathmell, J., 2016. A guide to immunometabolism for immunologists. Nat. Rev. Immunol. 16, 553–565.

O'Shea, D., Cawood, T.J., O'Farrelly, C., Lynch, L., 2010. Natural killer cells in obesity: impaired function and increased susceptibility to the effects of cigarette smoke. PLoS One 5, e8660.

O'Toole, A., Michielsen, A.J., Nolan, B., Tosetto, M., Sheahan, K., Mulcahy, H.E., Winter, D.C., Hyland, J.M., O'Connell, P.R., Fennelly, D., O'Donoghue, D., O'Sullivan, J., Doherty, G.A., Ryan, E.J., 2014. Tumour microenvironment of both early- and late-stage colorectal cancer is equally immunosuppressive. Br. J. Cancer 111, 927–32.

Oei, V.Y.S., Siernicka, M., Graczyk-Jarzynka, A., Hoel, H.J., Yang, W., Palacios, D., Almåsbak, H., Bajor, M., Clement, D., Brandt, L., Önfelt, B., Goodridge, J., Winiarska, M., Zagozdzon, R., Olweus, J., Kyte, J.-A., Malmberg, K.-J., 2018. Intrinsic Functional Potential of NK-Cell Subsets Constrains Retargeting Driven by Chimeric Antigen Receptors. Cancer Immunol. Res. 6, 467–480.

Ohira, M., Nishida, S., Tryphonopoulos, P., Tekin, A., Selvaggi, G., Moon, J., Levi, D., Ricordi, C., Ishiyama, K., Tanaka, Y., Ohdan, H., Tzakis, A.G., 2012. Clinical-scale isolation of interleukin-2-stimulated liver natural killer cells for treatment of liver transplantation with hepatocellular carcinoma. Cell Transplant. 21, 1397–406.

Orange, J.S., 2002. Human natural killer cell deficiencies and susceptibility to infection. Microbes Infect. 4, 1545–58.

Pallett, L.J., Davies, J., Colbeck, E.J., Robertson, F., Hansi, N., Easom, N.J.W., Burton, A.R., Stegmann, K.A., Schurich, A., Swadling, L., Gill, U.S., Male, V., Luong, T., Gander, A., Davidson, B.R., Kennedy, P.T.F., Maini, M.K., 2017. IL-2(high) tissue-resident T cells in the human liver: Sentinels for hepatotropic infection. J. Exp. Med. 214, 1567–1580.

Pardoll, D.M., 2001. Immunology. Stress, NK receptors, and immune surveillance. Science 294, 534–6.

Pardoll, D.M., 2012. The blockade of immune checkpoints in cancer immunotherapy. Nat. Rev. Cancer 12, 252–64.

Parham, P., 2005. MHC class I molecules and KIRs in human history, health and survival. Nat. Rev. Immunol. 5, 201–14.

Park, O., Jeong, W., Wang, L., Wang, H., Lian, Z., Gershwin, E., Gao, B., 2009. Diverse Roles of Invariant Natural Killer T Cells in Liver Injury and Fibrosis Induced by Carbon Tetrachloride. Hepatology 49, 1683–1694.

Parker, R., Weston, C., Adams, D., 2013. CXCR6 and CXCL16 in liver disease. Lancet 381, S83.

Pashine, A., Valiante, N.M., Ulmer, J.B., 2005. Targeting the innate immune response with improved vaccine adjuvants. Nat. Med. 11, S63–S68.

Patel, S.R., Karnad, A.B., Ketchum, N.S., Pollock, B.H., Sarantopoulos, J., Weitman, S., Mahalingam, D., 2014. Should we move beyond VEGF inhibition in metastatic colorectal cancer ? Lessons from early phase clinical trials. J. Gastrointest. Oncol. 5, 99–103.

Paust, S., Gill, H.S., Wang, B., Flynn, M.P., Ashley, E., Senman, B., Szczepanik, M., Telenti, A., Philip, W., Compans, R.W., Andrian, U.H. Von, 2011. Critical role for CXCR6 in NK cell-mediated antigen-specific memory to haptens and viruses. Nat. Immunol. 11, 1127–1135.

Pavlova, N.N., Thompson, C.B., 2016. The Emerging Hallmarks of Cancer Metabolism. Cell Metab. 23, 27–47.

Payen, V.L., Hsu, M.Y., Rädecke, K.S., Wyart, E., Vazeille, T., Bouzin, C., Porporato, P.E., Sonveaux, P., 2017. Monocarboxylate transporter MCT1 promotes tumor metastasis independently of its activity as a lactate transporter. Cancer Res. 77, 5591–5601.

Pegram, H.J., Andrews, D.M., Smyth, M.J., Darcy, P.K., Kershaw, M.H., 2011. Activating and inhibitory receptors of natural killer cells. Immunol. Cell Biol. 89, 216–24.

Pelicano, H., Martin, D.S., Xu, R.-H., Huang, P., 2006. Glycolysis inhibition for anticancer treatment. Oncogene 25, 4633–4646.

Pembroke, T., Christian, A., Jones, E., Hills, R.K., Wang, E.C.Y., Gallimore, A.M., Godkin, A., 2014. The paradox of NKp46+ natural killer cells: drivers of severe hepatitis C virus-induced pathology but in-vivo resistance to interferon α treatment. Gut 63, 515–24.

Peng, H., Jiang, X., Chen, Y., Sojka, D.K., Wei, H., Gao, X., Sun, R., Yokoyama, W.M., Tian, Z., 2013. Liver-resident NK cells confer adaptive immunity in skin-contact inflammation. J. Clin. Invest. 123, 1444–1456.

Peng, H., Wisse, E., Tian, Z., 2016. Liver natural killer cells: subsets and roles in liver immunity. Cell Mol Immunol 13, 328–336.

Peppa, D., Gill, U.S., Reynolds, G., Easom, N.J.W., Pallett, L.J., Schurich, A., Micco, L., Nebbia, G., Singh, H.D., Adams, D.H., Kennedy, P.T.F., Maini, M.K., 2013. Up-regulation of a death receptor renders antiviral T cells susceptible to NK cell-mediated deletion. J. Exp. Med. 210, 99–114.

Pietra, G., Manzini, C., Rivara, S., Vitale, M., Cantoni, C., Petretto, A., Balsamo, M., Conte, R., Benelli, R., Minghelli, S., Solari, N., Gualco, M., Queirolo, P., Moretta, L., Mingari, M.C., 2012. Melanoma cells inhibit natural killer cell function by modulating the expression of activating receptors and cytolytic activity. Cancer Res. 72, 1407–15.

Pinkoski, M.J., Green, D.R., 2003. Granzyme A: the road less traveled. Nat. Immunol. 4, 106–108.

Platten, M., Wick, W., Van den Eynde, B.J., 2012. Tryptophan Catabolism in Cancer: Beyond IDO and Tryptophan Depletion. Cancer Res. 72, 5435–5440.

Polanski, R., Hodgkinson, C.L., Fusi, A., Nonaka, D., Priest, L., Kelly, P., Trapani, F., Bishop, P.W., White, A., Critchlow, S.E., Smith, P.D., Blackhall, F., Dive, C., Morrow, C.J., 2014. Activity of the Monocarboxylate Transporter 1 Inhibitor AZD3965 in Small Cell Lung Cancer. Clin. Cancer Res. 20, 926–937.

Poli, A., Michel, T., Thérésine, M., Andrès, E., Hentges, F., Zimmer, J., 2009. CD56 bright natural killer (NK) cells: an important NK cell subset. Immunology 126, 458–465.

Pollmann, J., Rölle, A., Hofmann, M., Cerwenka, A., 2017. Hepatitis C Virus and Human Cytomegalovirus-Natural Killer Cell Subsets in Persistent Viral Infections. Front. Immunol. 8, 566.

Porporato, P.E., Payen, V.L., Pérez-Escuredo, J., De Saedeleer, C.J., Danhier, P., Copetti, T., Dhup, S., Tardy, M., Vazeille, T., Bouzin, C., Feron, O., Michiels, C., Gallez, B., Sonveaux, P., 2014. A Mitochondrial Switch Promotes Tumor Metastasis. Cell Rep. 8, 754–766.

Pötzl, J., Roser, D., Bankel, L., Hömberg, N., Geishauser, A., Brenner, C.D., Weigand, M., Röcken, M., Mocikat, R., 2017. Reversal of tumor acidosis by systemic buffering reactivates NK cells to express IFN-γ and induces NK cell-dependent lymphoma control without other immunotherapies. Int. J. Cancer 140, 2125–2133.

Protzer, U., Maini, M.K., Knolle, P. a, 2012. Living in the liver: hepatic infections. Nat. Rev. Immunol. 12, 201–13.

Pruvot, F.R., Navarro, F., Janin, A., Labalette, M., Masy, E., Lecomte-Houcke, M., Gambiez, L., Copin, M.C., Dessaint, J.P., 1995. Characterization, quantification, and localization of passenger T lymphocytes and NK cells in human liver before transplantation. Transpl. Int. 8, 273–9.

Pugh, S.A., Harrison, R.J., Primrose, J.N., Khakoo, S.I., 2014. T cells but not NK cells are associated with a favourable outcome for resected colorectal liver metastases. BMC Cancer 14, 180.

Qian, B.-Z., Pollard, J.W., 2010. Macrophage Diversity Enhances Tumor Progression and Metastasis. Cell 141, 39–51.

Racanelli, V., Sansonno, D., Piccoli, C., D'Amore, F.P., Tucci, F.A., Dammacco, F., 2001. Molecular characterization of B cell clonal expansions in the liver of chronically hepatitis C virus-infected patients. J. Immunol. 167, 21–9.

Radaeva, S., Sun, R., Jaruga, B., Nguyen, V.T., Tian, Z., Gao, B., 2006. Natural Killer Cells Ameliorate Liver Fibrosis by Killing Activated Stellate Cells in NKG2D-Dependent and Tumor Necrosis Factor–Related Apoptosis-Inducing Ligand–Dependent Manners. Gastroenterology 130, 435–452.

Ranson, T., Vosshenrich, C.A.J., Corcuff, E., Richard, O., Laloux, V., Santo, J.P. Di, 2003. IL-15 availability conditions homeostasis of peripheral natural killer T cells. Proc. Natl. Acad. Sci. U. S. A. 100, 2663–2668.

Raulet, D.H., 2003. Roles of the NKG2D immunoreceptor and its ligands. Nat. Rev. Immunol. 3, 781–90.

Reddy, N., Hernandez-Ilizaliturri, F.J., Deeb, G., Roth, M., Vaughn, M., Knight, J., Wallace, P., Czuczman, M.S., 2008. Immunomodulatory drugs stimulate natural killer-cell function, alter cytokine production by dendritic cells, and inhibit angiogenesis enhancing the anti-tumour activity of rituximab in vivo. Br. J. Haematol. 140, 36–45.

Renner, K., Singer, K., Koehl, G.E., Geissler, E.K., Peter, K., Siska, P.J., Kreutz, M., 2017. Metabolic Hallmarks of Tumor and Immune Cells in the Tumor Microenvironment. Front. Immunol. 8, 248.

Riaz, N., Havel, J.J., Makarov, V., Desrichard, A., Urba, W.J., Sims, J.S., Hodi, F.S., Martín-Algarra, S., Mandal, R., Sharfman, W.H., Bhatia, S., Hwu, W.J., Gajewski, T.F., Slingluff, C.L., Chowell, D., Kendall, S.M., Chang, H., Shah, R., Kuo, F., Morris, L.G.T., Sidhom, J.W., Schneck, J.P., Horak, C.E., Weinhold, N., Chan, T.A., 2017. Tumor and Microenvironment Evolution during Immunotherapy with Nivolumab. Cell 1–16.

Riccardi, C., Santoni, A., Barlozzari, T., Puccetti, P., Herberman, R.B., 1980. In vivo natural reactivity of mice against tumor cells. Int. J. cancer 25, 475–86.

Riihimäki, M., Hemminki, A., Sundquist, J., Hemminki, K., 2016. Patterns of metastasis in colon and rectal cancer. Sci. Rep. 6, 1–9.

Robinson, B.W., Pinkston, P., Crystal, R.G., 1984. Natural killer cells are present in the normal human lung but are functionally impotent. J. Clin. Invest. 74, 942–50.

Robinson, M.W., Harmon, C., O'Farrelly, C., 2016. Liver immunology and its role in inflammation and homeostasis. Cell. Mol. Immunol. 13.

Robson, A., Harris, L.K., Innes, B.A., Lash, G.E., Aljunaidy, M.M., Aplin, J.D., Baker, P.N., Robson, S.C., Bulmer, J.N., 2012. Uterine natural killer cells initiate spiral artery remodeling in human pregnancy. FASEB J. 26, 4876–85.

Rocca, Y.S., Roberti, M.P., Juliá, E.P., Pampena, M.B., Bruno, L., Rivero, S., Huertas, E., Sánchez Loria, F., Pairola, A., Caignard, A., Mordoh, J., Levy, E.M., 2016. Phenotypic and Functional Dysregulated Blood NK Cells in Colorectal Cancer Patients Can Be Activated by Cetuximab Plus IL-2 or IL-15. Front. Immunol. 7, 413.

Romero-Garcia, S., Moreno-Altamirano, M.M.B., Prado-Garcia, H., Sánchez-García, F.J., 2016. Lactate Contribution to the Tumor Microenvironment: Mechanisms, Effects on Immune Cells and Therapeutic Relevance. Front. Immunol. 7, 52.

Rouas-Freiss, N., Moreau, P., Ferrone, S., Carosella, E.D., 2005a. HLA-G proteins in cancer: do they provide tumor cells with an escape mechanism? Cancer Res. 65, 10139–44.

Rouas-Freiss, N., Moreau, P., Ferrone, S., Carosella, E.D., 2005b. HLA-G Proteins in Cancer: Do They Provide Tumor Cells with an Escape Mechanism? Cancer Res. 65, 10139–10144.

Rousalova, I., Krepela, E., 2010. Granzyme B-induced apoptosis in cancer cells and its regulation (Review). Int. J. Oncol. 37, 414–20.

Sagiv-Barfi, I., Czerwinski, D.K., Levy, S., Alam, I.S., Mayer, A.T., Gambhir, S.S., Levy, R., 2018. Eradication of spontaneous malignancy by local immunotherapy. Sci. Transl. Med. 10, eaan4488.

Salih, H.R., Goehlsdorf, D., Steinle, A., 2006. Release of MICB molecules by tumor cells: mechanism and soluble MICB in sera of cancer patients. Hum. Immunol. 67, 188–95.

Sayos, J., Wu, C., Morra, M., Wang, N., Zhang, X., Allen, D., Van Schaik, S., Notarangelo, L., Geha, R., Roncarolo, M.G., Oettgen, H., De Vries, J.E., Aversa, G., Terhorst, C., 1998. The X-linked lymphoproliferative-disease gene product SAP regulates signals induced through the co-receptor SLAM. Nature 395, 462–469.

Scatena, R., Bottoni, P., Pontoglio, A., Mastrototaro, L., Giardina, B., 2008. Glycolytic enzyme inhibitors in cancer treatment. Expert Opin. Investig. Drugs 17, 1533–1545.

Sceneay, J., Chow, M.T., Chen, A., Halse, H.M., Wong, C.S.F., Andrews, D.M., Sloan, E.K., Parker, B.S., Bowtell, D.D., Smyth, M.J., Möller, A., 2012. Primary tumor hypoxia recruits CD11b+/Ly6Cmed/Ly6G+ immune suppressor cells and compromises NK cell cytotoxicity in the premetastatic niche. Cancer Res. 72, 3906–11.

Schenkel, J.M., Masopust, D., 2014. Tissue-Resident Memory T Cells. Immunity 41, 886–897.

Schumacher, T.N., Schreiber, R.D., 2015. Neoantigens in cancer immunotherapy. Science (80-.). 348, 69–74.

Scott, K.E.N., Cleveland, J.L., 2016. Lactate Wreaks Havoc on Tumor-Infiltrating T and NK Cells. Cell Metab. 24, 649–650.

Seki, E., Brenner, D., 2008. Toll-like receptors and adaptor molecules in liver disease: update. Hepatology 48, 322–35.

Senoo, H., 2004. Structure and function of hepatic stellate cells. Med. Electron Microsc. 37, 3–15.

Serafini, N., Vosshenrich, C.A.J., Di Santo, J.P., 2015. Transcriptional regulation of innate lymphoid cell fate. Nat. Rev. Immunol. 15, 415–28.

Sharma, P., Hu-Lieskovan, S., Wargo, J.A., Ribas, A., 2017. Primary, Adaptive, and Acquired Resistance to Cancer Immunotherapy. Cell 168, 707–723.

Shellam, G.R., Allan, J.E., Papadimitriou, J.M., Bancroft, G.J., 1981. Increased susceptibility to cytomegalovirus infection in beige mutant mice. Proc. Natl. Acad. Sci. U. S. A. 78, 5104–8.

Shi, X., Moroso, V., Metselaar, H.J., Kwekkeboom, J., 2013. Long-lived donor leukocytes or relocated donor hematopoietic stem/progenitor cells cause long-term hematopoietic chimerism after liver transplantation. Hepatology 56, 2542.

Shiow, L.R., Rosen, D.B., Brdičková, N., Xu, Y., An, J., Lanier, L.L., Cyster, J.G., Matloubian, M., 2006. CD69 acts downstream of interferon-α/β to inhibit S1P1 and lymphocyte egress from lymphoid organs. Nature 440, 540–544.

Shiroishi, M., Kuroki, K., Rasubala, L., Tsumoto, K., Kumagai, I., Kurimoto, E., Kato, K., Kohda, D., Maenaka, K., 2006. Structural basis for recognition of the nonclassical MHC molecule HLA-G by the leukocyte Ig-like receptor B2 (LILRB2/LIR2/ILT4/CD85d). Proc. Natl. Acad. Sci. U. S. A. 103, 16412–7.

Shuai, Z., Leung, M.W., He, X., Zhang, W., Yang, G., Leung, P.S., Eric Gershwin, M., 2016. Adaptive immunity in the liver. Cell. Mol. Immunol. 13, 354–368.

Silva, A.S., Yunes, J.A., Gillies, R.J., Gatenby, R.A., 2009. The Potential Role of Systemic Buffers in Reducing Intratumoral Extracellular pH and Acid-Mediated Invasion. Cancer Res. 69, 2677–2684.

Simhadri, V.R., Reiners, K.S., Hansen, H.P., Topolar, D., Simhadri, V.L., Nohroudi, K., Kufer, T. a, Engert, A., Pogge von Strandmann, E., 2008. Dendritic cells release HLA-B-associated transcript-3 positive exosomes to regulate natural killer function. PLoS One 3, e3377.

Simmonds, P.C., 2000. Palliative chemotherapy for advanced colorectal cancer: systematic review and meta-analysis. Colorectal Cancer Collaborative Group. BMJ 321, 531–5.

Simon, H.U., Haj-Yehia, A., Levi-Schaffer, F., 2000. Role of reactive oxygen species (ROS) in apoptosis induction. Apoptosis 5, 415–8.

Simpson, N., Cho, Y.W., Cicciarelli, J.C., Selby, R.R., Fong, T.-L., 2006. Comparison of Renal Allograft Outcomes in Combined Liver-Kidney Transplantation Versus Subsequent Kidney Transplantation in Liver Transplant Recipients: Analysis of UNOS Database. Transplantation 82, 1298–1303.

Sivori, S., Parolini, S., Falco, M., Marcenaro, E., Biassoni, R., Bottino, C., Moretta, L., Moretta, A., 2000. 2B4 functions as a co-receptor in human NK cell activation. Eur. J. Immunol. 30, 787–793.

Smyth, M.J., Cretney, E., Kelly, J.M., Westwood, J.A., Street, S.E.A., Yagita, H., Takeda, K., van Dommelen, S.L.H., Degli-Esposti, M.A., Hayakawa, Y., 2005. Activation of NK cell cytotoxicity. Mol. Immunol. 42, 501–10.

Sojka, D.K., Plougastel-Douglas, B., Yang, L., Pak-Wittel, M.A., Artyomov, M.N., Ivanova, Y., Zhong, C., Chase, J.M., Rothman, P.B., Yu, J., Riley, J.K., Zhu, J., Tian, Z., Yokoyama, W.M., 2014a. Tissue-resident natural killer (NK) cells are cell lineages distinct from thymic and conventional splenic NK cells. Elife 3, e01659.

Sojka, D.K., Tian, Z., Yokoyama, W.M., 2014b. Tissue-resident natural killer cells and their potential diversity. Semin. Immunol. 1–5.

Som, P., Atkins, H.L., Bandoypadhyay, D., Fowler, J.S., MacGregor, R.R., Matsui, K., Oster, Z.H., Sacker, D.F., Shiue, C.Y., Turner, H., Wan, C.N., Wolf, A.P., Zabinski, S. V, 1980. A fluorinated glucose analog, 2-fluoro-2-deoxy-D-glucose (F-18): nontoxic tracer for rapid tumor detection. J. Nucl. Med. 21, 670–5.

Song, E., Chen, J., Ouyang, N., Su, F., Wang, M., Heemann, U., 2001. Soluble Fas ligand released by colon adenocarcinoma cells induces host lymphocyte apoptosis: an active mode of immune evasion in colon cancer. Br. J. Cancer 85, 1047–1054.

Sonveaux, P., Copetti, T., De Saedeleer, C.J., Végran, F., Verrax, J., Kennedy, K.M., Moon, E.J., Dhup, S., Danhier, P., Frérart, F., Gallez, B., Ribeiro, A., Michiels, C., Dewhirst, M.W., Feron, O., 2012. Targeting the Lactate Transporter MCT1 in Endothelial Cells Inhibits Lactate-Induced HIF-1 Activation and Tumor Angiogenesis. PLoS One 7, e33418.

Sonveaux, P., Végran, F., Schroeder, T., Wergin, M.C., Verrax, J., Rabbani, Z.N., De Saedeleer, C.J., Kennedy, K.M., Diepart, C., Jordan, B.F., Kelley, M.J., Gallez, B., Wahl, M.L., Feron, O., Dewhirst, M.W., 2008. Targeting lactate-fueled respiration selectively kills hypoxic tumor cells in mice. J. Clin. Invest. 118, 3930–3942.

Sotosek Tokmadzic, V., Laskarin, G., Mahmutefendic, H., Lucin, P., Mrakovcic-Sutic, I., Zupan, Z., Sustic, A., 2012. Expression of cytolytic protein–perforin in peripheral blood lymphocytes in severe traumatic brain injured patients. Injury 43, 624–631.

Spits, H., Di Santo, J.P., 2011. The expanding family of innate lymphoid cells: regulators and effectors of immunity and tissue remodeling. Nat. Immunol. 12, 21–7.

Spitzer, D., Spitzer, N.J., Deininger, M., Wirtz, C.R., König, R., Burster, T., Kapapa, T., 2017. Activation of Cytotoxic Natural Killer Cells After Aneurysmal Subarachnoid Hemorrhage. World Neurosurg. 101, 666–676.e1.

Stabile, H., Fionda, C., Gismondi, A., Santoni, A., 2017. Role of Distinct Natural Killer Cell Subsets in Anticancer Response. Front. Immunol. 8, 293.

Stegmann, K.A., Robertson, F., Hansi, N., Gill, U., Pallant, C., Christophides, T., Pallett, L.J., Peppa, D., Dunn, C., Fusai, G., Male, V., Davidson, B.R., Kennedy, P., Maini, M.K., 2016. CXCR6 marks a novel subset of T-betloEomeshi natural killer cells residing in human liver. Sci. Rep. 6, 26157.

Stern, R., Shuster, S., Neudecker, B.A., Formby, B., 2002. Lactate Stimulates Fibroblast Expression of Hyaluronan and CD44: The Warburg Effect Revisited. Exp. Cell Res. 276, 24–31.

Stojanovic, A., Cerwenka, A., 2011. Natural killer cells and solid tumors. J. Innate Immun. 3, 355–64.

Su, H.C., Nguyen, K.B., Salazar-mather, T.P., Ruzek, M.C., Marc, Y., Biron, C.A., 2001. NK cell functions restrain T cell responses during viral infections. Eur. J. Immunol. 31, 3048–3055.

Sun, C., Sun, H., Xiao, W., Zhang, C., Tian, Z., 2015. Natural killer cell dysfunction in hepatocellular carcinoma and NK cell-based immunotherapy. Acta Pharmacol. Sin. 1–9.

Sznurkowski, J.J., Zawrocki, A., Biernat, W., 2014. Subtypes of cytotoxic lymphocytes and natural killer cells infiltrating cancer nests correlate with prognosis in patients with vulvar squamous cell carcinoma. Cancer Immunol. Immunother. 63, 297–303.

Tacke, F., Zimmermann, H.W., 2014. Macrophage heterogeneity in liver injury and fibrosis. J. Hepatol. 60, 1090–1096.

Takanami, I., Takeuchi, K., Giga, M., 2001. The prognostic value of natural killer cell infiltration in resected pulmonary adenocarcinoma. J. Thorac. Cardiovasc. Surg. 121, 1058–63.

Takayama, T., Kamada, N., Chinen, H., Okamoto, S., Kitazume, M.T., Chang, J., Matuzaki, Y., Suzuki, S., Sugita, A., Koganei, K., Hisamatsu, T., Kanai, T., Hibi, T., 2010. Imbalance of NKp44(+)NKp46(-) and NKp44(-)NKp46(+) natural killer cells in the intestinal mucosa of patients with Crohn's disease. Gastroenterology 139, 882–92, 892–3.

Takeda, K., Cretney, E., Hayakawa, Y., Ota, T., Akiba, H., Yagita, H., Kinoshita, K., Okumura, K., Smyth, M.J., Ogasawara, K., 2005. TRAIL identifies immature natural killer cells in newborn mice and adult mouse liver TRAIL identifies immature natural killer cells in newborn mice and adult mouse liver. Blood 105, 2082–2089.

Takeda, K., Kojima, Y., Ikejima, K., Harada, K., Yamashina, S., Okumura, K., Aoyama, T., Frese, S., Ikeda, H., Haynes, N.M., Cretney, E., Yagita, H., Sueyoshi, N., Sato, N., Nakanuma, Y., Smyth, M.J., Okumura, K., 2008. Death receptor 5 mediated-apoptosis contributes to cholestatic liver disease. Proc. Natl. Acad. Sci. 105, 10895–10900.

Takeuchi, O., Akira, S., 2010. Pattern recognition receptors and inflammation. Cell 140, 805–20.

Tang, L., Peng, H., Zhou, J., Chen, Y., Wei, H., Sun, R., Yokoyama, W.M., Tian, Z., 2016. Differential phenotypic and functional properties of liver-resident NK cells and mucosal ILC1s. J. Autoimmun. 67, 29–35.

Taylor, R.C., Cullen, S.P., Martin, S.J., 2008. Apoptosis: controlled demolition at the cellular level. Nat. Rev. Mol. Cell Biol. 9, 231–241.

Tennant, D.A., Durán, R. V., Gottlieb, E., 2010. Targeting metabolic transformation for cancer therapy. Nat. Rev. Cancer 10, 267–277.

Theurich, S., Tsaousidou, E., Hanssen, R., Lempradl, A.M., Mauer, J., Timper, K., Schilbach, K., Folz-Donahue, K., Heilinger, C., Sexl, V., Pospisilik, J.A., Wunderlich, F.T., Brüning, J.C., 2017. IL-6/Stat3-Dependent Induction of a Distinct, Obesity-Associated NK Cell Subpopulation Deteriorates Energy and Glucose Homeostasis. Cell Metab. 26, 171–184.e6.

Thiruchelvam, U., Wingfield, M., O'Farrelly, C., 2016. Increased uNK Progenitor Cells in Women With Endometriosis and Infertility are Associated With Low Levels of Endometrial Stem Cell Factor. Am. J. Reprod. Immunol. 75, 493–502.

Thomson, A.W., Knolle, P.A., 2010. Antigen-presenting cell function in the tolerogenic liver environment. Nat. Rev. 10, 753–766.

Tobin, L.M., Mavinkurve, M., Carolan, E., Kinlen, D., O'Brien, E.C., Little, M.A., Finlay, D.K., Cody, D., Hogan, A.E., O'Shea, D., 2017. NK cells in childhood obesity are activated, metabolically stressed, and functionally deficient. JCI Insight 2, e94939.

Tokita, D., Sumpter, T.L., Raimondi, G., Zahorchak, A.F., Wang, Z., Nakao, A., Mazariegos, G. V, Abe, M., Thomson, A.W., 2008. Poor allostimulatory function of liver plasmacytoid DC is associated with pro-apoptotic activity, dependent on regulatory T cells. J. Hepatol. 49, 1008–18.

Tomlinson, J.S., Jarnagin, W.R., DeMatteo, R.P., Fong, Y., Kornprat, P., Gonen, M., Kemeny, N., Brennan, M.F., Blumgart, L.H., D'Angelica, M., 2007. Actual 10-year survival after resection of colorectal liver metastases defines cure. J. Clin. Oncol. 25, 4575–80.

Tosello-Trampont, A., Surette, F.A., Ewald, S.E., Hahn, Y.S., 2017. Immunoregulatory Role of NK Cells in Tissue Inflammation and Regeneration. Front. Immunol. 8, 301.

Tosello-Trampont, A.C., Krueger, P., Narayanan, S., Landes, S.G., Leitinger, N., Hahn, Y.S., 2016. NKp46+natural killer cells attenuate metabolism-induced hepatic fibrosis by regulating macrophage activation in mice. Hepatology 63, 799–812.

Uhlen, M., Zhang, C., Lee, S., Sjöstedt, E., Fagerberg, L., Bidkhori, G., Benfeitas, R., Arif, M., Liu, Z., Edfors, F., Sanli, K., von Feilitzen, K., Oksvold, P., Lundberg, E., Hober, S., Nilsson, P., Mattsson, J., Schwenk, J.M., Brunnström, H., Glimelius, B., Sjöblom, T., Edqvist, P.-H., Djureinovic, D., Micke, P., Lindskog, C., Mardinoglu, A., Ponten, F., 2017. A pathology atlas of the human cancer transcriptome. Science 357.

Uhrberg, M., Valiante, N.M., Shum, B.P., Shilling, H.G., Lienert-Weidenbach, K., Corliss, B., Tyan, D., Lanier, L.L., Parham, P., 1997. Human diversity in killer cell inhibitory receptor genes. Immunity 7, 753–63.

Urosevic, M., Dummer, R., 2008. Human leukocyte antigen-G and cancer immunoediting. Cancer Res. 68, 627–30.

van Domselaar, R., Quadir, R., van der Made, A.M., Broekhuizen, R., Bovenschen, N., 2012. All human granzymes target hnRNP K that is essential for tumor cell viability. J. Biol. Chem. 287, 22854–64.

Vander Heiden, M.G., Cantley, L.C., Thompson, C.B., 2009. Understanding the Warburg Effect: The Metabolic Requirements of Cell Proliferation. Science (80-.). 324, 1029–1033.

Vaupel, P., Kallinowski, F., Okunieff, P., 1989. Blood flow, oxygen and nutrient supply, and metabolic microenvironment of human tumors: a review. Cancer Res. 49, 6449–65.

Vegran, F., Boidot, R., Michiels, C., Sonveaux, P., Feron, O., 2011. Lactate Influx through the Endothelial Cell Monocarboxylate Transporter MCT1 Supports an NF- B/IL-8 Pathway that Drives Tumor Angiogenesis. Cancer Res. 71, 2550–2560.

Veillette, A., 2006. NK cell regulation by SLAM family receptors and SAP-related adapters. Immunol. Rev. 214, 22–34.

Velnar, T., Bailey, T., Smrkolj, V., 2009. The Wound Healing Process: An Overview of the Cellular and Molecular Mechanisms. J. Int. Med. Res. 37, 1528–1542.

Vermijlen, D., Luo, D., Froelich, C.J., Medema, J.P., Kummer, J.A., Willems, E., Braet, F., Wisse, E., 2002. Hepatic natural killer cells exclusively kill splenic/blood natural killer-resistant tumor cells by the perforin/granzyme pathway. J. Leukoc. Biol. 72, 668–76.

Viel, S., Marçais, A., Guimaraes, F.S.-F., Loftus, R., Rabilloud, J., Grau, M., Degouve, S., Djebali, S., Sanlaville, A., Charrier, E., Bienvenu, J., Marie, J.C., Caux, C., Marvel, J., Town, L., Huntington, N.D., Bartholin, L., Finlay, D., Smyth, M.J., Walzer, T., 2016. TGF-β inhibits the activation and functions of NK cells by repressing the mTOR pathway. Sci. Signal. 9, ra19.

Vilches, C., Parham, P., 2002. KIR: diverse, rapidly evolving receptors of innate and adaptive immunity. Annu. Rev. Immunol. 20, 217–51.

Villard, J., 2011. The role of natural killer cells in human solid organ and tissue transplantation. J. Innate Immun. 3, 395–402.

Villegas, F.R., Coca, S., Villarrubia, V.G., Jiménez, R., Chillón, M.J., Jareño, J., Zuil, M., Callol, L., 2002. Prognostic significance of tumor infiltrating natural killer cells subset CD57 in patients with squamous cell lung cancer. Lung Cancer 35, 23–8.

Vivier, E., Tomasello, E., Baratin, M., Walzer, T., Ugolini, S., 2008. Functions of natural killer cells. Nat. Immunol. 9, 503–10.

Voskoboinik, I., Whisstock, J.C., Trapani, J.A., 2015. Perforin and granzymes: function, dysfunction and human pathology. Nat. Rev. Immunol. 15, 388–400.

Vosshenrich, C.A.J., García-Ojeda, M.E., Samson-Villéger, S.I., Pasqualetto, V., Enault, L., Goff, O.R.-L., Corcuff, E., Guy-Grand, D., Rocha, B., Cumano, A., Rogge, L., Ezine, S., Di Santo, J.P., 2006. A thymic pathway of mouse natural killer cell development characterized by expression of GATA-3 and CD127. Nat. Immunol. 7, 1217–1224.

Waggoner, S.N., Cornberg, M., Selin, L.K., Welsh, R.M., 2012. Natural killer cells act as rheostats modulating antiviral T cells. Nature 481, 394–398.

Wagner, J.A., Rosario, M., Romee, R., Berrien-Elliott, M.M., Schneider, S.E., Leong, J.W., Sullivan, R.P., Jewell, B.A., Becker-Hapak, M., Schappe, T., Abdel-Latif, S., Ireland, A.R., Jaishankar, D., King, J.A., Vij, R., Clement, D., Goodridge, J., Malmberg, K.-J., Wong, H.C., Fehniger, T.A., 2017. CD56bright NK cells exhibit potent antitumor responses following IL-15 priming. J. Clin. Invest. 127, 4042–4058.

Walker, J.A., McKenzie, A.N., 2013. Development and function of group 2 innate lymphoid cells. Curr. Opin. Immunol. 25, 148–155.

Waller, L.P., Deshpande, V., Pyrsopoulos, N., 2015. Hepatocellular carcinoma: A comprehensive review. World J. Hepatol. 7, 2648–2663.

Wang, X.Q., Lo, C.M., Chen, L., Cheung, C.K.Y., Yang, Z.F., Chen, Y.X., Ng, M.N., Yu, W.C., Ming, X., Zhang, W., Ho, D.W.Y., Chan, S.C., Fan, S.T., 2012. Hematopoietic chimerism in liver transplantation patients and hematopoietic stem/progenitor cells in adult human liver. Hepatology 56, 1557–66.

Warburg, O., Wind, F., Negelein, E., 1927. THE METABOLISM OF TUMORS IN THE BODY. J. Gen. Physiol. 8, 519–30.

Wardle, E.N., 1987. Kupffer cells and their function. Liver 7, 63–75.

Wensveen, F.M., Jelenčić, V., Valentić, S., Šestan, M., Wensveen, T.T., Theurich, S., Glasner, A., Mendrila, D., Štimac, D., Wunderlich, F.T., Brüning, J.C., Mandelboim, O., Polić, B., 2015. NK cells link obesity-induced adipose stress to inflammation and insulin resistance. Nat. Immunol. 16, 376–385.

Westermann, B., 2010. Mitochondrial fusion and fission in cell life and death. Nat. Rev. Mol. Cell Biol. 11, 872–884.

Whitaker-Menezes, D., Martinez-Outschoorn, U.E., Lin, Z., Ertel, A., Flomenberg, N., Witkiewicz, A.K., Birbe, R., Howell, A., Pavlides, S., Gandara, R., Pestell, R.G., Sotgia, F., Philp, N.J., Lisanti, M.P., 2011. Evidence for a stromal-epithelial “lactate shuttle” in human tumors. Cell Cycle 10, 1772–1783.

Whiteside, T.L., Herberman, R.B., 1994. Human Natural Killer Cells in Health and Disease. Clin. Immunother. 1, 56–66.

Wieman, H.L., Wofford, J.A., Rathmell, J.C., 2007. Cytokine Stimulation Promotes Glucose Uptake via Phosphatidylinositol-3 Kinase/Akt Regulation of Glut1 Activity and Trafficking. Mol. Biol. Cell 18, 1437–1446.

Wiencke, K., 2001. Primary sclerosing cholangitis is associated to an extended B8-DR3 haplotype including particular MICA and MICB alleles. Hepatology 34, 625–630.

Wisse, E., Luo, D., Vermijlen, D., Kanellopoulou, C., De Zanger, R., Braet, F., 1997. On the function of pit cells, the liver-specific natural killer cells. Semin. Liver Dis. 17, 265–86.

Wisse, E., van’t Noordende, J.M., van der Meulen, J., Daems, W.T., 1976. The pit cell: Description of a new type of cell occurring in rat liver sinusoids and peripheral blood. Cell Tissue Res. 173, 423–435.

Wu, J., Meng, Z., Jiang, M., Zhang, E., Trippler, M., Broering, R., Bucchi, A., Krux, F., Dittmer, U., Yang, D., Roggendorf, M., Gerken, G., Lu, M., Schlaak, J.F., 2010. Toll-like receptor-induced innate immune responses in non-parenchymal liver cells are cell type-specific. Immunology 129, 363–74.

Wuensch, S.A., Spahn, J., Crispe, I.N., 2010. Direct, help-independent priming of CD8+ T cells by adeno-associated virus-transduced hepatocytes. Hepatology 52, 1068–77.

Xie, J., Wu, H., Dai, C., Pan, Q., Ding, Z., Hu, D., Ji, B., Luo, Y., Hu, X., 2015. Beyond Warburg effect – dual metabolic nature of cancer cells. Sci. Rep. 4, 4927.

Yaeger, R., Chatila, W.K., Lipsyc, M.D., Hechtman, J.F., Cercek, A., Sanchez-Vega, F., Jayakumaran, G., Middha, S., Zehir, A., Donoghue, M.T.A., You, D., Viale, A., Kemeny, N., Segal, N.H., Stadler, Z.K., Varghese, A.M., Kundra, R., Gao, J., Syed, A., Hyman, D.M., Vakiani, E., Rosen, N., Taylor, B.S., Ladanyi, M., Berger, M.F., Solit, D.B., Shia, J., Saltz, L., Schultz, N., 2018. Clinical Sequencing Defines the Genomic Landscape of Metastatic Colorectal Cancer. Cancer Cell 33, 125–136.e3.

Ying, H., Kimmelman, A.C., Lyssiotis, C.A., Hua, S., Chu, G.C., Fletcher-Sananikone, E., Locasale, J.W., Son, J., Zhang, H., Coloff, J.L., Yan, H., Wang, W., Chen, S., Viale, A., Zheng, H., Paik, J., Lim, C., Guimaraes, A.R., Martin, E.S., Chang, J., Hezel, A.F., Perry, S.R., Hu, J., Gan, B., Xiao, Y., Asara, J.M., Weissleder, R., Wang, Y.A., Chin, L., Cantley, L.C., DePinho, R.A., 2012. Oncogenic Kras Maintains Pancreatic Tumors through Regulation of Anabolic Glucose Metabolism. Cell 149, 656–670.

Younossi, Z., Anstee, Q.M., Marietti, M., Hardy, T., Henry, L., Eslam, M., George, J., Bugianesi, E., 2017. Global burden of NAFLD and NASH: trends, predictions, risk factors and prevention. Nat. Rev. Gastroenterol. Hepatol. 14, 11–20.

Younossi, Z.M., Koenig, A.B., Abdelatif, D., Fazel, Y., Henry, L., Wymer, M., 2016. Global epidemiology of nonalcoholic fatty liver disease-Meta-analytic assessment of prevalence, incidence, and outcomes. Hepatology 64, 73–84.

Yu, J., Freud, A.G., Caligiuri, M.A., 2013. Location and cellular stages of natural killer cell development. Trends Immunol. 34, 573–582.

Yu, X., Harden, K., C Gonzalez, L., Francesco, M., Chiang, E., Irving, B., Tom, I., Ivelja, S., Refino, C.J., Clark, H., Eaton, D., Grogan, J.L., 2009. The surface protein TIGIT suppresses T cell activation by promoting the generation of mature immunoregulatory dendritic cells. Nat. Immunol. 10, 48–57.

Zaiatz-Bittencourt, V., Finlay, D.K., Gardiner, C.M., 2018. Canonical TGF-β Signaling Pathway Represses Human NK Cell Metabolism. J. Immunol. 200, 3934–3941.

Zamai, L., Ponti, C., Mirandola, P., Gobbi, G., Papa, S., Galeotti, L., Cocco, L., Vitale, M., 2007. NK cells and cancer. J. Immunol. 178, 4011–4016.

Zhai, Y., Petrowsky, H., Hong, J.C., Busuttil, R.W., Kupiec-Weglinski, J.W., 2013. Ischaemia–reperfusion injury in liver transplantation—from bench to bedside. Nat. Rev. Gastroenterol. Hepatol. 10, 79–89.

Zhang, D.Y., Friedman, S.L., 2012. Fibrosis-dependent mechanisms of hepatocarcinogenesis. Hepatology 56, 769–75.

Zhang, J., Marotel, M., Fauteux-Daniel, S., Mathieu, A.-L., Viel, S., Marçais, A., Walzer, T., 2018. T-bet and Eomes govern differentiation and function of mouse and human NK cells and ILC1. Eur. J. Immunol. 48, 738–750.

Zhang, Z., Zhang, S., Zou, Z., Shi, J., Zhao, J., Fan, R., Qin, E., Li, B., Li, Z., Xu, X., Fu, J., Zhang, J., Gao, B., Tian, Z., Wang, F.-S., 2011. Hypercytolytic activity of hepatic natural killer cells correlates with liver injury in chronic hepatitis B patients. Hepatology 53, 73–85.

Zhao, T., Zhang, H., Guo, Y., Fan, Z., 2007. Granzyme K Directly Processes Bid to Release Cytochrome c and Endonuclease G Leading to Mitochondria-dependent Cell Death. J. Biol. Chem. 282, 12104–12111.

Zhao, T., Zhang, H., Guo, Y., Zhang, Q., Hua, G., Lu, H., Hou, Q., Liu, H., Fan, Z., 2007. Granzyme K cleaves the nucleosome assembly protein SET to induce single-stranded DNA nicks of target cells. Cell Death Differ. 14, 489–99.

Zook, E.C., Kee, B.L., 2016. Development of innate lymphoid cells. Nat. Immunol. 17, 775–782.

Appendix I

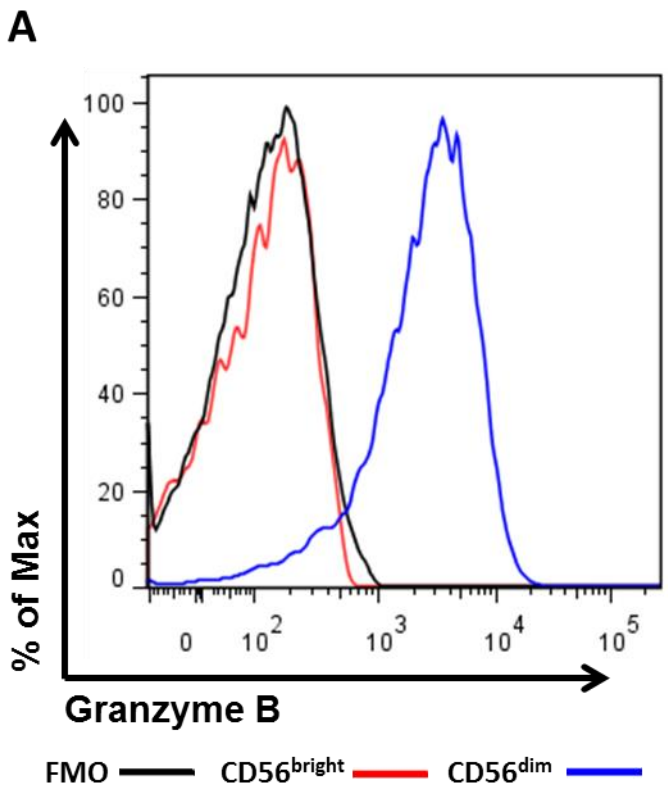

Appendix Figure 1 Granzyme B expression in freshly isolated PBMC sample

PBMC's were isolated from a healthy blood donor from local volunteer. NK cells were identified from the $CD45^{+}$ lymphocyte gate as $CD56^{+}CD3^{-}$. $CD56^{bright}$ $CD16^{-/+}$ and $CD56^{dim}$ $CD16^{+}$ subsets were then gated on. Non-viable cells were excluded by FVS780 staining. **(A)** Representative histograms of granzyme B expression in $CD56^{bright}$ (red) and $CD56^{dim}$ NK cells (blue).

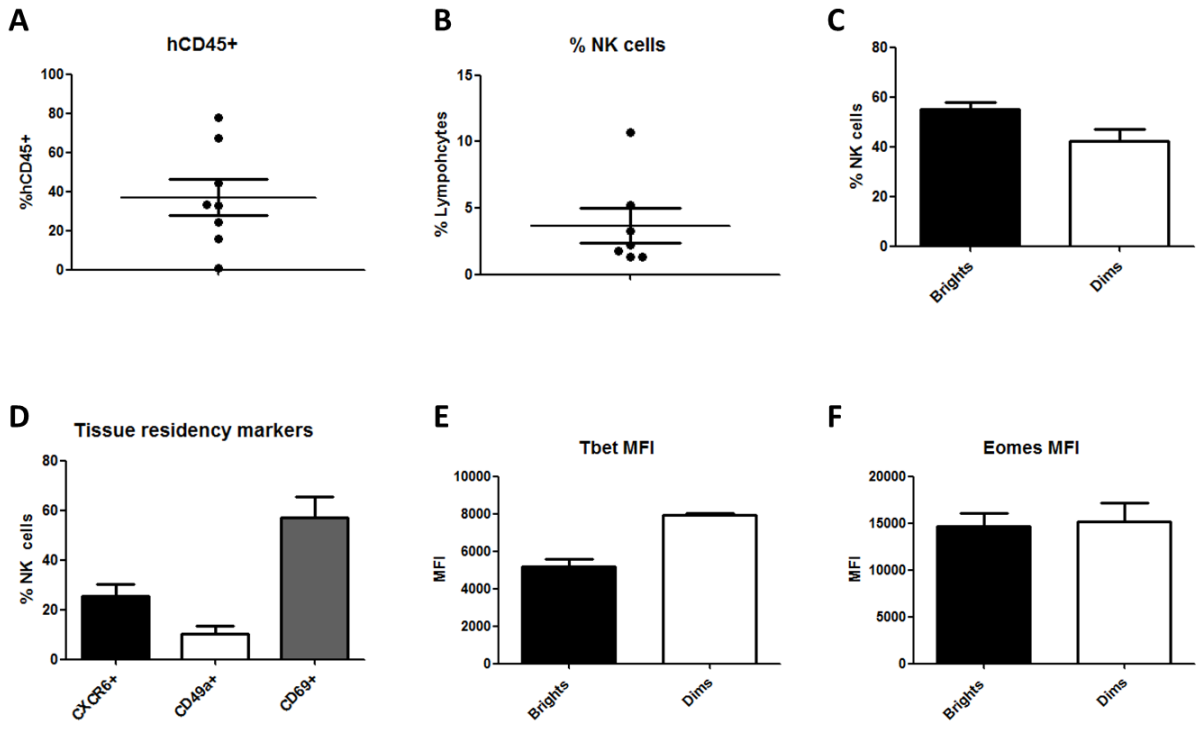

Appendix Figure 2 Characterisation of liver resident NK cells in humanised mice

Adult mice were irradiated and injected with human cord blood $CD34^{+}$ stem cells with analysis 12-13 weeks post stem cell transfer. Livers were harvested and single cell suspensions were prepared by mechanical digestion. Mononuclear cells were isolated from and stained with monoclonal antibodies. **(A)** Engraftment of human immune cells was measured by comparing the presence of human $CD45^{+}$ (hCD45) cells compared to murine CD45+ cells**. (B)** The proportion of NK cells in $hCD45^{+}$ lymphocytes. **(C)** Proportion of $CD56^{bright}$ (black bar) and $CD56^{dim}$ (white bar) NK cells in liver of humanised mice. **(D)** Percentage of tissue residency marker (CXCR6, CD49a and CD69) positive $CD56^{bright}$ NK cells from humanised mouse liver. **(E)** Expression of Tbet in liver $CD56^{bright}$ (black bar) and $CD56^{dim}$ (white bar) NK cells in liver of humanised mice. **(F)** Expression of Eomes in liver $CD56^{bright}$ (black bar) and $CD56^{dim}$ (white bar) NK cells in liver of humanised mice. Data presented as mean ± SEM. Data analysed using Wilcoxon matched pairs test. (n=6-8).

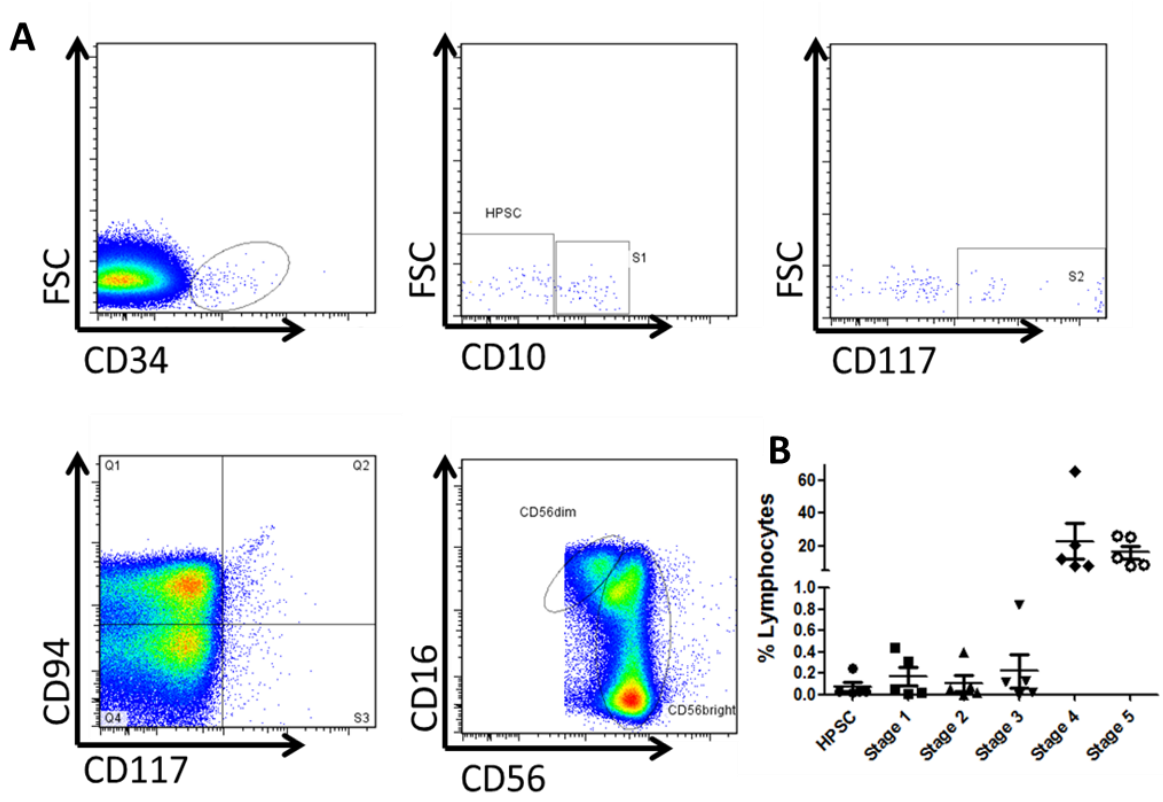

Appendix Figure 3 Presence of NK cell progenitors in liver perfusate

Mononuclear cells isolated from liver perfusate (LP) were stained with monoclonal antibodies. Progenitors and mature NK cells were identified from $CD45^{+}$ cells. Non-viable cells were excluded by FVS780 staining. **(A)** Representative FACS plots of NK cell progenitors in liver perfusate. **(B)** Percentage of NK progenitors in liver perfusate. (HPSC-Haematopoietic stem cell ($CD34^{+}$, $CD10^{-}$), S1- Stage 1 progenitor ($CD34^{+}$, $CD10^{+}$), S2-Stage 2 progenitor ($CD34^{+}$, $CD117^{+}$), S3-Stage 3 progenitor ($CD34^{-}$, $CD117^{+}$), Stage 4-$CD56^{bright}$ NK cell, Stage 5-$CD56^{dim}$ NK cell.)

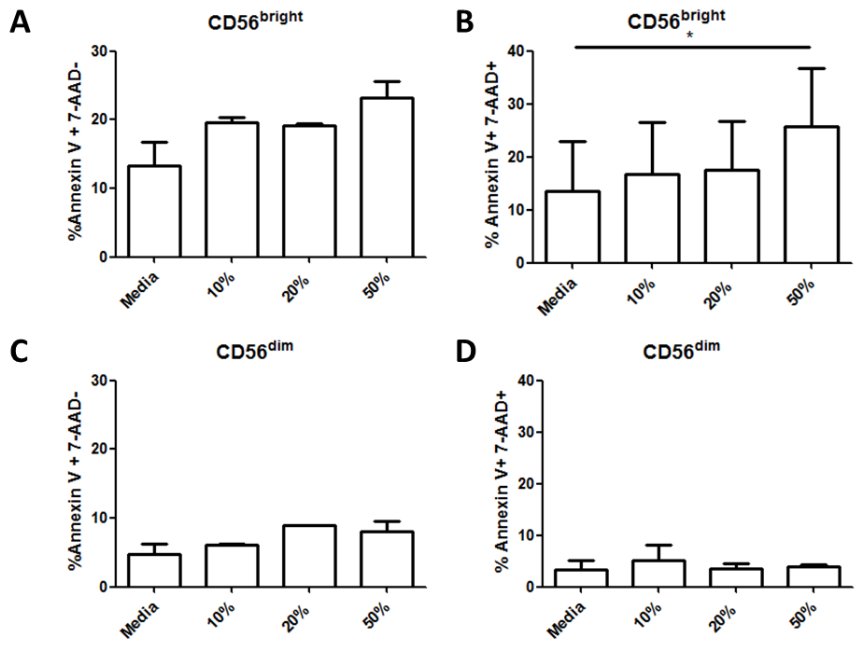

Appendix Figure 4 Optimisation of tumour conditioned media treatment

NK cell subsets were isolated from liver perfusate by FACS. Cells were cultured for 24 hours with increasing dose of tumour conditioned media; 10, 20 or 50% v/v conditioned media from colorectal liver metastasis tumours (CRLM). Apoptosis was assessed by annexin V and 7AAD staining. (A) Percentage of pro-apoptotic $CD56^{bright}$ NK cells. (B) Percentage of apoptotic $CD56^{bright}$ NK cells. (C) Percentage of pro-apoptotic $CD56^{dim}$ NK cells. (D) Percentage of apoptotic $CD56^{dim}$ NK cells. Data presented as mean ± SEM. Data analysed using Kruskal-Wallis test, with Dunn's multiple comparison test. (n=3, *, $p<0.05$)

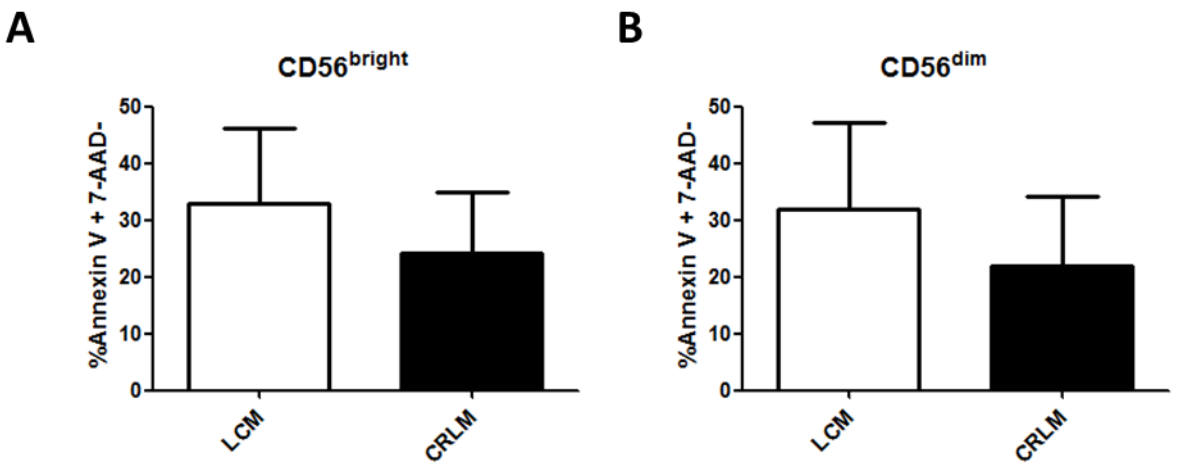

Appendix Figure 5 Pro-apoptotic NK cell subsets after treatment with LCM and CRLM conditioned media.

NK cell subsets were isolated from liver perfusate by FACS. Cells were cultured for 24 hours in the presence of 50% v/v healthy liver conditioned media (LCM) or conditioned media from colorectal liver metastasis tumours (CRLM). Apoptosis was assessed by annexin V and 7AAD staining. (A) Percentage of pro-apoptotic $CD56^{bright}$ NK cells. (B) Percentage of pro-apoptotic $CD56^{dim}$ NK cells. Data presented as mean ± SEM. Data analysed using Wilcoxon matched pairs test. (n=5).

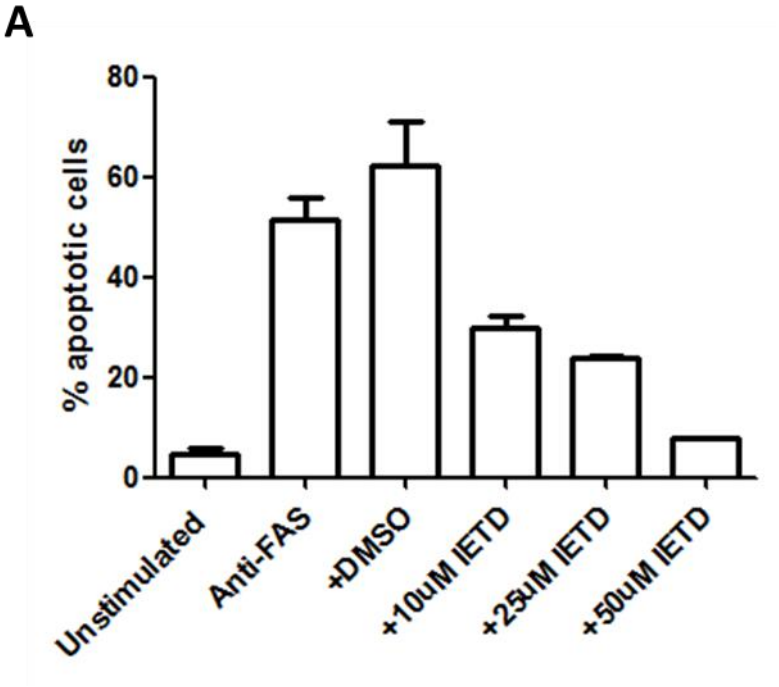

Appendix Figure 6 Optimisation of z-IETD-FMK treatment

Jurkat cells were treated with increasing concentrations of z-IETD-FMK (caspase-8 inhibitor) for 2 hours. Jurkat cells were then stimulated with an anti-FAS antibody for 24 hours. Apoptosis was measured by annexin V/7-AAD staining. (A) Percentage of apoptotic cells after incubation with anti-FAS and z-IETD-FMK.